Understanding the effects of environmental variability on demography in species with complex life histories through integrated population modeling

Amanda Warlick

A dissertation

submitted in partial fulfillment of the

requirements for the degree of

Doctor of Philosophy

University of Washington

2022

Reading Committee:

Sarah Converse, Chair

Beth Gardner

Devin Johnson

Program Authorized to Offer Degree:

School of Fishery and Aquatic Sciences

University of Washington

Abstract

Understanding the effects of environmental variability on demography in species with complex life histories through integrated population modeling

Amanda Warlick

Chair of the Supervisory Committee:
Sarah Converse
School of Aquatic and Fishery Sciences

Understanding the spatio-temporal variability in demography offers insight into factors underlying the dynamics and viability of wildlife populations. However, sparse monitoring data or persistent knowledge gaps can make it difficult to estimate vital rates for species with complex life histories. Even more challenging is identifying causal mechanisms that explain demographic patterns for long-lived, adaptive top predators due to the complexities of obtaining data about natural environmental variability or anthropogenic stressors at ecological scales most relevant to the population of interest. These challenges can be particularly acute in situations where the need for information is greatest; namely, for populations that are small, depleted, or declining and in need of conservation and management. Integrated population models (IPMs) that combine disparate data sources have emerged as an important tool for maximizing available information to improve the estimation of vital rates, abundance, and viability of wildlife populations.

The research presented here includes three case studies using data integration and hierarchical Bayesian state-space models to examine the effects of environmental conditions on the demography and viability of marine mammals and seabirds. First, I present a novel multi-event open-population model that extends nest survival and abundance modeling approaches to accomodate data where nest age, state, and fate may be unknown. I apply this model to Pigeon Guillemots (*Cepphus columba*) to provide the first estimates of fecundity for this indicator species in Puget Sound, Washington (Chapter 2) to facilitate future integrated population modeling using data collected by a community science program. Second, I developed an IPM to examine demographic and environmental factors contributing to divergent abundance trends observed across the range of the Endangered western distinct population segment of Steller sea lions (*Eumetopias jubatus*) in Alaska (Chapters 3-4). Third, I developed an IPM to examine environmental drivers of demography and viability for the Endangered Cook Inlet beluga whale in Alaska (Chapter 5). Unifying themes of this work include developing complex demographic models to reduce uncertainty in support of conservation and confronting the challenges of making inference about the effects of environmental variability at spatio-temporal scales relevant to long-lived, adaptive top predators living in dynamic and changing ecosystems.

TABLE OF CONTENTS

List of Figures ..... **ix**

List of Tables ..... **xv**

Chapter 1. Introduction **1**

1.1 Background 1

1.2 Research Objectives 3

1.3 Broader Impacts 4

1.4 References 5

Chapter 2. A Bayesian state-space nest survival and abundance model incorporating breeding phenology to address unknown age, state, or fate data **9**

2.1 Introduction 10

2.2 Methods 13

2.2.1 Study Species 13

2.2.2 Data 14

2.2.3 Model framework 15

2.2.4 Simulation analysis 18

2.2.5 Pigeon Guillemot case study 19

2.3 Results 20

2.3.1 Pigeon Guillemot case study 20

2.3.2 Simulation analysis 21

2.4 Discussion 23

2.5 Acknowledgements 27
2.6 Figures & Tables 28
2.7 References 33

Chapter 3. Identifying environmental drivers of demography and potential factors limiting the recovery of an endangered marine top predator 38

3.1 Introduction 39
3.2 Methods 42
3.2.1 Study system 42
3.2.2 Sea lion data 44
3.2.3 Oceanographic data 45
3.2.4 Statistical analyses 47
3.3 Results 53
3.3.1 Demography 53
3.3.2 Detection 55
3.3.3 Individual and oceanographic covariates 55
3.3.4 Model selection and evaluation 57
3.4 Discussion 58
3.4.1 Demography 59
3.4.2 Oceanographic effects 61
3.5 Conclusion 66
3.6 Acknowledgements 67
3.7 Figures & Tables 68
3.8 References 72

Chapter 4. Population viability analysis for the western distinct population segment of Steller sea lions in Alaska 84

4.1 Introduction 85

4.2 Methods 87

4.2.1 Study system 87

4.2.2 Data 88

4.2.3 Statistical analyses 90

4.2.4 Model assumptions and fitting 97

4.3 Results 98

4.3.1 Vital rates 98

4.3.2 Population growth rates, abundance, and age structure 99

4.3.3 Sensitivity and viability 100

4.4 Discussion 101

4.5 Acknowledgements 104

4.6 Figures and tables 105

4.7 References 112

Chapter 5. Demographic and environmental drivers of population dynamics and viability in an endangered top predator using an integrated model 123

5.1 Introduction 124

5.2 Methods 126

5.2.1 Study species 126

5.2.2 Population monitoring data 127

5.2.3 Statistical analyses 128
5.2.4 Environmental covariates 134
5.2.5 Model fitting 136
5.3 Results 136
5.3.1 Demographic rates 136
5.3.2 Population size and structure 137
5.3.3 Sensitivity and viability analyses 138
5.3.4 Environmental covariate effects 139
5.4 Discussion 139
5.5 Acknowledgements 144
5.6 Figures and tables 144
5.7 References 150
Appendix A 156
Appendix B 159
Appendix C 164
Appendix D 171
Appendix E 175
Appendix F 178
Appendix G 184

LIST OF FIGURES

Figure 2.1: Posterior mean and 95% credible intervals for egg and chick survival at a daily level, and reproductive success (probability a nest produces at least one fledgling) and stage-specific survival over the entire breeding season, derived for the latter by raising daily rates to the power of the mean peak transition age for each stage. 28

Figure 2.2: Posterior mean and 95% credible intervals for daily nest state transition probabilities for egg laying, egg hatching, and chick fledging by nest and chick age. 28

Figure 2.3: Mean and 95% credible intervals for the number of nests with at least one egg, hatchling, and fledging. 29

Figure 2.4: Mean and 95% credible intervals for daily burrow detection probability as a function of a categorical representation of the tidal cycle, where 1 represents burrow observations made closest in time to the morning's high tide and 4 represents burrow observations made farthest from the morning's high tide. 29

Figure 2.5: Relative bias (%) of (a) egg (ϕEgg) and chick (ϕChick) survival and nest success, (b) number of nests with at least one egg (N^L), hatchling (N^H), and fledgling (N^F), (c) stage-specific nest state transitions governing nest initiation (β1L and β2L), egg hatching (β1H and β2H), and chick fledging (β1F and β2F) and (d) observation process parameters nest detection (p) and state uncertainty (α) across levels of survey frequency (daily, three/week, once/week), nest detection probability (0.5, 0.75), and state uncertainty probability (none, 0.25, 0.5). Color scales are plot specific, but white always denotes 0 bias, while red and blue denote the percent positive and negative bias, respectively. Dark grey indicates where α is set at zero and therefore bias is not calculated. 30

Figure 2.6: Root mean squared error of (a) egg (ϕEgg) and chick (ϕChick) survival and nest success, (b) number of nests with at least one egg (N^L), hatchling (N^H), and fledgling (N^F), (c) stage-specific nest state transitions governing nest initiation (β1L and β2L), egg hatching (β1H and β2H), and chick fledging (β1F and β2F) and (d) observation process parameters nest detection (p) and state uncertainty (α) across levels of survey frequency (daily, three/week, once/week), nest detection probability (0.5, 0.75), and state uncertainty probability (none, 0.25, 0.5). Higher values indicated by darker colors reflect a higher degree of variance and bias. Dark grey indicates where α is set at zero and therefore RMSE is not calculated. 31

Figure 2.7: Credible interval coverage for (a) egg (ϕEgg) and chick (ϕChick) survival and nest success, (b) number of nests with at least one egg (N^L), hatchling (N^H), and fledgling (N^F), (c) stage-specific nest state transitions governing nest initiation (β1L and β2L), egg hatching (β1H and β2H), and

chick fledging (β1F and β2F) and (d) observation process parameters nest detection (p) and state uncertainty (α) across levels of survey frequency (daily, three/week, once/week), nest detection probability (0.5, 0.75), and state uncertainty probability (none, 0.25, 0.5). Color scales are plot specific, but white always denotes 95% coverage, while red and blue imply > 95% and < 95% coverage, respectively. Dark grey indicates where α is set at zero and therefore coverage is not calculated. 32

Figure 3.1: Steller sea lion branding locations in the eastern (blue triangles) and western (green squares) portions of the range, and rookeries (red) throughout the western distinct population segment (excluding Russia) and southeast Alaska (eastern DPS that extends along the U.S. West Coast). Black rectangles indicate locations from which satellite data were aggregated for use as covariates in the eastern (46.3° to 58.1°N and -177.9° to -159°W) and western (49.8° to 55.4°N and 169.9° to 175.6°E) portions of the range. Table shows the number of marked and released pups in each region over the study period. 68

Figure 3.2: Life cycle diagram for female and male Steller sea lions, with true ecological states shown in white (pup, juveniles age 1-3, pre-breeding subadults ages 4-5, breeding adult females (4^{+}B), non-breeding adult females (5^{+}NB), and adult males (6^{+}A). Survival (ϕ) and pupping (ψ) probabilities denote transitions between true states (black lines) and detection probabilities (p) denote possible observation events for each age and breeding (with or without pup) and non-breeding females (grey dotted lines). 68

Figure 3.3: Posterior mean and 95% credible intervals for age- and sex-specific survival and pupping probabilities for Steller sea lions in the eastern (black) and western (grey) portion of the wDPS range. 69

Figure 3.4: Posterior mean and 95% credible interval for time-varying age-specific (a) survival and (b) pupping probability for female Steller sea lions marked in the eastern portion of the wDPS range. 69

Figure 3.5: Posterior mean and 95% credible intervals for age- and sex-specific detection probability of Steller sea lions marked in the eastern (black) and western (grey) portion of the wDPS range. 70

Figure 3.6: Logit-scale posterior mean and 95% credible intervals for the fixed effects of environmental covariates in each season and pup mass at branding on pup and young (pooled effect for age 1-2) survival and pupping probabilities for individuals marked in the eastern and western portions of the wDPS range. 70

Figure 4.1: Steller sea lion field camps (blue triangles) in the eastern portion of the range, camera traps (green squares) in the western portion of the range, and rookeries (red) throughout the western distinct population segment (wDPS) (excluding Russia) and southeast Alaska (eastern DPS that extends along the U.S. West Coast). Rectangle indicates the spatial extent from which sea surface temperature data were aggregated. Table shows the number of branded and released pups in each subregion over the study period. 105

Figure 4.2: Reproduced from Warlick et al. (*in review*; Ch. 3), life cycle diagram for female and male Steller sea lions, indicating true ecological states (pup, juveniles age-1, age-2, and age-3, pre-breeding subadults age-4 and age-5, breeding adult females ($B(4^{+})$), non-breeding adult females ($NB(5^{+})$), and adult males ($A(6^{+})$). Survival (ϕ) and pupping (ψ) probabilities denote transitions between true states (black lines) and detection probabilities (p) denote possible observation events for each age and breeding (with or without pup) and non-breeding females (grey dotted lines). 106

Figure 4.3: Directed acyclic graph representing the integrated population model framework including subcomponent models using aerial survey and mark-resight data. 106

Figure 4.4: Posterior mean and 95% credible intervals for age-specific survival and pupping for female Steller sea lions across the six wDPS subregions, with the range-wide average represented by the dashed line. Male survival rates were similar (Appendix B) but are not shown for readability. 107

Figure 4.5: Posterior mean and 95% credible intervals for time-varying Steller sea lion female survival rates across the six wDPS subregions. 108

Figure 4.6: Posterior mean and 95% credible intervals of total abundance of Steller sea lions in the six wDPS subregions (colors) and range-wide (black). 109

Figure 4.7: Posterior mean and 95% credible intervals of Steller sea lion population growth rates in the six wDPS subregions and range-wide (grey dashed line) based on abundance estimates from the IPM and from aerial survey data treated with agTrend alone (red asterisks). 109

Figure 4.8: Posterior mean and 95% credible intervals of the ratio of total abundance to pup abundance range-wide (black) and in each of the six wDPS subregions (colors), with the traditional 4.5 “pup multiplier” (black dashed line) and the regional averages (colored dashed lines). 110

Figure 4.9: Total Steller sea lion abundance in each of the six wDPS subregions over the 100-year projection period. 110

Figure 4.10: Mean and 95% CI of population growth rates during the projection period across projection scenarios with varying mean and standard deviation of generated predictor variables compared with

the baseline scenario that adopts the mean and variability of historical conditions (dotted line). 111

Figure 5.1: Beluga whale study areas within Cook Inlet, Alaska. Aerial surveys occur two weeks in June. Photo-identification boat surveys and land-based operations occur from April-October primarily north of the Forelands..... 144

Figure 5.2: Life cycle diagrams reproduced from Himes Boor et al. (*In revision*) depicting (a) adult survival and reproduction; (b) calf survival; and (c) the full ecological process model with possible reproductive states and transitions based on fecundity and calf and adult female survival rates (excludes the transitions from a mother with two calves to one or zero calves when a calf dies or becomes independent for readability). 145

Figure 5.3: Directed acyclic graph of the integrated population model framework for Cook Inlet beluga whale abundance, including the multi-event mark-recapture model estimating fecundity and adult and calf survival, and the count model estimating group size through stochastic population growth equations based on aerial survey data and the associated detection probability. 146

Figure 5.4: Posterior mean and 95% credible intervals for time-varying survival of breeding females, the non-breeding group, young calf survival, apparent survival of older calves, and fecundity over the study period with mean rates represented by the dashed line. 146

Figure 5.5: (a) Predicted population abundance (black line), 95% credible interval (grey shading), aerial survey data during the study period (red circles), and posterior predictions for aerial survey data (blue points and error bars) that accounts for variability in aerial survey detection probability, and (b) projected abundance and annual extinction probability over a 150-year period for Cook Inlet belugas based on estimated demographic rates and abundance from mark-resight and aerial survey data. 147

Figure 5.6: Estimated annual population growth rates and demographic rates during the study period with posterior median correlation coefficients, *r*, and 95% credible intervals shown in parentheses for fecundity and adult, older calf, and young calf survival. 147

Figure 5.7: (a) Predicted abundance and (b) negative versus positive population growth rates (red-blue color scale) over hypothetical percent increases in demographic rates..... 148

Figure 5.8: Posterior mean and 95% credible intervals for the logit-scale effects of sea surface temperature and prey abundance on fecundity (ψB), and adult (S_B, S_N), older calf (ϕC), and young calf (S_Y) survival..... 148

Figure A1: WAIC values for models when each season-specific environmental variable was used as the only covariate. Dashed line represents a baseline WAIC value for the random effects-only model for the eastern portion of the range and a null model for the western portion of the range. 158

Figure B1: Posterior mean and 95% credible intervals for age-specific survival for Steller sea lions across the six wDPS subregions, with the range-wide average represented by the dashed line. ... 160

Figure B2: Posterior mean and 95% credible intervals of population age structure in each of the six wDPS subregions compared with the proportion expected according to a stable age distribution assumption (black dashed line). 161

Figure B3: Mean and 95% credible intervals of logit-scale effects of environmental conditions on male and female pup and yearling survival, breeding female survival, and first-time and repeat pupping probabilities. 162

Figure B4: Posterior mean and 95% credible intervals for correlation coefficients between population growth rates and female time-varying demographic rates. 162

Figure B5: Posterior mean and 95% credible intervals for correlation coefficients between population growth rates and female time-varying demographic rates across the six wDPS subregions.163

Figure C1: Posterior mean and 95% credible intervals for annual detection probabilities across priors for aerial survey detection probability using either maximum or median survey day counts. . 167

Figure C2: The overlap of prior (grey outline) and posterior (color fill) distributions across priors for aerial survey detection probability using either maximum or median survey day counts. . 167

Figure C3: Posterior mean and 95% credible intervals for stage-based survival and fecundity estimated across priors for aerial survey detection probability using either maximum or median survey day counts..... 168

Figure C4: Abundance trend during the time period informed by data across priors for aerial survey detection probability estimated using the "median" survey day data..... 168

Figure C5: Posterior mean and 95% credible intervals for projected abundance trends across priors for aerial survey detection probability and median and maximum survey day data..... 169

Figure C6: Posterior mean population growth rate across priors for aerial survey detection probability and median and maximum survey day data. 169

Figure C7: Posterior mean of population viability and extinction risk across priors for aerial survey detection probability and "median" and "maximum" survey day data. 170

Figure D1: Posterior mean and 95% credible intervals for demographic rates across ages at first reproduction..... 172

Figure D2: Posterior mean and 95% credible intervals for detection probabilities across ages at first reproduction..... 172
Figure D3: Posterior mean and 95% credible intervals for abundance estimates across ages at first reproduction..... 173
Figure D4: Posterior mean and 95% credible intervals for projected abundance estimates across ages at first reproduction. 173
Figure D5: Posterior mean population growth rates over the 150-year projection period across ages at first reproduction. 174
Figure D6: Posterior mean of population viability metrics, including the probability of a negative trend in abundance, of reaching the downlisting threshold (>520 individuals), of having no remaining female breeders, and of population extinction across a range of ages at first reproduction. 174
Figure E1. Results of a forward simulation grid search examining eventual extinction probabilities for population trajectories with a given population size at 50 years into the projection period.177
Figure F1: Mean and 95% CI of the logit-scale effects of seasonal and annual oceanographic covariate variables on beluga fecundity and adult, older calf, and young calf survival. 181
Figure F2: Mean and 95% CI of the logit-scale effects of annual covariate variables pertaining to proxies for prey availability, forage fish abundance, cumulative impacts, noise, and contaminants on beluga fecundity and adult, older calf, and young calf survival. 182
Figure F3: Mean and 95% CI of the logit-scale effects of seasonal prey-related covariate variables on beluga fecundity and adult, older calf, and young calf survival..... 183
Figure F4: WAIC values for models where each annual covariate for stressor categories was used alone (colored dots) compared to when no covariates were included (interannual random effects only; dotted black line). 183
Figure G1: Posterior mean and 95% credible intervals for time-varying stage-specific adult and calf detection over the study period with median of mean rates represented by the dashed line.185

LIST OF TABLES

Table 3.1: Posterior mean and 95% credible intervals for age- and sex-specific (M = male; F = female) survival and natality (proportion of females with a pup) parameters for the eastern (2000-2018) and western (2011-2018) portions of the wDPS. 71

Table 3.2: WAIC values for models of individuals marked in the eastern (null, random effects only, seasonal full models) and western (null and seasonal full models) portions of the range. ... 71

Table 4.1: Description of scenarios for generating predicted sea surface temperature and North Pacific Gyre Oscillation for examining the effects of environmental variability on population dynamics and viability, with mean and standard deviations of oceanographic predictors 75% smaller or larger than historical conditions. The percentage change represents the average change in population growth rates from the baseline scenario across regions. 111

Table 5.1: Model parameters, priors, and posterior median estimates. 149

Table 5.2. Posterior mean and 95% credible intervals for estimated age structure compared to that expected based on a stable age assumption and observed vital rates. 149

Table 5.3: WAIC values for the null, full, and the random effects-only models. 149

Chapter 1. INTRODUCTION

1.1 BACKGROUND

Understanding the processes driving trends in wildlife populations requires knowledge about population structure, survival, and reproductive success and how these metrics change over space and time. However, sparse monitoring data or persistent knowledge gaps about threats make it difficult to identify the drivers of population dynamics. Population dynamics have primarily been studied by either calculating population growth rates from counts or by constructing matrix models using demographic rate parameters estimated from mark-recapture data. In the first approach, inference is based on information related to state parameters. In the second, inference is based on information related to rate parameters. The former provides little insight into drivers of population dynamics and the latter is often limited to the smaller spatial extent of demographic studies. In neither case is inference based on the totality of information available about a population. Integrated population models (IPMs; Besbeas et al. 2002, Brooks et al. 2004) provide a formal framework for combining multiple data sources with differing spatio-temporal scales for inference on a joint likelihood that can leverage all available information to estimate parameters for which there is no explicit information and result in estimates with improved precision and reduced bias (Schaub et al. 2007, Tavecchia 2009, Abadi et al. 2010a).

In situations where small, depleted populations show continued evidence of decline for unknown reasons, IPMs can improve our understanding of demography, provide fundamental insights into factors that may be limiting recovery, and support conservation decision-making. Though the concept of data integration has been used in fisheries stock assessments since the 1980s (Methot 1990) IPMs are an emerging tool for identifying drivers of wildlife population

dynamics across a range of species and life history traits, including snow geese (Gauthier et al. 2007), shrikes (Schaub et al. 2013), beluga whales (Mosnier et al. 2015), waterfowl (Arnold et al. 2017), and brown bears (Bled et al. 2017), among many others. Researchers have also extended IPMs to estimate parameters for which there are no explicit data, as is often the case for immigration, fecundity, or the survival of unobservable age groups (e.g., Abadi et al. 2010a, Schaub et al. 2010). More recently, IPMs have been employed to examine other complex issues such as source-sink population dynamics (Weegman et al. 2016), synchrony (Schaub et al. 2015, Lahoz-Monfort et al. 2017), spatial dynamics (Chandler & Clark 2014), and the partitioning of mortality across different anthropogenic threats (Veran & Lebreton 2009, Rhodes 2011, Tenan et al. 2012). Several studies have also accounted for the effects of environmental variables and stochasticity on demographic rates and abundance estimates within an IPM framework (Oppel et al. 2014, Cleasby et al. 2017, Abadi et al. 2017).

Though IPMs have proven useful in a variety of applications, methods are still in development and the limitations of IPMs are being scrutinized. IPMs rely not only on the validity of all assumptions in each component likelihood but also on the assumption that the different data sets in the joint likelihood are independent (i.e., inclusion of an individual in one dataset is independent of its probability of inclusion in another data set). While some degree of dependence across data sets may result in negatively biased variance estimates (Abadi et al. 2010b, Goodman et al. 2004), bias in the parameter estimates themselves may arise when one data set dominates another, when sample sizes are small, or for parameters that would be unidentifiable in single likelihood frameworks (Besbeas et al. 2005, Riecke et al. 2019). Uncertainty can also be underestimated when conflicts between IPM likelihoods arise (Goudie et al. 2019, Johnson et al. 2022). Adding to the challenge is the dearth of tools for evaluating goodness-of-fit of the overall

joint likelihood. Recent efforts to use calibrated simulation for goodness-of-fit (Besbeas & Morgan 2014) have not been widely adopted. Instead, applications to date have generally relied on examining the fit of the component models. While the drawbacks may well be outweighed by the benefits of IPMs, they do highlight the importance of evaluating all model assumptions and the need for additional technical development.

1.2 Research Objectives

The overall goals of my research were to leverage the power of data integration within hierarchical Bayesian state-space models to examine the effects of environmental conditions on the demography of three case study species with complex life histories. Namely, I developed a novel nest success model for Pigeon Guillemots (*Cepphus columba*) in Puget Sound, Washington and IPMs for Steller sea lions (*Eumetopias jubatus*) and beluga whales (*Delphinapterus leucas*) in Alaska. These case study species have life history traits that often characterize species that are difficult to monitor, slow to recover from depleted levels, or more vulnerable to anthropogenic threats. In these instances, natural resource managers engaged in conservation can benefit from reliable and precise estimates of demographic rates, as well as an understanding of how environmental conditions affect these rates. Thus, the incorporation of environmental variability into IPM frameworks is a unifying theme throughout this work, ultimately lending insight into ecological drivers of population dynamics and how that information can be useful in resource management decision-making.

Each of these case studies represents a different example of developing and adapting IPM frameworks to maximize the knowledged gained based on the unique life histories, sources of uncertainty, and features of the given monitoring program. First, to estimate reproductive success for Pigeon Guillemots and develop an IPM in future work using data gathered by a community

science program, I developed a novel nest success model that generalizes nest survival models to estimate stage-specific survival and abundance when nest age, state, and fate may be unknown (Chapter 2). Second, to provide new insights into the potential drivers of the divergent abundance trends observed across the range of western Steller sea lions, I developed an IPM integrating mark-resight and aerial survey data to account for female reproductive state uncertainty and examine regional demographic differences (Chapters 3-4). Lastly, I adapted and built upon a newly introduced method of estimating fecundity and age-specific survival using mark-resight observations with uncertain ages (Himes Boor et al. *In revision*) to examine demographic drivers of trends in abundance and viability for Cook Inlet beluga whales (Chapter 5).

1.3 Broader Impacts

Taken together, these three case studies make both methodological and ecological contributions that can improve the quantitative tools and metrics available for recovery planning and other management decision making. Pigeon Guillemots have garnered local interest as a Puget Sound indicator species despite ongoing knowledge gaps about demography underlying observed abundance trends and the relationship between demography and environmental conditions. Despite extensive monitoring and research dedicated to examining the decline of both Cook Inlet belugas and Steller sea lions, factors limiting the recovery of these populations remain poorly understood. The methods and results described here provide new insights into the vital rates of these populations and represent model frameworks that can be applied to other study systems where enhanced information about the effects of environmental and demographic variability can affect population dynamics for species with complex life histories.

1.4 REFERENCES

Abadi, F., Barbraud, C., Gimenez, O. 2017. Integrated population modeling reveals the impact of climate on the survival of juvenile emperor penguins. Global Change Biology 23, 1353–1359. https://doi.org/10.1111/gcb.13538

Abadi, F., Gimenez, O., Arlettaz, R., Schaub, M. 2010a. An assessment of integrated population models: bias, accuracy, and violation of the assumption of independence. Ecology 91, 7–14. https://doi.org/10.1890/08-2235.1

Abadi, F., Gimenez, O., Ullrich, B., Arlettaz, R., Schaub, M. 2010b. Estimation of immigration rate using integrated population models. Journal of Applied Ecology 47, 393–400. https://doi.org/10.1111/j.1365-2664.2010.01789.x

Arnold, T.W., Clark, R.G., Koons, D.N., Schaub, M. 2017. Integrated population models facilitate ecological understanding and improved management decisions. The Journal of Wildlife Management 82, 266–274. https://doi.org/10.1002/jwmg.21404

Besbeas, P., Freeman, S.N., Morgan, B.J.T. 2005. The Potential of Integrated Population Modelling. Australian & New Zealand Journal of Statistics 47, 35–48. https://doi.org/10.1111/j.1467-842X.2005.00370.x

Besbeas, P., Lebreton, J.-D., Morgan, B.J.T. 2002. The efficient integration of abundance and demographic data. Journal of the Royal Statistical Society: Series C (Applied Statistics) 52, 95–102. https://doi.org/10.1111/1467-9876.00391

Besbeas, P., Morgan, B.J.T., 2014. Goodness-of-fit of integrated population models using calibrated simulation. Methods in Ecology and Evolution 5, 1373–1382. https://doi.org/10.1111/2041-210X.12279

Bled, F., Sauer, J., Pardieck, K., Doherty, P., Royle, J.A. 2013. Modeling Trends from North American Breeding Bird Survey Data: A Spatially Explicit Approach. PLOS ONE 8, e81867. https://doi.org/10.1371/journal.pone.0081867

Brooks S.P., King R., Morgan B.J.T. 2004. A Bayesian approach to combining animal abundance and demographic data. Anim Biodiv Conserv 27.1:515–529

Chandler, R.B., Clark, J.D. 2014. Spatially explicit integrated population models. Methods in Ecology and Evolution 5, 1351–1360. https://doi.org/10.1111/2041-210X.12153

Cleasby, I.R., Bodey, T.W., Vigfusdottir, F., McDonald, J.L., McElwaine, G., Mackie, K., Colhoun, K., Bearhop, S. 2017. Climatic conditions produce contrasting influences on

demographic traits in a long-distance Arctic migrant. J Anim Ecol 86, 285–295. https://doi.org/10.1111/1365-2656.12623

Gauthier, G., Besbeas, P., Lebreton, J.-D., Morgan, B.J.T. 2007. Population Growth in Snow Geese: A Modeling Approach Integrating Demographic and Survey Information. Ecology 88, 1420–1429. https://doi.org/10.1890/06-0953

Goodman, D. 2004. Methods for Joint Inference from Multiple Data Sources for Improved Estimates of Population Size and Survival Rates. Marine Mammal Science 20, 401–423. https://doi.org/10.1111/j.1748-7692.2004.tb01169.x

Goudie, R. J., Presanis, A. M., Lunn, D., De Angelis, D., & Wernisch, L. (2019). Joining and splitting models with Markov melding. Bayesian analysis, 14(1), 81.

Johnson, D. S., Brost, B. M., & Hooten, M. B. (2022). Greater than the sum of its parts: Computationally flexible Bayesian hierarchical modeling. Journal of Agricultural, Biological and Environmental Statistics, 27(2), 382-400.

Lahoz-Monfort, J.J., Harris, M.P., Wanless, S., Freeman, S.N., Morgan, B.J.T. 2017. Bringing It All Together: Multi-species Integrated Population Modelling of a Breeding Community. JABES 22, 140–160. https://doi.org/10.1007/s13253-017-0279-4.

Methot, R.D. 1990. Synthesis model: an adaptable framework for analysis of diverse stock assessment data. Int. N. Pac. Fish. Comm. Bull. 50, 259–277.

Mosnier, A., Doniol-Valcroze, T., Gosselin, J.-F., Lesage, V., Measures, L.N., Hammill, M.O. 2015. Insights into processes of population decline using an integrated population model: The case of the St. Lawrence Estuary beluga (Delphinapterus leucas). Ecological Modelling 314, 15–31. https://doi.org/10.1016/j.ecolmodel.2015.07.006

Oppel, S., Hilton, G., Ratcliffe, N., Fenton, C., Daley, J., Gray, G., Vickery, J., Gibbons, D., 2014. Assessing population viability while accounting for demographic and environmental uncertainty. Ecology 95, 1809–1818. https://doi.org/10.1890/13-0733.1

Rhodes, J.R., Ng, C.F., de Villiers, D.L., Preece, H.J., McAlpine, C.A., Possingham, H.P. 2011. Using integrated population modelling to quantify the implications of multiple threatening processes for a rapidly declining population. Biological Conservation, The New Conservation Debate: Beyond Parks vs. People 144, 1081–1088. https://doi.org/10.1016/j.biocon.2010.12.027

Riecke, T.V., Williams, P.J., Behnke, T.L., Gibson, D., Leach, A.G., Sedinger, B.S., Street, P.A., Sedinger, J.S. 2019. Integrated population models: model assumptions and inference. Methods Ecol Evol 2041–210X.13195. https://doi.org/10.1111/2041-210X.13195

Schaub, M., Aebischer, A., Gimenez, O., Berger, S., Arlettaz, R. 2010. Massive immigration balances high anthropogenic mortality in a stable eagle owl population: Lessons for conservation. Biological Conservation 143, 1911–1918. https://doi.org/10.1016/j.biocon.2010.04.047

Schaub, M., Gimenez, O., Sierro, A., Arlettaz, R. 2007. Use of Integrated Modeling to Enhance Estimates of Population Dynamics Obtained from Limited Data. Conservation Biology 21, 945–955. https://doi.org/10.1111/j.1523-1739.2007.00743.x

Schaub, M., Hirschheydt, J. von, Grüebler, M.U. 2015. Differential contribution of demographic rate synchrony to population synchrony in barn swallows. Journal of Animal Ecology 84, 1530–1541. https://doi.org/10.1111/1365-2656.12423

Schaub, M., Jakober, H., Stauber, W. 2013. Strong contribution of immigration to local population regulation: evidence from a migratory passerine. Ecology 94, 1828–1838. https://doi.org/10.1890/12-1395.1

Tavecchia, G., Besbeas, P., Coulson, T., Morgan, B.J.T., Clutton-Brock, T.H. 2009. Estimating Population Size and Hidden Demographic Parameters with State-Space Modeling. The American Naturalist 173, 722–733. https://doi.org/10.1086/598499

Tenan, S., Tavecchia, G., Oro, D., Pradel, R. 2019. Assessing the effect of density on population growth when modeling individual encounter data. Ecology 100, e02595. https://doi.org/10.1002/ecy.2595

Véran, S., Lebreton, J.-D. 2008. The potential of integrated modelling in conservation biology: A case study of the black-footed albatross (*Phoebastria nigripes*). Canadian Journal of Statistics 36, 85–98. https://doi.org/10.1002/cjs.5550360109

Weegman, M.D., Bearhop, S., Fox, A.D., Hilton, G.M., Walsh, A.J., McDonald, J.L., Hodgson, D.J. 2016. Integrated population modelling reveals a perceived source to be a cryptic sink. J Anim Ecol 85, 467–475. https://doi.org/10.1111/1365-2656.12481

Chapter 2. A BAYESIAN STATE-SPACE NEST SURVIVAL AND ABUNDANCE MODEL INCORPORATING BREEDING PHENOLOGY TO ADDRESS UNKNOWN AGE, STATE, OR FATE DATA

Publication history: This study was co-authored with Nathan J. Hostetter, Frances Wood, and Sarah J. Converse. At the time this dissertation was published, this chapter was not in review with a journal.

Abstract: Estimating reproductive success is fundamental to understanding the processes that drive avian population dynamics. Nest success models have traditionally required knowledge of the age and fate of monitored nests, which can be difficult to obtain in studies of wild populations due to imperfect observation processes, cryptic life history traits, and variability in fledging ages. Furthermore, standard methods condition on a subset of nests, precluding direct estimation of population-level reproductive success from nest monitoring data. We developed a multi-event Jolly-Seber model to estimate daily nest survival, the probability a nest produces a chick (i.e., nest success), and the total number of initiated and successful nests in a study area. Our approach extends nest survival models to situations where nest age, state (i.e., egg or chick stage), or fate may be unknown and can directly integrate information on species-specific breeding phenology (e.g., range of hatch and fledge ages) to estimate parameters of interest. The development of this modeling framework was motivated by a study of Pigeon Guillemots (*Cepphus columba*) in Puget Sound, Washington, an indicator species whose inaccessible burrows preclude traditional nest monitoring techniques. Using observations of burrow attendance documented by a community science monitoring program, we estimated daily egg and chick survival rates of 0.996 (95% Credible Interval: 0.989-1.000) and 0.988 (0.973-0.997),

respectively. Average egg incubation and chick rearing periods for successful nests were approximately 31 (29-34) and 37 (35-43) days, respectively. We estimated that 24 (13-33) nests produced at least one fledgling out of 42 (38-49) active nests for a reproductive success rate of 0.58 (0.30-0.78). A simulation study showed that the estimation of nest state transition probabilities degrades with decreasing data quality and quantity; however, the model produces unbiased and precise estimates of nest survival and abundance parameters that are of primary ecological interest. This work extends nest survival modeling techniques, highlights the utility of community science programs, provides the first estimates of Pigeon Guillemot demography in the region, and will ultimately lend insight into the relationship between population dynamics and environmental variability that will be useful for ongoing monitoring and conservation efforts for this ecosystem indicator species.

Keywords: Bayesian state-space model, nest success, Jolly-Seber, data augmentation, community science, Pigeon Guillemot, alcid, seabird

2.1 INTRODUCTION

An understanding of the demographic rates driving the dynamics of wild avian populations can improve the management of these populations. Specifically, knowledge about reproductive success and the productivity of avian populations is fundamental to gaining insights about potential environmental or anthropogenic drivers of population dynamics. However, the known-fate and known-age data that have traditionally been used to estimate nest success rates can be challenging to obtain due to imperfect observation processes. The literature documenting the expansion of nest survival modeling since Mayfield's (1961, 1975) emphasis on daily nest survival has included methods to address uncertainty in nest failure date (Dinsmore et al. 2002, Williams et al. 2002), heterogeneity in survival (Rotella et al. 2004, Royle & Dorazio 2008,

Schmidt et al. 2010), and individual-based and incompletely observed covariates (Nichols et al. 1992, Langrock and King 2013, Converse et al. 2013). Approaches have also been developed to estimate stage-specific survival with uncertainty in nest fate (Walsh et al. 2015) or nest age (Heisey and Nordheim 1995, He et al. 2001, Stanley 2004, Cao et al. 2009). However, taken together, existing approaches generally rely on either known-fate or known-age data to determine nest success. Furthermore, existing methods typically condition on a set of monitored nests, and therefore do not facilitate estimation of overall nest abundance and population-level productivity.

Two existing mark-recapture modeling frameworks offer potential for expanding our capacity to estimate nest abundance and survival: Jolly-Seber models (Jolly 1965, Seber 1965) and multi-event models (Kendall 2004, Pradel 2005). Abundance and nest survival estimation using open mark-recapture models has can be traced back to the methods of Jolly (1965) and Seber (1965), though these models have been adapted for situations when ages are known (Hostetter et al. 2020), when ages are unknown (Pledger et al. 2009, Lyons et al. 2016), and even for nest abundance when age is known (Péron et al. 2014), but have not yet been used to estimate nest abundance when nest age is unknown. Multi-event models were developed to address situations where the state of an individual is not observed perfectly, allowing for the estimation of demographic parameters when observations of individuals (i.e., events) map to multiple true states. Despite their wide applicability and recent use in the estimation of age-specific survival with unknown ages (McCrea et al. 2013, Matechou et al. 2013, Himes Boor et al. *in revision*), multi-event models have not yet been used to address uncertain nest ages, states, or fates in nest survival modeling.

Here we introduce a Bayesian multi-event Jolly-Seber model that extends nest survival modeling and nest abundance estimation to situations where nest age, state, or fate may be unknown. Our novel modeling framework extends existing methods in two ways: (1) by estimating daily nest survival and reproductive success while accounting for uncertainty in nest age, state, and fate through the incorporation of information on breeding phenology, and (2) by estimating nest abundance using an extension of Jolly-Seber mark-resight models with a multi-event observation process. Our approach includes life history-based constraints on nest state transition probabilities and is useful in a variety of situations where nest observations may not give complete or direct information about nest age, state, or fate, such as for species with nests that are inaccessible to observers. We used this model to estimate stage-specific daily nest survival, reproductive success, and nest abundance for Pigeon Guillemots (*Cepphus columba*), an indicator species in Puget Sound, Washington that nests on inaccessible cliffs, preventing direct observations of nest age, state, or fate.

As one of the most abundant seabird species nesting in Puget Sound, Pigeon Guillemots have been designated as a local indicator species, yet little is known about their demography. Our model provides a framework for estimating relationships between environmental factors and reproduction to inform our understanding of how trends in abundance might be indicative of localized changes in ecological processes or available habitat and prey resources for this indicator species. Research suggests that in seabirds, for example, oceanographic variability can impact not only seabird reproductive success, but the timing of nesting activities and overall population dynamics (Aebischer et al. 1990, Weimerskirch et al. 2003, Irons et al. 2008). We introduce this novel modeling framework using observations of Pigeon Guillemot chick provisioning collected through a community science monitoring program (Bishop et al. 2016),

making use of data at a spatio-temporal scale that would otherwise be prohibitively expensive to gather. This work highlights the value of community science initiatives and extends existing methods for the estimation of daily nest survival, reproductive success, and breeder and nest abundance across a wider variety of sampling scenarios, thus improving our understanding of metrics that are essential for the conservation of avian populations.

2.2 METHODS

2.2.1 *Study Species*

Pigeon Guillemots are cliff-nesting alcids (family Alcidae) with a range extending from California to Alaska and into Russia (Sowls 1978). Little is known about their winter habitat or distribution, but beginning in late spring, Pigeon Guillemots concentrate around colonies to nest in cliff burrows (other nesting habitats are used in some locations) along rocky shorelines spanning coastal areas and offshore islands. Nesting pairs typically arrive at the colony to occupy burrow sites several weeks in advance of egg laying, with experienced males arriving a few weeks before females (Robbins et al. 1966). Pigeon Guillemots (particularly experienced breeders) often lay 2-egg clutches where a second "beta" egg is laid ~4 days after the initial egg (Cairns 1987a). Once nests are established, eggs are incubated for an average of 30 days with both sexes tending the nest (Cairns 1987b). Once an egg hatches, adults alternately deliver food until chicks fledge after 35-42 days (Drent 1965, Vermeer 1993b). Fledging is difficult to observe as it generally occurs at night. Chick provisioning rates vary with brood size and change as chicks age, but prey deliveries are often concentrated in the early morning and evening, corresponding with optimal foraging periods and tidal conditions (Ainley & Lewis 1972, Petersen 1981, Vermeer et al. 1993a). Existing information on reproductive success in Pigeon Guillemots is largely limited to naïve estimates from the Farallon Islands, California, where the

nest success rate (i.e., probability a nest produces at least one fledgling) was estimated to be 0.4 (Vermeer et al. 1993b) and from Whidbey Island, Washington, where the nest success rate was estimated to be 0.31 (Kreamer 2011).

2.2.2 *Data*

Approximately 30 Pigeon Guillemot breeding colonies on Whidbey Island, Washington have been monitored through a community science program since 2003 (www.pigeonguillemot.org). Colony sites are located on cliffs that differ in height, length, and aspect, with the average number of active burrows observed per site per year ranging from 1 to 35. Volunteers observe coastal cliff sites from the beach for precisely one hour in the morning once per week during the breeding season, ranging from mid-June to mid-September (Kreamer 2011; Bishop et al. 2016). Volunteers record the number of adults nearshore adjacent to the colony and note visits to cliffside burrows. They also note whether adults have prey in their bill when visiting burrows. Burrow maps are developed to ensure that the burrows can be individually distinguished. Surveys are conducted approximately seven days apart, though the consistency and number of survey weeks vary by site due to logistics of beach access and because nesting activities occur somewhat asynchronously across the island. Surveys extend until at least two weeks without burrow activity have been observed. Data from a single site (Shore Meadows) and a single year (2014) were used here to demonstrate our novel model framework, which included 38 identified burrows observed over 11 weekly survey occasions that occurred from late May through early September. Less than one-third of these burrows were detected with a prey visit on at least one occasion.

2.2.3 *Model framework*

We describe a novel multi-event Jolly-Seber model for nest survival that facilitates estimating daily nest survival, reproductive success, and nest abundance while accounting for uncertainty in nest age, state, and fate through age-based constraints on the probability of transitioning between true states. We used the multi-event model structure because nests with hatchlings can be detected through either (1) prey delivery visits, (2) non-prey visits, or can be (3) undetected during a given observation period. Possible true states *s* in this model are representative of the life history stages of nests, namely nests not yet initiated ($z = 1$), with an egg ($z = 2$), with a hatchling ($z = 3$), fledged ($z = 4$), and not active ($z = 5$).

Following Royle and Dorazio (2008)'s Bayesian superpopulation formulation of a Jolly-Seber model, we used data augmentation to produce a dataset of *M* unique nests in which *n* nests are observed (with $n \leq N < M$, where *N* is the true superpopulation abundance of nests). We introduce a nest-specific inclusion parameter, w_i, with $w_i = 1$ if the nest is part of the superpopulation and $w_i = 0$ otherwise. We model this parameter as

$$w_i \sim \text{Bernoulli}(\psi)$$

where ψ is the probability of a nest ever entering the egg state. For any observed nest, we fix $w_i = 1$.

At occasion 0, all nests start as 'not initiated'. At subsequent occasions *k*, the state of nest *i* is categorically distributed based on the state in the previous occasion with entry, survival, and transition probabilities described by the matrix Θ. Specifically,

$$z_{i,k} \mid z_{i,k-1} \sim \text{categorical}(\Theta[z_{i,k-1}, i, k, 1{:}5])$$

where $\Theta =$

$$\begin{bmatrix} & \text{Not entered} & \text{Egg} & \text{Chick} & \text{Fledged} & \text{Not active} \\ \text{Not entered} & 1-\eta_k^{\text{Lay}} & \eta_k^{\text{Lay}} & 0 & 0 & 0 \\ \text{Egg} & 0 & \phi^{\text{Egg}}(1-\eta_{x_{i,k}}^{\text{Hatch}}) & \phi^{\text{Egg}}\eta_{x_{i,k}}^{\text{Hatch}} & 0 & 1-\phi^{\text{Egg}} \\ \text{Chick} & 0 & 0 & \phi^{\text{Chick}}(1-\eta_{c_{i,k}}^{\text{Fledge}}) & \phi^{\text{Chick}}\eta_{c_{i,k}}^{\text{Fledge}} & 1-\phi^{\text{Chick}} \\ \text{Fledged} & 0 & 0 & 0 & 0 & 1 \\ \text{Not active} & 0 & 0 & 0 & 0 & 1 \end{bmatrix}$$

which formulates nest transitions based on their underlying state-specific survival (ϕ^{state}) and transition probabilities ($\boldsymbol{\eta}^{\text{state}}$) at day *k* (for laying), nest age *x* (for hatching), and chick age *c* (for fledging). Here, η_k^{Lay} represents the probability of entry (egg laying) on day *k* given a nest has not yet entered. During the Egg state, a nest can survive (ϕ^{Egg}) and remain in the Egg state ($1-\eta_x^{\text{Hatch}}$), survive and transition to the Chick state (η_x^{Hatch}; i.e., hatch), or die ($1-\phi^{\text{Egg}}$). Similarly, in the Chick state, a nest can survive (ϕ^{Chick}) and remain in the Chick state ($1-\eta_c^{\text{Fledge}}$), survive and transition to the Fledged state (η_c^{Fledge}; i.e., fledge), or die ($1-\phi^{\text{Chick}}$).

Transitions between states are modeled as categorical processes that are non-zero during the ecologically relevant occasions and zero outside of those periods. Each transition (egg laying, egg hatching, and chick fledging) can have specific restrictions based on species life history (e.g., here laying could only occur on season days 2-47, hatching at nest ages 25-35, and fledging at chick ages 30-50). We modeled transition probabilities as quadratic functions of age-in-stage, given the expectation that laying, hatching, and fledging probabilities are lower at the extremes of the biological values (e.g., chicks are less likely to fledge at 30 or 50 days of chick age than at 40 days). We first specify (using θ to stand in for *k* season day, *x* nest age, or *c* chick age):

$$\eta_\theta^{\text{state}} = \frac{\pi_\theta^{\text{state}}}{(1-\sum_{l=1}^{(\theta-1)}\pi_\theta^{\text{state}})}, \quad \text{for } \theta_{\text{min}}:\theta_{\text{max}}$$

where θ_{min} and θ_{max} represent the minimum and maximum days of year, nest ages, or chick ages where transition probabilities are non-zero, such that transition probabilities $\eta_\theta^{\text{state}}$ describe the

probability of transitioning on θ conditional on having not yet transitioned, following Royle & Dorazio (2008). We then enforce the constraint that $\sum_\theta \pi_\theta^{\text{state}}$ sums to 1.0 over a given transition window, where nests must either transition or fail, using

$$\text{mlogit}(\pi_\theta^{\text{state}}) = \beta_1^{\text{state}}\theta + \beta_2^{\text{state}}\theta^2$$

where β_1^{state} and β_2^{state} are the state-specific parameters describing the quadratic changes in transition probabilities through time based on θ even if these processes are imperfectly observed. Together, the estimation of these multinomial transition probabilities (1) incorporates species-specific ecological process information, (2) allows transitions to occur across a defined range of ages instead of a specific age, and (3) directly quantifies the uncertainty associated with transition ages.

Observations are conditional on the state process and can take a variety of forms (e.g., direct observations of the state or an event linked to the state). For the Pigeon Guillemot case study, we had three observation events. At occasion 1, nests can only be observed with a non-prey visit (observation event 1) or go undetected (3), as all nests enter as eggs, and prey deliveries are only made to nests containing chicks. After occasion 1, observations $y_{i,k}$ conditional on true state *z* are modeled using a categorical distribution with observation probability matrix Ω, which indicates for nest *i* on occasion *k* the probability of observing events 1 or 2 or going undetected given the true state of the nest. The observation probability matrix is composed of burrow detection probability *p* and the multi-event classification probability, α, which represents the probability that a nest with a chick inside is detected via a non-prey visit, given that it is detected. Specifically,

$$y_{i,k} \mid z_{i,k}, w_i \sim \text{categorical}(\Omega[z_{i,k}, i, k, 1{:}3])$$

where Ω =

	Non-prey visit	Prey visit	Not detected
Not entered	0	0	1
Egg	p	0	$1-p$
Chick	$p\alpha$	$p(1-\alpha)$	$1-p$
Fledged	0	0	1
Not active	0	0	1

Summary statistics, such as the proportion of nests that produced a hatchling or fledgling (i.e., nest success) and their uncertainties, can be derived from the latent w_i and $z_{i,k}$ state variables. For example, the proportion of nests that produced a fledgling is the number of nests that ever entered the Fledged state ($w_i z_{i,k} = 4$) divided by the number of nests that ever entered the Egg state ($w_i z_{i,k} = 2$). These values were derived during each MCMC iteration, thus providing a posterior distribution for each metric. This eliminates the need to assign a fixed nest success age (e.g., a nest is successful if it reaches 40 days of age) and instead directly estimates the probability that a nest produced a fledgling without known-fate data. Reducing this model to a conditional-on-capture model to estimate survival and state transitions, but not abundance, could be achieved by simply removing the data augmentation process (w_i) and the associated entry and inclusion parameters (ψ and $\boldsymbol{\eta}^{\text{Lay}}$).

2.2.4 *Simulation analysis*

To assess model performance, we undertook a simulation analysis in which we examined three metrics: relative bias, $\frac{(\bar{e_i}-t)}{t} * 100$, as a measure of whether estimates were systematically over- or under-estimated compared to the true data-generating value, root mean square error (RMSE), $\sqrt{\mathrm{E}[(\bar{e_i}-t)^2]}$, as a combined measure of variance and bias, and credible interval coverage to examine the proportion of intervals containing the true data-generating parameter value. Each of

these were derived for each parameter in models fit to 100 simulated data sets representing different scenarios with varying daily nest detection probability (p = 0.50 versus 0.75), survey frequency (one/wk, three/wk, daily), and levels of nest state uncertainty (α = 0, 0.25, 0.5). Daily egg and chick survival were held constant at 0.98 and the number of nests initiated was set at 50. Our simulated data spanned 10-13 weeks in which surveys could be conducted in a 90-day survey season with nest initiation allowed in the first 1-30 survey days, with an incubation window during nest ages 26-33 days, and a slightly longer fledging window when chicks were 33-42 days old. The number of nests was augmented with a number M - n = 30% of the number of observed nests (n).

2.2.5 *Pigeon Guillemot case study*

In applying this model to the Pigeon Guillemot data, we estimated a constant daily nest detection probability, constant egg and chick survival, and constant multi-event classification probability. This is a simplification of what likely varies over the summer breeding season, but given model complexity, this simplification facilitated estimation of the parameters of interest. We set $L_{\min}$ as May 1 (i.e., no laying prior to May 1). The β_1 and β_2 coefficients representing the effects of nest, egg, and chick ages on the probabilities of daily initiation, hatching, and fledging were estimated using half normal distributions truncated to be positive and negative, respectively, to enforce an increasing and then decreasing daily probability over the course of the transition period. Priors for inclusion, ψ, state classification, α, daily survival, ϕ, were beta-distributed (1,1). Because foraging activities and chick provisioning behaviors have been noted as being influenced by tidal fluctuations (Emms & Verbeek 1991, Vermeer et al. 1993, *F. Wood pers comm*), daily nest detection probability, p, was modeled as a function of a beta(1,1)-distributed intercept and a four-level categorical fixed effect representing time (in minutes) from

the preceding high tide. Time from the preceding high tide was categorized as follows: observations made < 2 hrs from high tide = category 1; between 2-4 hrs = 2; between 4-5.5 hrs = 3; > 5.5 hrs = 4. Tidal data were obtained from near the study site using the `noaaoceans` R package; Warlick 2021. In the case study analysis, to account for nests that may never have been detected, capture histories were augmented with an additional $M - n$ nests equal to 300% of n, the number of nests observed at the colony.

For this analysis, the typical set of Jolly-Seber model assumptions applied. We assumed that there were no nest identification errors, survival and reproductive state of individuals were independent, and that there was no unmodeled heterogeneity in survival and detection probabilities. For both the simulated and real datasets, the model was implemented using the R package Nimble (NIMBLE Development Team 2019), with 40,000 iterations, 25,000 burn-in, thinning rate of 5, three chains, and MCMC chain convergence assessed with $\hat{R}$ values < 1.1.

2.3 RESULTS

2.3.1 *Pigeon Guillemot case study*

Posterior mean daily egg (ϕ^{Egg}) and chick (ϕ^{Chick}) survival rates were 0.996 (95% Credible Interval, CrI: 0.989-1.00) and 0.988 (0.973-0.997), respectively, which equated to an expected 0.89 (0.54-0.97) and 0.65 (0.16-0.82) for egg and chick survival over the average incubation (31 days) and chick rearing (37 days) periods, respectively (Figure 2.1). Stage-specific state transition probabilities were estimated with a high degree of uncertainty, particularly for egg laying, but yielded sensible daily transition probabilities (Figure 2.2).

The posterior mean abundance of initiated nests was 42 (95% CrI: 38-49). The mean abundance of nests with at least one hatchling (N^H) was 38 (35-42) and that with a fledgling (N^F) was 24 (13-33) (Figure 2.3). Hatching success (the proportion of nests that produced at least one

hatchling; $\frac{N^H}{N^L}$) was 0.91 (0.76-1.00) while fledging success (the proportion of nests that produced at least one fledgling; $\frac{N^F}{N^L}$) was 0.58 (0.30-0.78). The multi-event state assignment probability (α) was 0.78 (CI: 0.68-0.87), indicating that nests in the hatchling state were detected with non-prey visits a large proportion of the time. The data augmentation inclusion parameter ψ was sufficiently below 1.0 (mean = 0.37; CI: 0.27-0.47), indicating that the number of encounter histories by which the dataset was augmented was sufficiently large. Daily burrow detection probability was approximately 0.55 but was highest for burrow observations that were closest in time to high tide (Figure 2.4).

2.3.2 *Simulation analysis*

Overall, model performance in terms of both relative bias, RMSE (combined measure of bias and variance), and credible interval (CI) coverage improved with increasing detection, decreasing state uncertainty, and increasing survey frequency. Daily egg and chick survival rates were estimated with little to no bias across all simulation scenarios. In contrast, stage-specific abundance (number of nests with eggs, hatchlings, and fledglings) and nest state transition probabilities were more sensitive to deviations from "ideal" survey conditions, with increasing bias coinciding with decreasing data quality and quantity. Convergence was achieved for all model parameters in more than 90% of 100 simulations for scenarios with either daily or three times weekly surveys.

Daily egg and chick survival were estimated with a high degree of precision and low relative bias across all scenarios (Figure 2.5a, Figure 2.6). Even with low detection (p = 0.5), high state uncertainty (α = 0.5), and low survey frequency (once/wk), mean relative bias in daily egg and chick survival was approximately 0.01% and -0.43%, respectively. Similarly, RMSE for

egg and chick survival was less than 0.01 and mean CI coverage was approximately 94% for both egg and chick survival across all 18 simulation scenarios.

Model performance for the derived abundance metrics varied across scenarios and nest stages. The number of nests with a chick showed low relative bias (<0.1%) across all scenarios except the scenario with highest state uncertainty ($\alpha = 0.5$) and lowest survey frequency (once/wk) and detection ($p = 0.5$), where relative bias was approximately 4% (Figure 1a). However, while relative bias exhibited little to no pattern across levels of detection and state uncertainty, RMSE increased with decreasing detection and survey frequency. For the number of nests that produced at least one fledgling, relative bias was low (-0.1%) across all simulation scenarios. However, RMSE was higher for the number of nests with fledglings compared with the number of nests with hatchlings, with little pattern across levels of detection and state uncertainty.

Stage-based transition probabilities were estimated with varying degrees of bias and precision across the 18 simulation scenarios (Figure 2.5b, Figure 2.6). For nest initiation, relative bias was lower (5-20%) with daily surveys regardless of detection probability and remained low for three/wk survey frequency scenarios with higher detection. Bias increased for three/wk survey frequency scenarios with lower detection, particularly with higher state uncertainty, and increased even more (> 100%) for once/wk survey scenarios, though again was improved at higher detection levels. Increasing levels of state uncertainty only caused high bias when both the survey frequency and detection were low, indicating that state uncertainty alone did not inherently cause more bias. Though relative bias in this parameter was high in poor survey conditions, credible interval coverage was greater than 80% in all scenarios. In contrast to nest initiation transition probabilities, egg hatching and chick fledging transition probabilities were

estimated with lower relative bias across all scenarios. Relative bias increased notably with fewer than daily surveys, with no evident pattern across levels of detection and state uncertainty. It is important to note that though the estimation of these transition probabilities is tenuous under very low levels of detection and survey frequency, this merely over- or under-estimates the timing of the peak of nest transitions within the allowable window, not whether the transition happened. In other words, in cases where the estimation of these daily transition probabilities is biased, it does not affect the estimation of stage-specific abundance, only the timing and nest age phenology of initiation, hatching, and fledging.

Parameters in the observation process (p, α) were estimated with high precision and little to no bias across all simulation scenarios (Figure 2.5c, Figure 2.6). Relative bias in nest detection was low (<1%) and did not exhibit a pattern across levels of state uncertainty, survey frequency, or detection. RMSE did not vary across levels of state certainty but did increase with lower survey frequency. State uncertainty, α, was also estimated with very low bias (<2%), and though the precision of this state assignment parameter decreased with the deterioration of all levels of the observation process (increasing state uncertainty, decreasing detection, and decreasing survey frequency), credible interval coverage was nominal across all scenarios (Figure 2.7).

2.4 Discussion

We developed a novel multi-event Jolly-Seber nest survival model useful for estimating reproductive success and nest abundance in situations when nest age, state, and/or fate may be unknown. We applied this generalized nest survival model to estimate daily nest survival, stage-specific abundance, hatching success, and fledging success for a Pigeon Guillemot colony observed in 2014 on Whidbey Island, Washington, highlighting the usefulness of this framework for this and other cryptic nesting species.

We estimated a daily chick survival rate of 0.988 (0.973-0.997), hatching success of 0.91 (0.76-1.00), fledging success of 0.58 (0.30-0.78), a mean incubation period of 31 (29-34) days, and a mean chick rearing period of 37 (35-43) days. Our estimates were within the range estimated by others, though direct comparison is challenging as previous studies often distinguish between the survival and success rates of "alpha" versus "beta" chicks or 1-egg versus 2-egg nests, while our estimate should be interpreted as the probability that the nest produces at least one egg or chick. Litzow et al. (2002) found that Pigeon Guillemot beta chicks in Alaska had a daily survival rate between 0.971 and 0.998. Our estimates of stage-specific reproductive success were similar to the 0.56-0.87 hatching success and the 0.60-0.74 fledging success reported by McLaren (1991) for Pigeon Guillemots in Oregon.

Knowledge about how environmental conditions affect the demography and population dynamics of avian populations is fundamental to understanding responses to environmental perturbations and whether a species may be an indicator of ecosystem change. Pigeon Guillemots are thought to rely on nearshore, predictably distributed (but potentially lower quality) benthic forage fish species as opposed to (higher quality) pelagic species, allowing them to have higher provisioning rates to support 2-egg clutches (Cairns 1987). Pigeon Guillemot reproductive success in the Farallon Islands was lower in El Niño years (Ainley & Boekelheide 1990) and lower chick growth rates and brood sizes have occurred in years of lower prey abundance in British Columbia and Alaska (Vermeer et al. 1993b). Changing prey availability due to a shift in the Pacific Decadal Oscillation coincided with a notable decline in guillemot abundance in the Bering Sea and Gulf of Alaska in the 1990s (Litzow et al. 2002). Guillemot responses to environmental variability are complex and nuanced (Burger et al. 2004, Irons 2008, Litzow et al. 2004), but one thing is clear: oceanographic conditions matter and can affect everything from

nest initiation and attendance to chick provisioning and fledgling weights (Nelson 1987, Ainley & Boekelheide 1990, Nelson 1991, Golet et al. 2000, Wanless et al 2005). Future expansions of this work to include multiple colonies and years will allow us to directly link reproductive success and breeder abundance to environmental conditions for this Puget Sound indicator species.

Our novel modeling framework generalizes nest survival models and relaxes the requirements for known-age and/or known-fate data, adding to the expansion of model frameworks aimed at estimating nest success since Mayfield (1961, 1975). Though model performance varied across parameters and survey scenarios, simulation results indicated that the model generally produced unbiased estimates of the parameters of ecological interest. Daily egg and chick survival rates were returned with little to no bias and low RMSE even in scenarios with high state uncertainty, low nest detection, and infrequent surveys. The abundance of nests with at least one hatchling showed a small degree of positive bias while that of fledglings was estimated with a small degree of negative bias. The estimation of both of these parameters was strongly affected by survey frequency but not by levels of detection probability or state uncertainty. This is not unexpected, as abundance estimators tend to be relatively sensitive to the quality of the observation process (Link 2003, Grimm et al. 2014, Hickey & Sollmann, 2018). Our simulation results suggest that increasing the number of survey occasions could be more helpful than taking steps to improve daily nest detection or reduce state uncertainty in situations where nest ages and states may be unknown.

While the model framework produced relatively unbiased stage-specific survival and abundances, the estimation of daily transition probabilities was strongly biased, particularly for fledging probabilities with low survey frequency. The bias in these transition probabilities was

ameliorated by increasing the number of survey occasions, but was unaffected by levels of detection probability. It is important to restate that these apparent biases merely over- or under-estimate the timing of the peak of nest transitions, not whether the transition happened, which explains the low bias in stage-specific nest abundances. This framework is therefore very effective for estimating nest survival and nest abundance in a variety of survey situations, but a sufficient number of survey occasions would likely be necessary to robustly estimate the timing of stage-specific transitions. It is therefore unsurprising that the weekly monitoring survey protocol in the Pigeon Guillemot case study was somewhat problematic in applying this model framework to these data. Additionally challenging for the case study dataset were that there were very few surveys during and preceding the egg incubation period, providing little information to inform nest initiation date (which provides an anchoring foundation for subsequent hatching and fledging nest ages), ultimately leading to poor mixing and convergence when fitting the model to the full number of years and colony sites available in the dataset. A final complicating factor in using this model framework for the Pigeon Guillemot case study is the fact that we did not account for this species' ability to lay 2-egg clutches, which added additional uncertainty to the timing of nest state transitions. These issues would not be problematic in the application of this framework to species that lay 1-egg clutches or that are monitored more frequently with surveys beginning well before the start of nesting activity. Future work could examine model performance across different survival probabilities and nest-stage transition windows, as this is directly related to the frequency of survey occasions that would be needed to examine research questions related to nesting phenology.

Though some parameters were sensitive to prior distributions and scenarios with lower data quantity and quality, the novel multi-event Jolly-Seber model presented here advances nest

survival modeling methods and provides unbiased estimates of stage-specific nest survival and abundance even when nest age, state, and fate are unknown. This work highlights the valuable contributions of community science monitoring programs that are generating a growing quantity of information that can be used in ecological modeling and conservation science for this and other cryptic avian species around the world.

2.5 ACKNOWLEDGEMENTS

This work would not have been possible without the dedication and effort of the Guillemot Research Group and their countless volunteers observing Pigeon Guillemots throughout Puget Sound.

2.6 FIGURES & TABLES

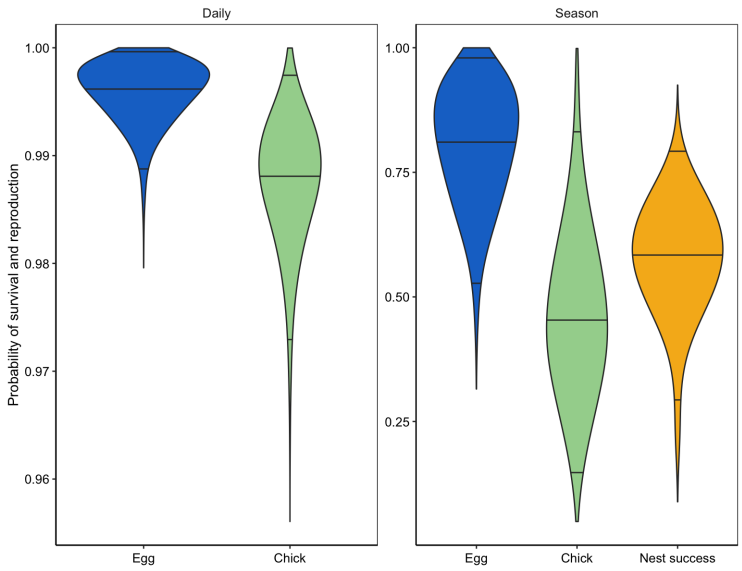

Figure 2.1: Posterior mean and 95% credible intervals for egg and chick survival at a daily level, and reproductive success (probability a nest produces at least one fledgling) and stage-specific survival over the entire breeding season, derived for the latter by raising daily rates to the power of the mean peak transition age for each stage.

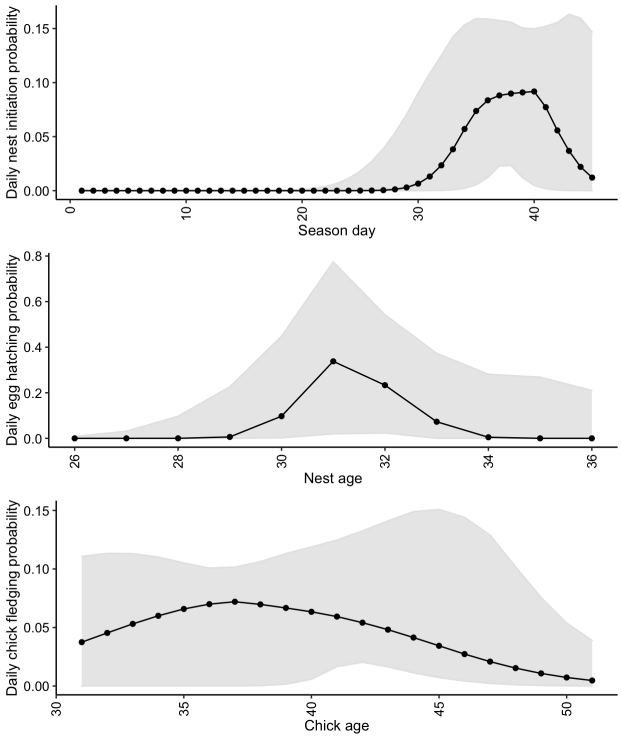

Figure 2.2: Posterior mean and 95% credible intervals for daily nest state transition probabilities for egg laying, egg hatching, and chick fledging by nest and chick age.

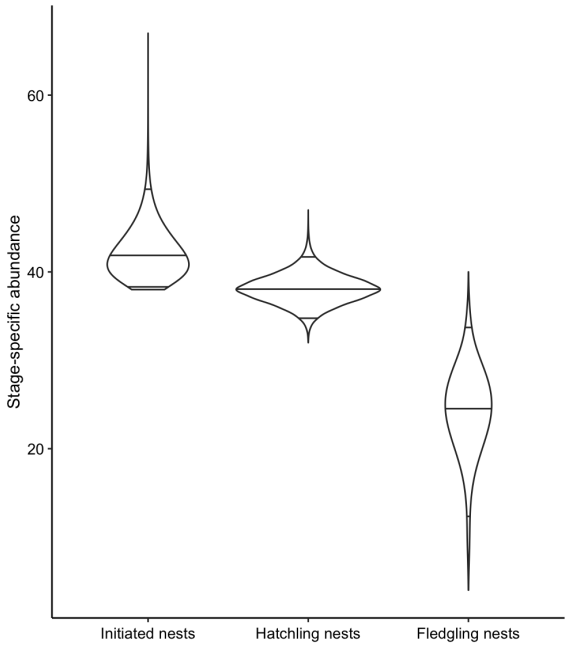

Figure 2.3: Mean and 95% credible intervals for the number of nests with at least one egg, hatchling, and fledging.

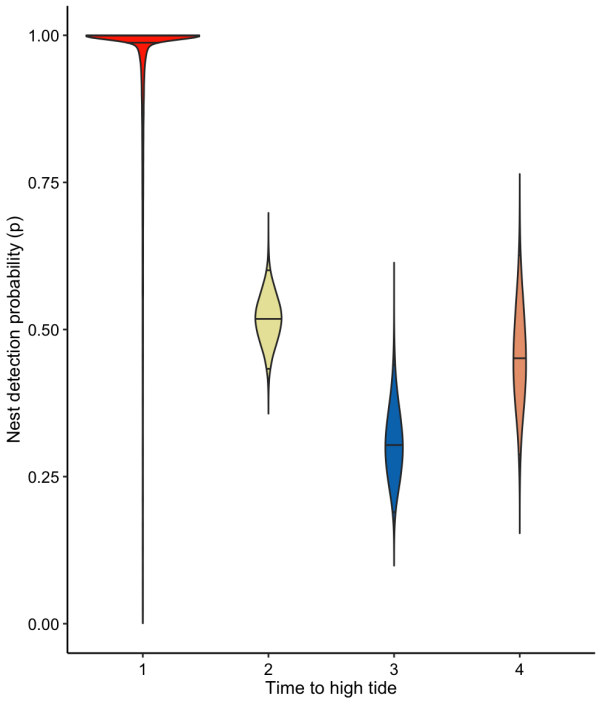

Figure 2.4: Mean and 95% credible intervals for daily burrow detection probability as a function of a categorical representation of the tidal cycle, where 1 represents burrow observations made closest in time to the morning's high tide and 4 represents burrow observations made farthest from the morning's high tide.

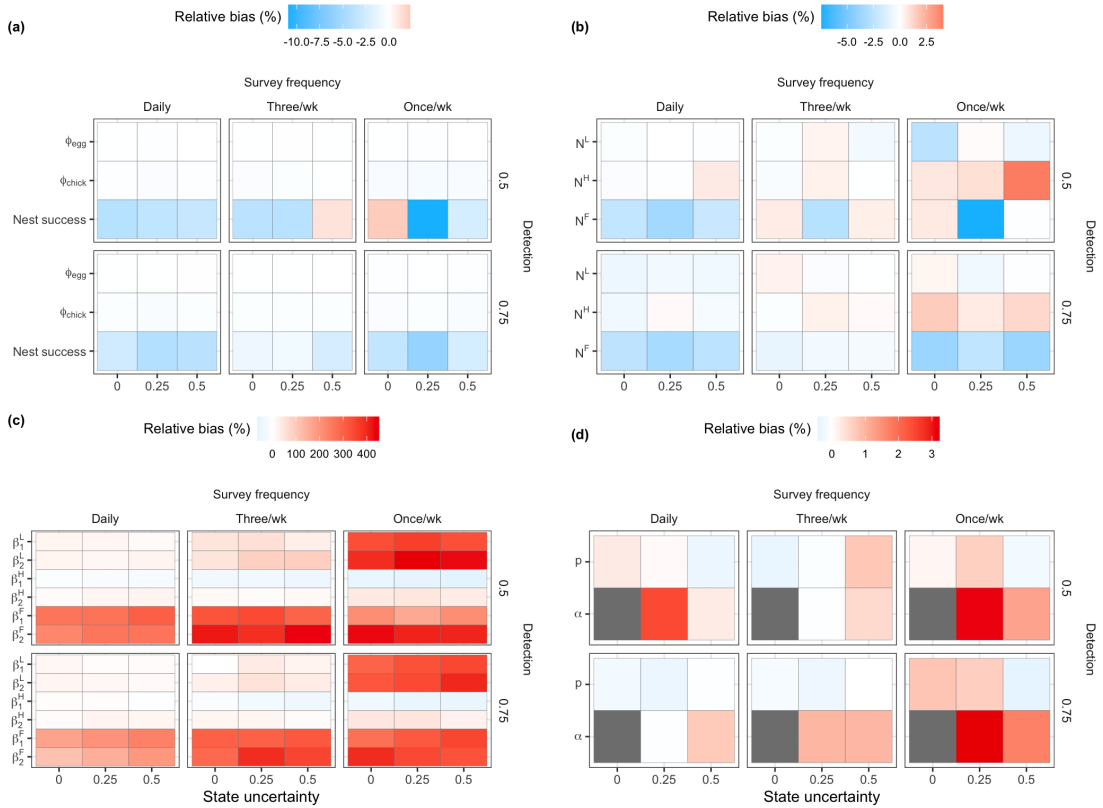

Figure 2.5: Relative bias (%) of (a) egg (ϕ^{Egg}) and chick (ϕ^{Chick}) survival and nest success, (b) number of nests with at least one egg (N^{L}), hatchling (N^{H}), and fledgling (N^{F}), (c) stage-specific nest state transitions governing nest initiation (β_1^{L} and β_2^{L}), egg hatching (β_1^{H} and β_2^{H}), and chick fledging (β_1^{F} and β_2^{F}) and (d) observation process parameters nest detection (p) and state uncertainty (α) across levels of survey frequency (daily, three/week, once/week), nest detection probability (0.5, 0.75), and state uncertainty probability (none, 0.25, 0.5). Color scales are plot specific, but white always denotes 0 bias, while red and blue denote the percent positive and negative bias, respectively. Dark grey indicates where α is set at zero and therefore bias is not calculated.

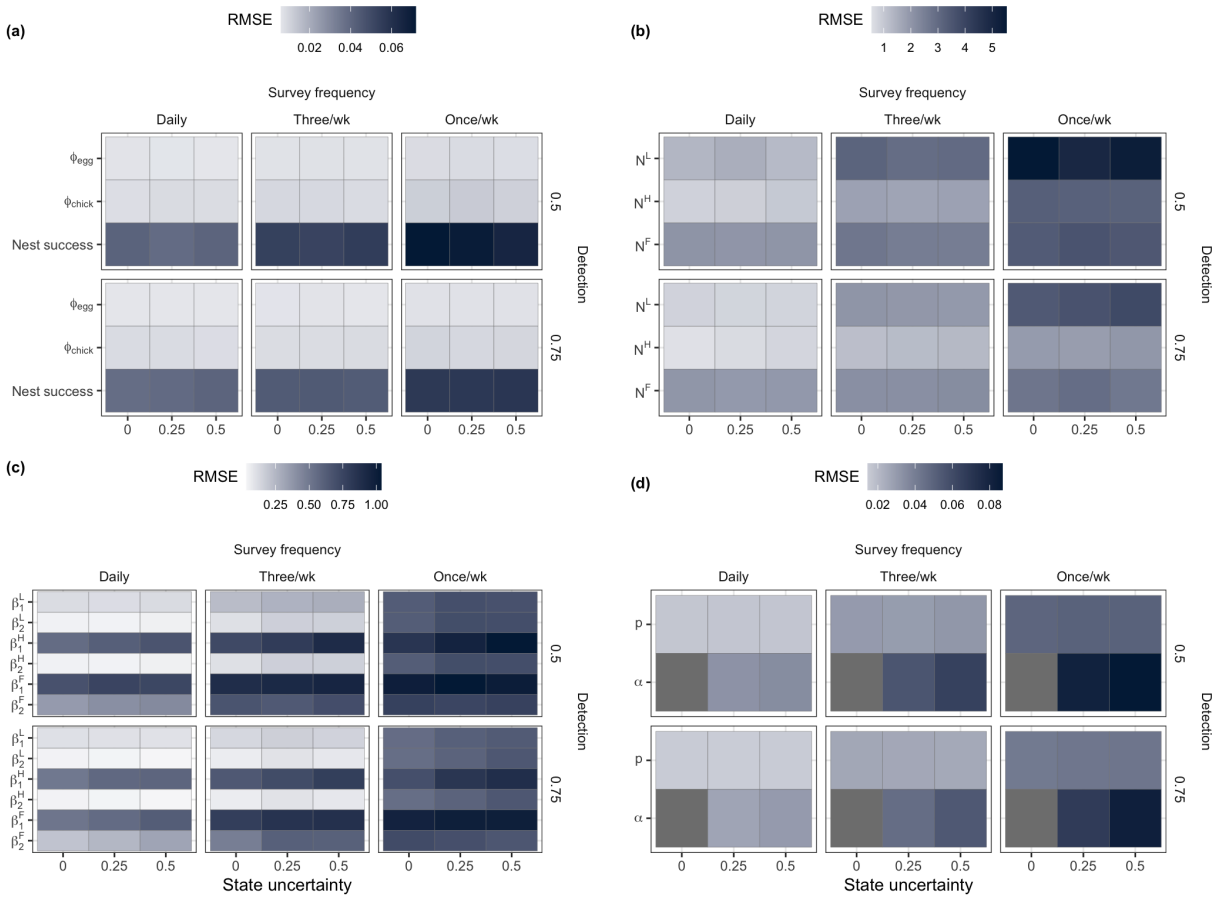

Figure 2.6: Root mean squared error of (a) egg (ϕ^{Egg}) and chick (ϕ^{Chick}) survival and nest success, (b) number of nests with at least one egg (N^L), hatchling (N^H), and fledgling (N^F), (c) stage-specific nest state transitions governing nest initiation (β_1^L and β_2^L), egg hatching (β_1^H and β_2^H), and chick fledging (β_1^F and β_2^F) and (d) observation process parameters nest detection (p) and state uncertainty (α) across levels of survey frequency (daily, three/week, once/week), nest detection probability (0.5, 0.75), and state uncertainty probability (none, 0.25, 0.5). Higher values indicated by darker colors reflect a higher degree of variance and bias. Dark grey indicates where α is set at zero and therefore RMSE is not calculated.

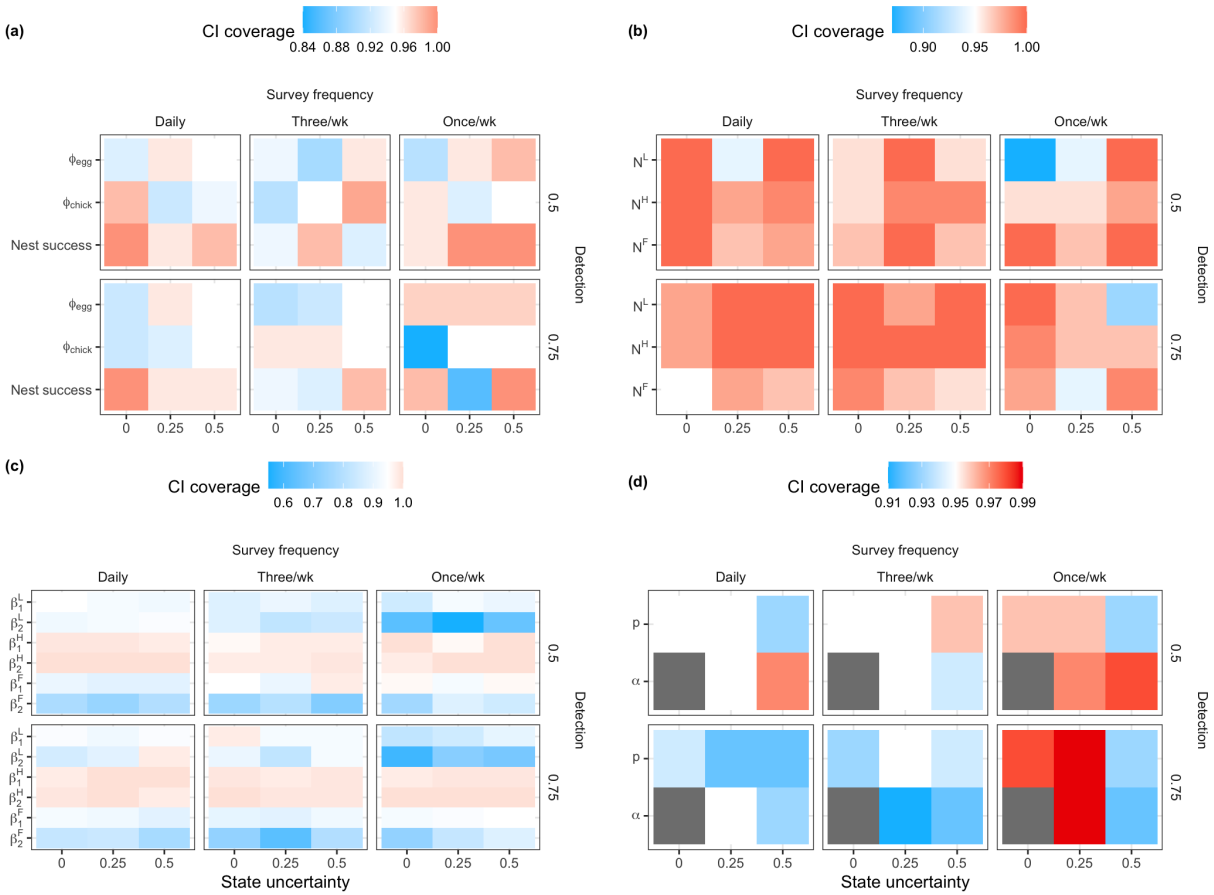

Figure 2.7: Credible interval coverage for (a) egg (ϕ^{Egg}) and chick (ϕ^{Chick}) survival and nest success, (b) number of nests with at least one egg (N^{L}), hatchling (N^{H}), and fledgling (N^{F}), (c) stage-specific nest state transitions governing nest initiation (β_1^L and β_2^L), egg hatching (β_1^H and β_2^H), and chick fledging (β_1^F and β_2^F) and (d) observation process parameters nest detection (p) and state uncertainty (α) across levels of survey frequency (daily, three/week, once/week), nest detection probability (0.5, 0.75), and state uncertainty probability (none, 0.25, 0.5). Color scales are plot specific, but white always denotes 95% coverage, while red and blue imply > 95% and < 95% coverage, respectively. Dark grey indicates where α is set at zero and therefore coverage is not calculated.

2.7 REFERENCES

Aebischer, N.J., Coulson, J.C., Colebrookl, J.M., 1990. Parallel long-term trends across four marine trophic levels and weather. Nature 347, 753–755. https://doi.org/10.1038/347753a0.

Ainley, D.G., T.J. Lewis. 1972. Colony attendance of Farallon Pigeon Guillemots. Pt Reyes Bird Observatory Newsletter 21: 4-5.

Ainley, D.G., R.J. Boekelheide. 1990. Seabirds of the Farallon Islands, Stanford, CA: Stanford University Press.

Bishop, E., Rosling, G., Kind, P., Wood, F., 2016. Pigeon Guillemots on whidbey island, washington: a six-year monitoring study. Northwestern Naturalist 97, 237–245.

Burger, A.E., Hitchcock, C.L., Davoren, G.K., 2004. Spatial aggregations of seabirds and their prey on the continental shelf off SW Vancouver Island. Marine Ecology Progress Series 283, 279–292.

Cairns, D.K., 1987a. Diet and foraging ecology of Black Guillemots in northeastern Hudson Bay. Canadian Journal of Zoology 65, 1257–1263. https://doi.org/10.1139/z87-196

Cairns, D.K., 1987b. The ecology and energetics of chick provisioning by Black Guillemots. The Condor 89, 627–635. https://doi.org/10.2307/1368652

Cao, J., He, C.Z., Wells, K.M.S., Millspaugh, J.J., Ryan, M.R., 2009. Modeling Age and Nest-Specific Survival Using a Hierarchical Bayesian Approach. Biometrics 65, 1052–1062. https://doi.org/10.1111/j.1541-0420.2009.01204.x

Converse, S.J., Royle, J.A., Adler, P.H., Urbanek, R.P., Barzen, J.A., 2013. A hierarchical nest survival model integrating incomplete temporally varying covariates. Ecology and Evolution 3, 4439–4447. https://doi.org/10.1002/ece3.822.

Cormack, R.M., 1964. Estimates of survival from the sighting of marked animals. Biometrika 51, 429–438. https://doi.org/10.2307/2334149

de Valpine, P., D. Turek, C.J. Paciorek, C. Anderson-Bergman, D. Temple Lang, an Bodik. NIMBLE Development Team. 2017. Programming with models: writing statistical algorithms for general model structures with NIMBLE. Journal of Computational and Graphical Statistics 26: 403-413. DOI:10.1080/10618600.2016.1172487.

Dinsmore, S.J., White, G.C., Knopf, F.L., 2002. Advanced Techniques for Modeling Avian Nest Survival. Ecology 83, 3476–3488.

Drent, R.H. 1965. Breeding biology of the Pigeon Guillemot, *Cepphus columba*. Ardea 53: 99-160.

Emms, S.K., Verbeek, N.A.M., 1991. Brood Size, Food Provisioning and Chick Growth in the Pigeon Guillemot Cepphus columba. The Condor 93, 943. https://doi.org/10.2307/3247729

Golet, G.H., Kuletz, K.J., Roby, D.D., Irons, D.B., 2000. Adult prey choice affects chick growth and reproductive success in pigeon guillemots. The Auk 117, 82–91. https://doi.org/10.1642/0004-8038(2000)117[0082:APCACG]2.0.CO;2

Grimm, A., Gruber, B., Henle, K., 2014. Reliability of Different Mark-Recapture Methods for Population Size Estimation Tested against Reference Population Sizes Constructed from Field Data. PLOS ONE 9, e98840. https://doi.org/10.1371/journal.pone.0098840

He, C.Z., Sun, D., Tra, Y., 2001. Bayesian Modeling of Age-Specific Survival in Nesting Studies Under Dirichlet Priors. Biometrics 57, 1059–1066. https://doi.org/10.1111/j.0006-341X.2001.01059.x

Heisey, D. M., and E. V. Nordheim. 1995. Modeling age-specific survival in nesting studies, using a general approach for doubly-censored and truncated data. *Biometrics* 51:51–60.

Hickey, J.R., Sollmann, R., 2018. A new mark-recapture approach for abundance estimation of social species. PLOS ONE 13, e0208726. https://doi.org/10.1371/journal.pone.0208726.

Himes Boor, G., McGuire, T.L., Warlick, A.J., Taylor, R.L., Converse, S.J., McClung, J.R., and A.D. Stephens. *In revision*. Estimating a reproductive rate when offspring ages are uncertain: a novel multievent mark-recapture model applied to an endangered beluga whale population.

Irons, D.B., Anker-Nilssen, T., Gaston, A.J., Byrd, G.V., Falk, K., Gilchrist, G., Hario, M., Hjernquist, M., Krasnov, Y.V., Mosbech, A., Olsen, B., Petersen, A., Reid, J.B., Robertson, G.J., Strøm, H., Wohl, K.D., 2008. Fluctuations in circumpolar seabird populations linked to climate oscillations. Global Change Biology 14, 1455–1463. https://doi.org/10.1111/j.1365-2486.2008.01581.x

Jolly, G.M., 1965. Explicit estimates from capture-recapture data with both death and immigration-stochastic model. *Biometrika* 52, 225-247.

Kreamer, K.A., 2011. Factors affecting the success of Pigeon Guillemots on Whidbey Island, Puget Sound, Washington, during the 2009 breeding season. 49.

Langrock, R., and R. King. 2013. Maximum likelihood estimation of mark-recapture-recovery models in the presence of continuous covariates. *Annals of Applied Statistics* 7(3): 1709-1732.

Link, W.A., 2003. Nonidentifiability of population size from capture-recapture data with heterogeneous detection probabilities. *Biometrics* 59, 1123–1130. https://doi.org/10.1111/j.0006-341x.2003.00129.x

Litzow, M.A., Piatt, J.F., Abookire, A.A., Robards, M.D., 2004. Energy density and variability in abundance of pigeon guillemot prey: support for the quality–variability trade-off hypothesis. *Journal of Animal Ecology* 73, 1149–1156. https://doi.org/10.1111/j.0021-8790.2004.00890.x

Litzow, M.A., Piatt, J.F., Prichard, A.K., Roby, D.D., 2002. Response of pigeon guillemots to variable abundance of high-lipid and low-lipid prey. *Oecologia* 132, 286–295. https://doi.org/10.1007/s00442-002-0945-1

Lyons, J.E., Kendall, W.L., Royle, J.A., Converse, S.J., Andres, B.A., Buchanan, J.B., 2016. Population size and stopover duration estimation using mark-resight data and Bayesian analysis of a superpopulation model: Mark-Resight Data and Superpopulation Model. Biom 72, 262–271. https://doi.org/10.1111/biom.12393.

Mayfield, H. R. 1961. Nesting success calculated from exposure. Wilson Bulletin 73:255–261.

Mayfield, H. R. 1975. Suggestions for calculating nest success. Wilson Bulletin 87:456–466.

Matechou, E., Pledger, S., Efford, M., Morgan, B.J.T., Thomson, D.L., 2013. Estimating age-specific survival when age is unknown: open population capture-recapture models with age structure and heterogeneity. *Methods Ecol Evol* 4, 654–664. https://doi.org/10.1111/2041-210X.12061

McCrea, R. S., B. J. T. Morgan, and D. J. Cole. 2013. Age dependent mixture models for recovery data on animals marked at unknown age. *Journal of the Royal Statistical Society, Series* C, 62(1), 101–113.

Mclaren, E.B., Richard, D., Castenhoiz, W., 1991. Clutch size in Pigeon Guillemots: an experimental manipulation and reproductive success in one and two egg clutches. MS Thesis, University of Oregon.

Nelson, D.A., 1991. Demography of the Pigeon Guillemot on Southeast Farallon Island, California. *The Condor* 93, 765–768. https://doi.org/10.2307/1368213

Nelson, D.A., 1987. Factors Influencing Colony Attendance by Pigeon Guillemots on Southeast Farallon Island, California. *The Condor* 89, 340. https://doi.org/10.2307/1368486

Nichols, J. D., J. R. Sauer, K. H. Pollock, and J. B. Hestbeck. 1992. Estimating transition probabilities for stage-based population projection matrices using capture-recapture data. *Ecology* 93:306–312.

Péron, G., Walker, J., Rotella, J., Hines, J.E., Nichols, J.D., 2014. Estimating nest abundance while accounting for time-to-event processes and imperfect detection. *Ecology* 95, 2548–2557. https://doi.org/10.1890/13-1779.1

Pledger, S., Efford, M., Pollock, K., Collazo, J., Lyons, J., 2009. Stopover Duration Analysis with Departure Probability Dependent on Unknown Time Since Arrival, in: Thomson, D.L., Cooch, E.G., Conroy, M.J. (Eds.), Modeling Demographic Processes In Marked Populations. Springer US, Boston, MA, pp. 349–363. https://doi.org/10.1007/978-0-387-78151-8_15

Pradel, R., 2005. Multievent: An Extension of Multistate Capture–Recapture Models to Uncertain States. *Biometrics* 61, 442–447. https://doi.org/10.1111/j.1541-0420.2005.00318.x

Robbins, C.S., Bruun, B., Zim, H.S., 1966. Birds of North America: a guide to field identification, A Golden field guide. Golden Press, New York.

Rotella JJ, Dinsmore SJ, Shaffer TL. 2004. Modeling nest-survival data: a comparison of recently developed methods that can be implemented in MARK and SAS. *Animal Biodiversity and Conservation* 27(1):187–205.

Royle JA, Dorazio RM. 2008. Hierarchical modeling and inference in ecology: the analysis of data from populations, metapopulations and communities. Academic, San Diego.

Schmidt, J.H., Walker, J.A., Lindberg, M.S., Johnson, D.S., Stephens, S.E., 2010. A General Bayesian Hierarchical Model for Estimating Survival of Nests and Young. *The Auk* 127, 379–386. https://doi.org/10.1525/auk.2009.09015.

Seber, G.A.F. 1965. A note on the multiple recapture census. *Biometrika* 52, 249-259.

Stanley, T. R. 2004. Estimating stage-specific daily survival probabilities of nests when nest age is unknown. *The Auk* 121:134–147.

Vermeer, K., Morgan, K.H., Smith, G.E.J., 1993a. Colony Attendance of Pigeon Guillemots as Related to Tide Height and Time of Day. *Colonial Waterbirds* 16, 1. https://doi.org/10.2307/1521550

Vermeer, K., Morgan, K.H., Smith, G.E.J., 1993b. Nesting Biology and Predation of Pigeon Guillemots in the Queen Charlotte Islands, British Columbia. *Colonial Waterbirds* 16, 119. https://doi.org/10.2307/1521430

Walsh, D.P., Dreitz, V.J., Heisey, D.M., 2015. Integrated survival analysis using an event-time approach in a Bayesian framework. *Ecology and Evolution* 5, 769–780. https://doi.org/10.1002/ece3.1399

Wanless, S., Harris, M., Redman, P., Speakman, J., 2005. Low energy values of fish as a probable cause of a major seabird breeding failure in the North Sea. *Marine Ecology Progress Series* 294, 1–8. https://doi.org/10.3354/meps294001

Weimerskirch, H., Ancel, A., Caloin, M., Zahariev, A., Spagiari, J., Kersten, M., Chastel, O., 2003. Foraging efficiency and adjustment of energy expenditure in a pelagic seabird provisioning its chick. *Journal of Animal Ecology* 72, 500–508. https://doi.org/10.1046/j.1365-2656.2002.00720.x.

Williams BK, Nichols JD, Conroy MJ. Analysis and management of animal populations. San Diego, CA, USA: Academic Press; 2002.

Chapter 3. IDENTIFYING ENVIRONMENTAL DRIVERS OF DEMOGRAPHY AND POTENTIAL FACTORS LIMITING THE RECOVERY OF AN ENDANGERED MARINE TOP PREDATOR

Publication history: This study was co-authored with Devin S. Johnson, Tom S. Gelatt, and Sarah J. Converse. At the time this dissertation was published, a version of this chapter was in review at *Ecosphere*.

Abstract: Understanding what drives changes in wildlife demography is fundamental to the conservation and management of depleted or declining populations, though making inference about the intrinsic and extrinsic factors that influence survival and reproduction remains challenging. Here we use 19 years of mark-resight data from 2000-2018 to examine the effects of environmental variability on age-specific survival and natality for the endangered western distinct population segment (wDPS) of Steller sea lions (*Eumetopias jubatus*) in Alaska, USA. Though this population has been studied extensively over the last four decades, the causes of divergent abundance trends that have been observed across the wDPS range remain unknown. We developed a Bayesian multi-event mark-resight model that accounts for female reproductive state uncertainty. Results indicated that survival rates for male pups (0.44; 0.36-0.53), female yearlings (0.63; 0.49-0.73), and male yearlings (0.62; 0.51-0.71) born in the western portion of the range and estimated here for the first time, were lower than the corresponding values in the eastern portion of the range: male pups (0.69; 0.65-0.74), female yearlings (0.76; 0.71-0.81), and male yearlings (0.71; 0.65-0.78). Additionally, pup mass had a positive effect on pup survival in the eastern portion of the range and a negative effect in the western portion of the range. Local and basin-scale

oceanographic features such as the Aleutian Low, the Arctic Oscillation Index, the North Pacific Gyre Oscillation, chlorophyll concentration, upwelling, and wind in certain seasons were correlated with vital rates. However, drawing strong inferences from these correlations is challenging given that relationships between ocean conditions and an adaptive top predator in a highly dynamic ecosystem are exceedingly complex. This study provides the first demographic rate estimates for the western portion of the population range where abundance estimates continue to decline. These estimates will advance efforts to identify factors driving regionally divergent abundance trends, with implications for population-level responses to future climate variability.

Keywords: Steller sea lion, demography, survival, oceanographic conditions, environmental variability, conservation, mark-resight, hierarchical model, western Distinct Population Segment

3.1 INTRODUCTION

Understanding the complex mechanisms linking environmental conditions to patterns in population dynamics is essential to developing effective conservation and management measures, but remains an ongoing challenge in most situations due to data availability and the complexities of making inferences across differing spatio-temporal scales. This is particularly true for top predators that inhabit vast and heterogenous landscapes, where there is often a mismatch between the ecological question and the data that are available to examine the relevant hypotheses (Conn et al. 2014). Pinnipeds exhibit a range of responses to oceanographic variability, including changes in body condition, reproductive output, maternal attendance patterns, diet, the timing of pupping or weaning, foraging effort, and levels of stranding and mortality (Sterling et al. 2014, Joy et al. 2015, Speakman et al. 2020). While it is important to study these relationships at the scale that is most relevant to the species or ecological process of interest, this is often difficult or impossible to do (Wiens 1989, Mannocci et al. 2017). The

challenge that lies at the crux of this issue is how to scale inference from a small sample of individual behaviors or physiological outcomes to the population level, particularly given that prey and predator responses to biophysical changes may not be consistent in degree or duration across space and time. Our objective with this work was to examine environmental drivers of demography and fill existing knowledge gaps about the spatio-temporal variability of survival and reproduction for the western distinct population segment (wDPS) of Steller sea lions (*Eumetopias jubatus*).

Though the population dynamics of Steller sea lions have been studied extensively, understanding the factors affecting demography is an ongoing area of research. Over the last four decades, researchers have proposed numerous competing hypotheses to explain the precipitous decline of the species during the 1970s and the divergent recovery rates that have been observed across the species' range. Factors that have been examined include nutritional stress (Pascual & Adkison 1994, Trites & Donnelly 2003, Atkinson et al. 2008) and reduced age-specific survival and fecundity (York 1994, Loughlin & York 2000, Holmes et al. 2007). However, existing demographic studies have been conducted at relatively small spatio-temporal scales and have not included the central and western Aleutian Islands, where abundance seemingly continues to decline (Sweeney et al. 2018). Additionally, evaluations of the effects of oceanographic conditions have thus far focused on correlations with trends in abundance rather than demography (Trites et al. 2007, Lander et al. 2013).

Existing research about the impacts of environmental variability on Steller sea lions has largely focused on examining body condition (Calkins et al. 1998), weaning (York et al. 2008), diet (Call & Loughlin 2005, Sinclair et al. 2013), and foraging behavior (Lander et al. 2010, 2011, 2020) spanning oceanographic regime shifts and the heterogenous landscape created by

the Aleutian Island passes. However, even though we have learned that Steller sea lion diet varies by region and over time (Sinclair & Zeppelin 2002, Call & Loughlin 2005, Sinclair et al. 2013), that female body condition and weaning age have varied across oceanographic regimes (Calkins et al. 1998, York et al. 2008), that diet diversity has traditionally been similar (Fritz et al. 2019) or lower (Merrick et al. 1997, Lander et al. 2009) in areas where the population continues to decline, and that sea lions likely use biophysical features of the landscape to locate nearshore prey aggregations (Fadely et al. 2005, Lander et al. 2010, 2011, 2020), these behavioral and physiological findings have not yet been linked to changes in demography.

Based on the assumption that seasonal and interannual variability in certain biophysical features affects the distribution and availability of Steller sea lion prey, we hypothesized that oceanographic features would be correlated with natality and survival of pups and young sea lions. Specifically, basin-scale processes such as the Pacific Decadal Oscillation (PDO), North Pacific Gyre Oscillation (NPGO), and the Aleutian Low (AL) can cause localized changes in sea surface temperature, upwelling, wind, and chlorophyll concentrations, which can affect the level of storminess or the distribution, density, and abundance of forage fish. The availability of prey can in turn affect foraging effort, energetic demands, the timing of weaning, reproductive output, and survival (Antonelis et al. 1997, Trites and Porter 2002, Hastings et al. 2021). On the one hand, sea lions are flexible foragers with numerous target prey species and can therefore likely adapt to both short- and long-term environmental variability (Loughlin et al. 2003). On the other hand, sea lions are central and multiple-central place foragers that rely to a great extent on the predictability of the distribution and quality of prey species near natal rookeries, which can be strongly affected by both static and dynamic oceanographic features (Sinclair & Zeppelin 2002, Raum-Suryan et al. 2004).

In this study, we use mark-resight data from 2000-2018 for the wDPS of Steller sea lions in Alaska to estimate the effects of individual characteristics and oceanographic conditions on age- and sex-specific survival and natality while accounting for uncertainty in reproductive state. This work will improve our ability to make inference about the factors underlying population dynamics by providing estimates of the effects of ocean conditions and comparing age- and sex-specific survival and natality over a greater spatio-temporal scale than has been examined to date. We report the first survival and natality estimates for individuals that breed in the far western Aleutian Islands, where abundance estimates have continued to decline, and provide insights into the links between environmental conditions and the demographic rates that drive abundance of this iconic top predator. Our results can inform conservation and management efforts in light of ongoing and future climatic change.

3.2 METHODS

3.2.1 *Study system*

The wDPS of Steller sea lions in the United States breeds on rookeries west of 144°W, an area that encompasses rookery and haul-out sites in the eastern, central, and western Gulf of Alaska and the eastern, central, and western Aleutian Islands (Figure 3.1). Each year, adult male bulls establish territories beginning in May. Females reach reproductive maturity between the ages of 3 and 6 (Pitcher & Calkins 1981) and arrive at rookeries to give birth from late May to early July depending on the region (Pitcher et al. 2001, Kuhn et al. 2017). At a given rookery, most pups are born within a relatively short time period and nurse throughout the summer. Females make short foraging trips throughout the summer breeding season, before going out to sea with their pups for the fall and winter (Raum-Suryan et al. 2002), during which time their activities can vary depending on environmental conditions and local bathymetric features (Burkanov et al.

2011, Lander et al. 2011). Females exhibit a high degree of natal rookery site fidelity (Pitcher & Calkins 1981), but recent research suggests a greater degree of movement between rookeries and regions within the Aleutian Islands and Gulf of Alaska, likely due to rookery-specific density dependence or prevailing environmental conditions (Fritz et al. 2016, Jemison et al. 2018).

The Aleutian Islands archipelago is a dynamic ecosystem that marks the boundary between the Pacific Ocean and the Bering Sea. The complex biological processes that drive primary production and foraging behavior of upper-level predators in the region are controlled largely by the dramatic bathymetry, hydrography, and biophysical characteristics of the numerous Aleutian passes, where heat exchange, nutrient mixing, and transport occur. While much remains unknown about this large region, researchers agree that the contrasting features to the east and west of Samalga Pass (~170°W) represent a notable ecological boundary (Ladd et al. 2005a). To the east of Samalga Pass, narrow shallow passes are supplied by the warmer waters of the Alaska Coastal Current and are often characterized by high nutrient concentration and productivity that support coastal zooplankton species, a higher diversity of forage fish, and abundant nearshore and piscivorous seabirds. Sea lion genetics and diet composition also differ on either side of Samalga Pass, with diet in the eastern portion of the range being more diverse and dominated largely by walleye pollock (*Gadus chalcogrammus*) (O'Corry-Crowe et al. 2006, Sinclair & Zeppelin 2002, Sinclair et al. 2005). In contrast, to the west of Samalga Pass, deep and wide passes are supplied by colder nutrient-rich waters of the Alaska Stream and are characterized by oceanic zooplankton, a lower diversity of potentially slower-growing forage fish (Hunt & Stabeno 2005), planktivorous seabirds, and a lower-diversity sea lion diet dominated by less densely aggregated Atka mackerel (*Pleurogrammus monopterygius*) (Sinclair et al. 2005, Rand et al. 2019). These generalized patterns likely oversimplify the fine-scale

variability that occurs seasonally, interannually, and across island rookeries (Mordy et al. 2005, Fadely et al. 2005), particularly given the influence of meso-scale habitat features such as eddies (Miller et al. 2005, Lander et al. 2010, Lander et al. 2021) that influence the availability, abundance, and distribution of predators and their prey.

3.2.2 *Sea lion data*

Our study is based on mark-resight data of sea lions that were hot-branded with an individually unique mark, weighed, measured, and released as pups from rookeries in five U.S. regions of the western DPS (n = 2,833). Approximately 13% of individuals were marked at Ulak and Agattu Island rookeries (hereafter, the "western portion of the wDPS range") beginning in 2011 (Agattu Island) and 2013 (Ulak Island), while the majority were marked in the eastern Aleutian Islands and central and eastern Gulf of Alaska (hereafter, the "eastern portion of the range") beginning in 2000 (Figure 3.1). Resightings occurred May through August during dedicated field camps (eastern portion of the range only) and vessel- and land-based surveys, generating a total of approximately 39,300 and 25,150 sighting records of marked females and males, respectively (for more details, see Fritz et al. 2014). Capture histories for individuals marked in the western portion of the range were primarily based on remote camera data, as in Altukhov et al. (2015). Across the range, 41% of marked female pups and 46% of marked male pups were not resighted. Based on the differences in sample size and sampling effort in addition to the biogeographic divide at Samalga Pass and divergent abundance trends noted above, we estimated distinct vital rates for individuals marked in the eastern versus western portions of the range.

In years when females were resighted, they were observed an average of six times. Multiple observations per season were collapsed into annual capture histories by adopting the observation with the greatest certainty in reproductive state (e.g., if a female was observed with a

pup at any point in the season, that status was applied for the whole year). To simplify model structure, we assumed that false positive identifications (pre-breeders or non-breeders observed with pups) did not occur. In order to minimize this error, a female was only recorded as being with a pup if it was observed nursing or very close physical contact with a single pup for a prolonged time (e.g., pup or dependent juvenile and female are sleeping together, or the pair reunite after female returns from foraging).

3.2.3 *Oceanographic data*

We examined metrics associated with both localized oceanographic conditions and basin-scale conditions as potential covariates on demography, assuming these features directly (e.g., storminess) or indirectly (forage fish availability) affect survival and reproduction through several ecological mechanisms. Basin-scale indices included the Arctic Oscillation Index (AOI), Pacific Decadal Oscillation (PDO), the North Pacific Gyre Oscillation (NPGO), and the Aleutian Low (AL). The AOI characterizes Arctic climate patterns, where positive phases represent stronger winds and warmer temperatures in northern latitudes (Higgins et al. 2000). The PDO, which quantifies large-scale, interdecadal variability in sea surface temperature, is associated with warm and cool phases that impact salinity, mixed layer depth, and ocean productivity (Zhang and Levitus 1997, Mantua et al. 1997). The NPGO is associated with patterns in circulation and ocean currents, where positive phases are marked by lower sea surface temperatures and higher salinity, chlorophyll, and nutrients, and is thus often considered a driver of plankton dynamics (Di Lorenzo et al. 2008). The AL is a measure of the strength and position of the atmospheric low-pressure system that persists in the Aleutian Basin during fall through spring each year and is associated with the timing, location, and duration of regional storms (Seckel 1993, Rodionov et al. 2005). Though years with stronger ALs have coincided with

warmer winters, the mechanisms underlying this connection are not well understood (Rodionov et al. 2007). Time series of these variables were obtained at the monthly level from the NOAA National Center for Environmental Information (NOAA NCEI 2020) and NOAA Physical Science Laboratory (NOAA PSL 2020) and applied as a proxy for both the eastern and western portions of the wDPS range.

Localized environmental variables were obtained from satellite reanalysis products and included sea surface temperature (SST; °C), chlorophyll-a concentration (mgm^{-3}), geostrophic meridional (north-south) and zonal (east-west) wind (ms^{-1}), and the Bakun upwelling index ($m^3s^{-1}100m^{-1}$ of coastline). Data for SST and wind were obtained from the Copernicus Marine Environment Monitoring Service (Martin et al. 2019). Monthly composites of chlorophyll-*a* concentration were obtained from Aqua MODIS and SeaWiFS satellite products (NASA 2018) using the NOAA ERDDAP server (Simons 2020). Monthly upwelling anomalies in the Gulf of Alaska (60°N, 149°W) were obtained from the NOAA Pacific Fisheries Environmental Laboratory.

All variables were obtained at monthly levels, aggregated to seasonal means, and converted to *Z*-scores (by subtracting the mean and dividing by the standard deviation) for the respective time series spanning the analyses for the western (2000–2018) and eastern (2011–2018) portions of the range. Sets of seasonal covariate values spanning the summer and fall of year *t* and the winter and spring of year *t*+1 were applied to demographic rates in year *t* to coincide with the seasonal sea lion breeding cycle. Because there is a high degree of uncertainty about age-specific sea lion foraging patterns, separate broad spatial extents were selected as bounding boxes from which to obtain satellite data for individuals marked and resighted in the eastern portion of the wDPS range (46.3°N to 58.1°N and 177.9°W to 159°W) and those in the

western portion of the wDPS range (49.8°N to 55.4°N and 169.9°E to 175.6°E) (Figure 3.1). Pairs of variables with high correlations ($r > 0.5$) were not included in the same model.

3.2.4 *Statistical analyses*

Age- or stage-specific demographic rates in wildlife populations can be estimated using multi-state mark-recapture models (Brownie et al. 1993), where repeated sightings of marked individuals allow inference about the true latent state or ecological process based on a capture history that arises from an observation process with imperfect detection. However, biases can occur when the state of a marked individual is not observed with perfect certainty. Multi-event models (Kendall 2004, Pradel 2005) allow for the estimation of parameters even when observations map to multiple true states and have led to improved parameter estimation compared with the strategy of dropping cases with state uncertainty (Kendall 2004). Multi-event models have been used extensively to assess reproductive status and survival in species with simple life histories, but have been increasingly used to examine vital rates and the effect of oceanographic conditions on demography for species with complex life histories (Fujiwara & Caswell 2002, Fay et al. 2015, Tavecchia et al. 2016, Payo-Payo et al. 2016, Santidrian Tomillo 2017, Sanz-Aguilar et al. 2017, Champagnon et al. 2018, Himes Boor et al. *In revision*). Here we use a multi-event model to account for reproductive state uncertainty, as a nursing female may be seen with or without her pup depending on a variety of circumstances.

3.2.4.1 Ecological process model

True states were defined by an individual's age, sex, and reproductive state. Immature age classes included pups (young of year), age-1 yearlings, age-2 individuals, and juveniles age 3-5 that had not yet entered the breeding population (pre-breeders). Adult states included males ages 6+ and females with pups at age 4, at age 5, and at ages 6+, and reproductively mature females

ages 5+ that did not have a pup in a given year (non-pupping). If a female has not pupped by age 6, she automatically transitions into the non-pupping state (Figure 3.2). The state process model,

$$z_{i,t}|z_{i,t-1} \sim \text{Categorical}(\Omega_{z_{i,t-1},i,t-1})$$

describes the state z of individual i at occasion t, conditional on the individual's state at the previous occasion, modeled as categorically distributed according to transition array Ω, describing the probability of an individual being in state z conditional on its previous state and individual- and time-specific effects. For Steller sea lions, this transition array is decomposed into survival ($\phi_{i,t}$) and pupping probability ($\psi_{i,t}$; the probability of a female that bred in year t having a pup in year t+1 conditional on survival).

Interannual variability in survival and pupping probabilities for individuals marked in the eastern portion of the range were modeled as functions of environmental and individual covariates and random effects of year. That is, for general demographic rate parameter γ,

$$\text{logit}(\gamma_{a,s,t}) = \mu^{\gamma}_{a,s} + \mathbf{x}'\boldsymbol{\beta}^{\gamma}_{a} + \epsilon^{\gamma}_{a,t}$$

where $\mu^{\gamma}_{s,a}$ is an age (a) and sex (s)-specific intercept, $\mathbf{x}$ is a vector of covariates with associated coefficients $\boldsymbol{\beta}^{\gamma}_{a}$, and $\epsilon^{\gamma}_{a,t}$ is an annual (t) random effect. The intercept $\mu^{\gamma}_{a,s}$ for a given demographic rate was estimated using a logit-transformed uniform U(0,1) prior distribution on the probability scale for individuals marked in the eastern portion of the wDPS range. For individuals marked in the western portion of the range where samples sizes were smaller, mean survival rates μ for each sex s for ages pup through age-5 juveniles were estimated using an intrinsic Gaussian conditional autoregressive (CAR) model prior distribution that enforced autocorrelation by age,

$$\mu^{\phi}_{pup:5,s} \sim \text{MVN}(0, \sigma\mathbf{Q})$$

where **Q** is the precision matrix of an intrinsic autoregression or order 2 (IAR(2); Speckman and Sun 2003) scaled by σ. The IAR(2) model imposes a smoothness constraint that estimates two fewer parameters relative to independent age random effects. As with the previous penalized complexity priors, we used $\sigma \sim \text{Exp}(\lambda = 1)$ as a prior for the scaling parameter σ.

To increase parameter estimability and regulate model complexity, we used a penalized complexity approach (Simpson et al. 2017, van Erp et al. 2019) for defining prior distributions on $\boldsymbol{\beta}_{\text{a}}^{\gamma}$ and $\epsilon_{\text{a,t}}^{\gamma}$. Using a penalized complexity prior shrinks the coefficient toward zero in the absence of strong support for a covariate effect. The effect of each univariate covariate *c* (e.g., pup mass x_{i} and oceanographic variable x_{t}) on demographic rate $\gamma_{\text{a,s}}$ was assumed to be drawn from a unique Gaussian distribution as $\beta_{\text{a,c}}^{\gamma} \sim \text{N}(0, \sigma_{a,c})$, with standard deviations distributed according to an exponential distribution with a fixed shrinkage rate $\sigma_{a,c} \sim \text{Exp}(\lambda = 1)$ to apply moderately strong shrinkage. Similarly, random year effects (estimated only for the eastern portion of the wDPS range) were assumed to be drawn from a Gaussian distribution as $\epsilon_{\text{a,t}}^{\gamma} \sim \text{N}(0, \sigma_{\text{a}}^{\gamma})$, with standard deviations $\sigma_{\text{a}}^{\gamma}$ distributed according to an exponential distribution with a fixed shrinkage rate as described above. Age- and sex-specific intercepts were estimated for each demographic rate, but fixed effects of environmental conditions were shared across sexes and only estimated for pup survival (ϕ_{P}), age 1-2 survival ("young", $\phi_{1:2}$), and first-time ($\psi_{3:5}$) and repeat (ψ_{B}) pupping, as we hypothesized that the survival of older individuals was likely to be relatively unaffected by environmental variability due to much larger energy storage capacity and foraging experience. Separate fixed effects were examined for the effect of pup mass for each sex. For survival, correlated random effects were assumed between sexes (except females with pups and adult males) and were also assumed for juvenile individuals ages 3-5 (i.e., year-specific deviations from the mean were modeled in common for these groups). For pupping

probabilities, correlated random effects were assumed for all first-time breeding transitions for age 3-5 individuals ($\psi_{3:5}$).

Age-specific natality (*f*, the number of offspring produced per female ages 4, 5, and 6+ in a given year, assuming only singleton births and different than pupping probability, which is a state transition probability) was calculated by taking the proportion of each female age class that had a pup at a given occasion according to the true *z* state. For the eastern portion of the range, age-specific and overall natality (proportion of females pupping in a given year) were calculated beginning in the 7th study year to allow for more than one marked cohort to have reached reproductive maturity. Due to the shorter study period and the biennial branding schedule in the western portion of the range, natality was calculated beginning in just the 4th year when at least one marked cohort had reached reproductive maturity.

3.2.4.2 Observation process model

Possible observations for adult females included being seen without a pup, seen with a pup, or not detected. These observations, combined with knowledge of an individual's age, define the events in the multi-event model,

$$y_{i,t}|z_{i,t} \sim \text{Categorical}(\Theta_{z_{i,t}i,t})$$

where an observation $y_{i,t}$ conditional on the true state $z_{i,t}$ is categorically distributed with probability array Θ. Components of detection probability for individual *i* at time *t* include the probability of detection, $p_{i,t}$, and the probability of correctly ascertaining the presence of a pup for breeders, $\delta_{i,t}$. Similar to demographic rates, detection probability was modeled as:

$$\text{logit}(p_{a,s}) = \mu_{a,s}^{p} + \beta^{p} + \epsilon_{t}^{p}$$

where the mean intercept $\mu^{p}_{a,s}$ for each sex *s* and age *a* was estimated using a logit-transformed prior that was uniform U(0,1) on the probability scale. For individuals marked in the eastern portion of the range, a categorical fixed effect parameter was included to account for markedly lower resight survey effort in three years during the study period (2006, 2017, 2018), where $\beta^{p} \sim \text{normal}(0,0.001)$ is drawn from a Gaussian distribution. Interannual variability in detection probability was estimated for the eastern portion of the range with random year effects assumed to be drawn from a Gaussian distribution as $\epsilon^{p}_{t} \sim \text{normal}(0, \sigma_p)$, with standard deviations σ_p estimated with shrinkage priors, distributed according to an exponential distribution with a fixed shrinkage rate as described above. We expected that the probability of correctly ascertaining whether a female had a pup would be a function of the number of times a female was seen in a season, and so we used the number of sightings per individual per year (with pups or without) as a categorical covariate for the multi-event classification probability parameter, $\delta_{i,t}$.

3.2.4.3 Variable and model selection

To reduce the number of covariates to a reasonable number with which to use shrinkage priors as a variable selection technique, we eliminated covariates that were not supported based on a comparison between Watanabe-Akaike information criterion (WAIC; Watanabe 2010) values of the null model versus models where each environmental variable was used as the sole covariate. We further eliminated some variables that did improve model fit based on WAIC values in order to avoid using strongly correlated covariates in the same model. For demographic models for individuals marked in the eastern portion of the range, this process of elimination left the AL, AOI, NPGO, upwelling, northward wind, and chlorophyll concentration for use in the "full" model. For the western portion of the range, the AOI, NPGO, upwelling, and northward wind were retained in the full model.

Once the final set of environmental covariates was determined, we used WAIC to compare the null model, an interannual random effects-only model (no environmental covariates), and a set of full models (interannual random effects, pup body mass, and season-specific environmental covariates). Season-specific environmental covariates were examined together (i.e., all covariates were from the same season in each model run) due to the infeasibility of examining all possible combinations of the four seasonal values of each environmental covariate. We summarized the results of the full model according to the proportion of MCMC chain sample estimates for the environmental effects that was above versus below zero.

3.2.4.4 Model fitting

Models were fit using NIMBLE (NIMBLE Development Team 2019) within the R programming environment (R Core Development 2022) using 20,000-40,000 iterations and 10,000-20,000 burn-in depending on the model, a thinning rate of 2, and an adaptation rate of 10. We evaluated model convergence using visual inspection of chains and the Brooks-Gelman-Rubin statistic (Gelman & Rubin 1992; Brooks & Roberts 1998) $\hat{R} < 1.1$. After fitting full models, we evaluated goodness-of-fit using Bayesian *p*-values, where we compared the number of observed versus predicted resightings of individuals by age at each occasion, and there were no indications of problematic lack of fit. The typical set of mark-recapture model assumptions applied in this study, where it was assumed that branding did not affect detection probability, survival and the reproductive state of individuals were independent, there were no identification errors, mortality during the sampling season was negligible, and there was no unmodeled heterogeneity in survival and detection probabilities.

3.3 RESULTS

3.3.1 *Demography*

3.3.1.1 Survival

Mean pup survival from 2000-2018 in the eastern portion of the wDPS range was 0.71 (95% credible interval = 0.67-0.76) and 0.69 (0.65-0.74) for females and males, respectively. Survival increased with age for both sexes, though survival for age-2 females (0.88; 0.82-0.92) was notably higher than that of age-2 males (0.76; 0.69-0.82; Figure 3.3, Table 3.1). Survival for females with a pup (0.94; 0.92-0.96) was higher than non-pupping females (0.83; 0.75-0.91; Figure 3.3, Table 3.1). Survival for individuals marked in the eastern portion of the range was most variable over years for pups, age-1, and age-2 individuals (Figure 3.4a). Mean annual male and female pup survival over the study period ranged from 0.31 to 0.95. Juvenile and pupping adult female survival remained relatively constant throughout the study period.

Age- and sex-specific survival rates for the western portion of the wDPS range from 2011-2018 had higher uncertainty than in the eastern portion of the wDPS range due to the smaller sample size. While female pup survival was similar to that in the east, male pup survival was 0.44 (0.36-0.53), which was significantly lower than that in the eastern portion of the wDPS range (Figure 3.3, Table 3.1). Additionally, female survival for age-1 through pre-breeding age groups (age-3 to age-5) was notably lower compared to that of individuals marked in the eastern portion of the wDPS range. Estimates were similar between the eastern and western portions of the range for adult males and females.

3.3.1.2 Pupping and natality

For the eastern portion of the wDPS range, the probability of first-time pupping was highest for age-5 individuals (i.e., giving birth for the first time at age 5; ψ_4) at 0.72 (0.62-0.8) and much lower for age-6 individuals (ψ_5) at 0.16 (0.01-0.38) and age-4 individuals (ψ_3) at 0.13 (0.08-0.21) (Figure 3.3, Table 3.1). The probability of females with a young of year also pupping in the following year (ψ_B) was high (0.98; 0.96-0.99) and remained relatively constant throughout the study period. The probability of pupping for females that had not given birth in the previous year (ψ_{NB}) was low (0.08; 0.03-0.16) and remained relatively low over the study period, with the exception of 2006-2007. Though estimated with a relatively high degree of uncertainty, the temporal standard deviation in pupping probabilities for first-time breeders was relatively high ($\sigma_{\psi_{PB}} = 1.26$), reflecting rates that fluctuated substantially throughout the study period (Figure 3.4b). Mean age-specific natality (calculated from the 7th year onward) was low for age-4 individuals (0.13; 0.04-0.28) and much higher for age-5 (0.81; 0.7-0.9). Overall natality (*f*, proportion of breeding-age females with a pup each year) was calculated as approximately 0.8 (0.74-0.84) in the last few years of the study period (Table 3.1).

For the western portion of the wDPS range, age-specific pupping probabilities mirrored that in the eastern portion (higher probability for age-5 individuals and existing breeders), though the mean probability of repeat pupping (ψ_B) was slightly lower and credible intervals were much wider due to the smaller sample size (only two marked cohorts had reached reproductive maturity by the end of the study, which covered fewer years compared to that in the eastern portion of the wDPS range; Figure 3.3). Mean age-specific natality (calculated from the 4th year onward) was 0.38 (0.12-0.89) for age-4 individuals and 0.76 (0.49-1) for age-5 individuals. Natality for age-6+ in the western portion of the wDPS range only included a single cohort and is

therefore not directly comparable to natality estimated for the eastern portion of the range. Overall natality for the study period was approximately 0.69 (0.47-0.96; Table 3.1). Time-varying demographic rates were not examined for individuals marked in the western portion of the range due to fewer marked individuals resighted over fewer occasions.

3.3.2 *Detection*

Detection probability increased with age for both males and females (Figure 3.5). Of note is that resightings in the western portion of the range are the product of both opportunistic observations and remote cameras, and though less certain, mean age- and sex-specific detection probabilities were higher than those estimated from rookery-based field camps in the eastern portion of the range. The probability of correctly identifying females as having a pup ($\delta_{i,t}$) increased with resighting frequency, ranging from 0.41 (0.38-0.45) for individuals resighted once or twice per year to 0.71 (0.68-0.75) for those resighted more than nine times.

3.3.3 *Individual and oceanographic covariates*

The effect of individual characteristics and environmental conditions ($\beta_{c,a}$) are reported on the logit scale, where values above zero indicate a positive correlation and values below zero a negative correlation. We report both the logit-scale value of $\beta_{c,a}$, which indicates the strength of the correlation, and the proportion of MCMC samples that were above or below zero ($p(\beta_{c,a} > 0)$), which indicates the probability that the correlation was positive versus negative. In general, the uncertainty around coefficient effects increased with the addition of random effects for vital rates and detection probabilities.

For individuals marked in the eastern portion of the wDPS range, pup mass had a positive effect on pup survival (ϕ_P) for both females ($\beta = 0.18$; 0, 0.37; $p(\beta > 0 = 0.98)$) and males ($\beta =$

0.29; 0.12, 0.48; p($\beta > 0 = 1$)), and young females age-1 to age-2 ($\phi_{1:2}$) as well (β = 0.07; -0.06, 0.25; p($\beta > 0$) = 0.82) (Figure 3.6). However, for individuals marked in the western portion of the range, pup mass had a negative effect on male pup survival (β = -0.26; -0.59, 0.02; p($\beta < 0$) = 0.95) and age 1-2 survival (β = -0.14; -0.66, 0.17; p($\beta < 0$) = 0.78). Uncertainty in the estimates for the effect of pup mass on these various demographic rates is much greater for individuals marked in the western portion of the range. We did not detect an effect of pup mass on that same female's probability of first-time pupping ($\psi_{3:5}$; Figure 3.6).

For the eastern portion of the range, the full model included the AL, AOI, NPGO, chlorophyll concentration, meridional winds, and upwelling. With the exception of upwelling, season-specific variables largely had a positive effect on the survival of pups (ϕ_P) that did not extend to individuals age 1-2 (Figure 3.6). More specifically, pup survival was positively correlated with positive-phase AL in the spring (β = 0.46; 0.04, 0.84; p($\beta > 0$) = 0.99), positive-phase AOI in the summer (β = 0.37; -0.22, 1.04; p($\beta > 0$) = 0.87) and positive-phase NPGO in the summer (β = 0.17; -0.17, 0.82; p($\beta > 0$) = 0.81) and fall (β = 0.31; -0.09, 0.76; p($\beta > 0$) = 0.91) (Figure 3.6). In terms of more localized conditions, pup survival was positively correlated with chlorophyll concentration during the winter (β = 0.45; 0.11, 0.73; p($\beta > 0$) = 0.99) and spring (β = 0.05; -0.19, 0.49; p($\beta > 0$) = 0.68) and negatively correlated with increased upwelling, particularly in the fall (β = -0.45; -1.13, 0.15; p($\beta < 0$) = 0.91) and winter (β = -0.68; -1.15, 0.07; p($\beta < 0$) = 0.99). In terms of reproduction, first-time pupping probability was positively correlated with summer positive-phase NPGO (β = 0.61; -0.02, 1.23; p($\beta > 0$) = 0.97) and increased summer upwelling (β = 0.31; -0.29, 1.05; p($\beta > 0$) = 0.84) and negatively correlated with stronger summer wind (β = -0.9; -1.6, 0.16; p($\beta < 0$) = 0.99). Repeat pupping

probability was positively correlated with chlorophyll concentrations in the fall ($\beta = 0.78$; -0.1, 2.05; $p(\beta > 0) = 0.93$), but showed little to no correlations with other environmental covariates.

For the western portion of the range, oceanographic variables included in the full model included the AOI, NPGO, wind, and upwelling, though their effects on pup and age 1-2 survival were estimated with less precision due to the smaller sample size (Figure 3.6). Some environmental effects were similar to those estimated for individuals marked in the eastern portion of the range, however, a notable difference was that the effects were evident not for pup survival, but for age 1-2 survival ($\phi_{1:2}$). Specifically, positive-phase AOI in the fall ($\beta = 0.84$; -0.12, 2.15; $p(\beta > 0) = 0.92$) and positive-phase NPGO in the fall ($\beta = 1.27$; 0.23, 2.2; $p(\beta > 0) = 0.99$), winter ($\beta = 0.89$; 0.01, 1.92; $p(\beta > 0) = 0.98$), and spring ($\beta = 1.25$; 0.48, 2.03; $p(\beta > 0) = 1$) exhibited strong evidence of a positive effect on age 1-2 survival. Stronger summer upwelling exhibited a positive correlation with age 1-2 survival ($\beta = 0.5$; -0.19, 1.4; $p(\beta > 0) = 0.9$) while stronger winds in spring and summer were correlated with lower survival rates. Environmental covariates were not included in the estimation of pupping probability for individuals marked in the western portion of the range due to the low sample size of reproductively mature individuals.

3.3.4 *Model selection and evaluation*

For the eastern portion of the range, both the models with time-varying demographic rates and the full seasonal models performed better than the null model in terms of lower WAIC values (Table 3.2). Much of the improvement in the full models compared with the null model ($\Delta_{WAIC} = 310$) was attributable to the addition of random effects ($\Delta_{WAIC} = 8.7$), with much smaller but meaningful improvements with the addition of individual and environmental covariates (Table 3.2). The best-fit model was the full model that included environmental covariates from the

winter season followed by the model that included covariates from the summer (Δ_{WAIC} = 9.3). A consequence of the larger number of covariates accommodated by the penalized complexity shrinkage priors is that it is more challenging to attribute the improvement in model fit to a specific environmental variable. To elucidate the effects of each season-specific environmental covariate, we examined WAIC values for models where each covariate was used alone. This revealed that upwelling and the Aleutian Low during winter and summer, the NPGO during the spring, and chlorophyll concentration over the entire non-breeding season explained the most variability when included alone (Appendix A).

For demographic estimates in the western portion of the range, all full seasonal models performed better than the null model (Table 3.2). The best-fit model included covariates from the spring, followed closely by the model that included environmental variables from the fall season (Δ_{WAIC} = 2.1). Similar to above, an examination of model fit with only one environmental covariate included at a time showed that these improvements in WAIC value could be attributed largely to the effect of spring and fall NPGO on age 1-2 survival, which in fact had the lowest WAIC value when included alone (Supplemental information).

3.4 Discussion

We used mark-resight data to estimate survival and natality and the effects of pup weight and oceanographic conditions for the wDPS of Steller sea lions in Alaska. This study provides the first demographic rate estimates for individuals marked in the western and central Aleutians where abundance continues to decline (Sweeney et al. 2018) and the first instance of examining correlations between environmental conditions and vital rates, providing insights into potential drivers of population dynamics for this population.

3.4.1 *Demography*

3.4.1.1 Regional comparisons

Researchers have hypothesized that the historical and ongoing decline in counts at rookeries in the western portion of the wDPS range may be due to a combination of demographic or environmental factors (Loughlin & York 2000, Holmes et al. 2007). With this study, we aimed to explore variation in age- and sex-specific vital rates to improve ecological understanding that can inform future management and recovery actions under the Endangered Species Act. In general, survival rates estimated in this study for the eastern portion of the wDPS range were similar to (or higher than) previous estimates (York 1994, Pendleton et al. 2006, Fritz et al. 2014, Maniscalco et al. 2015) and those estimated for the eastern DPS (Hastings et al. 2011, 2021, Wright et al. 2017). However, survival rates for the western portion of the wDPS range (western and central Aleutian Islands) estimated here for the first time are notably lower than those in the eastern portion of the range, particularly for male pups, yearlings of both sexes, and juvenile females ages 2-5. Survival estimates for individuals age 0-3 in the Asian stock of Steller sea lions in the Russian Far East (geographically closer to the western Aleutian Islands than other rookeries in the wDPS) ranged from approximately 0.6 to 0.8 (Altukhov et al. 2015), much higher than reported here. Though it is difficult to compare our natality estimates to previous studies that relied on proportions of observed breeders in aerial surveys, overall natality for the eastern portion of the wDPS range was similar to estimates from the late 2000s in the eastern Gulf of Alaska (Maniscalco et al. 2010, 2014) and those observed in stable or increasing pinniped populations (McKenzie et al. 2005, Lunn et al. 1994). In contrast, natality in the western portion of the wDPS range was lower. Though both survival and natality estimates for the western portion of the range had greater uncertainty compared to those for the eastern portion

of the range, the differences are striking and could be limiting population growth. Additional years of data will reduce the uncertainty in adult survival and natality estimates, which will round out our understanding of the intrinsic factors limiting recovery, as those vital rates are often the dominant drivers of population dynamics for long-lived species (Heppell et al. 2000).

3.4.1.2 Age- and sex-specific comparisons

Examining patterns in age- and sex-specific survival rates can lend insight into life history trade-offs, habitat conditions and prey availability, and reproductive fitness. Age-specific survival generally increased with age from pups to adults for both males and females, as expected for long-lived mammals according to the demographic buffering hypothesis (Gaillard et al. 1998, Pfister 1998, Eberhardt 2002, Rotella et al. 2012) and similar to previous studies of this species (Maniscalco et al. 2010, Hastings et al. 2011, 2018, Altukhov et al. 2015, Wright et al. 2017). However, this pattern was not uniformly observed for both sexes in each region. For males in the eastern portion of the range and females in the western portion of the range, a small drop was observed in survival for ages 1-2 compared to pups, as previously observed (Pendleton et al. 2006, Fritz et al. 2014, Maniscalco et al. 2014, Altukhov et al. 2015). The effect of pup mass was also different across sexes and regions, with a positive correlation in the eastern portion of the range versus a negative correlation (particularly pronounced for males) in the west. Taken together, these patterns in age-specific survival and the respective effects of pup mass likely stem from differential maternal investment strategies and age-at-weaning across the range.

Our results indicated that heavier pups had a higher probability of survival in their first year in the eastern portion of the range and a lower probability in the west, the effects of which were not strongly evident past the first year. Larger pups might be able to forage more effectively (if they were still larger when independent foraging begins) or might be born earlier

or to larger, more experienced females. Several authors have found this positive association between pup mass and first-year survival for the eastern DPS (Hastings et al. 2011, Maniscalco 2014, Wright et al. 2017) and for other pinniped species around the world, particularly fur seals (Boltnev et al. 1998) and Weddell seals (Hadley et al. 2007, Proffitt et al. 2010). However, females can compensate for smaller pup size by increasing maternal investment and/or weaning later (Trillmich 1990, Lee et al. 1991), providing support for the assertion that maternal care influences first-year survival more than birth mass for otariids (Boyd 1990, McMahon & Hindell 2003). Hastings et al. (2021) found that in certain rookeries in both the eastern and western DPSs, earlier weaned yearlings had a lower probability of survival, that heavier pups were more likely to wean by one year of age, and that pup body mass had a positive effect on survival. In applying these concepts to our findings, it is possible that larger pups in the western portion of the range incur a larger burden on lactating females (as was found in South American sea lions who foraged longer for heavier pups; Drago et al. 2021) and may habitually be weaned sooner and therefore ultimately experience lower survival rates despite their larger size. With additional years of data, a closer examination of the region-specific life history strategies for breeding females could lend insight into the trade-offs inherent in maximizing reproductive fitness given prevailing environmental conditions and physiological constraints.

3.4.2 *Oceanographic effects*

We examined numerous local and basin-scale oceanographic indices to identify potential correlations between environmental features and demography based on the hypothesis that these dynamic biophysical conditions either directly (e.g., through increased storminess) or indirectly (e.g., bottom-up forcing mechanisms that affect the quality, quantity, or distribution of prey species) impact survival and natality. Oceanographic conditions are known to influence many

aspects of foraging, health, maternal investment, and reproductive success in pinnipeds. Studies have shown that other otariids, primarily fur seals, associate with certain frontal features or oceanographic niches while foraging or migrating (Ream et al. 2005, Sterling et al. 2014, Joy et al. 2015, Speakman et al. 2020), but few studies have linked these features to demography. Existing examples include correlations between sea ice and recruitment in Weddell seals (Hadley et al. 2007), sea surface temperatures and first-year survival for subantarctic fur seals (Beauplet et al. 2005), and El Niño conditions and first-year survival in southern elephant seals (McMahon & Burton 2005). In this study, we found that there was strong evidence that the NPGO, the Aleutian Low, the AOI, northward wind, and chlorophyll concentration were positively correlated with pup and age 1-2 survival and that summer upwelling in the previous season was positively correlated with fecundity. Taken together, these results could indicate that lower sea surface temperatures, higher chlorophyll and nutrient concentrations (during positive-phase NPGO) and stronger winds and decreased storminess (during positive-phase AOI) represent conditions that may be more favorable for pup survival and reproductive success. However, the effects of these localized and basin-scale conditions were age-, region-, and season-specific. Namely, the Aleutian Low had the strongest effect in the spring while the AOI, chlorophyll concentration, and wind mattered more in the summer and winter for individuals marked in the eastern portion of the range. These seasons are likely important in terms of life history events, as research has shown that pups are most vulnerable during their first winter (York 1994, Trites & Larkin 1996), as they are limited to shallower diving and the physiological constraints of their smaller body size (Trites & Porter 2002). In the spring, environmental cues could be signaling adult females whether to wean their pups or continue nursing, and in the summer, lactating females would likely benefit from higher prey densities close to rookeries.

While identifying the precise mechanisms by which these features affect demography was outside the scope of this study, our findings improve our understanding of the population's response to environmental variability. For example, stronger winter Aleutian Lows may give way to spring and summer seasons with higher wind stress curl, stronger anticyclonic eddies, and increased chlorophyll concentrations (Prants et al. 2019), which could affect the aggregation of prey species and favorable foraging conditions for lactating females in the summer. Demographic rates in both regions were positively correlated with the NPGO, which has exhibited correlations with salmon productivity in the Gulf of Alaska (Jones et al. 2020) and may also influence plankton dynamics (Di Lorenzo et al. 2008) that affect both the availability and quality of groundfish and forage fish species. The NPGO was predominantly in a negative phase from 2013-2018 in the later part of the study, a time period coinciding with a persistently low body condition index seen in bottom trawls in the Aleutian Islands from 2012-2018 (NPFMC 2020). Notably absent from the group of variables that showed some degree of correlation with demographic rates is sea surface temperature, which has been shown to affect foraging behavior (Lander et al. 2010) and have lasting ecosystem effects long after marine heatwave events (Arimitsu et al. 2021, Suryan et al. 2021). It may be that sea surface temperature is more important at a highly localized scale as a behavioral cue rather than at broad regional scales. The fact that the effect of ocean conditions was limited to pup survival in the eastern portion of the range is likely an indication that these variables either directly affect pup survival (i.e., through increased storminess or maternal separation) or indirectly by affecting maternal investment (i.e., fat storage, weaning, nutrient transfer, prey quality). In contrast, the more notable effect of ocean conditions on yearling and age-2 individuals in the western portion of the range could be due to

earlier weaning of those heavier pups by their first summer, in which case yearling individuals could be strongly affected by prevailing ocean and foraging conditions.

When examining the complex relationships between environmental conditions and demography for an adaptive top predator, it is important to examine the effects of environmental variability and habitat features at the scale that is relevant to the species (Mannocci et al. 2017), but in this case, that is complicated by several factors. First, multiple spatio-temporal scales are likely important to sea lions, as both local and region-scale environmental conditions influence the quantity and quality of prey, for which data are patchily available. Second, the relationships between climate indices and the species they affect can themselves exhibit decadal-scale changes, as has been shown with the NPGO (Litzow et al. 2018, 2020). These complex issues of scale-matching and non-stationary relationships make it challenging to identify mechanistic pathways by which environmental variables affect demography. We know that landscape features are important, it is just that the reasons why they matter simultaneously vary by individual sea lion, rookery, region, season, and year. In addition to these inferential obstacles, the sea lions themselves present an additional challenge in that they are, by nature, adaptive and have evolved to maximize fitness in dynamic and variable environments. Nursing females can compensate for unfavorable foraging conditions or smaller pup birth weights by extending lactation or changing foraging behavior (Trites & Porter 2002, York et al. 2008, Maniscalco et al. 2014). While this flexibility may be particularly important in high-latitude environments with strong seasonality (Varpe et al. 2017), it does make it difficult to disentangle the effects of pup body size, maternal characteristics, regional differences, and environmental variability.

Future work could address some of these complexities through an individual-based integrated model combining mark-resight observations that included maternal attendance and

suckling of dependent young, telemetry data that could better inform the spatial extent of environmental covariates, localized measures of prey availability (though these are not readily available), and proxies for other stressors such as natural predation or contaminant exposure that may also vary across the range. These observational datasets could be used to estimate the effects of environmental variability within a stochastic antecedent model framework (Ogle et al. 2015) that could examine the lag time, duration, and intensity of the effects of ocean conditions. This framework could better account for the effects of maternal versus pup characteristics and would address the uncertainty about the strength, relative importance, and timing of the effects of seasonal environmental variability. Additionally, the results from this study could be used within a population viability framework to understand to what degree the age-specific effects of oceanographic variability estimated here could contribute to changes in population dynamics and trends in abundance.

This study has highlighted age- and sex-specific differences in base demographic rates that may inform ongoing investigation into the divergent abundance trends that have been observed between the eastern and western portions of the western DPS. Our results emphasize the improvement in precision that can be achieved with a longer-term dataset and the benefits of continued focus on obtaining additional years of data for the western portion of the wDPS range. Though the current study design precluded the identification of specific mechanisms by which ocean conditions affect demography, we have highlighted correlations that provide insight into ecological processes and patterns over the nearly 20-year study that could be explored further in future studies. This research has provided important information for the conservation and management of this species, particularly for portions of this endangered population that show continued evidence of decline, and will be foundational to future analyses of population viability

and extinction risk that will inform decision-making in light of ongoing and anticipated future climate variability.

3.5 CONCLUSION

This study examined interannual variability in age- and sex-specific demographic rates and the effects of pup mass and oceanographic conditions on survival and natality for the western DPS of Steller sea lions. Our results provide the first demographic rate estimates for individuals marked in the central and western Aleutian Islands, where low survival of male pups and young sea lions of both sexes may be contributing to or driving the continued declining abundance trends that contrast the stable or increasing trends at rookeries to the east of Samalga Pass. One of the strengths of this study is its broad spatio-temporal scope, which has facilitated the estimation of demographic rates with reasonable precision in the eastern portion of the wDPS range and highlight the importance of continued survey effort in the central and western Aleutians to reduce the uncertainty in age 1-2 survival probabilities and enable a more robust estimate of natality and adult survival, as those vital rates may also be factors limiting recovery. Pup mass had a positive effect on pup survival in stable or increasing population areas and a negative effect in the far western rookeries, potentially indicating differing maternal investment strategies between the two regions.

For both the eastern and western portions of the western DPS range, we found correlations of varying strength and degree between sea lion vital rates and seasonal oceanographic conditions. Namely, the spring Aleutian Lows, summer and winter AOI and wind velocities, fall and winter chlorophyll concentrations, and NPGO and upwelling throughout the year exhibited age- or region-specific positive or negative effects on survival and natality. However, because the effects of ocean conditions are dynamic, vary over time and three-

dimensional space, and are complicated by potential lag effects of unknown duration, the design of this study precluded specifically identifying the mechanisms underlying these observed correlations. Even so, improving our understanding of demography and the environmental factors that influence survival and natality across rookeries in the western DPS will enhance our ability to estimate population viability and trends in abundance and inform ongoing conservation and management strategies for this endangered species.

3.6 ACKNOWLEDGEMENTS

The fieldwork associated with the marking and resighting of sea lions was conducted under MMPA and ESA permit numbers 782-1532-00, 782-1532-01, 782-1532-02, 782-1532-03, 782-1768-00, 782-1768-01, 782-1889, 14326, 14326-01, 14326-02, and 18528-00 and animal care and use committee approvals A/NW 2010-4, A/NW 2013-2, and A/NW 2016-3. The findings and conclusions of the NOAA and USGS authors in the paper are their own and do not necessarily represent the views of the National Marine Fisheries Service, NOAA or United States Geological Survey. Any use of trade, firm, or product names is for descriptive purposes only and does not imply endorsement by the U.S. Government.

3.7 FIGURES & TABLES

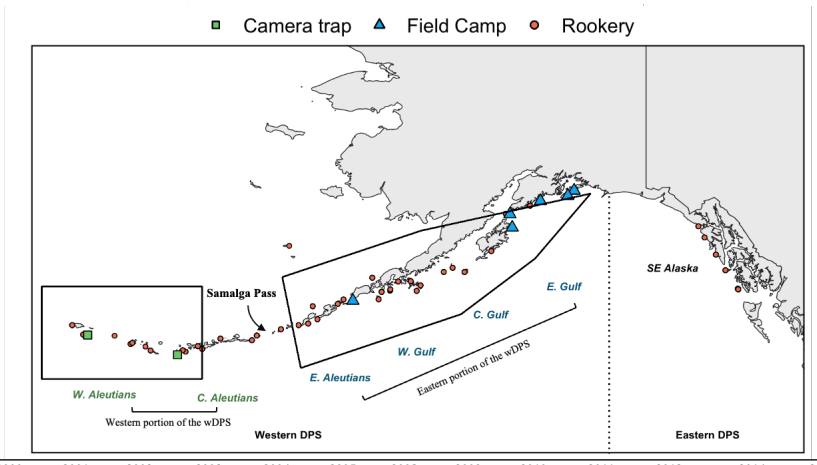

	2000	2001	2002	2003	2004	2005	2008	2009	2010	2011	2013	2014	2015	2017
E. GoA	--	107	--	100	--	80	--	--	--	--	--	--	--	--
C. GoA	258	--	194	--	185	--	178	--	178	--	--	191	--	--
E. Aleu	--	175	--	150	--	200	--	188	--	198	--	--	--	86
C. Aleu	--	--	--	--	--	--	--	--	--	--	58	--	51	50
W. Aleu	--	--	--	--	--	--	--	--	--	54	52	--	50	50

Figure 3.1: Steller sea lion branding locations in the eastern (blue triangles) and western (green squares) portions of the range, and rookeries (red) throughout the western distinct population segment (excluding Russia) and southeast Alaska (eastern DPS that extends along the U.S. West Coast). Black rectangles indicate locations from which satellite data were aggregated for use as covariates in the eastern (46.3° to 58.1°N and -177.9° to -159°W) and western (49.8° to 55.4°N and 169.9° to 175.6°E) portions of the range. Table shows the number of marked and released pups in each region over the study period.

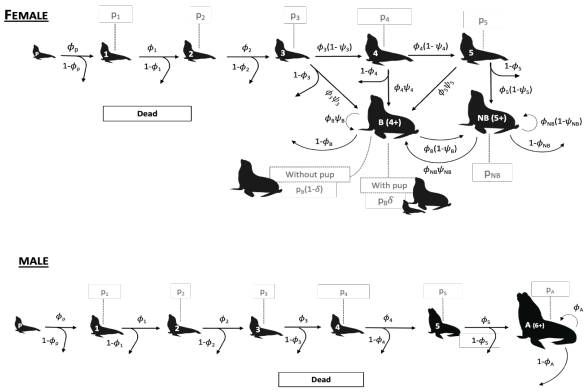

Figure 3.2: Life cycle diagram for female and male Steller sea lions, with true ecological states shown in white (pup, juveniles age 1-3, pre-breeding subadults ages 4-5, breeding adult females (4^{+}B), non-breeding adult females (5^{+}NB), and adult males (6^{+}A). Survival (ϕ) and pupping (ψ) probabilities denote transitions between true states (black lines) and detection probabilities (p) denote possible observation events for each age and breeding (with or without pup) and non-breeding females (grey dotted lines).

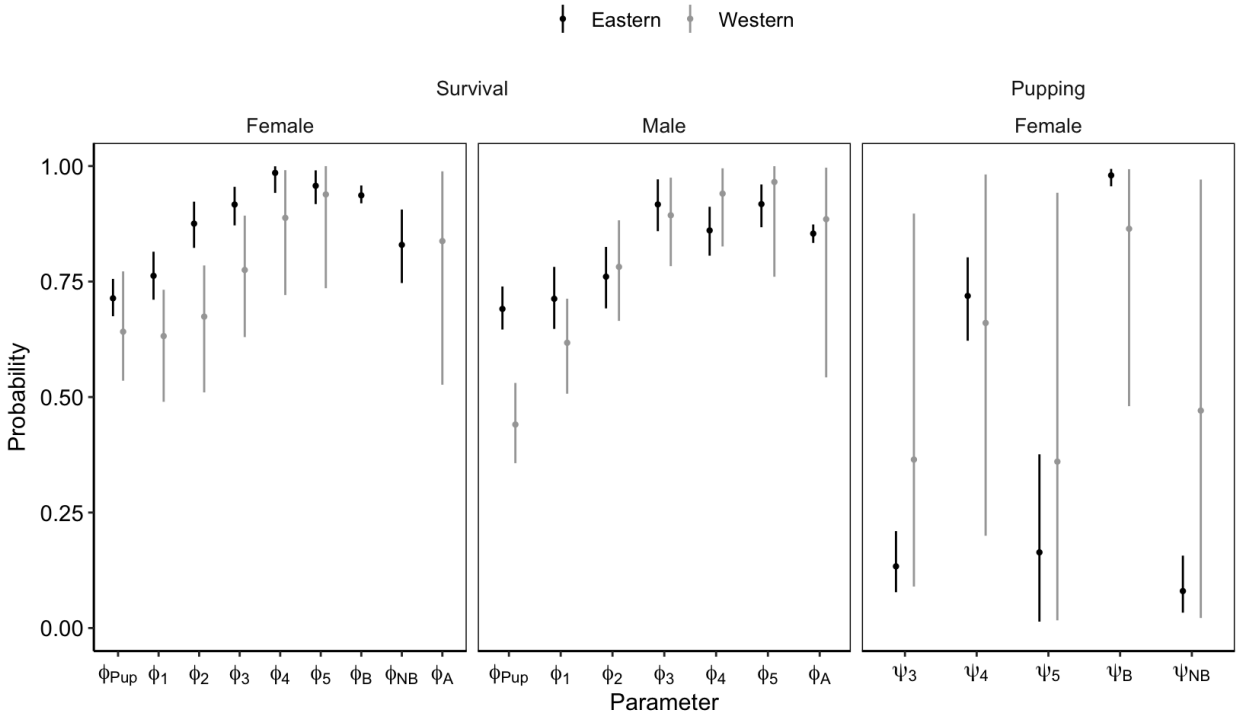

Figure 3.3: Posterior mean and 95% credible intervals for age- and sex-specific survival and pupping probabilities for Steller sea lions in the eastern (black) and western (grey) portion of the wDPS range.

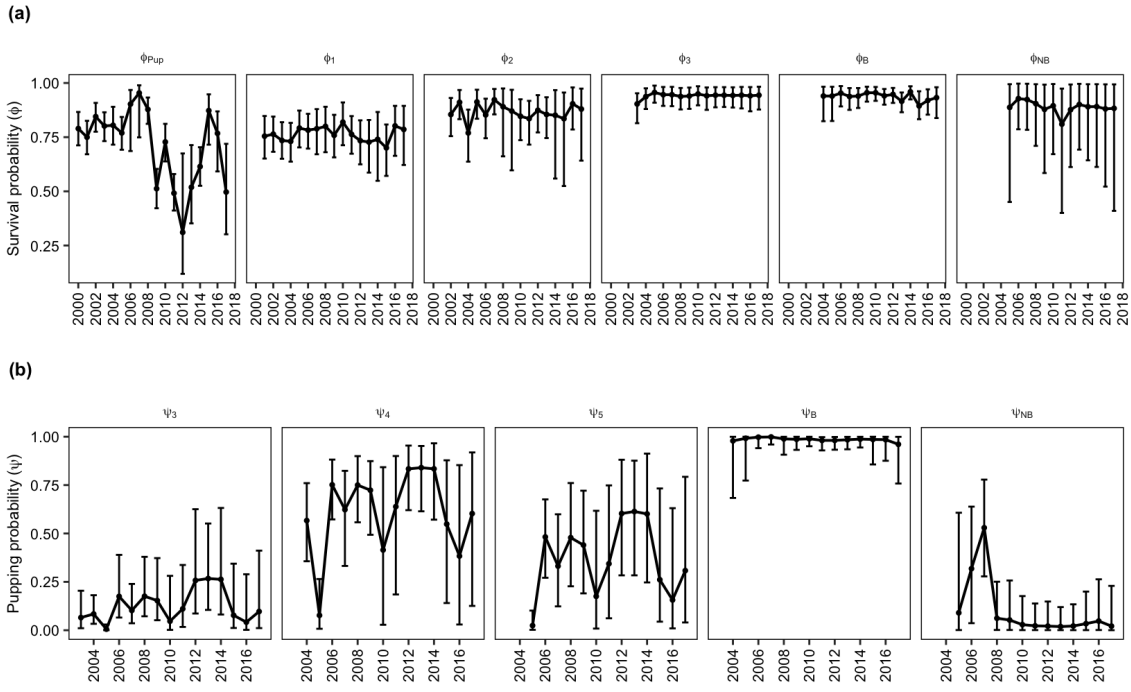

Figure 3.4: Posterior mean and 95% credible interval for time-varying age-specific (a) survival and (b) pupping probability for female Steller sea lions marked in the eastern portion of the wDPS range.

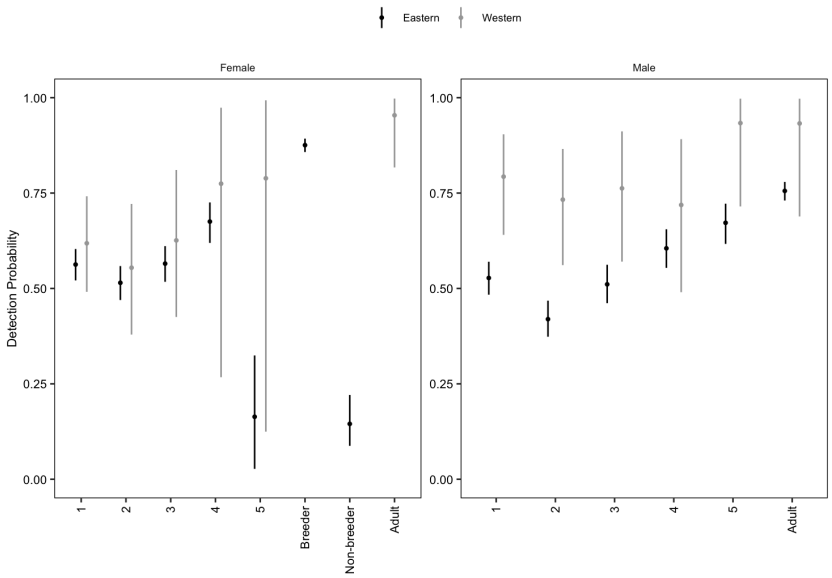

Figure 3.5: Posterior mean and 95% credible intervals for age- and sex-specific detection probability of Steller sea lions marked in the eastern (black) and western (grey) portion of the wDPS range.

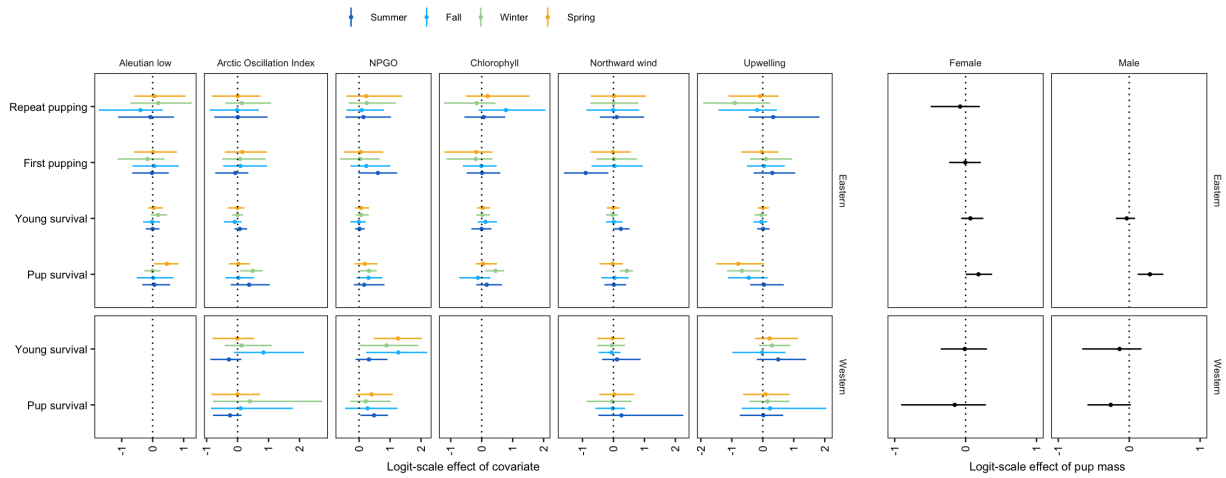

Figure 3.6: Logit-scale posterior mean and 95% credible intervals for the fixed effects of environmental covariates in each season and pup mass at branding on pup and young (pooled effect for age 1-2) survival and pupping probabilities for individuals marked in the eastern and western portions of the wDPS range.

Table 3.1: Posterior mean and 95% credible intervals for age- and sex-specific (M = male; F = female) survival and natality (proportion of females with a pup) parameters for the eastern (2000-2018) and western (2011-2018) portions of the wDPS.

Rate	Sex	Age	Eastern	95% CI	Western	95% CI
Survival	F	P	0.71	0.67-0.76	0.64	0.54-0.77
	M		0.69	0.65-0.74	0.44	0.36-0.53
	F	1	0.76	0.71-0.81	0.63	0.49-0.73
	M		0.71	0.65-0.78	0.62	0.51-0.71
	F	2	0.88	0.82-0.92	0.67	0.51-0.78
	M		0.76	0.69-0.82	0.78	0.66-0.88
	F	3	0.92	0.87-0.96	0.78	0.63-0.89
	M		0.92	0.86-0.97	0.89	0.78-0.97
	F	4	0.99	0.94-1.00	0.89	0.72-0.99
	M		0.86	0.81-0.91	0.94	0.83-1.00
	F	5	0.96	0.92-0.99	0.94	0.74-1.00
	M		0.92	0.87-0.96	0.97	0.76-1.00
	F	Adult w/ pup	0.94	0.92-0.96		
		Adult w/o pup	0.83	0.75-0.91		
	M	Adult	0.85	0.83-0.87	0.88	0.54-1.00
	F				0.84	0.53-0.99
Natality	F	4	0.13	0.04-0.28	0.38	0.12-0.89
		5	0.81	0.7-0.90	0.76	0.49-1.00
		all	0.80	0.74-0.84	0.69	0.47-0.96

Table 3.2: WAIC values for models of individuals marked in the eastern (null, random effects only, seasonal full models) and western (null and seasonal full models) portions of the range.

Region	Model	WAIC	ΔWAIC
Eastern	Full (Winter)	17,701.1	0.0
Eastern	Random effects only	17,709.8	8.7
Eastern	Full (Summer)	17,710.4	9.3
Eastern	Full (Spring)	17,714.4	13.3
Eastern	Full (Fall)	17,715.3	14.3
Eastern	Null	18,011.0	310.0
Western	Full (Spring)	919.2	0.0
Western	Full (Fall)	921.3	2.1
Western	Full (Winter)	922.9	3.7
Western	Full (Summer)	930.5	11.3
Western	Null	933.7	14.5

3.8 REFERENCES

Altukhov, A.V., Andrews, R.D., Calkins, D.G., Gelatt, T.S., Gurarie, E.D., Loughlin, T.R., Mamaev, E.G., Nikulin, V.S., Permyakov, P.A., Ryazanov, S.D., Vertyankin, V.V., Burkanov, V.N., 2015. Age Specific Survival Rates of Steller Sea Lions at Rookeries with Divergent Population Trends in the Russian Far East. PLOS ONE 10, e0127292. https://doi.org/10.1371/journal.pone.0127292

Antonelis, GA., EH. Sinclair, R. Ream, and BW. Robson. 1997. Inter-island variation in the diet of female northern fur seals (callorhinus ursinus) in the bering sea. Journal of zoology (london) 242: 435-451.

Arimitsu, M.L., Piatt, J.F., Hatch, S., Suryan, R.M., Batten, S., Bishop, M.A., Campbell, R.W., Coletti, H., Cushing, D., Gorman, K., Hopcroft, R.R., Kuletz, K.J., Marsteller, C., McKinstry, C., McGowan, D., Moran, J., Pegau, S., Schaefer, A., Schoen, S., Straley, J. and von Biela, V.R. 2021. Heatwave-induced synchrony within forage fish portfolio disrupts energy flow to top pelagic predators. Glob. Change Biol., 27: 1859-1878. https://doi.org/10.1111/gcb.15556

Atkinson, S., D.P. Demaster, and D.G. Calkins. 2008. Anthropogenic causes of the western Steller sea lion *Eumetopias jubatus* population decline and their threat to tecovery. Mammal Review 38: 1–18. doi:10.1111/j.1365-2907.2008.00128.x.

Beauplet, G., Barbraud, C., Chambellant, M., Guinet, C., 2005. Interannual variation in the post-weaning and juvenile survival of subantarctic fur seals: influence of pup sex, growth rate and oceanographic conditions. Journal of Animal Ecology 74, 1160–1172. https://doi.org/10.1111/j.1365-2656.2005.01016.x

Benson, A.J., and A.W. Trites. 2002. Ecological effects of regime shifts in the Bering Sea and eastern North Pacific Ocean. Fish and Fisheries 3 (2): 95–113. doi:10.1046/j.1467-2979.2002.00078.x.

Boltnev AI, York AE, Antonelis GA. 1998. Northern fur seal young: interrelationships among birth size, growth, and survival. Candian Journal of Zoology 76:843–854.

Boyd IL. 1990. State-dependent fertility in pinnipeds: contrasting capital and income breeders. Functional Ecology 14:623–630.

Brooks, S.P. & Roberts, G.O. 1998. Convergence assessment techniques for Markov chain Monte Carlo. Statistics and Computing, 8, 319-335.

Brownie, C., Hines, J.E., Nichols, J.D., Pollock, K.H., Hestbeck, J.B., 1993. Capture-Recapture Studies for Multiple Strata Including Non-Markovian Transitions. Biometrics 49, 1173. https://doi.org/10.2307/2532259

Burkanov, V., Gurarie, E., Altukhov, A., Mamaev, E., Permyakov, P., Trukhin, A., Waite, J., Gelatt, T., 2011. Environmental and biological factors influencing maternal attendance patterns of Steller sea lions (*Eumetopias jubatus*) in Russia. Journal of Mammalogy 92, 352–366. https://doi.org/10.1644/10-MAMM-A-194.1

Calkins, D. G., Becker, E. F. & Pitcher, K. W. 1998. Reduced body size of female Steller sea lions from a declining population in the Gulf of Alaska. Marine Mammal Science. 14, 232–244.

Call, K.A., Loughlin, T.R., 2005. An ecological classification of Alaskan Steller sea lion (*Eumetopias jubatus*) rookeries: a tool for conservation/management. Fisheries Oceanography 14, 212–222. https://doi.org/10.1111/j.1365-2419.2005.00370.x

Champagnon, J., Lebreton, J.-D., Drummond, H., Anderson, D.J., 2018. Pacific Decadal and El Niño oscillations shape survival of a seabird. Ecology 99, 1063–1072. https://doi.org/10.1002/ecy.2179

Conn, P.B., D.S. Johnson, L.W. Fritz, and B.S. Fadely. 2014. Examining the utility of fishery and survey data to detect prey removal effects on Steller Sea Lions (*Eumetopias jubatus*). Canadian Journal of Fisheries and Aquatic Sciences 71 (8): 1229–42. doi:10.1139/cjfas-2013-0602.

Copernicus Marine Environment Monitoring Service, 2020. https://resources.marine.copernicus.eu/documents/PUM/CMEMS-MOB-PUM-015-002.pdf

de Valpine, P., D. Turek, C.J. Paciorek, C. Anderson-Bergman, D. Temple Lang, an Bodik. NIMBLE Development Team. 2019. Programming with models: writing statistical algorithms for general model structures with NIMBLE. Journal of Computational and Graphical Statistics 26: 403-413. DOI:10.1080/10618600.2016.1172487.

Di Lorenzo E., Schneider N., Cobb K. M., Chhak, K, Franks P. J. S., Miller A. J., McWilliams J. C., Bograd S. J., Arango H., Curchister E., Powell T. M. and P. Rivere, 2008: North Pacific Gyre Oscillation links ocean climate and ecosystem change. Geophys. Res. Lett., 35, L08607, doi:10.1029/2007GL032838.

Drago, M., Cardona, L., Franco-Trecu, V., Riet-Sapriza, F.G., Crespo, E.A., García, N., Inchausti, P., 2021. Relationship between the female attendance pattern and pup growth rate in the South American sea lion (Carnivora). Scimar 85, 81–90. https://doi.org/10.3989/scimar.05128.008

Eberhardt, L.L., 2002. A Paradigm for Population Analysis of Long-Lived Vertebrates. Ecology 83, 2841–2854. https://doi.org/10.1890/0012-9658(2002)083[2841:APFPAO]2.0.CO;2

Fay, R., Weimerskirch, H., Delord, K., Barbraud, C., 2015. Population density and climate shape early-life survival and recruitment in a long-lived pelagic seabird. Journal of Animal Ecology 84, 1423–1433. https://doi.org/10.1111/1365-2656.12390

Fadely, B.S., Robson, B.W., Sterling, J.T., Greig, A., Call, K.A., 2005. Immature Steller sea lion (*Eumetopias jubatus*) dive activity in relation to habitat features of the eastern Aleutian Islands. Fisheries Oceanography 14, 243–258. https://doi.org/10.1111/j.1365-2419.2005.00379.x

Fritz, L., K. Sweeney, D. Johnson, M. Lynn, T. Gelatt, and J. Gilpatrick. 2013. Aerial and ship-based surveys of Steller sea lions (*Eumetopias jubatus*) conducted in Alaska in June-July 2008 through 2012, and an update on the status and trend of the western distinct population segment in Alaska. U.S. Dep. Commer., NOAA Tech. Memo. NMFS-AFSC- 251, 92 p.

Fritz L., R. Towell, T. Gelatt, D. Johnson, and T. Loughlin. 2014. Recent increases in survival of western Steller sea lions in Alaska and implications for recovery. Endangered Species Research 26(1):13–24. doi: 10.3354/esr00634.

Fritz, L., K. Sweeney, R. Towell, and T. Gelatt. 2016. Aerial and ship- based surveys of Steller sea lions (*Eumetopias jubatus*) conducted in Alaska in June-July 2013 through 2015, and an update on the status and trend of the western distinct population segment in Alaska. U.S. Dep. Commer., NOAA Tech. Memo. NMFS-AFSC-321, 72 p. doi:10.7289/V5/TM-AFSC-321.

Fritz, L., Brost, B., Laman, E., Luxa, K., Sweeney, K., Thomason, J., Tollit, D., Walker, W., Zeppelin, T., 2019. A re-examination of the relationship between Steller sea lion (*Eumetopias jubatus*) diet and population trend using data from the Aleutian Islands. Canadian Journal of Zoology. https://doi.org/10.1139/cjz-2018-0329

Fujiwara, M., Caswell, H., 2002. Estimating Population Projection Matrices from Multi-Stage Mark–Recapture Data. Ecology 83, 3257–3265. https://doi.org/10.1890/0012-9658(2002)083[3257:EPPMFM]2.0.CO;2

Gaillard J.M., Festa-Bianchet M, Yoccoz NG. 1998. Population dynamics of large herbivores: variable recruitment with constant adult survival. Trends Ecol Evol 13:58–63.

Gelman, A. & Rubin, D.B. 1992. Inference from iterative simulation using multiple sequences. Statist. Sci., 7, 457-472.

Hadley, G.L., Rotella, J.J., Garrott, R.A., 2007. Influence of maternal characteristics and oceanographic conditions on survival and recruitment probabilities of Weddell seals. Oikos 116, 601–613. https://doi.org/10.1111/j.0030-1299.2007.15528.x

Jemison, L.A., Pendleton, G.W., Fritz, L.W., Hastings, K.K., Maniscalco, J.M., Trites, A.W., Gelatt, T.S., 2013. Inter-population movements of steller sea lions in Alaska with implications for population separation. PLoS ONE 8, e70167. https://doi.org/10.1371/journal.pone.0070167

Joy, R., Dowd, M.G., Battaile, B.C., Lestenkof, P.M., Sterling, J.T., Trites, A.W., Routledge, R.D., 2015. Linking northern fur seal dive behavior to environmental variables in the eastern Bering Sea. Ecosphere 6, art75. https://doi.org/10.1890/ES14-00314.1

Hastings, K.K., 2017. Survival of Steller sea lion (*Eumetopias jubatus*) pups during the first months of life at the Forrester Island complex, Alaska. J Mammal 98, 397–409. https://doi.org/10.1093/jmammal/gyw182

Hastings, K.K., Jemison, L.A., Gelatt, T.S., Laake, J.L., Pendleton, G.W., King, J.C., Trites, A.W., Pitcher, K.W., 2011. Cohort effects and spatial variation in age-specific survival of Steller sea lions from southeastern Alaska. Ecosphere 2, art111. https://doi.org/10.1890/ES11-00215.1

Hastings, K.K., Jemison, L.A., Pendleton, G.W., 2018. Survival of adult Steller sea lions in Alaska: senescence, annual variation and covariation with male reproductive success. Royal Society Open Science 5, 170665. https://doi.org/10.1098/rsos.170665

Hastings, K.K., Johnson, D.S., Pendleton, G.W., Fadely, B.S., Gelatt, T.S., 2021. Investigating life-history traits of Steller sea lions with multistate hidden Markov mark–recapture models: Age at weaning and body size effects. Ecol. Evol. 11, 714–734. https://doi.org/10.1002/ece3.6878

Heppell, S.S., Caswell, H., Crowder, L.B., 2000. Life Histories and Elasticity Patterns: Perturbation Analysis for Species with Minimal Demographic Data. Ecology 81, 654–665.

Higgins, R. W., A. Leetmaa, Y. Xue, and A. Barnston, 2000: Dominant factors influencing the seasonal predictability of U.S. precipitation and surface air temperature. J. Climate, 13, 3994-4017.

Himes Boor, G., McGuire, T.L., Warlick, A.J., Taylor, R.L., Converse, S.J., McClung, J.R., and A.D. Stephens. *In revision*. Estimating a reproductive rate when offspring ages are uncertain: a novel multievent mark-recapture model applied to an endangered beluga whale population.

Holmes, E.E., L.W. Fritz, A.E. York, and K. Sweeney. 2007. Age-structured modeling reveals long-term declines in the natality of western Steller sea lions. Ecological Applications 17 (8): 2214–32. doi:10.1890/07-0508.1.

Hunt, G.L., Stabeno, P.J., 2005. Oceanography and ecology of the Aleutian Archipelago: spatial and temporal variation. Fisheries Oceanography 14, 292–306. https://doi.org/10.1111/j.1365-2419.2005.00378.x

Jones, LA, Schoen, ER, Shaftel, R, et al. 2021. Watershed-scale climate influences productivity of Chinook salmon populations across southcentral Alaska. Glob Change Biol. 26: 4919–4936. https://doi.org/10.1111/gcb.15155

Joy, R., Dowd, M.G., Battaile, B.C., Lestenkof, P.M., Sterling, J.T., Trites, A.W., Routledge, R.D., 2015. Linking northern fur seal dive behavior to environmental variables in the eastern Bering Sea. Ecosphere 6, art75. https://doi.org/10.1890/ES14-00314.1

Kendall, W.L., Langtimm, C.A., Beck, C.A., Runge, M.C., 2004. Capture-Recapture Analysis for Estimating Manatee Reproductive Rates. Marine Mammal Science 20, 424–437. https://doi.org/10.1111/j.1748-7692.2004.tb01170.x

Kuhn, C.E., K.C., D. Johnson, and L. Fritz. 2017. A re-examination of the timing of pupping for Steller sea lions *Eumetopias jubatus* breeding on two islands in Alaska. Endangered Species Research 32: 213–22. doi:10.3354/esr00796.

Ladd, C., Hunt, G.L., Mordy, C.W., Salo, S.A., Stabeno, P.J., 2005. Marine environment of the eastern and central Aleutian Islands. Fisheries Oceanography 14, 22–38. https://doi.org/10.1111/j.1365-2419.2005.00373.x

Lander, M.E., Fritz, L.W., Johnson, D.S., Logsdon, M.G., 2013. Population trends of Steller sea lions (*Eumetopias jubatus*) with respect to remote sensing measures of chlorophyll-a in critical habitat. Mar Biol 160, 195–209. https://doi.org/10.1007/s00227-012-2077-4

Lander, M.E., Loughlin, T.R., Logsdon, M.G., VanBlaricom, G.R., Fadely, B.S., Fritz, L.W., 2009. Regional differences in the spatial and temporal heterogeneity of oceanographic habitat used by Steller sea lions. Ecological Applications 19, 1645–1659. https://doi.org/10.1890/08-0159.1

Lander, M., T. Loughlin, M. Logsdon, G. VanBlaricom, and B. Fadely. 2010. Foraging effort of juvenile Steller sea lions *Eumetopias Jubatus* with respect to heterogeneity of sea surface temperature. Endangered Species Research 10: 145–58. doi:10.3354/esr00260.

Lander, M.E., M.L. Logsdon, T.R. Loughlin, and G. Van Blaricom. 2011. Spatial patterns and scaling behaviors of Steller sea lion (*Eumetopias jubatus*) distributions and their environment. Journal of Theoretical Biology 274 (1): 74–83. doi:10.1016/j.jtbi.2011.01.015.

Lander, M.E., Fadely, B.S., Gelatt, T.S., Sterling, J.T., Johnson, D.S., Pelland, N.A., 2020. Mixing it up in Alaska: Habitat use of adult female Steller sea lions reveals a variety of foraging strategies. Ecosphere 11, e03021. https://doi.org/10.1002/ecs2.3021

Lee PC, Majluf P, Gordon IJ. 1991. Growth, weaning and maternal investment from a comparative perspective. Journal of Zoology 225:9–114.

Loughlin, T.R. 1997. Using the phylogeographic method to identify Steller sea lion stocks. Molecular Genetics of Marine Mammals 3:159-171.

Loughlin, T.R., and A.E. York. 2000. "An accounting of the sources of Steller sea lion, *Eumetopias jubatus*, mortality." Marine Fisheries Review, 6.

Lunn, N.J., I.L. Boyd, and J.P. Croxall, 1994. Reproductive performance of female Antarctic fur seals: the influence of age, breeding experience, environmental variation, and individual quality. Journal of Animal Ecology 63: 827-840.

Maniscalco, J.M., Springer, A.M., Parker, P., 2010. High natality rates of endangered Steller sea lions in Kenai fjords, Alaska and perceptions of population status in the Gulf of Alaska. PLOS ONE 5, e10076. https://doi.org/10.1371/journal.pone.0010076

Maniscalco, J.M., A.M., Springer, P. Parker, M.D. Adkinson. 2014. A longitudinal study of Steller sea lion natality rates in the Gulf of Alaska with comparisons to census data. PLOS One 9:e111523.

Maniscalco, J.M., 2014. The Effects of Birth Weight and Maternal Care on Survival of Juvenile Steller Sea Lions (*Eumetopias jubatus*). PLOS ONE 9, e96328. https://doi.org/10.1371/journal.pone.0096328

Maniscalco, J.M., Springer, A.M., Adkison, M.D., Parker, P., 2015. Population Trend and Elasticities of Vital Rates for Steller Sea Lions (*Eumetopias jubatus*) in the Eastern Gulf of Alaska: A New Life-History Table Analysis. PLOS ONE 10, e0140982. https://doi.org/10.1371/journal.pone.0140982

Mannocci, L., A.M. Boustany, J.J. Roberts, D.M. Palacios, D.C. Dunn, P.N. Halpin, S. Viehman, et al. 2017. Temporal Resolutions in Species Distribution Models of Highly Mobile Marine Animals: Recommendations for Ecologists and Managers. Diversity and Distributions 23 (10): 1098–1109. doi:10.1111/ddi.12609.

Mantua, N. J., S. R. Hare, Y., Zhang, J. M. Wallace, and R. C. Francis, 1997: A Pacific interdecadal climate oscillation with impacts on salmon production. Bull. Am. Met. Soc., 76, 1069-1079.

Martin, M., McLaren, A., Good, S., 2019. PRODUCT USER MANUAL For Global Ocean GMPE Sea Surface Temperature Multi Product Ensemble SST_GLO_SST_L4_NRT_OBSERVATIONS_010_005 16.

McKenzie, J.L., J. Parry, B. Page, and S.D. Goldsworthy. 2005. Estimation of pregnancy rates and reproductive failure in New Zealand fur seals. Journal of Mammalogy 86:1237-1246.

McMahon CR, Hindell MA. 2003. Twinning in southern elephant seals: implications of resource allocation by mothers. Wildlife Research 30:35–39.

McMahon, C.R., Burton, H.R., 2005. Climate change and seal survival: evidence for environmentally mediated changes in elephant seal, Mirounga leonina, pup survival. Proceedings of the Royal Society B: Biological Sciences 272, 923–928. https://doi.org/10.1098/rspb.2004.3038

Merrick, R.L., M.K. Chumbley, and G.V Byrd. 1997. Diet Diversity of Steller Sea Lions (*Eumetopias Jubatus*) and Their Population Decline in Alaska: A Potential Relationship. Canadian Journal of Fisheries and Aquatic Sciences 54 (6): 1342–8. doi:10.1139/f97-037.

Miller, A. J., et al. 2005. Interdecadal changes in mesoscale eddy variance in the Gulf of Alaska circulation: possible implications for the Steller sea lion decline. Atmosphere-Ocean 43:231–240.

Mordy, C.W., Stabeno, P.J., Ladd, C., Zeeman, S., Wisegarver, D.P., Salo, S.A., Hunt, G.L., 2005. Nutrients and primary production along the eastern Aleutian Island Archipelago. Fisheries Oceanography 14, 55–76. https://doi.org/10.1111/j.1365-2419.2005.00364.x

NASA Goddard Space Flight Center, Ocean Ecology Laboratory, Ocean Biology Processing Group. 2018. Sea-viewing Wide Field-of-view Sensor (SeaWiFS) R2018.0 Chlorophyll Data; NASA OB.DAAC, Greenbelt, MD, USA. doi: https://dx.doi.org/10.5067/ORBVIEW-2/SEAWIFS/L3M/CHL/2018.

NOAA NCEI, 2020. NOAA Climate monitoring teleconnections: Arctic Oscillation. https://www.ncdc.noaa.gov/teleconnections/ao/ accessed July 1, 2020.

NOAA PSL, 2020. NOAA Physical Sciences Laboratory: Gridded Climate Datasets. https://psl.noaa.gov/data/gridded/tables/ocean.html accessed July 1, 2020.

North Pacific Fisheries Management Council, 2020. Ecosystem Status Report 2020 Aleutian Islands. Bering Sea and Aleutian Islands SAFE, *Eds* Ortiz, I. and Zador, S. Anchorage, AK.

O'Corry-Crowe, G., Taylor, B.L., Gelatt, T., Loughlin, T.R., Bickham, J., Basterretche, M., Pitcher, K.W., DeMaster, D.P., 2006. Demographic independence along ecosystem boundaries in Steller sea lions revealed by mtDNA analysis: implications for management of an endangered species. Can. J. Zool. 84, 1796–1809. https://doi.org/10.1139/z06-167

Ogle, K., Barber, J.J., Barron-Gafford, G.A., Bentley, L.P., Young, J.M., Huxman, T.E., Loik, M.E., Tissue, D.T., 2015. Quantifying ecological memory in plant and ecosystem processes. Ecol. Lett. 18, 221–235. https://doi.org/10.1111/ele.12399

Pascual, M.A., and M.D. Adkison. 1994. The Decline of the Steller Sea Lion in the Northeast Pacific: Demography, Harvest or Environment? Ecological Applications 4 (2): 393–403. doi:10.2307/1941942.

Payo-Payo, A., Genovart, M., Bertolero, A., Pradel, R., Oro, D., 2016. Consecutive cohort effects driven by density-dependence and climate influence early-life survival in a long-lived bird. Proc. R. Soc. B 283, 20153042. https://doi.org/10.1098/rspb.2015.3042

Pendleton, G.W., Pitcher, K.W., Fritz, L.W., York, A.E., Raum-Suryan, K.L., Loughlin, T.R., Calkins, D.G., Hastings, K.K., Gelatt, T.S., 2006. Survival of Steller sea lions in Alaska: a comparison of increasing and decreasing populations. Can. J. Zool. 84, 1163–1172. https://doi.org/10.1139/z06-103

Pitcher, K.W., and D.G. Calkins. 1981. Reproductive Biology of Steller Sea Lions in the Gulf of Alaska. Journal of Mammalogy 62 (3): 599–605. doi:10.2307/1380406.

Pitcher, K.W., V.N. Burkanov, D.G. Calkins, B.J. Le Boeuf, E.G. Mamaev, R.L. Merrick, and G.W. Pendleton. 2001. Spatial and Temporal Variation in the Timing of Births of Steller Sea Lions. Journal of Mammalogy 82 (4): 1047–53. doi:10.1644/1545-1542(2001)082<1047:SATVIT>2.0.CO;2.

Pfister CM. 1998. Patterns of variance in stage-structured populations: evolutionary predictions and ecological implications. Proc Nat Acad Sci. 1998; 95: 213–218. PMID: 9419355

Pradel, R., 2005. Multievent: An Extension of Multistate Capture–Recapture Models to Uncertain States. Biometrics 61, 442–447. https://doi.org/10.1111/j.1541-0420.2005.00318.x

Prants, S.V., Andreev, A.G., Uleysky, M.Y., Budyansky, M.V., 2019. Lagrangian study of mesoscale circulation in the Alaskan Stream area and the eastern Bering Sea. Deep Sea Research Part II: Topical Studies in Oceanography S096706451830153X. https://doi.org/10.1016/j.dsr2.2019.03.005

Proffitt KM, Rotella JJ, Garrott RA. 2010. Effects of pup age, maternal age, and birth date on pre-weaning survival rates of Weddell seals in Erebus Bay, Antarctica. Oikos 119:1255–1264.

Rand, K., McDermott, S., Logerwell, E., Matta, M.E., Levine, M., Bryan, D.R., Spies, I.B., Loomis, T., 2019. Higher Aggregation of Key Prey Species Associated with Diet and Abundance of the Steller Sea Lion *Eumetopias jubatus* across the Aleutian Islands. Marine and Coastal Fisheries 11, 472–486. https://doi.org/10.1002/mcf2.10096

Raum-Suryan, K.L., K.W. Pitcher, D.G. Calkins, J.L. Sease, and T.R. Loughlin. 2002. Dispersal, Rookery Fidelity, and Metapopulation Structure of Steller Sea Lions (*Eumetopias Jubatus*) in an Increasing and a Decreasing Population in Alaska. Marine Mammal Science 18 (3): 746–64. doi:10.1111/j.1748-7692.2002.tb01071.x.

Rodionov, S.N., Bond, N.A., Overland, J.E., 2007. The Aleutian Low, storm tracks, and winter climate variability in the Bering Sea. Deep Sea Research Part II: Topical Studies in Oceanography 54, 2560–2577. https://doi.org/10.1016/j.dsr2.2007.08.002

Rodionov, S.N., Overland, J.E., Bond, N.A., 2005. Spatial and temporal variability of the Aleutian climate. Fisheries Oceanography 14, 3–21. https://doi.org/10.1111/j.1365-2419.2005.00363.x

Rotella JJ, Link WA, Chambert T, Stauffer GE, Garrott RA. 2012. Evaluating the demographic buffering hypothesis with vital rates estimated for Weddell seals from 30 years of mark-recapture data. J Anim Ecol. 2012; 81: 162–173. doi: 10.1111/j.1365-2656.2011.01902.x PMID: 21939440

Ream, R.R., Sterling, J.T., Loughlin, T.R., 2005. Oceanographic features related to northern fur seal migratory movements. Deep Sea Research Part II: Topical Studies in Oceanography, Linkages between coastal and open ocean ecosystems 52, 823–843. https://doi.org/10.1016/j.dsr2.2004.12.021

Sanz-Aguilar, A., Igual, J.M., Oro, D., Genovart, M., Tavecchia, G., 2017. Estimating recruitment and survival in partially monitored populations. Functional Ecology 73–82. https://doi.org/10.1111/1365-2664.12580@10.1111/(ISSN)1365-2435.DemographyBehindthePopulation

Seckel, G.R. 1993. Zonal gradient of the winter sea level atmospheric pressure at 50 N: an indicator of atmospheric forcing of North Pacific surface conditions. J. Geophys. Res. 98:22615–22628.

Simons, R.A. (2019). ERDDAP. https://coastwatch.pfeg.noaa.gov/erddap. Monterey, CA: NOAA/NMFS/SWFSC/ERD.

Simpson, D., Rue, H., Riebler, A., Martins, T.G., Sørbye, S.H., 2017. Penalising Model Component Complexity: A Principled, Practical Approach to Constructing Priors. Statist. Sci. 32, 1–28. https://doi.org/10.1214/16-STS576

Sinclair, E.H., Zeppelin, T.K., 2002. Seasonal and Spatial Differences in Diet in the Western Stock of Steller Sea Lions (*Eumetopias jubatus*). Journal of Mammalogy 83, 973–990.

Sinclair, E. H., D. S. Johnson, T. K. Zeppelin, and T. S. Gelatt. 2013. Decadal variation in the diet of Western Stock Steller sea lions (*Eumetopias jubatus*). U.S. Dep. Commer., NOAA Tech. Memo. NMFS-AFSC-248, 67 p.

Speakman, C.N., Hoskins, A.J., Hindell, M.A., Costa, D.P., Hartog, J.R., Hobday, A.J., Arnould, J.P.Y., 2020. Environmental influences on foraging effort, success and efficiency in female Australian fur seals. Scientific Reports 10, 17710. https://doi.org/10.1038/s41598-020-73579-y

Speckman, P.L. and Sun, D., 2003. Fully Bayesian spline smoothing and intrinsic autoregressive priors. Biometrika. 90:289–302.

Stabeno, P. J., J. D. Schumacher, and K. Ohtani. 1999. The physical oceanography of the Bering Sea. Pages 1–28 in T. R. Loughlin and K. Ohtani, editors. Dynamics of the Bering Sea. AK–SG–99–03. University of Alaska Sea Grant, Fairbanks, Alaska, USA.

Sterling, J.T., Springer, A.M., Iverson, S.J., Johnson, S.P., Pelland, N.A., Johnson, D.S., Lea, M.-A., Bond, N.A., 2014. The Sun, Moon, Wind, and Biological Imperative–Shaping Contrasting Wintertime Migration and Foraging Strategies of Adult Male and Female Northern Fur Seals (Callorhinus ursinus). PLOS ONE 9, e93068. https://doi.org/10.1371/journal.pone.0093068

Suryan, R.M., Arimitsu, M.L., Coletti, H.A. et al. 2021. Ecosystem response persists after a prolonged marine heatwave. Sci Rep 11, 6235 (2021).

Sweeney, K., Towell, R., Gelatt, T. 2018. Results of Steller Sea Lion Surveys in Alaska, June-July 2017. NOAA Fisheries Alaska Fisheries Science Center Marine Mammal Laboratory, Seattle, WA. https://media.fisheries.noaa.gov/dam-migration/ssl_aerial_survey_2018_final.pdf

Tavecchia, G., Sanz-Aguilar, A., Cannell, B., 2016. Modelling survival and breeding dispersal to unobservable nest sites. Wildlife Research 43, 411. https://doi.org/10.1071/WR15187

Thomas JA, DeMaster DP. 1983. Parameters affecting survival of Weddell seal pups (Leptonychotes weddelli) to weaning. Canadian Journal of Zoology 61:2078–2083.

Tomillo, P.S., Robinson, N.J., Sanz-Aguilar, A., Spotila, J.R., Paladino, F.V., Tavecchia, G., 2017. High and variable mortality of leatherback turtles reveal possible anthropogenic impacts. Ecology 98, 2170–2179. https://doi.org/10.1002/ecy.1909

Trillmich F. 1990. The behavioral ecology of maternal effort in fur seals and sea lions. Behaviour 114:3–20.

Trites, A. W., and C. P. Donnelly. 2003. The Decline of Steller Sea Lions *Eumetopias jubatus* in Alaska: A Review of the Nutritional Stress Hypothesis. Mammal Review 33 (1): 3–28. doi:10.1046/j.1365-2907.2003.00009.x.

Trites, A.W., Larkin, P.A., 1996. Changes in the abundance of Steller sea lions (*Eumetopias jubatus*) in Alaska from 1956 to 1992: how many were there? Aquatic Mammals 22: 153-166.

Trites, A.W., Miller, A.J., Maschner, H.D.G., Alexander, M.A., Bograd, S.J., Calder, J.A., Capotondi, A., Coyle, K.O., Lorenzo, E.D., Finney, B.P., Gregr, E.J., Grosch, C.E., Hare, S.R., Hunt, G.L., Jahncke, J., Kachel, N.B., Kim, H.-J., ... Winship, A.J., 2007. Bottom-up forcing and the decline of Steller sea lions (*Eumetopias jubatus*) in Alaska: assessing the ocean climate hypothesis. Fisheries Oceanography.

Trites, A.W., Porter, B.T., 2002. Attendance patterns of Steller sea lions (*Eumetopias jubatus*) and their young during.

van Erp, S., Oberski, D.L., Mulder, J., 2019. Shrinkage priors for Bayesian penalized regression. Journal of Mathematical Psychology 89, 31–50. https://doi.org/10.1016/j.jmp.2018.12.004

Varpe, Ø., 2017. Life History Adaptations to Seasonality. Integrative and Comparative Biology 57, 943–960. https://doi.org/10.1093/icb/icx123

Watanabe, S., 2010. Asymptotic Equivalence of Bayes Cross Validation and Widely Applicable Information Criterion in Singular Learning Theory. Journal of Machine Learning Research 11.

Wiens JA .1989. Spatial scaling in ecology. Funct Ecol 3: 385 – 397.

Wright, B.E., Brown, R.F., DeLong, R.L., Gearin, P.J., Riemer, S.D., Laake, J.L., Scordino, J.J., 2017. Survival rates of Steller sea lions from Oregon and California. J Mammal 98, 885–894. https://doi.org/10.1093/jmammal/gyx033

York, A.E. 1994. The Population Dynamics of Northern Sea Lions, 1975-1985. Marine Mammal Science 10 (1): 38–51. doi:10.1111/j.1748-7692.1994.tb00388.x.

York, A. E., J. R. Thomason, E. H. Sinclair, and K.A. Hobson. 2008. Stable carbon and nitrogen isotope values in teeth of Steller sea lions: Age of weaning and the impact of the 1975-1976 regime shift in the North Pacific Ocean. Can. J. Zool. 86: 33-44.

Zhang, R.H. and S. Levitus, 1997: Structure and cycle of decadal variability of upper-ocean temperature in the North Pacific. J. Climate, 10, 710-727.

Chapter 4. POPULATION VIABILITY ANALYSIS FOR THE WESTERN DISTINCT POPULATION SEGMENT OF STELLER SEA LIONS IN ALASKA

Publication history: This study was co-authored with Devin S. Johnson, Tom S. Gelatt, and Sarah J. Converse. At the time this dissertation was published, this chapter was not in review with a journal.

Abstract: Understanding the spatio-temporal variability in demography offers insight into the factors that underlie population dynamics and viability of wildlife populations. This is particularly true for species with divergent demographic patterns across large geographic areas. The divergent demographic trends across the range of Steller sea lions (*Eumetopias jubatus*) have been studied extensively but remain poorly understood. We developed a Bayesian integrated population model for the western distinct population segment of Steller sea lions in Alaska that combines rookery counts and capture-recapture data from 2000-2021 to estimate demography, abundance trends, and the effects of environmental variability on population growth and viability. Our results show declining age-specific survival rates in the latter part of the study period and highlight demographic differences between subregions, including reduced pup survival in the central Aleutian Islands and reduced yearling survival in the central and western Aleutians Islands. Range-wide abundance increased by 1.15% yr^{-1} (95% credible interval: -8.2;11.2%) over the study period, with variable growth rates across the range. We estimated higher rates of annual growth (~3% yr^{-1}) east of Samalga Pass and a decline (-2.5% yr^{-1}) west of Samalga Pass. Our model framework represents an improvement upon existing approaches for estimating abundance, facilitates accounting for uncertainty in future viability due

to environmental variability, and will be useful in evaluating the efficacy of ongoing monitoring and conservation actions for the species across its range.

Keywords: Steller sea lion, population viability, integrated population model, Bayesian hierarchical model, endangered species, sensitivity analysis, environmental variability

4.1 INTRODUCTION

For species that exhibit divergent demographic patterns across large geographic areas, understanding the spatio-temporal variability in demography provides valuable insight into the drivers of population dynamics. For depleted or declining populations, the accuracy of demographic estimates can directly affect managers' abilities to develop effective conservation strategies. However, estimating vital rates and detecting trends in abundance for a depleted top predator with a complex life history and a large geographic range is a challenging endeavor, where inferences about broadscale patterns are necessarily made from spatio-temporally limited datasets or covariates. Combining multiple data sources within the formal framework of an integrated population model (IPMs; Besbeas et al. 2002, Brooks et al. 2004) can often improve precision, reduce bias, and facilitate the estimation of parameters not directly informed by data (Schaub et al. 2007, Tavecchia 2009, Abadi et al. 2010). Integrated population models can also facilitate the estimation of spatio-temporal variance in demographic parameters, which is fundamental to conducting population viability analyses (PVA; Beissinger & Westphal 1998) that allow managers to understand the population-level implications of this variability while facilitating the evaluation of extinction risk, developing quantitative recovery criteria, or proposed recovery strategies.

IPMs are an emerging and evolving tool in wildlife applications that have proven useful for examining population dynamics of species with complex life histories (e.g., brown bears,

Bled et al. 2017; polar bears, Regehr et al. 2018), and other issues of management importance such as the effects of anthropogenic stressors and environmental variability on demography (e.g., Rhodes 2011, Cleasby et al. 2017, Abadi et al. 2017, Pirotta et al. 2018). Using an IPM as the foundation of a PVA can improve demographic estimates and facilitate a full accounting of uncertainty when examining viability or progress toward established recovery criteria. IPM-based PVAs have been used to evaluate the effects of climate change and management actions on wildlife populations of conservation concern (Saunders et al. 2018), including beluga whales (Mosnier et al. 2015, Ch. 5), harbor seals (Boveng et al. 2018), and emperor penguins (Jenouvrier et al. 2019).

The western distinct population segment (wDPS) of Steller sea lions (*Eumetopias jubatus*) in Alaska exhibited substantial and rapid declines during the 1980s, which have been followed by divergent trends in abundance over the large geographic range of this population. Abundance in the central and western Aleutian Island rookeries west of Samalga Pass continues to decline while abundance in eastern regions of the wDPS range has increased since the early 2000s (Fritz & Stinchcomb 2005, Fritz et al. 2016). Despite extensive research aimed at identifying drivers of regional population dynamics, the underlying drivers of divergent abundance trends remain poorly understood. These patterns have been attributed at least partly to reduced and variable age-specific survival and fecundity (York 1994, Holmes et al. 2007), with recent evidence suggesting depressed pup survival (Warlick et al. *in review*; Ch. 3) in areas of ongoing decline and lower apparent survival of female breeders in the late 2010s in the Gulf of Alaska (Maniscalco 2018).

Here, we build on the analyses of Warlick et al. (*in review*; Ch. 3) and present a PVA for the wDPS of Steller sea lions based on an IPM informed by mark-resight and aerial survey data

from 2000-2021. Our goals were to (1) identify regional differences in vital rates that may be driving divergent abundance trends, (2) improve upon the existing approach of estimating abundance, and (3) examine the population-level implications of environmental variability and spatio-temporal differences in demography. Our results can inform future research, management decisions, and the evaluation of progress towards recovery criteria. More generally, our approach serves as a useful framework for studying the effects of environmental variability on population dynamics and viability with applicability to other species of conservation concern, especially those with a high degree of spatio-temporal variability in demography over their range.

4.2 METHODS

4.2.1 *Study system*

The range of the wDPS of Steller sea lions includes rookery and haulout sites along the coastline of the eastern, central, and western Gulf of Alaska (GoA) and the numerous islands that comprise the eastern, central, and western Aleutian Island (AI) management subregions (Figure 4.1). The biological processes driving primary production and ecosystem dynamics in the GoA and across the Aleutian archipelago are shaped by a dividing line at Samalga Pass (170°W; Stabeno et al. 1999, Ladd et al. 2005). The shallower passes to the east of Samalga Pass are characterized by a higher diversity of forage fish that supports a more diverse sea lion diet (Sinclair & Zeppelin 2002) compared to the deeper, colder, nutrient-rich passes to the west of Samalga Pass that are dominated by slower-growing forage fish (Hunt & Stabeno 2005, Sinclair et al. 2005, Rand et al. 2019). These generalized regional characteristics, supplemented by finer-scale variability, affect the foraging conditions experienced by individual sea lions.

During the breeding season, adult male bulls establish rookery territories starting in May before reproductively mature females arrive to give birth from late May to early July (Pitcher et

al. 2001, Kuhn et al. 2017). Throughout the summer, females with pups make short foraging trips that allow them to remain close to the rookery in order to nurse their young and build up energy reserves before going out to sea with their pups for the fall and winter (Raum-Suryan et al. 2002). Females exhibit a high degree of natal site fidelity and begin reproducing between the ages of 3 and 6 (Pitcher & Calkins 1981).

4.2.2 *Data*

Two data sources were combined in our model: (1) mark-resight data from sea lions that were hot-branded with individual marks as pups and resighted in five subregions of the wDPS range from 2000-2018 and (2) annual count estimates (Johnson & Fritz 2014) based on aerial survey data from 2000-2021 across the wDPS range.

The mark-resight data are conditioned on pup cohorts that were marked late in the summer breeding seasons from 2000-2017 at specific rookeries in five of the six subregions. Three cohorts were marked (2001, 2003, 2005) at rookeries in the eastern GoA (Seal Rocks, Wooded, n = 287), six cohorts were marked nearly biennially starting in 2000 at rookeries in the central GoA (Marmot and Sugarloaf Is., n = 1,184) and eastern AI (Ugamak Is., n = 997), three cohorts were marked (2013, 2015, 2017) in the central AI (Ulak Is., n = 159), and four cohorts were marked (2011, 2013, 2015, 2017) in the western AI (Agattu Is., n = 206). No cohorts were marked in the western GoA. In the eastern portion of the wDPS range (eastern-central GoA, eastern AI), resighting effort occurred May through August during vessel- and land-based surveys, generating a total of approximately 39,300 and 25,150 sighting records of branded females and males, respectively. In the western portion of the range (central and western AI), resightings were primarily based on observations generated from remote cameras.

Aerial surveys of Steller sea lions throughout Alaska have been conducted since the 1980s, though with more spatio-temporal consistency beginning in the 2000s (Fritz et al. 2016). Surveys generally occur from late June to early July after most pups are born and when haulout rates are highest (Fritz et al. 2016). Approximately 200 survey sites have been identified within the range of the wDPS and grouped according to the six management subregions. Images of sea lion rookeries and haulouts taken during aerial surveys were processed by two analysts who independently counted and designated individuals as pups and non-pups (the latter including juveniles, sub-adult males, adult females, and male bulls). These raw counts from 2000 to 2021 were then modeled using the agTrend R package (Johnson & Fritz 2014) to derive predicted subregion-specific abundance for pups and non-pups across both surveyed and unsurveyed sites in each year (Sweeney et al. 2022). All areas are not surveyed each year due to the costs and logistics of conducting aerial surveys in remote areas.

In addition to these two sea lion datasets, we examined the effects of environmental covariates on demography. Based on the results of Warlick et al. (*in review*; Ch. 3) and evidence documenting widespread impacts of the marine heatwave that persisted in the North Pacific from 2015-2017 (Suryan et al. 2021, Arimitsu et al. 2021), we chose to examine the effect of two covariates that may influence sea lion demography: the North Pacific Gyre Oscillation (NPGO) and sea surface temperature (SST). The NPGO is an oceanographic index that has been linked to the growth and abundance of various salmon and groundfish species (Kilduff et al. 2015, Ohlberger et al. 2016, Litzow et al. 2018) and changes in SST coincide with varying localized and basin-scale oceanographic conditions ranging from increased storminess to changes in prey distribution and availability, all of which could affect sea lion survival and reproduction. Monthly data for the NPGO in summer months were obtained from the NOAA National Center

for Environmental Information (NOAA NCEI 2020) and NOAA Physical Science Laboratory (NOAA PSL 2020), averaged to create annual values, and *Z*-scored. Monthly data for SST around the Gulf of Alaska and the Aleutian Island chain (47.5°N to 58.1°N and 174.5°W to 159°W) in summer months (June-Aug) were obtained from the Copernicus Marine Environment Monitoring Service (Martin et al. 2019), averaged over time and space to create a single annual time series, and *Z*-scored. Though we recognize the spatio-temporal complexity and nuance of the effect of localized environmental conditions on long-lived, adaptive top predators, we used a single timeseries for each covariate in the estimation of vital rates in all subregions even though these conditions and their effects likely vary across the wDPS range. We expected that these large-scale predictors could have common effects across the range and that the sample sizes in subregions in the western portion of the wDPS range would not support independent estimates of covariate effects. We therefore relied on other elements of model structure (e.g., random effects over time and space) to capture critical spatio-temporal variability in demographic rates.

4.2.3 *Statistical analyses*

Our IPM has two subcomponent models: a multi-event model (Kendall 2004, Pradel 2005) to estimate demographic rates based on mark-resight data, and a state-space model based on aerial survey data to estimate abundance. Multi-event models have been increasingly used to examine vital rates for species with complex life histories (Tavecchia et al. 2016, Payo-Payo et al. 2016, Santidrian Tomillo 2017, Sanz-Aguilar et al. 2017, Champagnon et al. 2018, Regehr et al. 2018, Himes Boor et al. *In revision*). As described in Warlick et al. (*in review*; Ch. 3), we use a multi-event model to account for reproductive state uncertainty, as a nursing female may be seen with or without her pup.

4.2.3.1 Multi-event model

The multi-event model used for the analysis of mark-resight data is defined by both an ecological process, in which animals transition between true states according to demographic rates, and an observation process, in which individuals are resighted according to detection and state classification probabilities. States were defined by an individual's age, sex, and reproductive state and included pups, yearlings, age-2 individuals, age-3 individuals, age-4 individuals, age-5 individuals, breeding adult females, non-breeding adult females, and adult males. Females can first be in the breeder state starting at age 4 and must transition into one of the adult female states by age 6 (Figure 4.2) conditional on survival. Males are defined as adults at age 6. The state process model,

$$z_{i,t}|z_{i,t-1} \sim \text{categorical}(\Omega_{z_{i,t-1},i,t-1})$$

describes the state z of individual i at occasion t, conditional on the individual's state at the previous occasion, modeled as categorically distributed according to transition array Ω, which is composed of survival ($\phi_{i,t}$) and, for some transitions, pupping probability ($\psi_{i,t}$). We estimate survival for each sex and age, and pupping probabilities describe transitions between states (e.g., first-time pupping probability, ψ_3, describes the probability of pregnancy at age 3 resulting in having a pup at age 4; pupping probability for repeat breeding, ψ_B, describes the probability that an established breeder has a pup in successive years; pupping probability for non-breeders, ψ_{NB}, describes the probability that a female that was a non-breeder in the previous year breeds). Spatio-temporally varying survival and pupping probabilities for each state were modeled as functions of fixed effects of natal subregion, environmental covariates, and smoothed random effects of year:

$$\text{logit}(\gamma_{a,s,r,t}) = \mu^{\gamma}_{a,s} + \mathbf{x}'\boldsymbol{\beta}^{\gamma}_{a} + \epsilon^{\gamma}_{a,r,t}$$

where $\gamma_{a,s,r,t}$ is a general demographic parameter for age *a,* sex *s,* region *r*, and year *t*; $\mu_{a,s}^{\gamma}$ is an age and sex-specific intercept; **x** is a vector of covariates (including natal region and environmental variables) with associated coefficients $\boldsymbol{\beta}_a^{\gamma}$; and $\epsilon_{a,r,t}^{\gamma}$ is a smoothed annual random effect. We used informed priors to estimate age- and sex-specific demographic rates, where each $\mu_{a,s}^{\gamma}$, was assumed to be drawn from a Gaussian distribution with a mean and a standard deviation based on similar age- and sex-specific survival and natality estimates from sea lions marked and resighted in southeast Alaska and Russia during the early 2000's (Hastings et al. 2018, A. Altukhov *unpublished data*). Separate fixed effects of natal region were estimated for survival of pups, yearlings, age-2 individuals, and breeding females, and for pupping probabilities of age-3, age-4, and age-5 individuals, established breeders, and previous non-breeders. A pooled effect of natal region was estimated for the survival of male and female juvenile age groups (age-3, age-4, and age-5 individuals) for subregions in the eastern versus western portions of the wDPS range. The effects of environmental covariates (SST, NPGO) were estimated for the survival of male and female pups, yearlings, age-2 individuals, breeding females, and pupping probabilities for first-time and repeat breeders based on the assumption that those demographic rates would be the strongest drivers of population dynamics and most susceptible to environmental perturbation.

We applied penalized complexity (PC) priors (Simpson et al. 2017, van Erp et al. 2019) for defining prior distributions on fixed effects of natal region and environmental variables and on random year effects. This approach shrinks the coefficients toward zero in the absence of strong support for an effect and can improve parameter estimability and regulate model complexity. The PC priors for the fixed effects of natal region and environmental covariates were constructed by defining the conditional prior distribution $\beta_{a,r}^{\gamma} \sim \mathrm{N}(0, \sigma_{\gamma_a})$ with standard deviations σ_{γ_a}, which were subsequently distributed according to an exponential distribution with

a fixed shrinkage rate $\sigma_{\gamma_a} \sim \text{Exp}(\lambda = 1)$ to apply moderately strong shrinkage. Random year effects were shared between sexes and estimated only for subregions in the eastern portion of the wDPS range (due to insufficient sample sizes in the central and western AI) using an intrinsic Gaussian conditional autoregressive (CAR) model prior distribution that enforced autocorrelation between years,

$$\boldsymbol{\epsilon}^{\gamma}_{a,r} \sim \text{MVN}(0, \sigma\mathbf{Q}),$$

where $\mathbf{Q}$ is the precision matrix of an intrinsic autoregression of order 2 (IAR(2); Speckman and Sun 2003) scaled by σ and $\boldsymbol{\epsilon}^{\gamma}_{a,r}$ is a vector of temporal random effects, $\epsilon^{\gamma}_{a,r,t}$. The IAR(2) model imposes a smoothness constraint that reduces model complexity relative to independent random effects. For survival of pups, yearlings, age-2 individuals, and breeding females, separate random effects were estimated for each of the four subregions in the eastern portion of the wDPS range (western GoA-eastern AI). For survival of age-3, age-4, and age-5 males and females and pupping probabilities for age-4 individuals and established breeders, random year effects were shared across all four of the easternmost subregions. Temporal variability was not estimated for several demographic rates due to poor estimability; namely, non-breeding female adult survival and first-time pupping probability for age-3 individuals, age-5 individuals, and previous non-breeders. As no individuals were marked in the western GoA during the study period, demographic rate estimates for that subregion were largely informed by aerial survey data.

The events in the multi-event model are defined by the possible observations of individuals. For all states except for breeding females, events are detected and not detected. For breeding females, events are: seen without a pup, seen with a pup, or not detected. These events are modeled as:

$$y_{i,t}|z_{i,t} \sim \text{ categorical}(\Theta_{z_{i,t}i,t})$$

where observations $y_{i,t}$ conditional on the true state $z_{i,t}$ are categorically distributed with observation array Θ, which is composed of an individual's detection probability at time *t*, $p_{i,t}$, and the probability of correctly ascertaining the presence of a pup for female breeders, $\delta_{i,t}$. Temporal variation was modeled as,

$$\text{logit}(p_{a,s}) = \mu_{a,s}^{p} + \epsilon_{t}^{p}$$

where the mean intercept $\mu_{a,s}^{p}$ for each sex *s* and age *a* was estimated using a logit-transformed uniform (0,1) prior distribution. Interannual variability in detection probability was estimated with random year effects assumed to be drawn from a Gaussian distribution as $\epsilon_{t}^{p} \sim \text{N}(0, \sigma_{p})$, with standard deviations σ_{p} *a priori* distributed according to an exponential distribution with a fixed shrinkage rate as described above. As in Warlick et al. (*in review*; Ch. 3), we used the number of sightings per individual per year (with pups or without) as a categorical covariate for the multi-event classification probability parameter, $\delta_{i,t}$.

4.2.3.2 State-space model to estimate pup abundance

A state-space model was used to estimate pup abundance in year *t* in subregion *r* using the modeled posterior median and standard deviation of 'realized' counts for all rookeries and haulout sites across the range (surveyed and unsurveyed).

$$\text{N}_{\text{pup}_{r,t}} \sim \text{normal}(\text{N}^{\text{F}}_{\text{pup}_{r,t}} + \text{N}^{\text{M}}_{\text{pup}_{r,t}}, \sigma^{\text{pup}}_{r,t})$$

where annual pup abundance $\text{N}_{\text{pup}_{r,t}}$ in region *r* is normally distributed with a mean of annual pup abundance estimated in the stochastic population growth equations (described below) and variance $\sigma^{\text{pup}}_{r,t}$ equal to the known variance of the counts estimated from the agTrend analysis (Sweeney et al. 2022).

4.2.3.3 Integrated population model

The multi-event model was combined with the pup abundance model in an IPM framework using stochastic growth equations (Figure 4.3). The population process model was initialized one year prior to the start of the mark-resight data (2000) using a discrete uniform distribution with minimum and maximum values set at 75% and 125% of the expected counts based on the stable age distribution proportions. For example, for breeding females,

$$\mathrm{N}_{\mathrm{B}_{r,1}} \sim \mathrm{uniform}(\mathrm{N}_{\mathrm{min}_{r,1}} \cdot SA_{\mathrm{B}} \cdot 0.75, \mathrm{N}_{\mathrm{min}_{r,1}} \cdot SA_{\mathrm{B}} \cdot 1.25)$$

where $\mathrm{N}_{\mathrm{min}_{r,1}}$ is the sum of pup and non-pup in each region *r* in the initial year and *SA* is the stable age distribution proportions calculated using the eigen values and range-wide demographic rates estimated in Warlick et al. (*in review*; Ch. 3).

In each year *t* +1, the number of individuals at a given age was modeled using a Poisson distribution based on the number of individuals and survival and pupping probabilities in the previous year *t*:

$$\begin{bmatrix}
\mathrm{N}^{\mathrm{F}}_{\mathrm{pup}_{r,t+1}} \sim \mathrm{Binomial}(0.5, \mathrm{N}^{\mathrm{F}}_{\mathrm{B}_{r,t+1}}) \\
\mathrm{N}^{\mathrm{F}}_{1_{r,t+1}} \sim \mathrm{Poisson}(\mathrm{N}^{\mathrm{F}}_{\mathrm{pup}_{r,t}} \phi^{\mathrm{F}}_{\mathrm{pup}_{r,t}} \cdot m) \\
\mathrm{N}^{\mathrm{F}}_{2_{r,t+1}} \sim \mathrm{Poisson}(\mathrm{N}^{\mathrm{F}}_{1_{r,t}} \phi^{\mathrm{F}}_{1_{r,t}}) \\
\mathrm{N}^{\mathrm{F}}_{3_{r,t+1}} \sim \mathrm{Poisson}(\mathrm{N}^{\mathrm{F}}_{2_{r,t}} \phi^{\mathrm{F}}_{2_{r,t}}) \\
\mathrm{N}^{\mathrm{F}}_{4_{r,t+1}} \sim \mathrm{Poisson}(\mathrm{N}^{\mathrm{F}}_{3_{r,t}} \phi^{\mathrm{F}}_{3_t}(1-\psi_3)) \\
\mathrm{N}^{\mathrm{F}}_{5_{r,t+1}} \sim \mathrm{Poisson}(\mathrm{N}^{\mathrm{F}}_{4_{r,t}} \phi^{\mathrm{F}}_{4_t}(1-\psi_4)) \\
\mathrm{N}^{\mathrm{F}}_{\mathrm{B}_{r,t+1}} \sim \mathrm{Poisson}(\mathrm{N}^{\mathrm{F}}_{3_{r,t}} \phi_{3_t} \psi_3) + \mathrm{Poisson}(\mathrm{N}^{\mathrm{F}}_{4_{r,t}} \phi_{4_t} \psi_4) + \mathrm{Poisson}(\mathrm{N}^{\mathrm{F}}_{5_{r,t}} \phi_{5_t} \psi_5) + \mathrm{Poisson}(\mathrm{N}^{\mathrm{F}}_{\mathrm{B}_{r,t}} \phi_{\mathrm{B}_t} \psi_{\mathrm{B}}) + \mathrm{Poisson}(\mathrm{N}^{\mathrm{F}}_{\mathrm{NB}_{r,t}} \phi_{\mathrm{NB}_t} \psi_{\mathrm{NB}}) \\
\mathrm{N}^{\mathrm{F}}_{\mathrm{NB}_{r,t+1}} \sim \mathrm{Poisson}(\mathrm{N}^{\mathrm{F}}_{\mathrm{B}_{r,t}} \phi_{\mathrm{B}_t}(1-\psi_{\mathrm{B}})) + \mathrm{Poisson}(\mathrm{N}^{\mathrm{F}}_{\mathrm{NB}_{r,t}} \phi_{\mathrm{NB}_t}(1-\psi_{\mathrm{NB}})) + \mathrm{Poisson}(\mathrm{N}^{\mathrm{F}}_{5_{r,t}} \phi^{\mathrm{F}}_{5_t}(1-\psi_5)) \\
\mathrm{N}^{\mathrm{M}}_{\mathrm{pup}_{r,t+1}} \sim \mathrm{Binomial}(0.5, \mathrm{N}^{\mathrm{F}}_{\mathrm{B}_{r,t+1}}) \\
\mathrm{N}^{\mathrm{M}}_{1_{r,t+1}} \sim \mathrm{Poisson}(\mathrm{N}^{\mathrm{M}}_{\mathrm{pup}_{r,t}} \phi^{\mathrm{M}}_{\mathrm{pup}_{r,t}} \cdot m) \\
\mathrm{N}^{\mathrm{M}}_{2_{r,t+1}} \sim \mathrm{Poisson}(\mathrm{N}^{\mathrm{M}}_{1_{r,t}} \phi^{\mathrm{M}}_{1_{r,t}}) \\
\mathrm{N}^{\mathrm{M}}_{3_{r,t+1}} \sim \mathrm{Poisson}(\mathrm{N}^{\mathrm{M}}_{2_{r,t}} \phi^{\mathrm{M}}_{2_{r,t}}) \\
\mathrm{N}^{\mathrm{M}}_{4_{r,t+1}} \sim \mathrm{Poisson}(\mathrm{N}^{\mathrm{M}}_{3_{r,t}} \phi^{\mathrm{M}}_{3_t}) \\
\mathrm{N}^{\mathrm{M}}_{5_{r,t+1}} \sim \mathrm{Poisson}(\mathrm{N}^{\mathrm{M}}_{4_{r,t}} \phi^{\mathrm{M}}_{4_t}) \\
\mathrm{N}^{\mathrm{M}}_{6_{r,t+1}} \sim \mathrm{Poisson}(\mathrm{N}^{\mathrm{M}}_{5_{r,t}} \phi^{\mathrm{M}}_{5_t}) \\
\mathrm{N}^{\mathrm{M}}_{\mathrm{A}_{r,t+1}} \sim \mathrm{Poisson}(\mathrm{N}^{\mathrm{M}}_{5_{r,t}} \phi^{\mathrm{M}}_{5_t}) + \mathrm{Poisson}(\mathrm{N}^{\mathrm{M}}_{\mathrm{A}_{r,t}} \phi^{\mathrm{M}}_{\mathrm{A}_t})
\end{bmatrix}$$

Poisson distributions were used here (i.e., instead of sequential binomial distributions) because a Poisson-distributed age structure offered more stability in the population model, improved convergence, approximated binomial outcomes with these large numbers, and theoretically allowed for a small degree of emigration of age-specific individuals into regional populations (i.e., it was possible, but not probable, that $N_{age_{r,t+1}} > N_{age_{r,t}}$). Total abundance in each year and subregion was then calculated as the sum of all age classes and states, $N_{Tot_{r,t}} = \sum(N_{age_{r,t}})$. Neonate mortality *m* (i.e., the mortality that occurs between birth and marking) was assumed to be 5% (Merrick 1987), though this value likely varies considerably from year to year (Maniscalco et al. 2008). We also calculated the ratio of total abundance to the number of pups ($w_{r,t} = \frac{N_{Tot_{r,t}}}{N_{pup_{r,t}}}$); previously assumed to be a fixed value of $w = 4.5$ (known as a "pup multiplier") that has been used to derive total abundance from pup abundance (Calkins & Pitcher 1982).

4.2.3.4 Sensitivity and viability analyses

We conducted a sensitivity analysis for each of the six management subregions by examining the correlation coefficient (*r*) between posterior mean annual population growth rates (λ_t) and annual age-specific female survival and pupping rates.

To examine the viability of populations in each of the six management subregions, we projected the population forward in time for $T = 100$ years using the posterior distributions of the vital rate parameters estimated for the timeframe informed by mark-resight data (2000-2018). For each year in the 100-year projection period, we randomly selected posterior samples of random effect deviates from one of the eighteen data years (with replacement) and added this to posterior samples of the relevant intercept term and the relevant effect of environmental variability given generated SST and NPGO values, and back-transformed to derive stage-specific

abundance at $t + 1$. We randomly generated sets of predicted SST and NPGO values based on eight scenarios that increased or decreased the mean and/or standard deviation of each predictor for the 100-year projection period (Table 4.1). Due to the complex and variable nature of a top predator's response to environmental conditions, the comparison of projection scenarios is intended not as a predictive tool but instead to provide a general sense of how meaningful system change (e.g., under climate change) might impact population growth rates via the underlying demography. Posterior distributions of the population projections were summarized in terms of the average population growth rate $\lambda_t = \frac{N_{\mathrm{Tot}_{t+1}}}{N_{\mathrm{Tot}_t}}$, the probability of extinction, Pr(N_{Tot}<1), the probability of having no remaining breeding females, Pr(N_{B}<1), and the probability of experiencing positive population growth.

4.2.4 *Model assumptions and fitting*

For the multi-event model, the typical set of mark-recapture model assumptions applies, including that branding did not affect detection probability, that there were no identification errors, that mortality during the sampling season was negligible, that individuals were independent, that there was no unmodeled heterogeneity in survival and detection probabilities, and that marked individuals are representative of the entire population. Lack of fit issues were not apparent in the analysis of these data in Warlick et al. (*in review*; Ch. 3). For the abundance model, we assumed that there were no errors in classifying pups and that the pup count is nearly a complete census, as the surveys occur when pups are still remaining onshore.

The IPM was fit using NIMBLE (NIMBLE Development Team 2019) within the R programming environment (R Core Development 2018) using 45,000 iterations, 20,000 burn-in, an adaptation rate of 10, and thinning rate of 1. Convergence was evaluated using visual

inspection of chains and the Brooks-Gelman-Rubin statistic (Gelman & Rubin 1992; Brooks & Roberts 1998) $\hat{R} < 1.1$. Population projections were carried out in R using the MCMC chains from NIMBLE.

4.3 RESULTS

4.3.1 *Vital rates*

Age-specific vital rates varied notably by region. Female pup survival (ϕ_P) was lower in the central AI (0.31, 95% CI: 0.24-0.41) and higher in the western AI (0.71, 0.62-0.81), with a range-wide average of 0.54 (0.38-0.75; Figure 4.4). Pup survival rates in each of the four subregions where we were able to estimate temporally varying survival (eastern GoA-eastern AI) were lower toward the end of the study period (Figure 4.5). Female yearling survival (ϕ_1) was notably lower in the central AI (0.49, 0.28-0.71) and western AI (0.59, 0.46-0.73), with a range-wide average of 0.72 (0.54-0.87). Male pup and yearling survival was slightly lower than that of females but followed similar regional and temporal patterns. Survival of older juveniles (ϕ_3, ϕ_4, ϕ_5) did not vary notably across the subregions but exhibited a slightly negative trend over the study period. Female adult breeding survival (ϕ_B) was relatively similar across subregions with the exception of a lower average rate in the eastern AI, where rates declined between 2000-2008 (Figure 4.5). Age-specific first-time pupping probability was highest for age-5 individuals (ψ_4) and similar across regions. The probability of pupping for age-4 individuals (ψ_3) was lower in the eastern portion of the wDPS range and higher in the western portion relative to the range-wide average (Figure 4.4). The probability of pupping for repeat breeders (ψ_B) increased from eastern to western subregions with the exception of the western AI where the rate was lowest.

Pupping probabilities for repeat breeders were lower in the latter half of the study period (Figure 4.5).

4.3.2 *Population growth rates, abundance, and age structure*

Over the twenty-year study period, the range-wide abundance of the wDPS increased from 33,568 (95% CI: 31,430-35,723) in 2000 to 48,278 (43,267-53,900) in 2021, representing an average growth rate of 1.15% (-7.4; 8.4%) per year (Figure 4.6, Figure 4.7). However, abundance trends in each of the subregions varied, with an increasing abundance trend in the subregions in the eastern portion of the wDPS and a decreasing trend in the central and western AI subregions (Figure 6). The mean annual population growth rate was highest in the eastern AI (3.7%, 95% CI: -4.5; 14.0%) and central (3.1%, -9.6; 14.2%) and western (3.4%, -8.4; 20.9%) GoA followed by the eastern GoA (1.8%, -11.6; 11.5%). The mean annual population growth rate was lowest, and negative, in the central (-1.8%, -5.8; 1.4%) and western AI (-3.2%, -9.3; 5.0%) (Figure 4.7).

The average age structure across the six subregions was approximately 20% pups, 20% breeding females, 12% yearlings, 19.1% juveniles, 5.6% non-breeding females, and 15.4% adult males. However, there were a few notable exceptions, including a lower proportion of pups and of female breeders in the western AI relative to what would be expected based on a range-wide stable age distribution (Appendix B). In contrast, in the central AI, there was a higher proportion of pups and breeding females with a lower proportion of yearlings and juveniles. In the wDPS as a whole, the $\frac{N_{Tot}}{N_{pup}}$ ratio was approximately 4.4 (95% CI: 3.2-5.4) but varied over time and across the six subregions. Specifically, this ratio was lower than the range-wide average in the eastern

and western GoA and central AI, and higher than the range-wide average in the western AI (Figure 4.8).

4.3.3 *Sensitivity and viability*

Most female demographic rates were positively correlated with population growth rates, though credible intervals of many region-specific correlation coefficients overlapped zero with the exception of repeat pupping probability and survival of females with pups (Appendix B). Based on demographic rate estimates during the data period, abundance during the 100-year projection period increased in subregions east of Samalga Pass and declined in the western subregions (Figure 4.9). The probability of extinction in 100 years was close to zero for the subregions with increasing population trends in the eastern portion of the wDPS range and in the central AI, but was approximately 2% (95% CI: 1.7-2.5%) in the western AI. Similarly, the probability of having no remaining female breeders was effectively zero in all subregions except the western AI (11.5%, 10.7-12.6%). The probability of a negative abundance trend was close to zero for all subregions in the eastern portion of the wDPS range and was approximately 99.2% and 100% for the central and western AI subregions, respectively.

Estimated effects of summer SST and positive-phase NPGO conditions on pupping probability and the survival of pups and yearlings were positive (Appendix B). Our prediction scenarios indicated that adjusting the mean of environmental covariates drove the greatest percentage changes in population growth rates compared with adjusting the variability (Table 4.1). However, the magnitude of the change in population growth rates varied based on the underlying demography in each of the six subregions, with particularly notable effects in the western AI, where rates of decline were lower in scenarios with warmer SST and warm-phase NPGO conditions and less variability, and faster and more uncertain in scenarios with lower

mean SST and cool-phase NPGO and greater variability relative to baseline conditions (Figure 10).

4.4 DISCUSSION

We combined mark-resight data and annual pup abundance estimates from aerial surveys to examine the demographic factors underlying divergent trends in abundance within six management subregions across the range of the wDPS of Steller sea lions in Alaska. We undertook this analysis in order to (1) identify regional differences in vital rates that may be driving divergent abundance trends, (2) improve upon the existing approach of estimating abundance, and (3) examine the population-level implications of environmental variability and spatio-temporal differences in demography. Our results indicated that sea lion population dynamics vary due to average regional demographic differences, environmental factors, and residual temporal variance. This information can inform future research priorities and the design of management strategies for this population.

Understanding regional differences in survival and natality over time and across the wDPS range is fundamental to gaining insights about the drivers of observed trends in Steller sea lion abundance. Empirical evidence and ecological theory suggest that population dynamics are most sensitive to changes in adult survival (Heppell et al. 2000, Runge et al. 2004, Gormley et al. 2012), but also to fecundity and offspring survival, as these rates tend to be more variable (Lacy et al. 2017, Manlik et al. 2017). Our results indicated that populations to the west of Samalga Pass may be continuing to decline via two different demographic mechanisms. In the central Aleutian Islands, pup and yearling survival is low and apparently not offset by higher reproductive rates. In the western Aleutian Islands, the decline may be driven by lower juvenile survival, as the lower reproductive rates combined with high pup survival indicate high maternal

investment. Our IPM also allowed us to estimate lower survival rates for pups and breeding females during the latter part of the study period in subregions east of Samalga Pass. Lower breeding female survival was also seen in the eastern GoA in the late 2010's (Maniscalco 2018) and could dampen population growth rates in areas with stable or growing populations or cause further declines if survival and pupping probabilities have also decreased in the western and central AI subregions where sample sizes were too small to estimate temporal variance.

Despite the complexities of quantifying the effects of ocean conditions on long-lived top predators, our simplified example of the effects of environmental perturbations highlights the importance of understanding the effects of environmental variability on population viability. Under prediction scenarios where environmental conditions (i.e., NPGO and SST) were projected to remain similar to historical conditions, the estimated probability of extinction for the western Aleutian Island subregion was still relatively small (~2%), though the 100-year time horizon is relatively short for a long-lived mammal and there was a high probability of a continued declining trend. Our results revealed that the potential effects of changing oceanographic conditions were largest in the western AI subregion, where the population is smallest and key demographic rates, namely survival of pups and yearlings and repeat pupping probabilities were depressed relative to the range-wide average. In other words, the regional response to environmental perturbation is dependent on the magnitude of the covariate effect as well as baseline demographic rates and age structure. Our analysis contained several simplifying assumptions that could be improved upon in future studies with additional years of monitoring data, including estimating region-specific covariate effects; estimating temporally lagged covariate effects; examining the effect of an increased frequency of extreme environmental conditions; and including temporal autocorrelation that would accurately capture the cyclic

nature of basin-scale indices such as the NPGO. However, as is, our analysis provides insights into the population's resilience to oceanographic changes despite our lack of knowledge about underlying causal mechanisms such as changes in prey availability. An improved understanding of a population's sensitivity to environmental perturbation is fundamental to the assessment of threats and the development of recovery criteria under the U.S. Endangered Species Act.

Accurate and timely estimates of demographic parameters can be valuable for the development of effective conservation measures and monitoring strategies that aim to maintain the resilience of stable populations or recover depleted ones. However, estimating these parameters can be challenging for marine mammals due to the high cost of surveys, small sample sizes, and the longer time series needed for long-lived organisms. While past approaches – involving summing aerial survey counts or using a "pup multiplier" to derive total abundance – have provided convenient metrics for tracking trends, our IPM-based PVA framework provides a more robust framework for estimation of abundance and other demographic parameters that accounts for uncertainty in female reproductive state and imperfect detection in mark-resight and aerial surveys. While the $\frac{N_{Tot_r}}{N_{pup_r}}$ ratios estimated in this study were approximately 4.4 (3.2-5.4), similar to the traditional 4.5 "pup multiplier", a closer examination of the regional and temporal variability in that ratio revealed how using it as an abundance multiplier may lead to biased or inaccurate abundance estimates of population growth rates for regions or time periods where age structure may not be stable, such as was found in this study for the central and western AI subregions (Figure 4.7). Relying on biased estimates of population growth rates for the subregions west of Samalga Pass (which have been a deciding factor in evaluating whether downlisting criteria have been met; NMFS 2020) may become increasingly problematic if abundance in these areas continues to decline. This work highlights the importance of developing

a unified approach for monitoring demographic trends in Steller sea lions that maximizes available resources to obtain precise and unbiased information. Incorporating additional information on stressors to the population within this framework will be useful in examining the abundance and long-term viability of Steller sea lions in Alaska and across the species' range as new data on climate variability become available.

Identifying causal mechanisms underlying changes in demography for highly mobile, long-lived top predators remains a challenge for conservation biologists, particularly for species that exhibit divergent abundance trends across a large geographic range. Integrated population modeling facilitates reducing and accounting for all sources of uncertainty when examining the effects of natural or anthropogenic stressors on the population dynamics and viability of declining or depleted populations. Improving estimation and reducing uncertainty in spatio-temporal demographic patterns can inform the decision-making process, as reliable estimates are needed in assessing progress toward recovery or downlisting criteria under the U.S. Endangered Species Act.

4.5 ACKNOWLEDGEMENTS

We thank the staff of NOAA Fisheries Marine Mammal Lab and other institutions for the effort and time dedicated to mark-resight and aerial survey fieldwork, which was conducted under MMPA and ESA permit numbers 782-1532-00, 782-1532-01, 782-1532-02, 782-1532-03, 782-1768-00, 782-1768-01, 782-1889, 14326, 14326-01, 14326-02, 18528, and 22289, and animal care and use committee approvals A/NW 2010-4, A/NW 2013-2, and A/NW 2016-3. The findings and conclusions of the NOAA and USGS authors in the paper are their own and do not necessarily represent the views of the National Marine Fisheries Service, NOAA or United States

Geological Survey. Any use of trade, firm, or product names is for descriptive purposes only and does not imply endorsement by the U.S. Government.

4.6 FIGURES AND TABLES

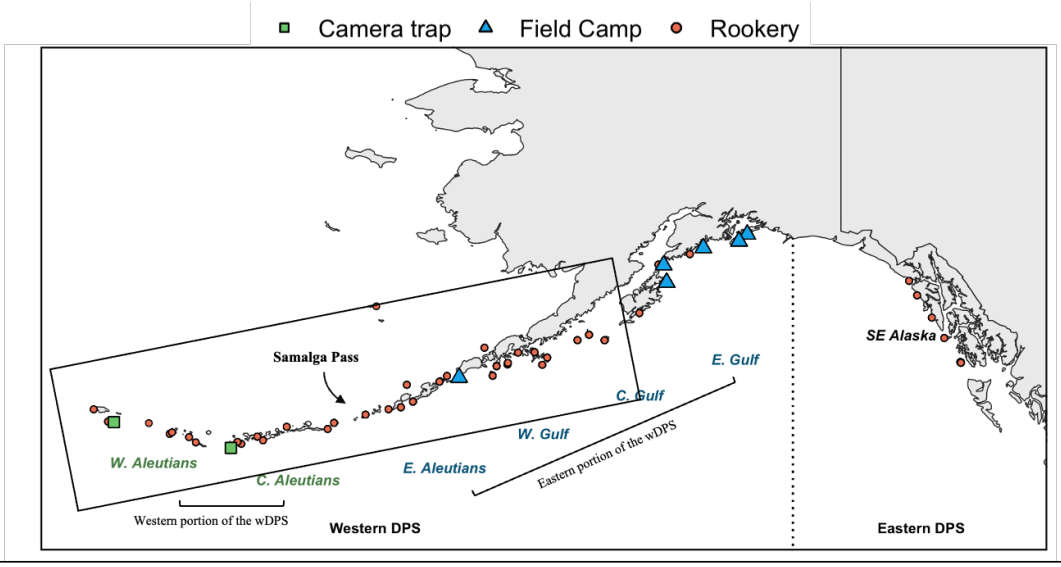

	2000	2001	2002	2003	2004	2005	2008	2009	2010	2011	2013	2014	2015	2017
E. GoA	--	107	--	100	--	80	--	--	--	--	--	--	--	--
C. GoA	258	--	194	--	185	--	178	--	178	--	--	191	--	--
E. Aleu	--	175	--	150	--	200	--	188	--	198	--	--	--	86
C. Aleu	--	--	--	--	--	--	--	--	--	--	58	--	51	50
W. Aleu	--	--	--	--	--	--	--	--	--	54	52	--	50	50

Figure 4.1: Steller sea lion field camps (blue triangles) in the eastern portion of the range, camera traps (green squares) in the western portion of the range, and rookeries (red) throughout the western distinct population segment (wDPS) (excluding Russia) and southeast Alaska (eastern DPS that extends along the U.S. West Coast). Rectangle indicates the spatial extent from which sea surface temperature data were aggregated. Table shows the number of branded and released pups in each subregion over the study period.

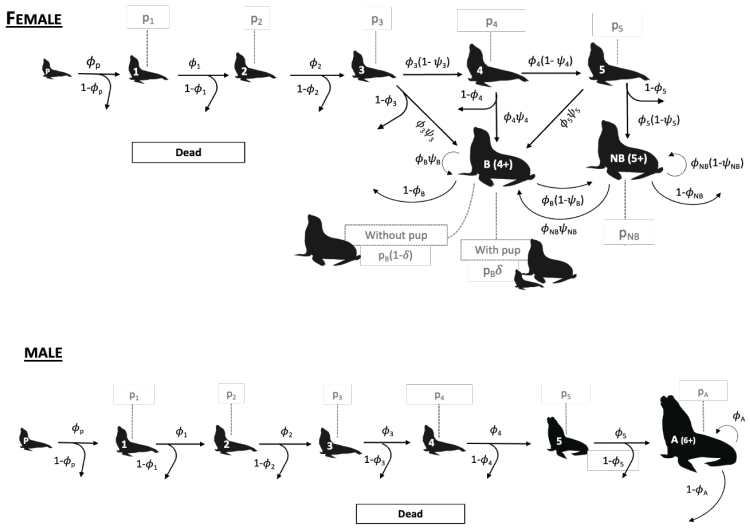

Figure 4.2: Reproduced from Warlick et al. (*in review*; Ch. 3), life cycle diagram for female and male Steller sea lions, indicating true ecological states (pup, juveniles age-1, age-2, and age-3, pre-breeding subadults age-4 and age-5, breeding adult females (B(4^+)), non-breeding adult females (NB(5^+)), and adult males (A(6^+)). Survival (ϕ) and pupping (ψ) probabilities denote transitions between true states (black lines) and detection probabilities (p) denote possible observation events for each age and breeding (with or without pup) and non-breeding females (grey dotted lines).

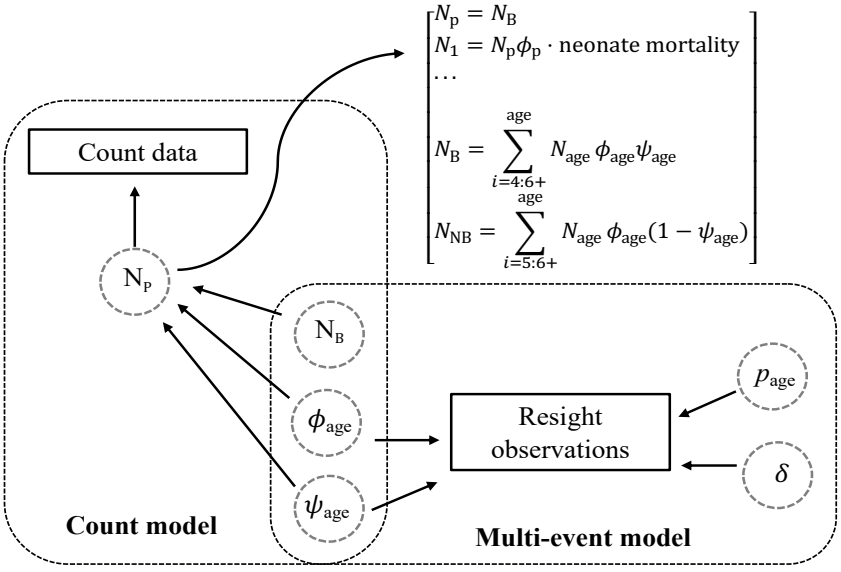

Figure 4.3: Directed acyclic graph representing the integrated population model framework including subcomponent models using aerial survey and mark-resight data.

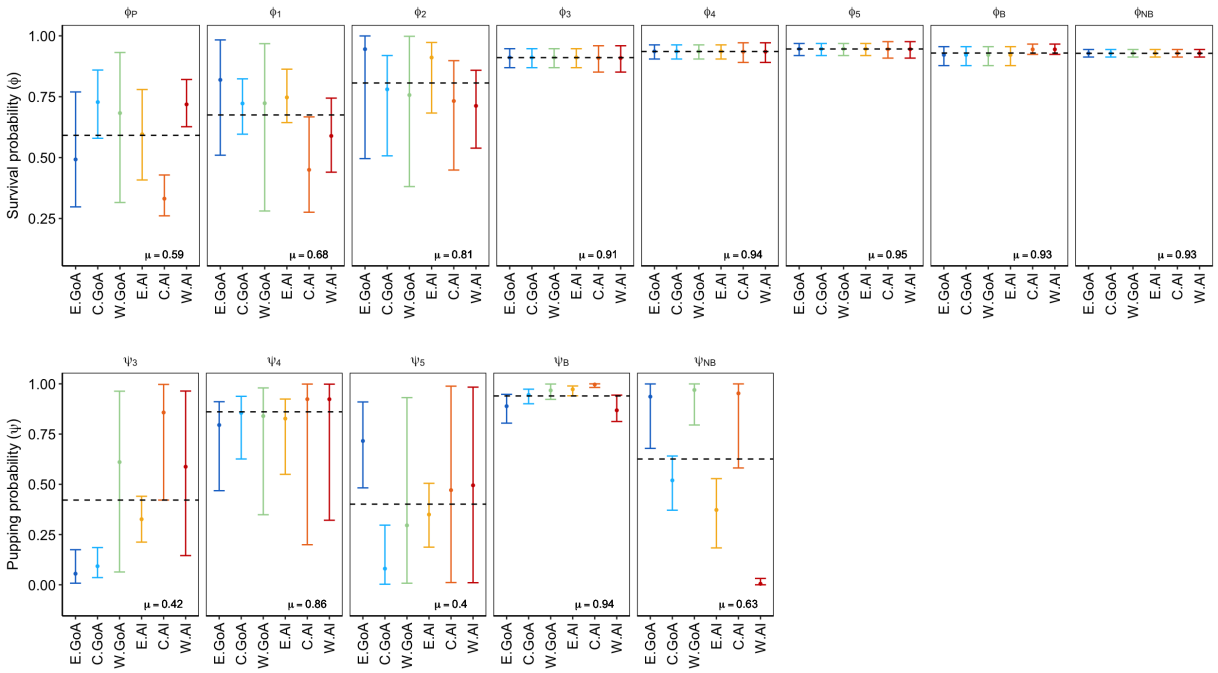

Figure 4.4: Posterior mean and 95% credible intervals for age-specific survival and pupping for female Steller sea lions across the six wDPS subregions, with the range-wide average represented by the dashed line. Male survival rates were similar (Appendix B) but are not shown for readability.

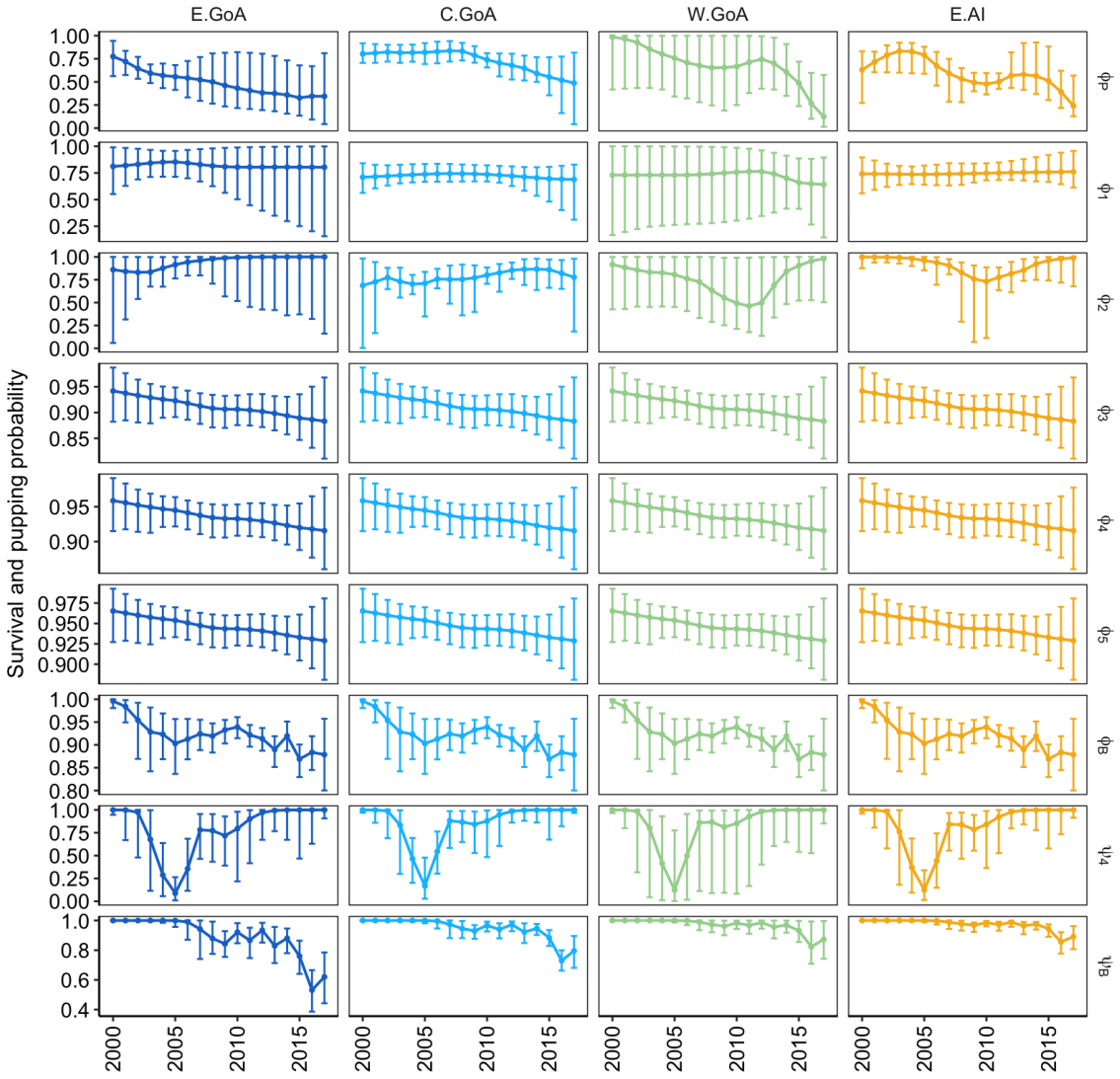

Figure 4.5: Posterior mean and 95% credible intervals for time-varying Steller sea lion female survival rates across the six wDPS subregions.

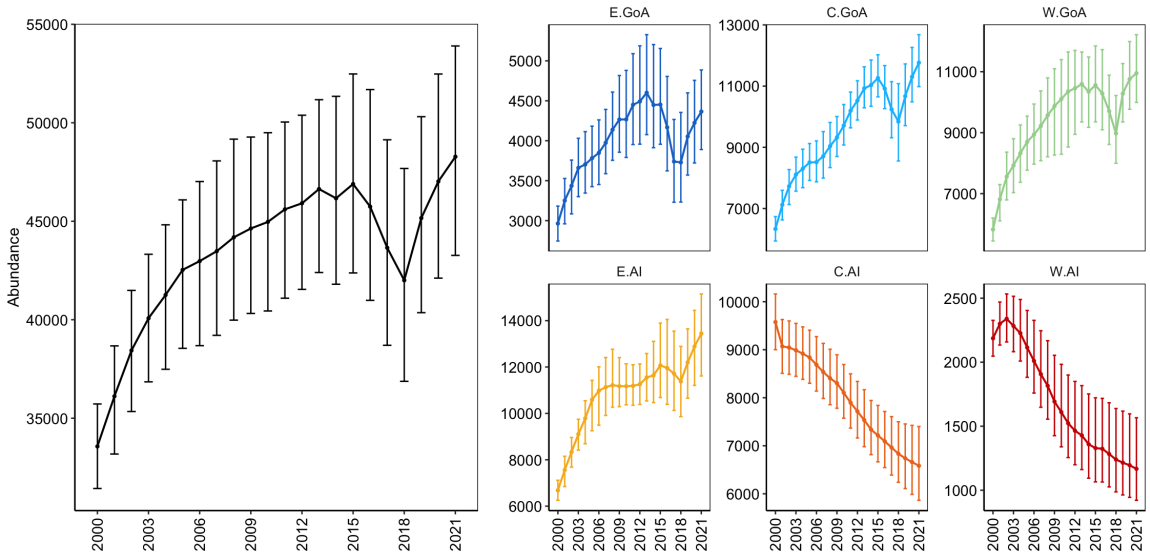

Figure 4.6: Posterior mean and 95% credible intervals of total abundance of Steller sea lions in the six wDPS subregions (colors) and range-wide (black).

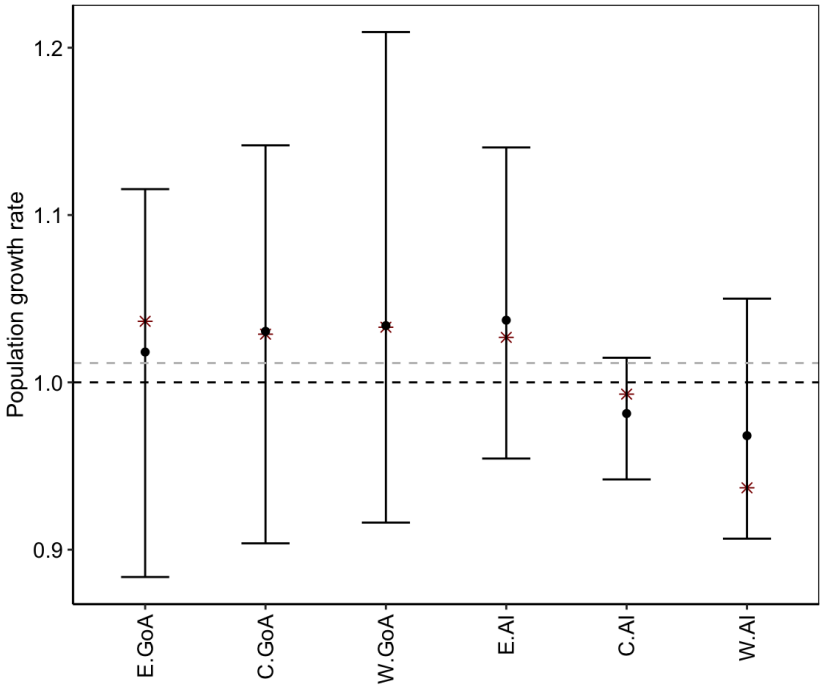

Figure 4.7: Posterior mean and 95% credible intervals of Steller sea lion population growth rates in the six wDPS subregions and range-wide (grey dashed line) based on abundance estimates from the IPM and from aerial survey data treated with agTrend alone (red asterisks).

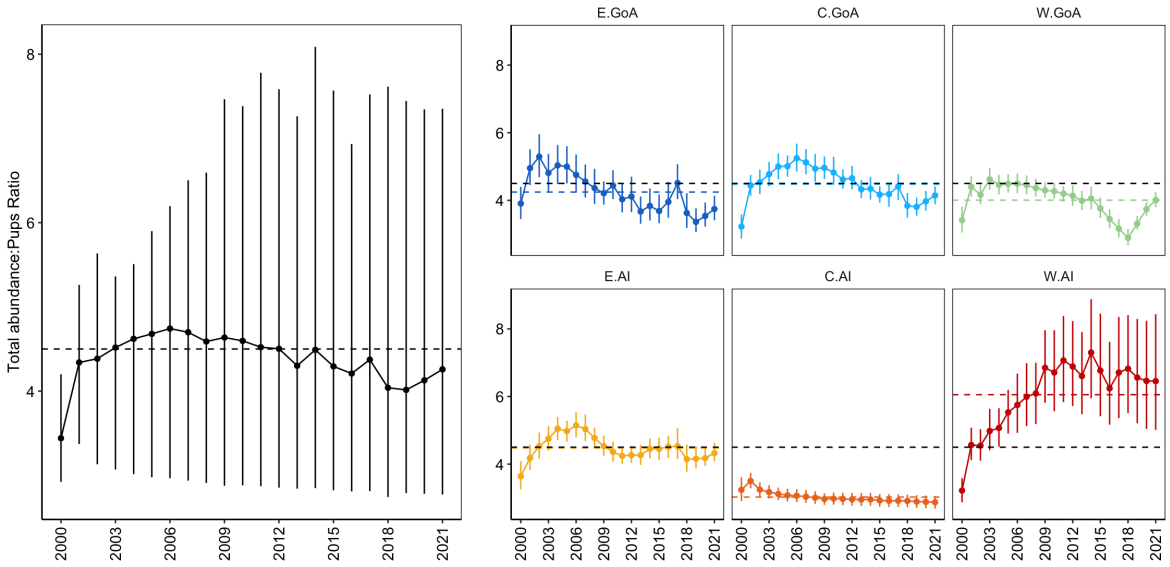

Figure 4.8: Posterior mean and 95% credible intervals of the ratio of total abundance to pup abundance range-wide (black) and in each of the six wDPS subregions (colors), with the traditional 4.5 "pup multiplier" (black dashed line) and the regional averages (colored dashed lines).

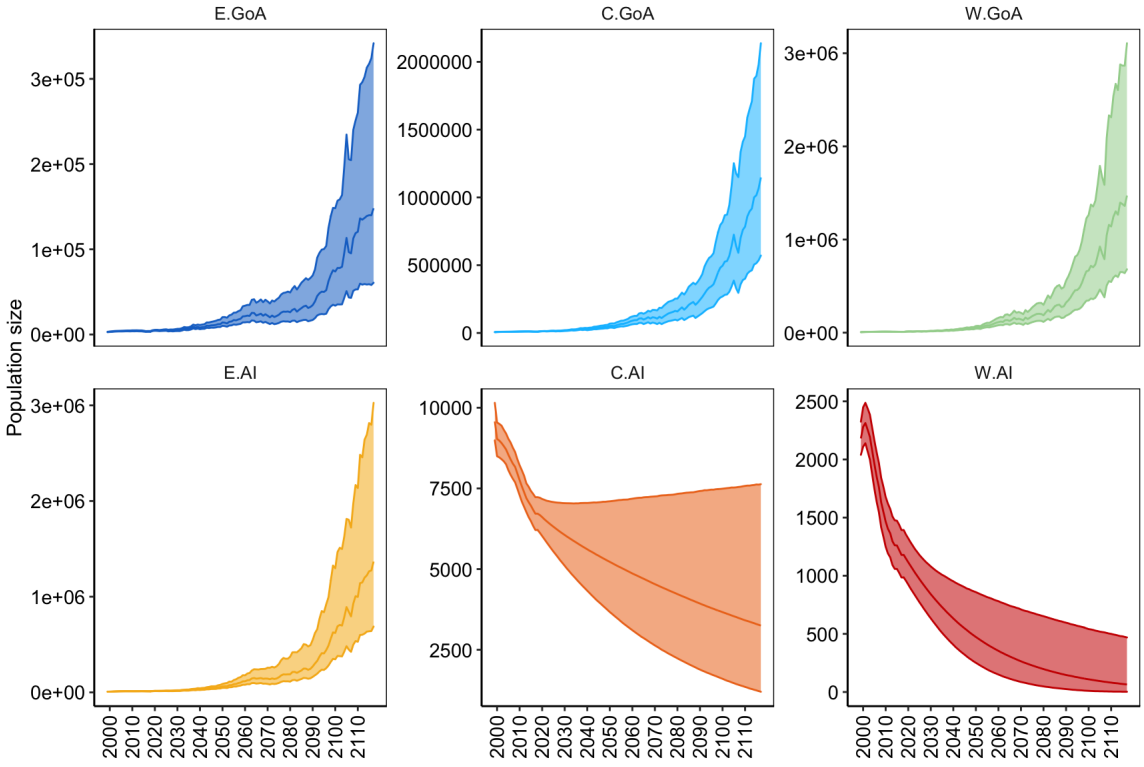

Figure 4.9: Total Steller sea lion abundance in each of the six wDPS subregions over the 100-year projection period.

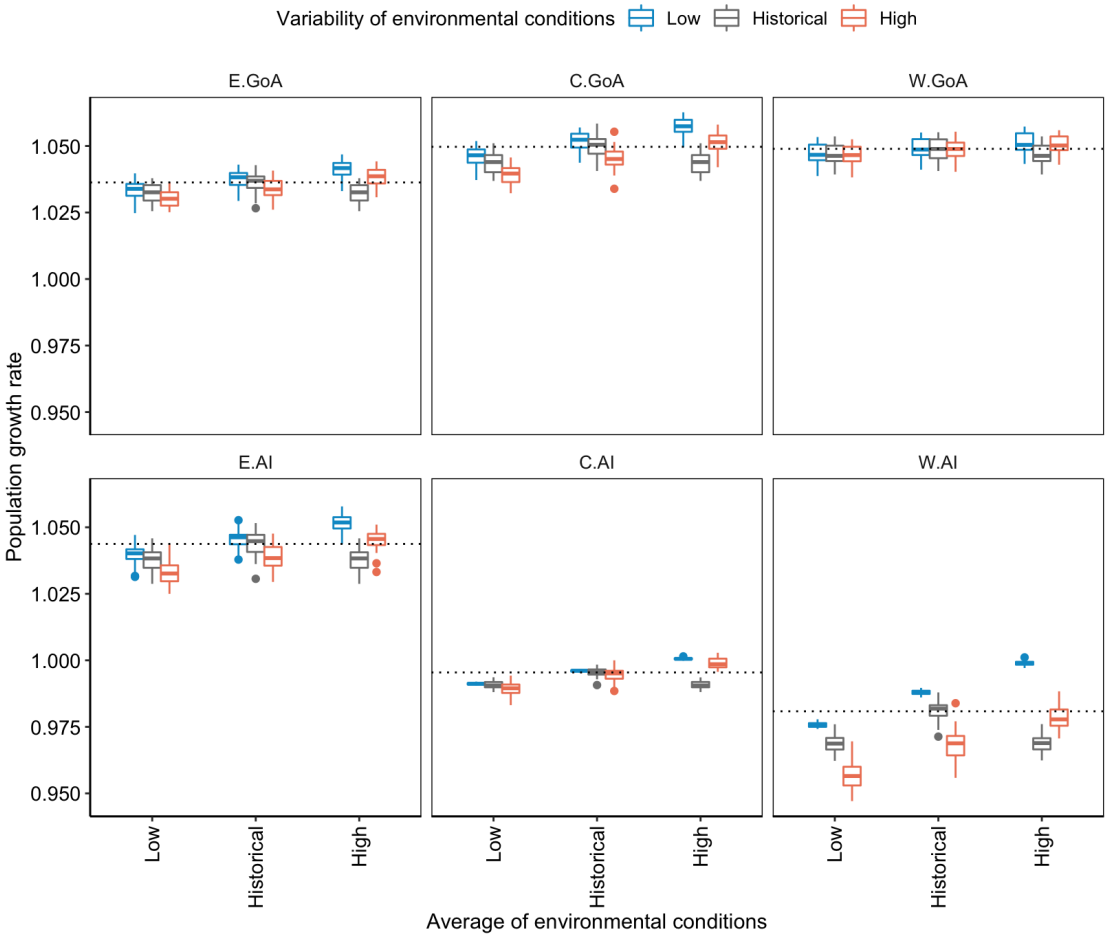

Figure 4.10: Mean and 95% CI of population growth rates during the projection period across projection scenarios with varying mean and standard deviation of generated predictor variables compared with the baseline scenario that adopts the mean and variability of historical conditions (dotted line).

Table 4.1: Description of scenarios for generating predicted sea surface temperature and North Pacific Gyre Oscillation for examining the effects of environmental variability on population dynamics and viability, with mean and standard deviations of oceanographic predictors 75% smaller or larger than historical conditions. The percentage change represents the average change in population growth rates from the baseline scenario across regions.

Scenario	Mean	Standard deviation	Percentage change (%)
1	Historical	Historical	0.000
2		Smaller	0.22
3		Larger	-0.42
4	Low	Smaller	-0.36
5		Historical	-0.57
6		Larger	-0.98
7	High	Smaller	0.75
8		Historical	-0.57
9		Larger	0.12

4.7 REFERENCES

Abadi, F., Gimenez, O., Ullrich, B., Arlettaz, R., Schaub, M. 2010. Estimation of immigration rate using integrated population models. Journal of Applied Ecology 47, 393–400. https://doi.org/10.1111/j.1365-2664.2010.01789.x

Abadi, F., Barbraud, C., Gimenez, O. 2017. Integrated population modeling reveals the impact of climate on the survival of juvenile emperor penguins. Global Change Biology 23, 1353–1359. https://doi.org/10.1111/gcb.13538

Arimitsu, M.L., Piatt, J.F., Hatch, S., Suryan, R.M., Batten, S., Bishop, M.A., Campbell, R.W., Coletti, H., Cushing, D., Gorman, K., Hopcroft, R.R., Kuletz, K.J., Marsteller, C., McKinstry, C., McGowan, D., Moran, J., Pegau, S., Schaefer, A., Schoen, S., Straley, J. and von Biela, V.R. 2021. Heatwave-induced synchrony within forage fish portfolio disrupts energy flow to top pelagic predators. Glob. Change Biol., 27: 1859-1878. https://doi.org/10.1111/gcb.15556

Atkinson, S., D.P. Demaster, and D.G. Calkins. 2008. Anthropogenic Causes of the Western Steller Sea Lion *Eumetopias jubatus* Population Decline and Their Threat to Recovery. Mammal Review 38 (1): 1–18. doi:10.1111/j.1365-2907.2008.00128.x.

Beissinger, S.R., Westphal, M.I., 1998. On the Use of Demographic Models of Population Viability in Endangered Species Management. The Journal of Wildlife Management 62, 821. https://doi.org/10.2307/3802534

Benson, A.J., and A.W. Trites. 2002. Ecological Effects of Regime Shifts in the Bering Sea and Eastern North Pacific Ocean. Fish and Fisheries 3 (2): 95–113. doi:10.1046/j.1467-2979.2002.00078.x.

Besbeas, P., Freeman, S.N., Morgan, B., Catchpole, E.A. 2002. Integrating mark-recapture-recovery and census data to estimate animal abundance and demographic parameters. Biometrics 58, 540–547.

Bled, F., Sauer, J., Pardieck, K., Doherty, P., Royle, J.A. 2013. Modeling Trends from North American Breeding Bird Survey Data: A Spatially Explicit Approach. PLOS ONE 8, e81867. https://doi.org/10.1371/journal.pone.0081867

Boltnev A.I., York A.E., Antonelis G.A. 1998. Northern fur seal young: interrelationships among birth size, growth, and survival. Candian Journal of Zoology 76:843–854.

Boyd I.L. 1990. State-dependent fertility in pinnipeds: contrasting capital and income breeders. Functional Ecology 14:623–630.

Boveng, P.L., Hoef, J.M.V., Withrow, D.E., London, J.M. 2018. A Bayesian Analysis of Abundance, Trend, and Population Viability for Harbor Seals in Iliamna Lake, Alaska. Risk Analysis 0. https://doi.org/10.1111/risa.12988

Brooks, S.P. & Roberts, G.O. 1998. Convergence assessment techniques for Markov chain Monte Carlo. Statistics and Computing, 8, 319-335.

Brooks, S.P., King, R., Morgan, B.J.T. 2004. A Bayesian approach to combining animal abundance and demographic data. Animal Biodiversity and Conservation 27, 515–529.

Calkins, D.G., and K.W. Pitcher. 1982. Population assessment, ecology and trophic relationships of Steller sea lions in the Gulf of Alaska. Environmental Assessment of the Alaskan Continental Shelf. Final reports 19:455-546.

Champagnon, J., Lebreton, J.D., Drummond, H., Anderson, D.J. 2018. Pacific Decadal and El Niño oscillations shape survival of a seabird. Ecology 99, 1063–1072. https://doi.org/10.1002/ecy.2179

Cleasby, I.R., Bodey, T.W., Vigfusdottir, F., McDonald, J.L., McElwaine, G., Mackie, K., Colhoun, K., Bearhop, S. 2017. Climatic conditions produce contrasting influences on demographic traits in a long-distance Arctic migrant. J Anim Ecol 86, 285–295. https://doi.org/10.1111/1365-2656.12623

Conn, P.B., D.S. Johnson, L.W. Fritz, and B.S. Fadely. 2014. Examining the Utility of Fishery and Survey Data to Detect Prey Removal Effects on Steller Sea Lions (*Eumetopias jubatus*). Canadian Journal of Fisheries and Aquatic Sciences 71 (8): 1229–42. doi:10.1139/cjfas-2013-0602.

Copernicus Marine Environment Monitoring Service, 2020. https://resources.marine.copernicus.eu/documents/PUM/CMEMS-MOB-PUM-015-002.pdf

de Valpine, P., D. Turek, C.J. Paciorek, C. Anderson-Bergman, D. Temple Lang, an Bodik. NIMBLE Development Team. 2019. Programming with models: writing statistical algorithms for general model structures with NIMBLE. Journal of Computational and Graphical Statistics 26: 403-413. DOI:10.1080/10618600.2016.1172487.

Di Lorenzo E., Schneider N., Cobb K. M., Chhak, K, Franks P. J. S., Miller A. J., McWilliams J. C., Bograd S. J., Arango H., Curchister E., Powell T. M. and P. Rivere. 2008: North Pacific

Gyre Oscillation links ocean climate and ecosystem change. Geophys. Res. Lett., 35, L08607, doi:10.1029/2007GL032838.

Fritz, L., K. Sweeney, D. Johnson, M. Lynn, T. Gelatt, and J. Gilpatrick. 2013. Aerial and ship-based surveys of Steller sea lions (*Eumetopias jubatus*) conducted in Alaska in June-July 2008 through 2012, and an update on the status and trend of the western distinct population segment in Alaska. U.S. Dep. Commer., NOAA Tech. Memo. NMFS-AFSC- 251, 92 p.

Fritz L., R. Towell, T. Gelatt, D. Johnson, and T. Loughlin. 2014. Recent increases in survival of western Steller sea lions in Alaska and implications for recovery. Endang. Spec. Res. 26(1):13–24. doi: 10.3354/esr00634.

Fritz, L., K. Sweeney, R. Towell, and T. Gelatt. 2016. Aerial and ship- based surveys of Steller sea lions (*Eumetopias jubatus*) conducted in Alaska in June-July 2013 through 2015, and an update on the status and trend of the western distinct population segment in Alaska. U.S. Dep. Commer., NOAA Tech. Memo. NMFS-AFSC-321, 72 p. doi:10.7289/V5/TM-AFSC-321.

Gelman, A. & Rubin, D.B. 1992. Inference from iterative simulation using multiple sequences. Statist. Sci., 7, 457-472.

Gormley, A.M., Slooten, E., Dawson, S., Barker, R.J., Rayment, W., du Fresne, S., Bräger, S. 2012. First evidence that marine protected areas can work for marine mammals. Journal of Applied Ecology 49, 474–480. https://doi.org/10.1111/j.1365-2664.2012.02121.x

Hastings, K.K. 2017. Survival of Steller sea lion (*Eumetopias jubatus*) pups during the first months of life at the Forrester Island complex, Alaska. J Mammal 98, 397–409. https://doi.org/10.1093/jmammal/gyw182

Hastings, K.K., Jemison, L.A., Gelatt, T.S., Laake, J.L., Pendleton, G.W., King, J.C., Trites, A.W., Pitcher, K.W. 2011. Cohort effects and spatial variation in age-specific survival of Steller sea lions from southeastern Alaska. Ecosphere 2, art111. https://doi.org/10.1890/ES11-00215.1

Hastings, K.K., Jemison, L.A., Pendleton, G.W. 2018. Survival of adult Steller sea lions in Alaska: senescence, annual variation and covariation with male reproductive success. Royal Society Open Science 5, 170665. https://doi.org/10.1098/rsos.170665

Hastings, K.K., Johnson, D.S., Pendleton, G.W., Fadely, B.S., Gelatt, T.S. 2021. Investigating life-history traits of Steller sea lions with multistate hidden Markov mark–recapture

models: Age at weaning and body size effects. Ecol. Evol. 11, 714–734. https://doi.org/10.1002/ece3.6878

Heppell, S.S., Caswell, H., Crowder, L.B. 2000. Life Histories and Elasticity Patterns: Perturbation Analysis for Species with Minimal Demographic Data. Ecology 81, 654–665.

Higgins, R. W., A. Leetmaa, Y. Xue, and A. Barnston. 2000: Dominant factors influencing the seasonal predictability of U.S. precipitation and surface air temperature. J. Climate, 13, 3994-4017.

Himes Boor, G.K., T.L. McGuire, A.J. Warlick, R.L. Taylor, S.J. Converse, J.R. McClung, and A.D. Stephens. *In revision*. Estimating reproductive rates and juvenile survival when offspring ages are uncertain using a novel multievent mark-recapture model. Methods in Ecology and Evolution.

Holmes, E.E., L.W. Fritz, A.E. York, and K. Sweeney. 2007. Age-Structured Modeling Reveals Long-Term Declines in the Natality of Western Steller Sea Lions. Ecological Applications 17 (8): 2214–32. doi:10.1890/07-0508.1.

Jenouvrier, S., Holland, M., Iles, D., Labrousse, S., Landrum, L., Garnier, J., Caswell, H., Weimerskirch, H., LaRue, M., Ji, R., Barbraud, C. 2019. The Paris Agreement objectives will likely halt future declines of emperor penguins. Global Change Biology 26, 1170–1184. https://doi.org/10.1111/gcb.14864

Johnson, D. S., and L. W. Fritz. 2014. agTrend: A Bayesian approach for estimating trends of aggregated abundance. Methods in Ecology and Evolution 5(10): 1110-1115.

Kendall, W.L., Langtimm, C.A., Beck, C.A., Runge, M.C. 2004. Capture-Recapture Analysis for Estimating Manatee Reproductive Rates. Marine Mammal Science 20, 424–437. https://doi.org/10.1111/j.1748-7692.2004.tb01170.x

Kilduff, D.P., Lorenzo, E.D., Botsford, L.W., Teo, S.L.H. 2015. Changing central Pacific El Niños reduce stability of North American salmon survival rates. PNAS 112, 10962–10966. https://doi.org/10.1073/pnas.1503190112.

Kuhn, C.E., K.C., D. Johnson, and L. Fritz. 2017. A Re-Examination of the Timing of Pupping for Steller Sea Lions *Eumetopias jubatus* Breeding on Two Islands in Alaska. Endangered Species Research 32: 213–22. doi:10.3354/esr00796.

Lacy, R.C., Williams, R., Ashe, E., Balcomb III, K.C., Brent, L.J.N., Clark, C.W., Croft, D.P., Giles, D.A., MacDuffee, M., Paquet, P.C. 2017. Evaluating anthropogenic threats to

endangered killer whales to inform effective recovery plans. Sci Rep 7, 14119. https://doi.org/10.1038/s41598-017-14471-0

Ladd, C., Hunt, G.L., Mordy, C.W., Salo, S.A., Stabeno, P.J. 2005. Marine environment of the eastern and central Aleutian Islands. Fisheries Oceanography 14, 22–38. https://doi.org/10.1111/j.1365-2419.2005.00373.x

Lander, M., T. Loughlin, M. Logsdon, G. VanBlaricom, and B. Fadely. 2010. Foraging Effort of Juvenile Steller Sea Lions *Eumetopias jubatus* with Respect to Heterogeneity of Sea Surface Temperature. Endangered Species Research 10 (March): 145–58. doi:10.3354/esr00260.

Lander, M.E., M.L. Logsdon, T.R. Loughlin, and G. Van Blaricom. 2011. Spatial Patterns and Scaling Behaviors of Steller Sea Lion (*Eumetopias jubatus*) Distributions and Their Environment. Journal of Theoretical Biology 274 (1): 74–83. doi:10.1016/j.jtbi.2011.01.015.

Lander, M.E., Fadely, B.S., Gelatt, T.S., Sterling, J.T., Johnson, D.S., Pelland, N.A. 2020. Mixing it up in Alaska: Habitat use of adult female Steller sea lions reveals a variety of foraging strategies. Ecosphere 11, e03021. https://doi.org/10.1002/ecs2.3021

Lee P.C., Majluf P., Gordon I.J. 1991. Growth, weaning and maternal investment from a comparative perspective. Journal of Zoology 225:9–114.

Litzow, M.A., Ciannelli, L., Puerta, P., Wettstein, J.J., Rykaczewski, R.R., Opiekun, M., 2018. Non-stationary climate–salmon relationships in the Gulf of Alaska. Proc Biol Sci 285, 20181855. https://doi.org/10.1098/rspb.2018.1855

Loughlin, T.R. 1997. Using the phylogeographic method to identify Steller sea lion stocks. Molecular Genetics of Marine Mammals 3:159-171.

Loughlin, T.R., and A.E. York. 2000. "An Accounting of the Sources of Steller Sea Lion, Eumetopias Jubatus, Mortality." Marine Fisheries Review, 6.

Maniscalco, J.M., Springer, A.M., Parker, P. 2010. High Natality Rates of Endangered Steller Sea Lions in Kenai Fjords, Alaska and Perceptions of Population Status in the Gulf of Alaska. PLOS ONE 5, e10076. https://doi.org/10.1371/journal.pone.0010076

Maniscalco, J.M., A.M., Springer, P. Parker, M.D. Adkinson. 2014. A longitudinal study of Steller sea lion natality rates in the Gulf of Alaska with comparisons to census data. PLOS One 9:e111523.

Maniscalco, J.M. 2014. The Effects of Birth Weight and Maternal Care on Survival of Juvenile Steller Sea Lions (*Eumetopias jubatus*). PLOS ONE 9, e96328. https://doi.org/10.1371/journal.pone.0096328

Maniscalco, J.M. 2018. NOAA/NMFS 5-year status review for Endangered Steller sea lions – Comments.

Manlik, O., McDonald, J.A., Mann, J., Raudino, H.C., Bejder, L., Krützen, M., Connor, R.C., Heithaus, M.R., Lacy, R.C., Sherwin, W.B., 2016. The relative importance of reproduction and survival for the conservation of two dolphin populations. Ecology and Evolution 6, 3496–3512.

Mannocci, L., A.M. Boustany, J.J. Roberts, D.M. Palacios, D.C. Dunn, P.N. Halpin, S. Viehman, et al. 2017. Temporal Resolutions in Species Distribution Models of Highly Mobile Marine Animals: Recommendations for Ecologists and Managers. Diversity and Distributions 23 (10): 1098–1109. doi:10.1111/ddi.12609.

Mantua, N. J., S. R. Hare, Y., Zhang, J. M. Wallace, and R. C. Francis. 1997: A Pacific interdecadal climate oscillation with impacts on salmon production. Bull. Am. Met. Soc., 76, 1069-1079.

Martin, M., McLaren, A., Good, S. 2019. PRODUCT USER MANUAL For Global Ocean GMPE Sea Surface Temperature Multi Product Ensemble SST_GLO_SST_L4_NRT_OBSERVATIONS_010_005 16.

McMahon C.R., Hindell M.A. 2003. Twinning in southern elephant seals: implications of resource allocation by mothers. Wildlife Research 30:35–39.

McMahon, C.R., Burton, H.R. 2005. Climate change and seal survival: evidence for environmentally mediated changes in elephant seal, Mirounga leonina, pup survival. Proceedings of the Royal Society B: Biological Sciences 272, 923–928. https://doi.org/10.1098/rspb.2004.3038

Merrick, R.L. 1987. Behavioral and demographic characteristics of northern sea lion rookeries. Master of Science thesis, Oregon State University, Corvallis. 124 pp.

Merrick, R.L., M.K. Chumbley, and G.V Byrd. 1997. Diet Diversity of Steller Sea Lions (*Eumetopias jubatus*) and Their Population Decline in Alaska: A Potential Relationship. Canadian Journal of Fisheries and Aquatic Sciences 54 (6): 1342–8. doi:10.1139/f97-037.

Mosnier, A., Doniol-Valcroze, T., Gosselin, J.-F., Lesage, V., Measures, L.N., Hammill, M.O. 2015. Insights into processes of population decline using an integrated population model: The case of the St. Lawrence Estuary beluga (*Delphinapterus leucas*). Ecological Modelling 314, 15–31.

National Marine Fisheries Service. 2020. Western Distinct Population Segment Steller sea lion (*Eumetopias jubatus*) 5-Year Review: Summary and Evaluation. NMFS Protected Resources Division, Juneau, Alaska.

NASA Goddard Space Flight Center, Ocean Ecology Laboratory, Ocean Biology Processing Group. 2018. Sea-viewing Wide Field-of-view Sensor (SeaWiFS) R2018.0 Chlorophyll Data; NASA OB.DAAC, Greenbelt, MD, USA. doi: https://dx.doi.org/10.5067/ORBVIEW-2/SEAWIFS/L3M/CHL/2018.

NOAA NCEI, 2020. NOAA Climate monitoring teleconnections: Arctic Oscillation. https://www.ncdc.noaa.gov/teleconnections/ao/ accessed July 1, 2020.

NOAA PSL, 2020. NOAA Physical Sciences Laboratory: Gridded Climate Datasets. https://psl.noaa.gov/data/gridded/tables/ocean.html accessed July 1, 2020.

Ohlberger, J., Scheuerell, M.D., Schindler, D.E. 2016. Population coherence and environmental impacts across spatial scales: a case study of Chinook salmon. Ecosphere 7, e01333. https://doi.org/10.1002/ecs2.1333

Pascual, M.A., and M.D. Adkison. 1994. The Decline of the Steller Sea Lion in the Northeast Pacific: Demography, Harvest or Environment? Ecological Applications 4 (2): 393–403. doi:10.2307/1941942.

Payo-Payo, A., Genovart, M., Bertolero, A., Pradel, R., Oro, D. 2016. Consecutive cohort effects driven by density-dependence and climate influence early-life survival in a long-lived bird. Proc. R. Soc. B 283, 20153042. https://doi.org/10.1098/rspb.2015.3042

Pfister C.M. 1998. Patterns of variance in stage-structured populations: evolutionary predictions and ecologi- cal implications. Proc Nat Acad Sci. 1998; 95: 213–218. PMID: 9419355

Pitcher, K.W., and D.G. Calkins. 1981. Reproductive Biology of Steller Sea Lions in the Gulf of Alaska. Journal of Mammalogy 62 (3): 599–605. doi:10.2307/1380406.

Pitcher, K.W., V.N. Burkanov, D.G. Calkins, B.J. Le Boeuf, E.G. Mamaev, R.L. Merrick, and G.W. Pendleton. 2001. Spatial and Temporal Variation in the Timing of Births of Steller

Sea Lions. Journal of Mammalogy 82 (4): 1047–53. doi:10.1644/1545-1542(2001)082<1047:SATVIT>2.0.CO;2.

Pirotta, E., Thomas, L., Costa, D.P., Hall, A.J., Harris, C.M., Harwood, J., Kraus, S.D., Miller, P.J.O., Moore, M.J., Photopoulou, T., Rolland, R.M., Schwacke, L., Simmons, S.E., Southall, B.L., Tyack, P.L. 2022. Understanding the combined effects of multiple stressors: A new perspective on a longstanding challenge. Science of The Total Environment 821, 153322. https://doi.org/10.1016/j.scitotenv.2022.153322

Pradel, R. 2005. Multievent: An Extension of Multistate Capture–Recapture Models to Uncertain States. Biometrics 61, 442–447. https://doi.org/10.1111/j.1541-0420.2005.00318.x

Proffitt K.M., Rotella J.J., Garrott R.A. 2010. Effects of pup age, maternal age, and birth date on pre-weaning survival rates of Weddell seals in Erebus Bay, Antarctica. Oikos 119:1255–1264.

Rand, K., McDermott, S., Logerwell, E., Matta, M.E., Levine, M., Bryan, D.R., Spies, I.B., Loomis, T., 2019. Higher Aggregation of Key Prey Species Associated with Diet and Abundance of the Steller Sea Lion *Eumetopias jubatus* across the Aleutian Islands. Marine and Coastal Fisheries 11, 472–486. https://doi.org/10.1002/mcf2.10096

Raum-Suryan, K.L., K.W. Pitcher, D.G. Calkins, J.L. Sease, and T.R. Loughlin. 2002. Dispersal, Rookery Fidelity, and Metapopulation Structure of Steller Sea Lions (Eumetopias Jubatus) in an Increasing and a Decreasing Population in Alaska. Marine Mammal Science 18 (3): 746–64. doi:10.1111/j.1748-7692.2002.tb01071.x.

Regehr, E.V., Hostetter, N.J., Wilson, R.R., Rode, K.D., Martin, M.S., Converse, S.J. 2018. Integrated Population Modeling Provides the First Empirical Estimates of Vital Rates and Abundance for Polar Bears in the Chukchi Sea. Scientific Reports 8, 16780. https://doi.org/10.1038/s41598-018-34824-7

Rhodes, J.R., Ng, C.F., de Villiers, D.L., Preece, H.J., McAlpine, C.A., Possingham, H.P. 2011. Using integrated population modelling to quantify the implications of multiple threatening processes for a rapidly declining population. Biological Conservation 144, 1081–1088.

Rodionov, S.N., Bond, N.A., Overland, J.E. 2007. The Aleutian Low, storm tracks, and winter climate variability in the Bering Sea. Deep Sea Research Part II: Topical Studies in Oceanography 54, 2560–2577. https://doi.org/10.1016/j.dsr2.2007.08.002

Rodionov, S.N., Overland, J.E., Bond, N.A. 2005. Spatial and temporal variability of the Aleutian climate. Fisheries Oceanography 14, 3–21. https://doi.org/10.1111/j.1365-2419.2005.00363.x

Rotella J.J., Link W.A., Chambert T., Stauffer G.E., Garrott RA. 2012. Evaluating the demographic buffering hypothesis with vital rates estimated for Weddell seals from 30 years of mark-recapture data. J Anim Ecol. 2012; 81: 162–173. doi: 10.1111/j.1365-2656.2011.01902.x PMID: 21939440.

Runge, M.C., Langtimm, C.A., Kendall, W.L. 2004. A stage-based model of manatee population dynamics. Marine Mammal Science 20: 361-385.

Saunders, S.P., Cuthbert, F.J., Zipkin, E.F. 2018. Evaluating population viability and efficacy of conservation management using integrated population models. Journal of Applied Ecology 55, 1380–1392. https://doi.org/10.1111/1365-2664.13080

Schaub, M., Gimenez, O., Sierro, A., Arlettaz, R. 2007. Use of Integrated Modeling to Enhance Estimates of Population Dynamics Obtained from Limited Data. Conservation Biology 21, 945–955. Seber, G., 1965. A note on the multiple recapture census. Biometrika 52, 249–259.

Seckel, G.R. 1993. Zonal gradient of the winter sea level atmospheric pressure at 50 N: an indicator of atmospheric forcing of North Pacific surface conditions. J. Geophys. Res. 98:22615–22628.

Simons, R.A. (2019). ERDDAP. https://coastwatch.pfeg.noaa.gov/erddap. Monterey, CA: NOAA/NMFS/SWFSC/ERD.

Sinclair, E.H., Zeppelin, T.K. 2002. Seasonal and Spatial Differences in Diet in the Western Stock of Steller Sea Lions (*Eumetopias jubatus*). Journal of Mammalogy 83, 973–990. https://doi.org/10.1644/1545-1542(2002)083<0973:SASDID>2.0.CO;2

Sinclair, E. H., D. S. Johnson, T. K. Zeppelin, and T.S. Gelatt. 2013. Decadal variation in the diet of Western Stock Steller sea lions (*Eumetopias jubatus*). U.S. Dep. Commer., NOAA Tech. Memo. NMFS-AFSC-248, 67 p.

Simpson, D., Rue, H., Riebler, A., Martins, T.G., Sørbye, S.H. 2017. Penalising Model Component Complexity: A Principled, Practical Approach to Constructing Priors. Statist. Sci. 32, 1–28. https://doi.org/10.1214/16-STS576

Speckman, P.L. and Sun, D. 2003. Fully Bayesian spline smoothing and intrinsic autoregressive priors. Biometrika. 90:289–302.

Stabeno, P. J., J. D. Schumacher, and K. Ohtani. 1999. The physical oceanography of the Bering Sea. Pages 1–28 in T. R. Loughlin and K. Ohtani, editors. Dynamics of the Bering Sea. AK–SG–99–03. University of Alaska Sea Grant, Fairbanks, Alaska, USA.

Fritz, L.W., and C. Stinchcomb. 2005. Aerial, ship, and land-based surveys of Steller sea lions (*Eumetopias jubatus*) in the western stock in Alaska, June and July 2003 and 2004. U.S. Department of Commerce, NOAA Technical Memorandum NMFS-AFSC-153. 56 pp.

Suryan, R.M., Arimitsu, M.L., Coletti, H.A. et al. 2021. Ecosystem response persists after a prolonged marine heatwave. Sci Rep 11, 6235 (2021). https://doi.org/10.1038/s41598-021-83818-5

Sweeney, K., Towell, R., Gelatt, T. 2018. Results of Steller Sea Lion Surveys in Alaska, June-July 2017. NOAA Fisheries Alaska Fisheries Science Center Marine Mammal Laboratory, Seattle, WA. https://media.fisheries.noaa.gov/dam-migration/ssl_aerial_survey_2018_final.pdf

Sweeney, K. L., Birkemeier, B., Luxa, K., and Gelatt, T. 2022. Results of Steller Sea LionSurveys in Alaska, June-July 2021. Memorandum to The Record. Feb 7, 2022. https://media.fisheries.noaa.gov/2022-02/ssl_aerial_survey_2021_final.pdf

Tavecchia, G., Besbeas, P., Coulson, T., Morgan, B.J.T., Clutton-Brock, T.H. 2009. Estimating Population Size and Hidden Demographic Parameters with State-Space Modeling. The American Naturalist 173, 722–733. https://doi.org/10.1086/598499

Thomas J.A., DeMaster D.P. 1983. Parameters affecting survival of Weddell seal pups (*Leptonychotes weddelli*) to weaning. Canadian Journal of Zoology 61:2078–2083.

Tomillo, P.S., Robinson, N.J., Sanz-Aguilar, A., Spotila, J.R., Paladino, F.V., Tavecchia, G. 2017. High and variable mortality of leatherback turtles reveal possible anthropogenic impacts. Ecology 98, 2170–2179. https://doi.org/10.1002/ecy.1909

Trillmich F. 1990. The behavioral ecology of maternal effort in fur seals and sea lions. Behaviour 114:3–20.

Trites, A. W., and C. P. Donnelly. 2003. The Decline of Steller Sea Lions Eumetopias Jubatus in Alaska: A Review of the Nutritional Stress Hypothesis. Mammal Review 33 (1): 3–28. doi:10.1046/j.1365-2907.2003.00009.x.

van Erp, S., Oberski, D.L., Mulder, J. 2019. Shrinkage priors for Bayesian penalized regression. Journal of Mathematical Psychology 89, 31–50. https://doi.org/10.1016/j.jmp.2018.12.004

York, A.E. 1994. The Population Dynamics of Northern Sea Lions, 1975-1985. Marine Mammal Science 10 (1): 38–51. doi:10.1111/j.1748-7692.1994.tb00388.x.

York, A. E., J. R. Thomason, E. H. Sinclair, and K.A. Hobson. 2008. Stable carbon and nitrogen isotope values in teeth of Steller sea lions: Age of weaning and the impact of the 1975-1976 regime shift in the North Pacific Ocean. Can. J. Zool. 86: 33-44.

Watanabe, S. 2010. Asymptotic Equivalence of Bayes Cross Validation and Widely Applicable Information Criterion in Singular Learning Theory. Journal of Machine Learning Research 11.

Wiens J.A. 1989. Spatial scaling in ecology. Funct Ecol 3: 385 – 397.

Wright, B.E., Brown, R.F., DeLong, R.L., Gearin, P.J., Riemer, S.D., Laake, J.L., Scordino, J.J. 2017. Survival rates of Steller sea lions from Oregon and California. J Mammal 98, 885–894. https://doi.org/10.1093/jmammal/gyx033

Zhang, R.H. and S. Levitus. 1997: Structure and cycle of decadal variability of upper-ocean temperature in the North Pacific. J. Climate, 10, 710-727.

Chapter 5. DEMOGRAPHIC AND ENVIRONMENTAL DRIVERS OF POPULATION DYNAMICS AND VIABILITY IN AN ENDANGERED TOP PREDATOR USING AN INTEGRATED MODEL

Publication history: This study was co-authored with Gina K. Himes Boor, Tamara L. McGuire, Kim E.W. Shelden, Eiren K. Jacobson, Charlotte Boyd, Paul R. Wade, Andre E. Punt, Sarah J. Converse. At the time this dissertation was published, this chapter was not in review with a journal.

Abstract: Knowledge about the demographic and environmental factors underlying population dynamics is fundamental to designing effective conservation measures to recover depleted wildlife populations. However, sparse monitoring data or persistent knowledge gaps about threats make it difficult to identify the drivers of population dynamics. In situations where small, depleted populations show continued evidence of decline for unknown reasons, integrated population models can improve our understanding of demography, provide fundamental insights into factors that may be limiting recovery, and support conservation decision-making. We used mark-resight and aerial survey data from 2004-2018 to build an integrated population model for the Cook Inlet population of beluga whales (*Delphinapterus leucas*), which is listed as endangered under the U.S. Endangered Species Act. We examined the relationships between beluga vital rates and available information on prey availability and environmental conditions and conducted a population viability analysis to predict extinction risk across a range of hypothetical changes in beluga survival and reproduction. Our results indicate that while mean survival rates of breeding females (0.97) and young-of-year (0.92) are relatively high, that of

non-breeding adults (0.94) and fecundity (0.27) may be depressed, and that prey availability and environmental variability may be impacting demography. If vital rates and environmental variability remain similar to those estimated from the latter part of the study period, the population will likely continue to decline, with a 19-32% probability of extinction in 150 years. This framework could be broadly applied and highlights the utility of integrated population modeling for capitalizing on available information and accounting for uncertainty when evaluating the efficacy of conservation actions and identifying factors contributing to the failure of this and other protected populations to recover.

Keywords: Bayesian integrated population model, population viability analysis, Cook Inlet beluga whale, extinction risk, environmental variability, prey availability

5.1 INTRODUCTION

Understanding the demographic and environmental factors driving trends in abundance is fundamental to designing effective conservation measures for wildlife populations. However, knowledge about population dynamics is challenging to obtain, particularly for populations that are small, declining, patchily distributed, or difficult to survey. In these situations, individual data streams might indicate that the population is declining without lending insight into the drivers of the observed trend, or might fail to provide sufficient information to detect a trend at all. This can be particularly true for cetacean populations, where costly survey methods and cryptic life history stages (e.g., smaller calves hidden underneath females) lead to insufficient statistical power for detecting trends (Taylor et al. 2007, Boyd & Punt 2021). Population models that integrate all available data can improve our ability to quantify the importance of various stressors in shaping population dynamics while accounting for uncertainty and variability in underlying ecological processes.

Integrated population models (IPMs; Besbeas et al. 2002, Brooks et al. 2004) constitute a formal framework for combining multiple data sources through a joint likelihood designed to simultaneously model demographic rates and abundance. By integrating multiple data streams in the same model, IPMs can produce parameter estimates with improved precision and reduced bias (Schaub et al. 2007, Abadi et al. 2010), as well as estimates of parameters that would be unidentifiable using traditional approaches (Schaub et al. 2010, Veran & Lebreton 2009). IPMs maximize the utility of available data, which is typically expensive to collect on management-relevant time horizons, particularly for long-lived species (Zipkin & Saunders 2018, Regehr et al. 2018) and are therefore useful to conduct population viability analyses (PVA) that quantify extinction risk and evaluate the efficacy of management alternatives (Beissinger & Westphal 1998, Converse et al. 2013, Heard et al. 2013). Despite the usefulness of this approach, few IPM-based PVAs have been implemented to examine viability across varying climate change or management scenarios for wildlife populations of conservation concern (Saunders et al. 2018, Boveng et al. 2018, Leasure et al. 2019, Jenouvrier et al. 2019).

While marine mammals tend to be sensitive to environmental variability and anthropogenic disturbance (Moore 2008, Evans et al. 2010, Santora et al. 2020, Wade et al. 2012, Moore 2018), it can be challenging to disentangle the effects of multiple environmental factors that directly or indirectly affect demography. An exemplar of this challenge is the Cook Inlet population of beluga whales (*Delphinapterus leucas*), which is estimated to have declined dramatically during the 1990s (Hobbs et al. 2006) and is listed as endangered under the U.S. Endangered Species Act (ESA). Despite the cessation of hunting and increased monitoring efforts since its precipitous decline, the best available estimates from aerial surveys suggest that the population is continuing to decline (Shelden & Wade 2019), and a clear cause for the failure

of this population to recover has not been identified. The leading hypotheses for the lack of recovery include reduced prey availability due to environmental change, reduced foraging success due to anthropogenic noise or other disturbance, natural predation, pollution, small population effects, or some combination of these factors (Hobbs et al. 2015). However, existing modeling approaches have not been able to identify putative causes of decline due to a lack of empirical estimates of demographic rates and sparse data on threats (Hobbs et al. 2015, Jacobson et al. 2020, Norman et al. 2019). Consequently, it has been challenging to develop targeted conservation actions for advancing recovery.

To improve our understanding of factors affecting the demography and viability of Cook Inlet belugas, we developed a Bayesian IPM-based PVA using mark-resight and aerial survey data from 2004-2018. Using this framework, we examine the effects of environmental conditions and prey availability on vital rates, identify demographic drivers of population dynamics, and assess extinction risk across a range of hypothetical changes in survival and reproduction. Our model provides insights into the sensitivity of population dynamics to changes in demography and environmental conditions, examines external factors potentially limiting recovery, and establishes a framework to evaluate future viability and management alternatives as additional data become available. Our analysis highlights the usefulness of IPMs for capitalizing on available information and accounting for uncertainty when examining factors contributing to wildlife population declines and the failure of this and other protected species to recover.

5.2 METHODS

5.2.1 *Study species*

Of the five beluga whale stocks in Alaskan waters, the geographically and genetically isolated population in Cook Inlet, Alaska (Figure 5.1) is the smallest in number. Belugas exhibit life

history traits typical of large, long-lived odontocetes (i.e., late maturing with a long inter-birth interval), common amongst many species of conservation concern. Females are thought to reach reproductive maturity around age 10 (Shelden et al. 2020, McGuire et al. 2020), with calves remaining dependent until 2-5 years old. Calving begins in late July and extends into October (McGuire et al. 2020). Belugas are known to inhabit coastal and offshore waters of the inlet, and this population likely remains in Cook Inlet year-round, aggregating in estuaries and near river mouths to feed in summer (Shelden et al. 2015). Cook Inlet is a dynamic semi-enclosed tidal estuary extending roughly 370 km (200 nm) north from the Gulf of Alaska, with beluga habitat seasonally influenced by ice cover and freshwater discharge from large rivers (Moore et al. 2000). Belugas are adaptive foragers, feeding on a variety of species in Cook Inlet (Moore et al. 2000) at different times of the year and in various areas of their range (Quakenbush et al. 2015; Nelson et al. 2018).

5.2.2 *Population monitoring data*

The population was monitored using land and boat-based mark-resight surveys in Cook Inlet from May through October, 2005-2017, resulting in over 1,900 left-side sightings records of the 400+ identifiable beluga whales in the photographic catalog (McGuire et al. 2020). When cataloged individuals were resighted, it was noted whether they were unambiguously associated with a young of the year (YOY), a calf (age 1-5), or both. Calves and YOY were associated with adult whales in just under 20% of sightings and calf age determination was based on color, size, and the presence of fetal folds (McGuire et al. 2020, Himes Boor et al. *In revision*). Belugas generally only become individually identifiable (using scars or other skin markings) once they are 5 years old or older. These data alone cannot be used to produce robust abundance estimates

due to individual heterogeneity in range and behavior that impacts sighting probability (Boyd et al. 2019).

The population was also monitored using aerial surveys annually from 1993-2012 and biennially from 2012 to the present, though only data since 2004 were used in this study due to a change in methodology that year. Aerial surveys were conducted strategically over the course of several days, with variable daily survey effort that was spatio-temporally concentrated when and where belugas were most likely to be present – at low tide near shore – covering 100% of the coastline and just under half of the area of the entire inlet (Shelden and Wade 2019). Aerial surveys were executed from twin-engine aircraft with two observers recording the number of belugas observed resulting in daily population size estimates (sum of all surveyed beluga groups; Shelden and Wade 2019, Boyd et al. 2019). Annual population sizes were estimated from repeated aerial survey counts using a Bayesian hierarchical model to account for availability, perception, and visibility bias due to the difficulty of detecting darker, smaller animals in turbid waters and the uncertainty surrounding dive synchrony and time spent at the surface (Boyd et al. 2019). The median and standard deviations of the posterior distributions of daily population size estimates from Boyd et al. (2019) were used here as data in the abundance model described below.

5.2.3 *Statistical analyses*

5.2.3.1 Multi-event model

We implemented the multi-event model introduced by Himes Boor et al. (*In revision*) to estimate mean fecundity and age-specific survival using mark-resight data of mother-calf pairs with uncertain offspring ages. In brief, this model framework includes 14 life-history states based on reproductive status (breeder versus non-breeder) and the number of associated dependent

offspring in various age combinations (YOY, 1-4+) (Figure 5.2). Due to the long inter-birth interval, we assumed that females cannot give birth in consecutive years, with the state process model reflecting this constraint (i.e., a breeder cannot have both YOY and a 1-year-old calf). The state process is defined as,

$$z_{i,t}|z_{i,t-1} \sim \text{categorical}(\Omega_{z_{i,t-1},i,t-1})$$

where the state z of individual i at occasion t, conditional on the individual's state at the previous occasion, is categorically distributed according to matrix Ω, which is composed of survival, calf aging, and breeding transition matrices. Stage-specific survival was estimated for four groups: breeding females (S_B); non-breeding subadults and adults (independent age 6+ belugas including subadults of both sexes, adult males, and non-breeding females; S_N); young calves (age 0-1; S_Y); and older dependent calves (age 2-5; apparent survival ϕ_C). Survival of young and older calves was conditioned on breeding female survival to account for young calves dying if the female dies and older calves becoming independent. Breeding transition matrices allow reproductively mature individuals to breed for the first time (ψ_N, though this is of limited ecological interest because the pool of pre-breeders includes males) and thereafter (ψ_B; e.g., fecundity), conditional on female breeder and calf survival. Breeding probability (ψ_B) also encompasses neonate survival prior to the start of the mark-resight surveys each year.

The model framework was adapted here to estimate temporal variation for stage-specific demographic rate ξ, modeled as a function of environmental covariates and random effects of year,

$$\text{logit}(\xi_a) = \mu_a^{\xi} + \beta_{a,c}^{\xi} \cdot x_{c_t} + \epsilon_{a,t}^{\xi}$$

where μ_a^{ξ} is the intercept for demographic rate ξ and age group a, coefficients $\beta_{a,c}^{\xi}$ describe the effects of covariate c on each age-specific vital rate, and $\epsilon_{a,t}^{\xi}$ are random year effects. All

covariates were *Z*-scored prior to inclusion in the analysis, so the intercept μ_a^{ξ} represents the mean rate. Intercepts μ_a^{ξ} were logit-transformed parameters with uniform(0,1) prior distributions. To improve parameter estimability and regulate model complexity, we applied penalized complexity priors (Simpson et al. 2017, van Erp et al. 2019) on covariate coefficients and random year effects, which shrink the parameter toward zero in the absence of strong support for larger values. Thus, the random year effects and the effect of any covariate *c* on demographic rate ξ were assumed to be drawn from a Gaussian distribution with standard deviations distributed according to an exponential distribution with a fixed shrinkage rate; $\epsilon_{a,t}^{\xi} \sim \text{normal}(0, \sigma_a^{\xi} \sim \text{exponential}(\nu = 1))$ and $\beta_{a,c}^{\xi} \sim \text{normal}(0, \sigma_{a,c} \sim \text{exponential}(\nu = 1))$. Parameter estimates were insensitive to the choice of the penalized complexity prior fixed shrinkage rate (results not shown).

The observation process model accounts for the uncertainty in both female reproductive status and calf age determination. Specifically,

$$y_{i,t} \mid z_{i,t} \sim \text{categorical}(\Theta_{z_{i,t-1,i,t}})$$

where observations *y* conditional on life history state *z* are categorically distributed with probability matrix Θ. Components of this matrix for individual *i* at time *t* include age-specific detection probabilities and calf age assignment probabilities. Detection probabilities include those for young (δ_Y) and older calves (δ_C) (conditional on detecting the female; e.g., the multi-event state assignment probabilities), non-breeding adults (p_N), and breeding females with (p_{B_C}) and without (p_{B_N}) calves. Similar to demographic rates, detection probabilities for each age class *a* were modeled as

$$\text{logit}(p_a) = \mu_a^p + \beta_p \cdot x_t^p + \epsilon_{a,t}^p$$

where the intercept μ_a^p for each age group *a* was estimated using a logit-transformed parameter with a uniform(0,1) prior distribution. A fixed effect β_p accounted for variable survey effort x_t^p, the *Z*-scored number of vessel- and land-based surveys that occurred each year, with prior distribution normal(0, variance = 1000). Interannual random effects for each age group were estimated using penalized complexity priors as above with a fixed shrinkage rate for the standard deviations, $\epsilon_{a,t}^p \sim \text{normal}(0, \sigma_p \sim \text{exponential}(\nu = 1))$.

The parameters involved in estimating calf age assignment probability given the calf's true age (discussed in detail by Himes Boor et al. (*In revision*)) included the probabilities of assigning the individual to an age category (γ), assigning calf age with perfect certainty (α), assigning an uncertain age that matched the true age (ω), assigning an uncertain age that is different than true age by one year (κ), and the probability of the true age being at the upper limit of its assigned age category (η, e.g., yearling calf placed in the <1 yo category).

5.2.3.2 Abundance model

The second component of the IPM is the state-space model for estimating annual population size using aerial survey data. Belugas are difficult to detect in the turbid waters of Cook Inlet, and their group sizes vary widely depending on location, season, and tidal flux. To account for highly variable annual counts derived from the aerial survey data, population size is modeled as,

$$\widehat{N}_{\mu_t} \sim \text{normal}(N_t, \widehat{\sigma}_t)$$

$$N_t \sim \text{binomial}(N_{\text{Tot}_t}, p_{\text{Ab}_t})$$

where annual aerial survey population size estimates $\widehat{N}_{\mu_t}$ are modeled as arising from a normal distribution with mean equal to N_t (the population size in year *t* subject to detection in the aerial survey) and standard deviation $\widehat{\sigma}_t$. Both the annual estimates $\widehat{N}_{\mu_t}$ and their sampling standard

deviations $\widehat{\sigma}_t$ were estimated by Boyd et al. (2019) and Shelden and Wade (2019). In turn, N_t is modeled as arising from a binomial distribution with index equal to the total abundance, N_{Tot_t}, from the IPM process model (described below), and the probability equal to the aerial survey detection probability p_{Ab_t}. Due to the uncertainty surrounding the degree to which underlying assumptions in the aerial survey are met (namely the proportion of the population missed on a given survey day and whether groups are consistently missed or missed at random), we examined the sensitivity of both abundance and vital rates to the prior used for the aerial survey detection probability, p_{Ab_t} (Appendix C). We ultimately used an uninformative prior ($p_{\mathrm{Ab}_t} \sim \mathrm{Beta}(1,1)$, but also considered two weakly informative priors, $p_{\mathrm{Ab}_t} \sim \mathrm{Beta}(2,1)$ and $p_{\mathrm{Ab}_t} \sim \mathrm{Beta}(10,3)$, which suggest most individuals are observed but allow for the possibility of lower detection probabilities; and a strongly informative prior, $p_{\mathrm{Ab}_t} \sim \mathrm{Beta}(15,1)$, with the majority of the prior mass above 0.90, representing the idea that the aerial survey represents a near census of the population due to the strategic survey methodology.

5.2.3.3 Integrated model

Abundance for each age group and life history state were modeled using stochastic population growth equations with vital rate and population size estimates from the two subcomponent models (Figure 5.3). The age at first reproduction was set at 10 years, though due to uncertainty in this parameter, we examined the sensitivity of model results to a range of age at first reproduction from 8 to 16 years (Appendix D). The age structure in the first model year was established using a multinomial distribution based on the assumption of a stable age distribution, and parameter estimates were robust to this assumption (results not shown). In each subsequent year *t*, the number of individuals in the YOY age class was equal to the number of females with YOYs in that year, and the numbers of individuals in all other age classes were modeled as

binomial outcomes given survival and breeding transition probabilities and abundances in the previous year:

$$\begin{bmatrix} N_{\mathrm{YOY}_{t+1}} = N_{\mathrm{B_{YOY}}_{t+1}} \\ N_{1_{t+1}} \sim \mathrm{Bin}(N_{\mathrm{YOY}_t}, S_{\mathrm{Y}_t}) \\ N_{\mathrm{C}_{t+1}} \sim \mathrm{Bin}(N_{\mathrm{C}_t}, \phi_{C_t}) \\ N_{\mathrm{J}_{t+1}} \sim \mathrm{Bin}(N_{\mathrm{J}_t}, S_{\mathrm{N}_t}) \\ N_{\mathrm{B_{YOY}}_{t+1}} \sim \mathrm{Bin}(N_{\mathrm{J}_t}, S_{\mathrm{N}_t}\psi_{\mathrm{N}}) + \mathrm{Bin}(N_{\mathrm{NB}_t}, S_{\mathrm{N}_t}\psi_{\mathrm{N}}) + \mathrm{Bin}(N_{\mathrm{B_{Sk}}_t}, S_{\mathrm{B}_t}\psi_{\mathrm{B}_t}) \\ N_{\mathrm{B_{Sk}}_{t+1}} \sim \mathrm{Bin}(N_{\mathrm{B_{YOY}}_t}, S_{\mathrm{B}_t}) + \mathrm{Bin}(N_{\mathrm{B_{Sk}}_t}, S_{\mathrm{B}_t} \cdot (1 - \psi_{\mathrm{B}_t})) \\ N_{\mathrm{NB}_{t+1}} \sim \mathrm{Bin}(N_{\mathrm{J}_t}, S_{\mathrm{N}_t}(1 - \psi_{\mathrm{N}})) + \mathrm{Bin}(N_{\mathrm{NB}_t}, S_{\mathrm{N}_t}(1 - \psi_{\mathrm{N}})) \end{bmatrix}$$

Total abundance in each year was then calculated as the sum of YOY (N_{YOY_t}), yearlings (N_{1_t}), calves age 2-5 (N_{C_t}), juveniles age 6-8 (N_{J_t}), non-breeders age 9+ (N_{NB_t}), established breeders with YOY ($N_{\mathrm{B_{YOY}}_t}$), and without YOY ($N_{\mathrm{B_{Sk}}_t}$): $N_{\mathrm{Tot}_t} = \sum(N_{\mathrm{age}_t})$.

5.2.3.4 Sensitivity and viability analyses

We examined the sensitivity of population growth to specific demographic rates by examining the correlation coefficient (r) between posterior mean annual population growth rate, $\lambda_t = \frac{N_{\mathrm{Tot}t+1}}{N_{\mathrm{Tot}_t}}$, and annual fecundity and survival of breeding females, non-breeders, and calves. For each demographic rate, we calculated the probability of the correlation coefficient being positive or negative.

To examine future viability, we projected the population forward in time for 150 years (appropriate to capture the accelerated extinction risks after 100 years for a long-lived mammal) using the posterior distributions for the estimated demographic rates and age-specific abundance. The estimated deviates from the random effect distributions, $\epsilon^{\xi}_{a,t}$, for the 12 years informed by mark-resight data (2005-2017) were randomly sampled with replacement and used to simulate all survival and breeding probabilities in each given year of the projection, representing a demographic "status quo". To examine the effect of potential changes in demography on

viability, we also projected the population forward under all possible combinations of three hypothetical percent increases in vital rates; namely, breeding female and non-breeding group survival (1%, 1.5%, 2%), young calf survival (1%, 2%, 4%), older calf survival (5%, 10%, 15%), and fecundity (5%, 10%, 15%) (e.g., 1% increase raises survival from 0.90 to 0.909).

We summarized the posterior distributions of population projections in terms of the probability of extinction ($\Pr(N_{\mathrm{Tot}_{2117}}<2)$), the probability of having no remaining breeding females ($\Pr(N_{\mathrm{B_{YOY}}_{2117}}<1)$), the probability of exceeding the ESA downlisting criterion of 520 individuals ($\Pr(N_{\mathrm{Tot}_{2117}}>520)$), the average population growth rate (λ), and the probability of positive population growth ($\Pr(N_{\mathrm{Tot}_{2004}} < \mathrm{N}_{\mathrm{Tot}_{2117}})$). Additionally, we estimated a quasi-extinction threshold as called for in the Cook Inlet beluga whale Recovery Plan (NMFS 2016; Appendix E).

5.2.4 *Environmental covariates*

To evaluate the effects of oceanographic conditions and prey availability on beluga vital rates, we compiled Gulf of Alaska summer (July-Sept) sea surface temperatures (SST) and derived a proxy for prey abundance in tributaries within Cook Inlet. Monthly SSTs were compiled from a large geographic space (approximately 54°N to 60°N and 137°W to 157°W) using the NOAA GOES satellite data accessed from the ERDDAP server (Simons 2020) and averaged to produce annual means spanning October of year t to September of year $t + 1$. The prey abundance metric was derived by compiling summer in-river reconstructed run estimates for Chinook (*Oncorhynchus tshawytscha*), escapement counts for coho (*Oncorhynchus kisutch*), chum (*Oncorhynchus keta*), sockeye (*Oncorhynchus nerka*), and pink salmon (*Oncorhynchus gorbuscha*), and recreational harvest of eulachon (*Thaleichthys pacificus*) from areas within the

Susitna Delta, Knik Arm, and Chinitna Bay in Cook Inlet (Alaska Department of Fish and Game). Escapement data were multiplied by species-specific average weights and energy content (O'Neill et al. 2014), summed across all species, and then Z-scored and scaled for an overall proxy for prey abundance. Both covariates were applied to fecundity and survival rates (shared coefficient between breeding females and the non-breeding group) in year t. In addition to reporting the median logit-scale effect size, we also include the probability of MCMC samples for each covariate coefficient $\beta_{a,c}^{\xi}$ being above versus below zero. We compared a "full" model fit with both covariates to a base model without covariates using the Watanabe-Akaike information criterion (WAIC; Watanabe 2010) and made inference and conducted the viability analysis using the base model to align with our intention of examining covariates in an exploratory manner due to the uncertain link between covariates and demography and the challenges of projecting covariates forward in time.

Sea surface temperature and prey abundance were selected as covariates in this analysis based on our hypothesis that demographic rates could be affected by oceanographic conditions that affect the availability of prey. The Pacific Decadal Oscillation (PDO) and the North Pacific Gyre Oscillation (NPGO) are both oceanographic indices that have been identified as predictors of the growth and abundance of various salmon and groundfish species (Kilduff et al. 2015, Ohlberger et al. 2016, Dorner et al. 2018, Litzow et al. 2018) that are important beluga prey (Quakenbush et al. 2015). However, due to the high degree of correlation between SST, the NPGO, and PDO, and the changing relationships that have been identified between these variables (Litzow et al. 2018), we chose to use SST, as it is one of the strongest underlying drivers and identifying features of these two climatic patterns. It should be noted, however, that regional SST in the Gulf of Alaska may not reflect conditions experienced by belugas foraging in

upper Cook Inlet, where conditions are strongly influenced by river features and tidal fluctuations. Though we focused on Gulf of Alaska SST and a single metric of prey abundance, examining the effects of environmental variability, prey availability, and proxies for anthropogenic stressors on vital rates in a data-limited situation is a complex and ongoing challenge that is fundamental to informing potential conservation actions. We include an expanded analysis of potential covariates in Appendix F, which includes season-specific oceanographic indices, species-specific prey abundances, and proxies for forage fish availability, pollution, and cumulative impacts.

5.2.5 *Model fitting*

The model was fitted in JAGS (Plummer 2019) using package jagsUI (Kellner 2019) in the R statistical programming language (R Core Development 2022). Posterior distributions were calculated using Markov chain Monte Carlo (MCMC) estimation with three independent chains run for 40,000 iterations after a burn-in period of 28,000 iterations with a thinning rate of 2. We evaluated model convergence with visual inspection of traceplots and the Brooks-Gelman-Rubin statistic (Gelman & Rubin 1992) $\hat{R} < 1.1$. Model fit was evaluated by generating a posterior predictive distribution for population size.

5.3 RESULTS

5.3.1 *Demographic rates*

Posterior mean breeding female survival (S_B) was 0.97 (95% credible interval: 0.95-0.99) (Table 1), with lower rates in 2011 and 2014 (Figure 5.4). Posterior mean survival of the non-breeding adult group (S_N; including older juveniles, non-breeding females, and males) was 0.94 (0.91-0.97), with observed random effect deviates leading to lower survival (S_N = 0.87-0.90) from

2006-2008 and in 2011. Posterior mean survival of young calves (S_Y) was approximately 0.92 (0.80-0.98). Posterior mean apparent survival of older calves (ϕ_C) was approximately 0.55 (0.35-0.77). Annual estimates of younger and older calf survival had greater uncertainty compared with adult survival and were lower in 2011, dropping to $S_Y = 0.89$ and $\phi_C = 0.51$ (Figure 5.4). Mean fecundity (ψ_B; breeding probability for previously established breeders) was 0.27 (0.21-0.35) over the study period (Table 5.1), ranging from a low of 0.22 in 2011-2012 to a high of 0.35 in 2013. Demographic rate estimates varied little across the range of possible ages at first reproduction (Appendix D). Models fitted with mark-resight data alone (excluding aerial survey data) produced similar estimates (Himes Boor et al. *In revision*). Detection and state assignment probabilities from the mark-resight model were variable and dependent on state (Appendix G).

5.3.2 *Population size and structure*

During the period informed by data (2004-2021), the average population growth rate λ was 1.00 yr^{-1} (95% credible interval: 0.91-1.09), though the population increased at a rate of 1.01 yr^{-1} (0.92-1.09) from 2004-2010 and subsequently declined at a rate of 0.99 yr^{-1} (0.89-1.07). Annual abundance was higher during the early part of the study period and started declining in 2010 to reach 369 (294-450) individuals in 2018 (Figure 5.5a). Abundance estimates were somewhat sensitive to the prior distribution on the detection probability in the population size model, with lower estimated abundance resulting from informative priors that placed more prior weight on higher detection probabilities (Appendix C). Over the study period, the posterior mean age structure was similar to that expected with a stable age distribution (Table 5.2).

5.3.3 *Sensitivity and viability analyses*

In terms of the sensitivity analysis, fecundity had the strongest correlation with λ_t, with $r = 0.48$ (95% credible interval: -0.13, 0.82) followed by breeding adult survival $r = 0.46$ (-0.23, 0.83) (Figure 5.6). Younger and older calf survival rates were also correlated with population growth with $r = 0.43$ (-0.24, 0.82) and $r = 0.39$ (-0.25, 0.81), respectively. Estimates of non-breeder survival were not strongly correlated with population growth ($r = 0.25$; -0.38, 0.74).

Over 10,000 150-year population projections, the population declined on average (Figure 5.5b), with a mean population growth rate of approximately 0.983 (0.982-0.985). The posterior mean probability of extinction, $Pr(N_{Tot}<2)$, was 4.1% (2.5-6.4%) at 100 years into the future and 25.6% (19.6-32.4%) at 150 years into the future. The probability of reaching a point with no breeding females remaining in the population, $Pr(N_{B_{YOY}}<1)$, was 32.9% (26.5-39.3%) 150 years into the future (Table 5.1). The probability of exceeding the downlisting criterion, $Pr(N_{Tot}>520)$, at any point during the study period was 1.5% (0.5-3.4%).

In examining how changes in demography affected population viability, mean population growth rates exceeded 1.0 when adult (breeder and non-breeder) survival was increased by 2% regardless of other demographic changes (Figure 5.7a). A positive population growth rate could also be achieved with a 1.5% increase in adult survival in conjunction with (a) a minimum 2% increase in young calf survival and a 5% increase in fecundity or (b) a 10% increase in fecundity (Figure 5.7b). The probability of extinction at 150 years was reduced from the baseline of 25.6% to 1.9% with a 2% increase in adult survival and was reduced to 1.5% with a simultaneous 2% increase in young calf survival and a 15% increase in fecundity. The probability of exceeding the population size downlisting criterion at any point during the 150-year projection period was close to zero under the demographic status quo, and notably varied only with changes in adult

survival, increasing to 26% (18.2-34.2%) with 2% higher adult survival when all other rates remained unchanged.

5.3.4 *Environmental covariate effects*

The results of the full model indicated that Gulf of Alaska SST was weakly positively correlated with fecundity (β_{SST} = 0.23; -0.06, 0.65; Pr($\beta_{SST} > 0$) = 0.92) and older calf survival (β_{SST} = 0.17; -0.23, 0.89; Pr($\beta_{SST} > 0$) = 0.79) (Figure 5.8). The combined prey availability metric was positively correlated with fecundity (β_{prey} = 0.14; -0.04, 0.40; Pr($\beta_{prey} > 0$) = 0.91) and older calf survival (β_{prey} = 0.1; -0.28, 0.7; Pr($\beta_{prey} > 0$) = 0.73) (Figure 5.8). Notable correlations were not apparent between adult and young calf survival and either SST or prey abundance. Though effect sizes were relatively small, the inclusion of Gulf of Alaska sea surface temperature and the proxy for combined-species prey abundance resulted in an improvement in model fit compared to when covariates were excluded (Δ_{WAIC} = 5) (Table 5.3).

5.4 DISCUSSION

We developed an IPM-based PVA to evaluate drivers of population dynamics and future viability of Cook Inlet belugas, a population that has failed to recover from past depletion despite its protected status. Based on our results, the population experienced a period of stability and has subsequently declined since 2011 with an estimated abundance of 369 (294-450) individuals as of 2018. The population is projected to decline at an average rate of 1.7% per year in the coming decades assuming constant environmental variability and that vital rates remain the same as during the latter part of the study period rather than experiencing more above-average years similar to pre-2011 values. This projected trend results in a 2-6% probability of extinction over the next 100 years, a 19-32% probability of extinction over the next 150 years, and less than 1%

probability that the population will meet the criterion for downlisting from endangered to threatened. The extinction risk reported here is likely an underestimate, as our model does not account for changing climate, potential mortality due to catastrophic events, or the exacerbating effects of temporal autocorrelation in vital rates in a declining population. Ultimately, the population is unlikely to experience positive growth or reach the ESA downlisting criterion unless conservation actions can be identified that will promote and maintain higher rates of adult survival and fecundity. Though a paucity of data about stressors remains a barrier, our IPM provides a framework for testing hypotheses about threats and evaluating future management alternatives.

Understanding a population's sensitivity to changes in demographic rates is fundamental to developing hypotheses about factors that underlie changes in abundance. For long-lived mammals with late maturity and high maternal investment, ecological theory and empirical evidence suggest that adult survival is a stronger driver of population dynamics compared with juvenile survival or fecundity (Heppell et al. 2000, Runge et al. 2004). Our results indicated that young calf survival (estimated robustly for the first time here and in Himes Boor et al. *In revision*; 0.92, 0.80-0.98) and breeding adult survival (0.97, 0.95-0.99) were high and similar to rates reported for other stable, long-lived cetacean populations (Jordaan et al. 2020). It is therefore unlikely that increasing breeding female survival is a logistically practical or biologically feasible way to bolster population growth rates. However, we found that though non-breeding survival included subadults, the estimate (0.94, 0.91-0.97) was lower than that of breeding females and consistent with the declining population of belugas in St. Lawrence Estuary (Lesage & Kingsley 1998, Mosnier et al. 2015) and other depleted, declining, or hunted cetacean populations (Luque & Ferguson 2010, Fearnbach et al. 2012). Additionally, as noted by

Himes Boor et al. (*In revision*), fecundity (0.27, 0.21-0.35; equivalent to a 4.6-year inter-birth interval; $1+\frac{1}{0.27}$) was lower than that previously estimated for this and other beluga populations (2- to 3-year inter-birth interval; Sergeant 1973, Mosnier et al. 2015, Jacobson et al. 2020). Despite the theoretical importance of adult survival in long-lived species, fecundity rates generally exhibit greater fluctuations (Gaillard et al. 1998) and are more sensitive to environmental variability and habitat disturbance (Benton & Grant 1996). Because adult survival is often high for long-lived mammals, there is likely greater potential for increasing fecundity, which was found to be the case for Southern Resident killer whales (*Orcinus orca*; Lacy et al. 2017) and bottlenose dolphins (*Tursiops aduncus*; Manlik et al. 2017). Our results suggest that increasing fecundity, young calf survival, non-breeding adult survival, and maintaining high rates of breeding female survival would improve the viability of Cook Inlet belugas, though identifying and implementing conservation actions that might facilitate achieving those targets is challenging.

Even when conservation actions can be designed to ameliorate the impact of anthropogenic activities, the efficacy of these measures is often hindered by the effects of underlying environmental variability. Our results indicated that fecundity and survival rates of Cook Inlet belugas are likely affected by prey abundance and oceanographic conditions. Over the study period, survival and fecundity were lower during 2011 and 2012, suggesting that environmental conditions may have been suboptimal or anthropogenic stressors more acute in those years. The productivity of Chinook salmon populations throughout Cook Inlet from 2003-2007 was poor due to adverse freshwater conditions, which contributed to diminished returns of adult salmon in subsequent years (Jones et al. 2020). Despite the uncertainty in the spatio-temporal alignment of available prey data and beluga foraging, it is conceivable that these trends

impacted foraging conditions, particularly during late gestation and lactation when energetic demands are high. In terms of SST, Suryan et al. (2021) and Arimitsu et al. (2021) concluded that the 2014-2016 marine heatwave in the northern Gulf of Alaska led to declines in forage species, leading to large-scale declines in abundance and breeding success of salmon, groundfish, birds, and mammals. It is therefore challenging to identify the mechanism(s) by which warmer ocean conditions would facilitate increased beluga survival and reproduction as indicated by our analysis, but as an underlying component of basin-scale atmospheric processes that affect both physical (e.g., winds, currents, storms) and biological (e.g., nutrient concentrations, prey abundance) processes, it is possible that elevated SST confer benefits (up to a point) as a shorter-term foraging cue or coincide with the availability of preferred prey. However, these somewhat ambiguous findings related to the effects of SST exemplify the challenges of understanding the ecological scale at which oceanographic conditions are most meaningful for top predators. For this small and isolated population of whales that forages primarily in the upper Cook Inlet, it may be that prey availability and environmental conditions are more strongly influenced by highly localized processes such as river outflow compared with broadscale climatic patterns.

For long-lived top predators that are able to switch target prey or move to avoid disturbances, it is highly unlikely that even the most robust model could identify a single root cause of an apparent decline. For Cook Inlet belugas, it may be the product of cumulative effects: perhaps underwater noise is reducing foraging opportunities in situations when prey availability is already diminished due to dwindling salmon abundance, which is hindering the recovery of the population after decades of hunting pressure and recent habitat constriction. Though we examined the effects of additional anthropogenic stressors and the season-specific effects of

environmental conditions, a more nuanced understanding of the strength, duration, and lag times of environmental effects should be explored in future research.

The paucity of data about anthropogenic stressors and their impacts on demography highlights the importance of developing strategies for implementing recovery actions despite the all-too-common limitations of missing or imperfect information. In an examination of the threats facing over 150 species listed under the ESA, more than one-third of the associated recovery plans lacked information about either the magnitude, timing, frequency, or severity of the threats (Lawler et al. 2002). Identifying conservation measures that aim to mitigate a combination of stressors is challenging but essential: if cumulative effects are indeed one of the largest threats as outlined in the Recovery Plan (NMFS 2016), interventions targeting only a single threat would likely need to reduce the impacts of that threat to implausibly low levels to counteract other stressors (Rhodes et al. 2011, Pirotta et al. 2022). In a recent viability analysis for St. Lawrence Estuary beluga whales, which are also assumed to suffer from cumulative effects of multiple stressors (Lesage 2021), Williams et al. (2017) found that the projected decline was only reversed in simulation scenarios where the three greatest stressors (increased noise and pollution and decreased prey) were simultaneously addressed.

The IPM-based PVA framework presented here could be applied to other species or populations where the causal mechanisms driving changes in abundance remain unknown. This work provided novel insights into temporal variance in demography, the effects of environmental variability, and the sensitivity of Cook Inlet beluga population dynamics and viability to changes in vital rates. Though uncertainty remains, this foundational information is critical for ongoing monitoring and future conservation and recovery planning efforts. This approach highlights the importance and means of capitalizing on the significant resources that have already been

dedicated to monitoring declining populations so that tangible measures can be implemented to understand and reverse the current trajectory of this and other endangered populations.

5.5 Acknowledgements

This work would not be possible without the tremendous effort and dedication of research teams from the Cook Inlet PhotoID Project and from NOAA Fisheries. Aerial surveys were conducted under NMFS Scientific Research Permits 782–1719, 14245, and 20465. CIBW photo-ID surveys were conducted under General Authorization, Letter of Confirmation No. 481-1759, and NMFS Scientific Research Permits 14210 and 18016.

5.6 Figures and Tables

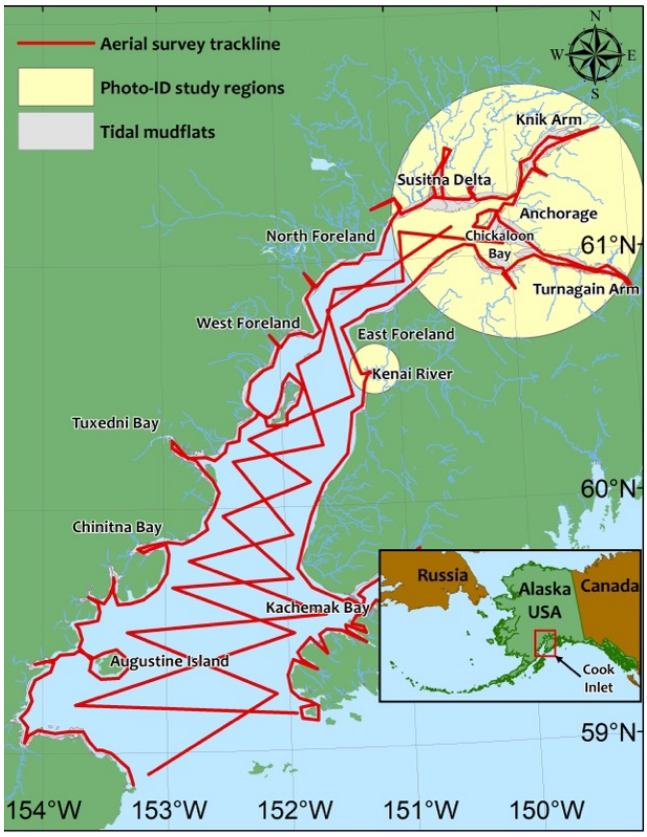

Figure 5.1: Beluga whale study areas within Cook Inlet, Alaska. Aerial surveys occur two weeks in June. Photo-identification boat surveys and land-based operations occur from April-October primarily north of the Forelands.

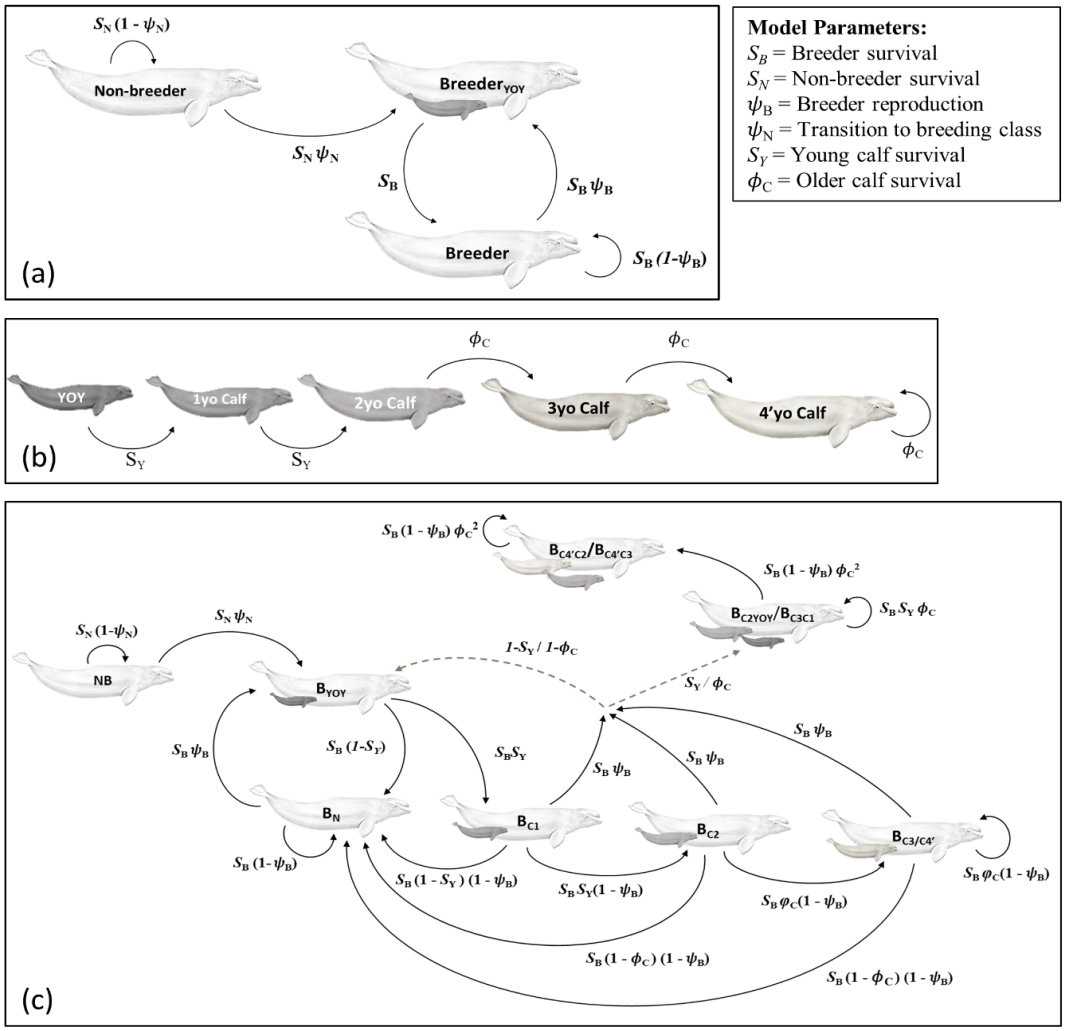

Codes: YOY = young-of-the-year calf, 1yo = 1-year-old calf, 4'yo = 4-year-old or older calf, NB = non-breeder, B_N = breeder with no calf, B_{C1} = breeder with a 1-year-old calf, B_{C2YOY} = breeder with a 2-year-old calf and a YOY

Figure 5.2: Life cycle diagrams reproduced from Himes Boor et al. (*In revision*) depicting (a) adult survival and reproduction; (b) calf survival; and (c) the full ecological process model with possible reproductive states and transitions based on fecundity and calf and adult female survival rates (excludes the transitions from a mother with two calves to one or zero calves when a calf dies or becomes independent for readability).

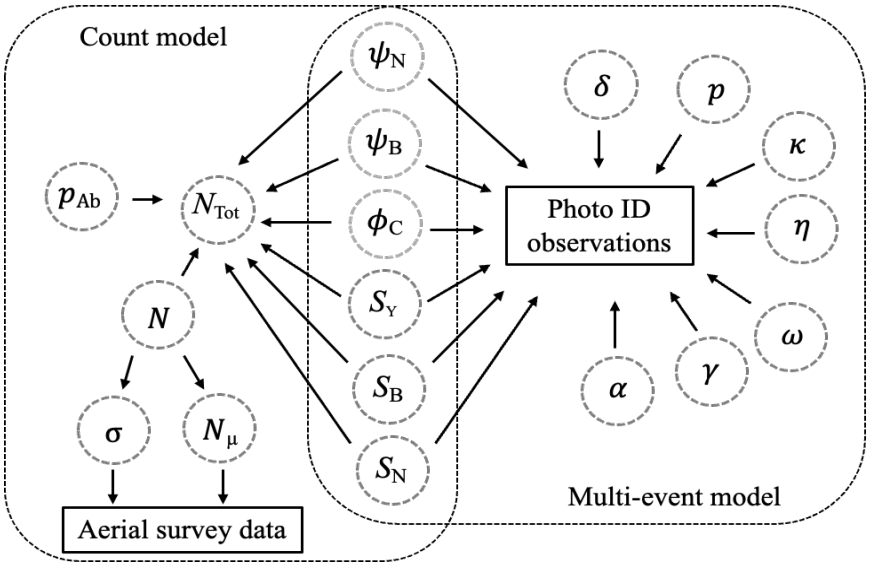

Figure 5.3: Directed acyclic graph of the integrated population model framework for Cook Inlet beluga whale abundance, including the multi-event mark-recapture model estimating fecundity and adult and calf survival, and the count model estimating group size through stochastic population growth equations based on aerial survey data and the associated detection probability.

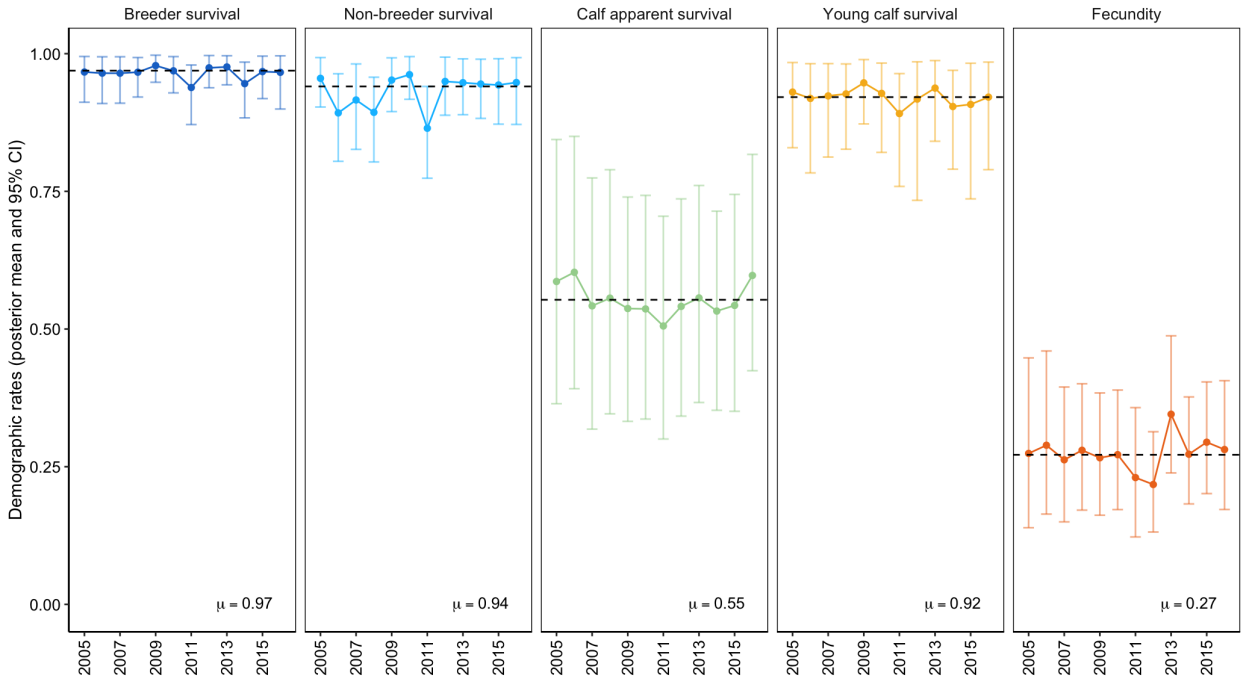

Figure 5.4: Posterior mean and 95% credible intervals for time-varying survival of breeding females, the non-breeding group, young calf survival, apparent survival of older calves, and fecundity over the study period with mean rates represented by the dashed line.

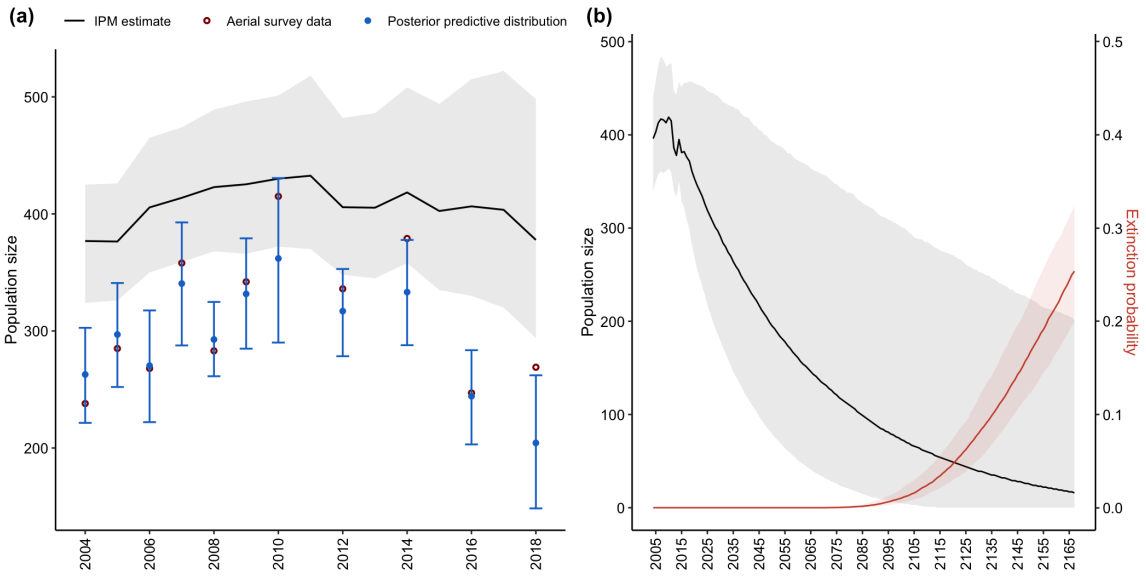

Figure 5.5: (a) Predicted population abundance (black line), 95% credible interval (grey shading), aerial survey data during the study period (red circles), and posterior predictions for aerial survey data (blue points and error bars) that accounts for variability in aerial survey detection probability, and (b) projected abundance and annual extinction probability over a 150-year period for Cook Inlet belugas based on estimated demographic rates and abundance from mark-resight and aerial survey data.

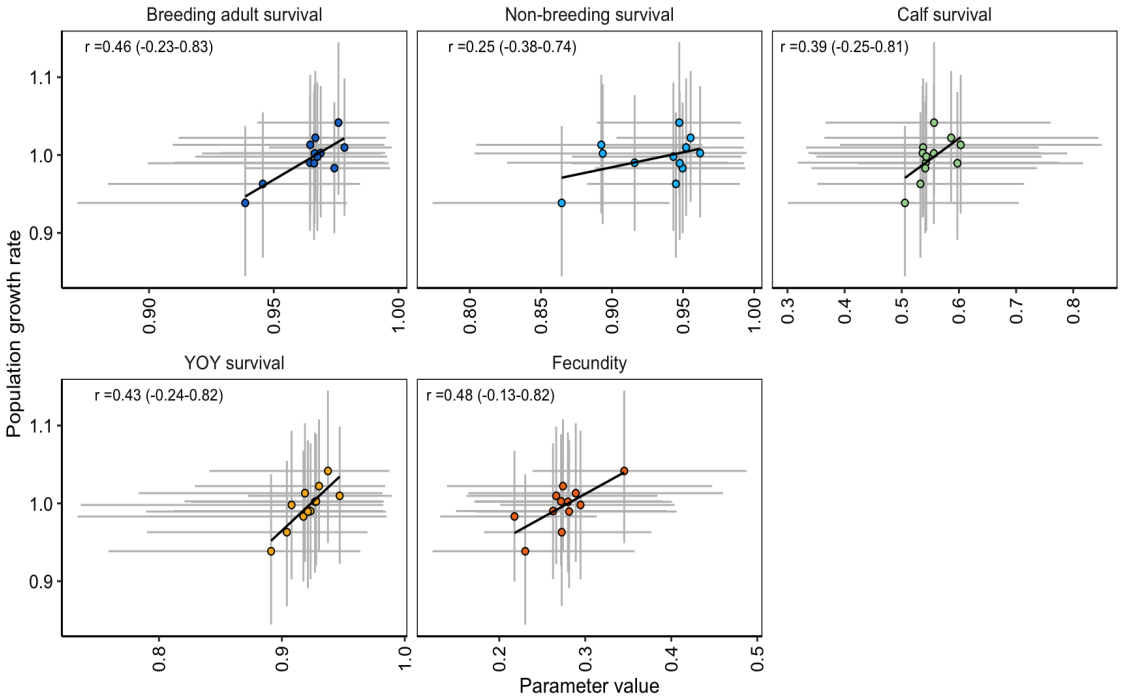

Figure 5.6: Estimated annual population growth rates and demographic rates during the study period with posterior median correlation coefficients, *r*, and 95% credible intervals shown in parentheses for fecundity and adult, older calf, and young calf survival.

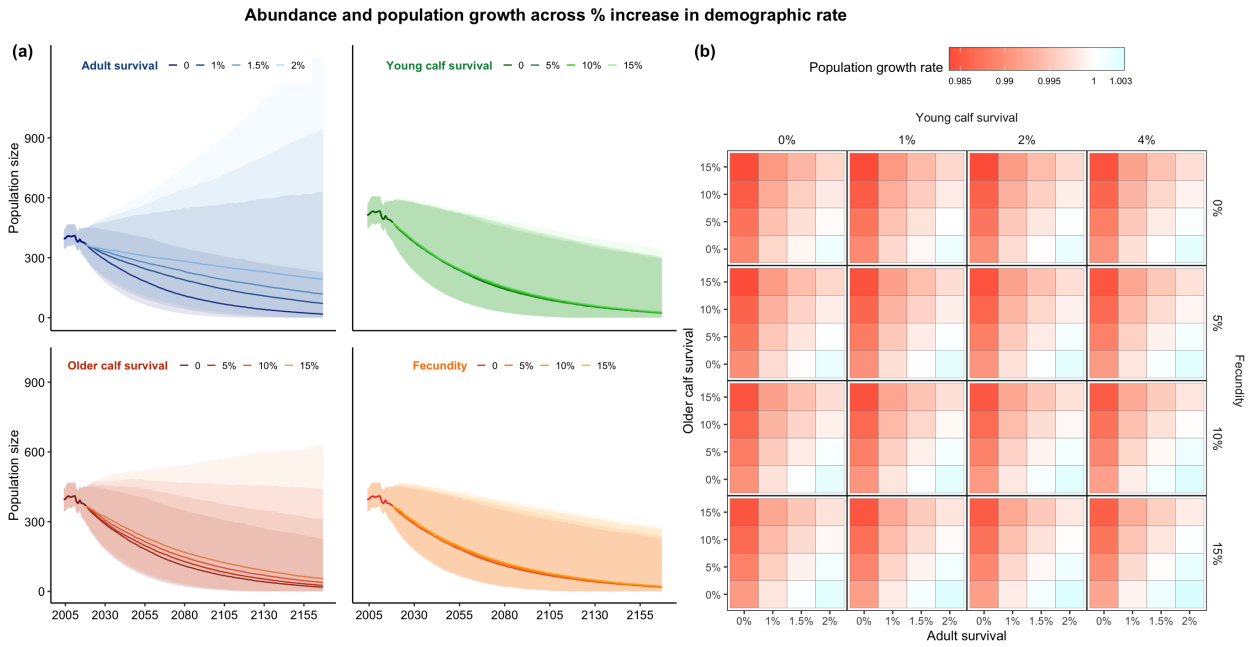

Figure 5.7: (a) Predicted abundance and (b) negative versus positive population growth rates (red-blue color scale) over hypothetical percent increases in demographic rates.

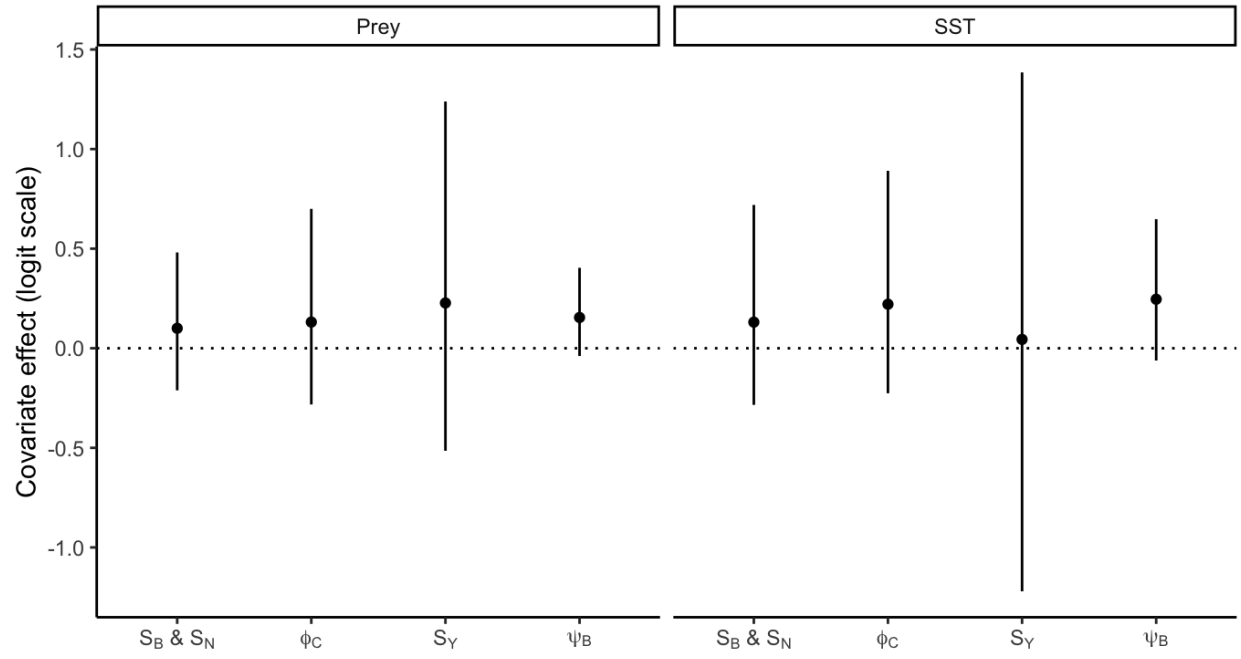

Figure 5.8: Posterior mean and 95% credible intervals for the logit-scale effects of sea surface temperature and prey abundance on fecundity (ψ_B), and adult (S_B, S_N), older calf (ϕ_C), and young calf (S_Y) survival.

Table 5.1: Model parameters, priors, and posterior median estimates.

Parameter	Description	Prior	Median	CI
S_{B}	Female breeder survival	U(0,1)	0.97	0.95-0.99
S_{N}	Non-breeding survival	U(0,1)	0.94	0.91-0.97
ϕ_C	Apparent calf survival	U(0,1)	0.55	0.35-0.77
S_{Y}	Young calf survival	U(0,1)	0.92	0.8-0.98
ψ_{B}	Fecundity	U(0,1)	0.27	0.21-0.35
ψ_{N}	First-time breeding probability	U(0,1)	0.07	0.06-0.09
p_{N}	Non-breeder detection	U(0,1)	0.47	0.38-0.56
p_{Bc}	Breeder with calf detection	U(0,1)	0.68	0.54-0.79
p_{Bn}	Breeder without calf detection	U(0,1)	0.73	0.59-0.87
δ_{C}	Older calf detection	U(0,1)	0.45	0.33-0.58
δ_{Y}	Young calf detection	U(0,1)	0.55	0.46-0.65
p_{Ab}	Aerial survey detection probability	Beta(1,1)	0.77	0.63-0.91
N_{2018}	Abundance in 2018	--	369	294-450
λ	Population growth rate	--	0.98	0.982-0.985
$\Pr(N_{\mathrm{Tot}_{2167}} < N_{\mathrm{Tot}_{2004}})$	Probability of decline	--	0.99	0.98-0.99
$\Pr(N_{\mathrm{Tot}} < 2)_{100}$	Extinction probability - 100 yrs	--	0.04	0.02-0.06
$\Pr(N_{\mathrm{Tot}} < 2)_{150}$	Extinction probability - 150 yrs	--	0.26	0.19-0.32
$\Pr(N_{\mathrm{B_{YOY}}} < 1)_{150}$	Probability of no remaining breeding females	--	0.33	0.26-0.39
$\Pr(N_{\mathrm{Tot}} > 520)_{150}$	Probability of exceeding downlisting criterion	--	0.01	0.005-0.034

Table 5.2. Posterior mean and 95% credible intervals for estimated age structure compared to that expected based on a stable age assumption and observed vital rates.

	Stable age (%)	Estimated age (%)	
Life cycle stage		Mean	95% credible interval
YOY (age 0-1)	8.3	10.1	7.0-12.9
Calves (age 2-5)	25.3	26.2	15.5-36.6
Subadults (age 6-8)	6.1	5.1	1.3-10.1
Breeding females w/ YOY	8.3	10.1	7.0-12.9
Breeding females w/o YOY	29.2	33.2	30.3-35.2
Non-breeding adults (age 9^{+})	22.6	14.8	12.2-17.0

Table 5.3: WAIC values for the null, full, and the random effects-only models.

Model	WAIC	ΔWAIC
Annual random effects + covariates	5,381	0
Annual random effects, no covariates	5,386	5
Null	5,561	180

5.7 REFERENCES

Abadi, F., Gimenez, O., Arlettaz, R., Schaub, M. 2010. An assessment of integrated population models: bias, accuracy, and violation of the assumption of independence. Ecology 91, 7–14.

Arimitsu, M.L., Piatt, J.F., Hatch, S., Suryan, R.M., Batten, S., Bishop, M.A., Campbell, R.W., Coletti, H., Cushing, D., Gorman, K., Hopcroft, R.R., Kuletz, K.J., Marsteller, C., McKinstry, C., McGowan, D., Moran, J., Pegau, S., Schaefer, A., Schoen, S., Straley, J. and von Biela, V.R. 2021. Heatwave-induced synchrony within forage fish portfolio disrupts energy flow to top pelagic predators. Glob. Change Biol., 27: 1859-1878. https://doi.org/10.1111/gcb.15556

Benton, T.G, Grant, A. 1996. How to keep fit in the real world: elasticity analysis and selection pressures on life histories in variable environments American Naturalist, 147, pp. 115-139.

Besbeas, P., Freeman, S.N., Morgan, B., Catchpole, E.A. 2002. Integrating mark-recapture-recovery and census data to estimate animal abundance and demographic parameters. Biometrics 58, 540–547.

Beissinger, S.R., Westphal, M.I. 1998. On the Use of Demographic Models of Population Viability in Endangered Species Management. The Journal of Wildlife Management 62, 821. https://doi.org/10.2307/3802534

Boyd, C., Hobbs, R.C., Punt, A.E., Shelden, K.E.W., Sims, C.L., Wade, P.R. 2019. Bayesian estimation of group sizes for a coastal cetacean using aerial survey data. Marine Mammal Science 0. https://doi.org/10.1111/mms.12592

Boyd, C. and Punt, A.E. 2021. Shifting trends: Detecting changes in cetacean population dynamics in shifting habitat. PloS one, 16(5), p.e0251522.

Boveng, P.L., Hoef, J.M.V., Withrow, D.E., London, J.M. 2018. A Bayesian Analysis of Abundance, Trend, and Population Viability for Harbor Seals in Iliamna Lake, Alaska. Risk Analysis 0. https://doi.org/10.1111/risa.12988

Brooks, S.P., King, R., Morgan, B.J.T. 2004. A Bayesian approach to combining animal abundance and demographic data. Animal Biodiversity and Conservation 27, 515–529.

Converse, S.J., Moore, C.T., Armstrong, D.P. 2013. Demographics of reintroduced populations: Estimation, modeling, and decision analysis. The Journal of Wildlife Management 77, 1081–1093.

Evans, K., Thresher, R., Warneke, R.M., Bradshaw, C.J.A., Pook, M., Thiele, D., Hindell, M.A. 2005. Periodic variability in cetacean strandings: links to large-scale climate events. Biology Letters 1, 147–150. https://doi.org/10.1098/rsbl.2005.0313

Gaillard J.M., Festa-Bianchet M., Yoccoz N.G. 1998. Population dynamics of large herbivores: variable recruitment with constant adult survival. Trends Ecol Evol 13:58–63

Gelman, A., Rubin, D.B. 1992. Inference from iterative simulation using multiple sequences. Statistical Science 7, 457–472.

Heppell, S.S., Caswell, H., Crowder, L.B. 2000. Life Histories and Elasticity Patterns: Perturbation Analysis for Species with Minimal Demographic Data. Ecology 81, 654–665.

Himes Boor, G.K., T.L. McGuire, A.J. Warlick, R.L. Taylor, S.J. Converse, J.R. McClung, and A.D. Stephens. *In revision*. Estimating reproductive rates and juvenile survival when offspring ages are uncertain using a novel multievent mark-recapture model. Methods in Ecology and Evolution.

Hobbs, R.C., K.E.W. Shelden, D.J. Vos, K.T. Goetz, and D.J. Rugh. 2006. Status review and extinction assessment of Cook Inlet belugas (*Delphinapterus leucas*). AFSC Processed Rep. 2006-16, 74 p. Alaska Fish. Sci. Cent., NOAA, Natl. Mar, Fish. Serv., 7600 Sand Point Way NE, Seattle WA 98115.

Hobbs, R.C., Wade, P.R., Shelden, K.E.W. 2015. Viability of a small, geographically-isolated population of beluga whale, *Delphinapterus leucas*: effects of hunting, predation, and mortality events in Cook Inlet, Alaska. Marine Fisheries Review 77(2), 59–88. https://doi.org/10.7755/MFR.77.2.4

IJsseldijk, L.L., Hessing, S., Mairo, A. et al. 2021. Nutritional status and prey energy density govern reproductive success in a small cetacean. Sci Rep 11, 19201.

Jacobson, E.K., Boyd, C., McGuire T.L., Shelden K.E.W., Himes-Boor G.K.H, and A.E. Punt. 2020. Assessing cetacean populations using integrated population models: an example with Cook Inlet beluga whales. Ecological Applications 30: e02114. https://doi.org/10.1002/eap.2114

Jenouvrier, S., Holland, M., Iles, D., Labrousse, S., Landrum, L., Garnier, J., Caswell, H., Weimerskirch, H., LaRue, M., Ji, R., Barbraud, C. 2020. The Paris Agreement objectives will likely halt future declines of emperor penguins. Global Change Biology 26, 1170–1184. https://doi.org/10.1111/gcb.14864

Jones, LA, Schoen, ER, Shaftel, R, et al. 2020. Watershed-scale climate influences productivity of Chinook salmon populations across southcentral Alaska. Glob Change Biol; 26: 4919–4936. https://doi.org/10.1111/gcb.15155

Jordaan, R.K., Oosthuizen, W.C., Reisinger, R.R., Bruyn, P.J.N.D. 2020. Abundance, survival and population growth of killer whales Orcinus orca at subantarctic Marion Island. wbio 2020, wlb.00732. https://doi.org/10.2981/wlb.00732

Kellner, K. 2019. A Wrapper Around 'rjags' to Streamline 'JAGS' Analyses. https://github.com/kenkellner/jagsUI

Lacy, R.C., Williams, R., Ashe, E., Balcomb III, K.C., Brent, L.J.N., Clark, C.W., Croft, D.P., Giles, D.A., MacDuffee, M., Paquet, P.C., 2017. Evaluating anthropogenic threats to endangered killer whales to inform effective recovery plans. Sci Rep 7, 14119. https://doi.org/10.1038/s41598-017-14471-0

Lawler, J.J., Campbell, S.P., Guerry, A.D., Kolozsvary, M.B., O'Connor, R.J., Seward, L.C.N. 2002. The Scope and Treatment of Threats in Endangered Species Recovery Plans. Ecological Applications 12, 663–667. https://doi.org/10.2307/3060975

Leasure, D.R., Wenger, S.J., Chelgren, N.D., Neville, H.M., Dauwalter, D.C., Bjork, R., Fesenmyer, K.A., Dunham, J.B., Peacock, M.M., Luce, C.H., Lute, A.C., Isaak, D.J. 2019. Hierarchical multi-population viability analysis. Ecology 100, e02538. https://doi.org/10.1002/ecy.2538

Lesage, V., and M.C.S. Kingsley. 1998. Updated status of the St. Lawrence River population of the beluga, *Delphinapterus leucas*. Can. Field-Nat. 112(1): 98–114. [Canada] St. Lawrence population. Leslie, P.H., 1948. Some Further Notes on the Use of Matrices in Population Mathematics. Biometrika 35, 213.

Luque, S.P., and S.H Ferguson. 2010. Age structure, growth, mortality, and density of belugas (*Delphinapterus leucas*) in the Canadian Arctic: responses to environment? Polar Biol 33, 163–178. https://doi.org/10.1007/s00300-009-0694-2

Manlik, O., McDonald, J.A., Mann, J., Raudino, H.C., Bejder, L., Krützen, M., Connor, R.C., Heithaus, M.R., Lacy, R.C., Sherwin, W.B. 2016. The relative importance of reproduction and survival for the conservation of two dolphin populations. Ecology and Evolution 6, 3496–3512. https://doi.org/10.1002/ece3.2130

McGuire, T.L., Stephens, A.D., McClung, J.R., Garner, C.D., Shelden, K.E.W., Himes Boor, G.K. & Wright, B. 2020. Reproductive natural history of endangered Cook Inlet Beluga whales: insights from a long-term photo-identification study. Polar Biology, 43, 1851-1871

Moore, S.E. 2008. Marine Mammals as Ecosystem Sentinels. J Mammal 89, 534–540. https://doi.org/10.1644/07-MAMM-S-312R1.1

Moore, S.E. 2018. Climate Change. pp 194-197 *In* The Encyclopedia of Marine Mammals, 3rd Edition, B. Würsig, J.G.M. Thewissen, K.M. Kovacs (eds.), Academic Press/Elsevier, San Diego, CA USA.

Moore, S.E., K.E.W. Shelden, D.J. Rugh, B.A. Mahoney and L.K. Litzky. 2000. Beluga whale habitat associations in Cook Inlet, Alaska. *Marine Fisheries Review* 62(3): 60-80.

Mosnier, A., Doniol-Valcroze, T., Gosselin, J.-F., Lesage, V., Measures, L.N., Hammill, M.O. 2015. Insights into processes of population decline using an integrated population model: The case of the St. Lawrence Estuary beluga (*Delphinapterus leucas*). Ecological Modelling 314, 15–31.

National Marine Fisheries Service. 2016. Recovery Plan for the Cook Inlet Beluga Whale (*Delphinapterus leucas*). National Marine Fisheries Service, Alaska Region, Protected Resources Division, Juneau, AK.

Nelson, M., Quakenbush, L., Mahoney, B., Taras, B., Wooller, M. 2018. Fifty years of Cook Inlet beluga whale feeding ecology from isotopes in bone and teeth. Endangered Species Research 36, 77–87. https://doi.org/10.3354/esr00890

Norman, S. A., Hobbs, R. C., Beckett, L. A., Trumble, S. J., and Smith, W.A. 2019. Relationship between per capita births of Cook Inlet belugas and summer salmon runs: age-structured population modeling. Ecosphere 11(1):e02955. 10.1002/ecs2.2955

O'Neill, S.M., Ylitalo, G.M., West, J.E. 2014. Energy content of Pacific salmon as prey of northern and southern resident killer whales. Endanger. Species Res. 25, 265–281. https://doi.org/10.3354/esr00631

Pirotta, E., Thomas, L., Costa, D.P., Hall, A.J., Harris, C.M., Harwood, J., Kraus, S.D., Miller, P.J.O., Moore, M.J., Photopoulou, T., Rolland, R.M., Schwacke, L., Simmons, S.E., Southall, B.L., Tyack, P.L. 2022. Understanding the combined effects of multiple stressors: A new perspective on a longstanding challenge. Science of The Total Environment 821, 153322. https://doi.org/10.1016/j.scitotenv.2022.153322

Plummer, M. 2019. rjags: Bayesian Graphical Models using MCMC. R package version 4-10. https://CRAN.R-project.org/package=rjags.

Quakenbush, L.T., Suydam, R.S., Brown, A.L., Lowry, L.F., Frost, K.J., Mahoney, B.A. 2015. Diet of beluga whales, *Delphinapterus leucas*, in Alaska from stomach contents, March-November. Marine Fisheries Review 77(1), 70–84.

R Core Development. 2022. R: A Language and Environment for Statistical Computing.

Regehr, E.V., Hostetter, N.J., Wilson, R.R., Rode, K.D., Martin, M.S., Converse, S.J. 2018. Integrated Population Modeling Provides the First Empirical Estimates of Vital Rates and Abundance for Polar Bears in the Chukchi Sea. Scientific Reports 8, 16780. https://doi.org/10.1038/s41598-018-34824-7

Rhodes, J.R., Ng, C.F., de Villiers, D.L., Preece, H.J., McAlpine, C.A., Possingham, H.P. 2011. Using integrated population modelling to quantify the implications of multiple threatening processes for a rapidly declining population. Biological Conservation 144, 1081–1088.

Romero, M.A., Grandi, M.F., Koen-Alonso, M., Svendsen, G., Ocampo Reinaldo, M., García, N.A., Dans, S.L., González, R., Crespo, E.A. 2017. Analysing the natural population growth of a large marine mammal after a depletive harvest. Nature Publishing Group 7, 597–16.

Runge, M.C., Langtimm, C.A., Kendall, W.L. 2004. A stage-based model of manatee population dynamics. Marine Mammal Science 20: 361-385.

Santora, J.A., Mantua, N.J., Schroeder, I.D., Field, J.C., Hazen, E.L., Bograd, S.J., Sydeman, W.J., Wells, B.K., Calambokidis, J., Saez, L., Lawson, D., Forney, K.A., 2020. Habitat compression and ecosystem shifts as potential links between marine heatwave and record whale entanglements. Nat Commun 11, 536. https://doi.org/10.1038/s41467-019-14215-w

Saunders, S.P., Cuthbert, F.J., Zipkin, E.F. 2018. Evaluating population viability and efficacy of conservation management using integrated population models. Journal of Applied Ecology 55, 1380–1392. https://doi.org/10.1111/1365-2664.13080

Schaub, M., Gimenez, O., Sierro, A., Arlettaz, R., 2007. Use of Integrated Modeling to Enhance Estimates of Population Dynamics Obtained from Limited Data. Conservation Biology 21, 945–955. Seber, G., 1965. A note on the multiple recapture census. Biometrika 52, 249–259.

Schaub, M., Abadi, F., 2010. Integrated population models: a novel analysis framework for deeper insights into population dynamics. Journal of Ornithology 152, 227–237.

Shelden, K.E.W. and P.R. Wade. 2019. Aerial surveys, distribution, abundance, and trend of belugas (*Delphinapterus leucas*) in Cook Inlet, Alaska, June 2018. AFSC Processed Rep. 2019-09, 93 p. https://doi.org/10.25923/kay8-7p06

Shelden K.E.W., K.T. Goetz, D.J. Rugh, D.G. Calkins, B.A. Mahoney, & R.C. Hobbs. 2015. Spatio-temporal changes in beluga whale, *Delphinapterus leucas*, distribution: Results from aerial surveys (1977-2014), opportunistic sightings (1975-2014), and satellite tagging (1999-2003) in Cook Inlet, Alaska. Marine Fisheries Review 77(2):1-31. DOI: 10.7755/MFR.77.2.1

Shelden K.E.W., J.J. Burns, T.L. McGuire, K.A. Burek-Huntington, D.J. Vos, C.E.C. Goertz, G. O'Corry-Crowe, & B.A. Mahoney. 2020. Reproductive status of female beluga whales from the endangered Cook Inlet population. Marine Mammal Science 36(2):690-699. DOI: 10.1111/mms.12648

Suryan, R.M., Arimitsu, M.L., Coletti, H.A. et al. 2021. Ecosystem response persists after a prolonged marine heatwave. Sci Rep 11, 6235. https://doi.org/10.1038/s41598-021-83818-5

Taylor, B.L., Martinez, M., Gerrodette, T., Barlow, J., Hrovat, Y.N. 2007. Lessons from monitoring trends in abundance of marine mammals. Marine Mammal Science 23, 157–175.

Véran, S., Lebreton, J.-D. 2008. The potential of integrated modelling in conservation biology: A case study of the black-footed albatross (*Phoebastria nigripes*). Canadian Journal of Statistics 36, 85–98. https://doi.org/10.1002/cjs.5550360109

Wade, P.R., Reeves, R.R., Mesnick, S.L. 2012. Social and Behavioural Factors in Cetacean Responses to Overexploitation: Are Odontocetes Less "Resilient" Than Mysticetes? Journal of Marine Biology 2012, 1–15.

Williams, P.J., Hooten, M.B., Womble, J.N., Esslinger, G.G., Bower, M.R., Hefley, T.J. 2017. An integrated data model to estimate spatiotemporal occupancy, abundance, and colonization dynamics. Ecology 98, 328–336. https://doi.org/10.1002/ecy.1643

Zipkin, E.F., Saunders, S.P. 2018. Synthesizing multiple data types for biological conservation using integrated population models. Biological Conservation 217, 240–250. https://doi.org/10.1016/j.biocon.2017.10.017.

APPENDIX A

Model selection and seasonal covariates for Steller sea lion demography (Chapter 3)

We examined the effects of environmental variability on age- and sex-specific demographic rates for Steller sea lions in the western distinct population segment (wDPS) in Alaska. Our aim was to identify correlations between changes in vital rates and oceanographic conditions for individuals branded in both the eastern and western portions of the wDPS range where divergent abundance trends have been observed.

To examine these relationships for a top predator in a highly variable and complex ecosystem, we used both localized and basin-scale ocean conditions as covariates for pup and dependent young (age 1-2) survival and first-time and repeat female breeding probabilities. Estimating the effects of numerous environmental conditions simultaneously was facilitated by using penalized complexity priors as a variable selection tool. However, due to the temporal correlations within and between season-specific environmental values, not all possible variables could be simultaneously included and only one set of seasonal values could be used at a time. This limitation precluded identifying which environmental variable(s) were the strongest predictors based on changes in WAIC values. To address this issue, we ran models where each environmental variable was the sole predictor within the 'full' model framework, which included random effects of year for survival, breeding, and detection probabilities for individuals branded in the eastern portion of the range. The WAIC values for each of these single-covariate models were compared to that of the random effects-only model for the eastern portion of the range and the null model for the western portion of the range. This additional analysis both facilitated the initial elimination of numerous environmental variables and then ultimately provided insight into

potential optimal season-specific combinations of different variables (e.g., AOI in summer and PDO in winter) that could be explored in future work.

For models estimating vital rates for individuals branded in the eastern portion of the range, results when all variables were used indicated that best-fit models based on WAIC values included environmental variables from the winter season followed by the summer. However, only by examining the single-variable model runs was it possible to ascertain that winter Aleutian Low, upwelling, and eastward wind, year-round SST and chlorophyll-a concentration, and spring North Pacific Gyre Oscillation (NPGO) conditions were the strongest drivers of improved model fit when used alone (Figure A1). As can be seen, model runs with these predictors as the sole covariate had the lowest WAIC values. Additionally, these results provided support for the elimination of PDO, productivity, wind stress, and wind velocity based on the general lack of improvement in WAIC values across seasons compared to the random effects-only model.

For models estimating vital rates for individuals branded in the western portion of the range, results when all variables were included indicated that best-fit models based on WAIC values included environmental variables from the fall and winter. Examining the single-variable model runs revealed that these gains in model fit were likely most attributable to the conditions of the NPGO during fall and spring that made the biggest contributions to improved model fit when used alone (Figure A1). These results provide justification for the elimination of wind variables, productivity, and PDO.

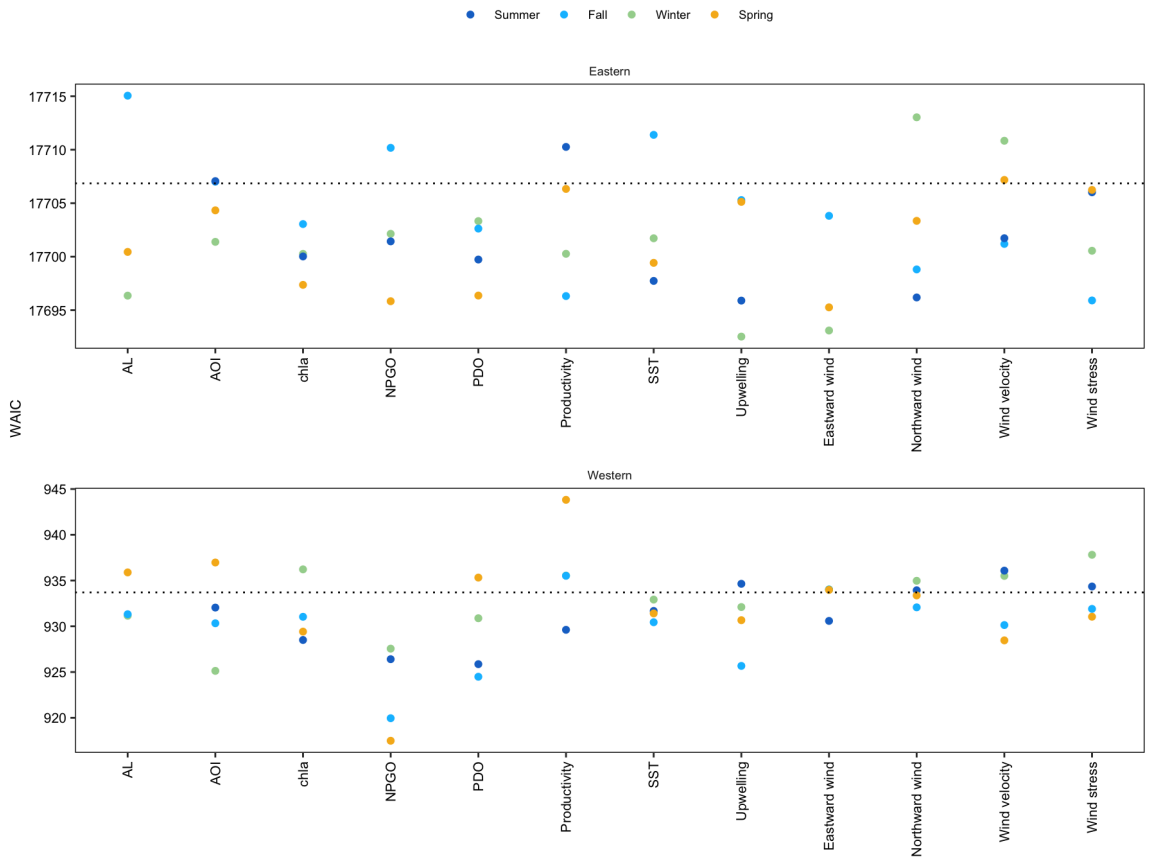

Figure A1: WAIC values for models when each season-specific environmental variable was used as the only covariate. Dashed line represents a baseline WAIC value for the random effects-only model for the eastern portion of the range and a null model for the western portion of the range.

APPENDIX B

Age- and sex-specific demography and population sensitivity in an integrated population model and viability analysis for Steller sea lions (Chapter 4)

This appendix contains additional information pertaining to understanding age- and sex-specific demographic rates, age structure, and the effects of environmental conditions on Steller sea lions in the six management subregions of the wDPS in Alaska

Using an integrated population model (IPM) framework with mark-resight and aerial survey data, we estimated age- and sex-specific vital rates as functions of fixed effects of natal subregion and random effects of time with varying levels of complexity depending on the vital rate of interest (see main text). Our results showed that male and female vital rates were similar to each other for each age, but varied by region (Figure B1).

In addition to examining population structure in terms of the $\frac{N_{Tot}}{N_{pup}}$ ratio, we also here show a more complex age structure that compares estimated age structure to the age proportions that would be expected based on estimated demographic rates and our assumption of the stable age distribution that was used to initiate the population model (Figure B2). This more nuanced picture provides additional insight into the subregional deviations in the overall $\frac{N_{Tot}}{N_{pup}}$ ratio that we see in the subregions with declining abundance trends. Specifically, we estimated a higher proportion of pups (and therefore female breeders) in the central AI subregion, where pup and yearling survival are notably lower than the range-wide average. Additionally, in the western AI subregion, the proportion of non-female breeders is high while that of female breeders is low, but pup survival is high. These differences may be providing insights into the different maternal investment strategies in these two subregions, where survival and pupping probabilities are likely influenced by pup mass, weaning age, maternal body condition, and environmental conditions.

In terms of the effects of environmental conditions on vital rates of Steller sea lions, as noted in the main text, sea surface temperature and warm-phase North Pacific Gyre Oscillation were positively correlated with survival and pupping probabilities, though credible intervals overlapped zero (Figure B3). In considering how these or other environmental variables may affect population dynamics, it is important to examine the sensitivity of population growth rates to changes in demographic rates. As noted in the main text but illustrated in more detail here, population growth rates were most consistently and strongly correlated with female breeder survival and repeat pupping probabilities (Figure B4), though the variability in these correlations varied across subregions (Figure B5).

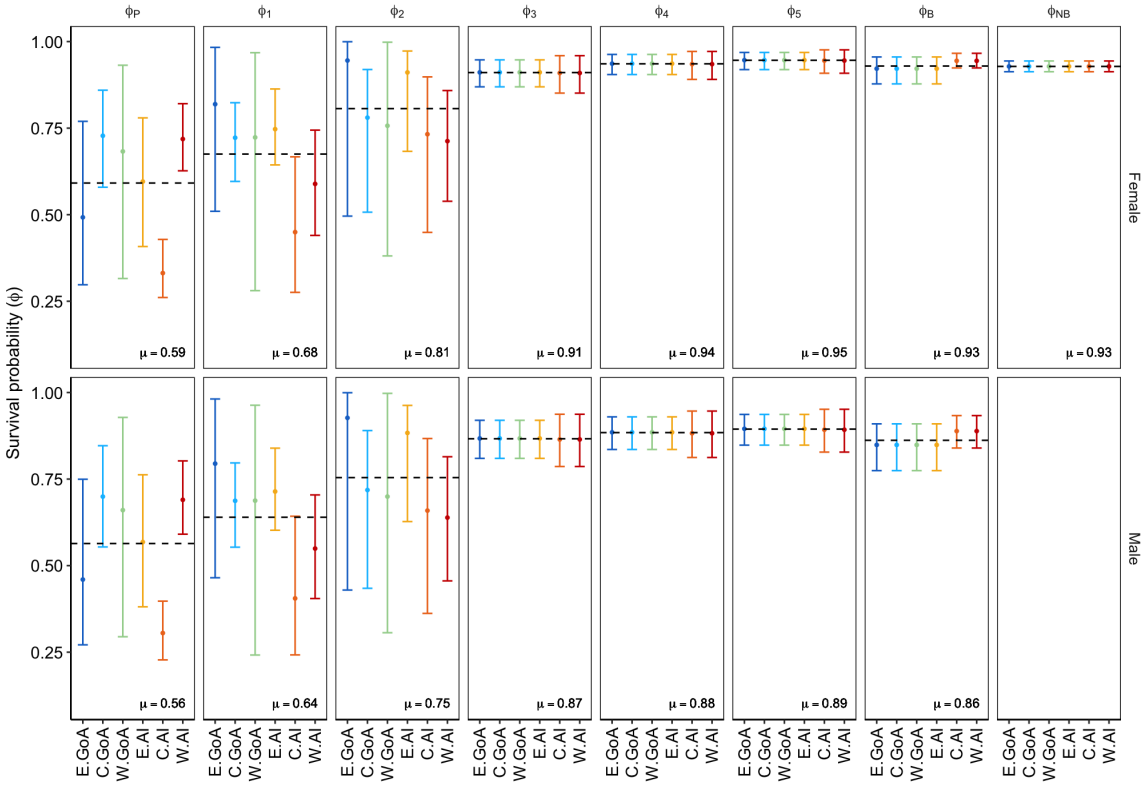

Figure B1: Posterior mean and 95% credible intervals for age-specific survival for Steller sea lions across the six wDPS subregions, with the range-wide average represented by the dashed line.

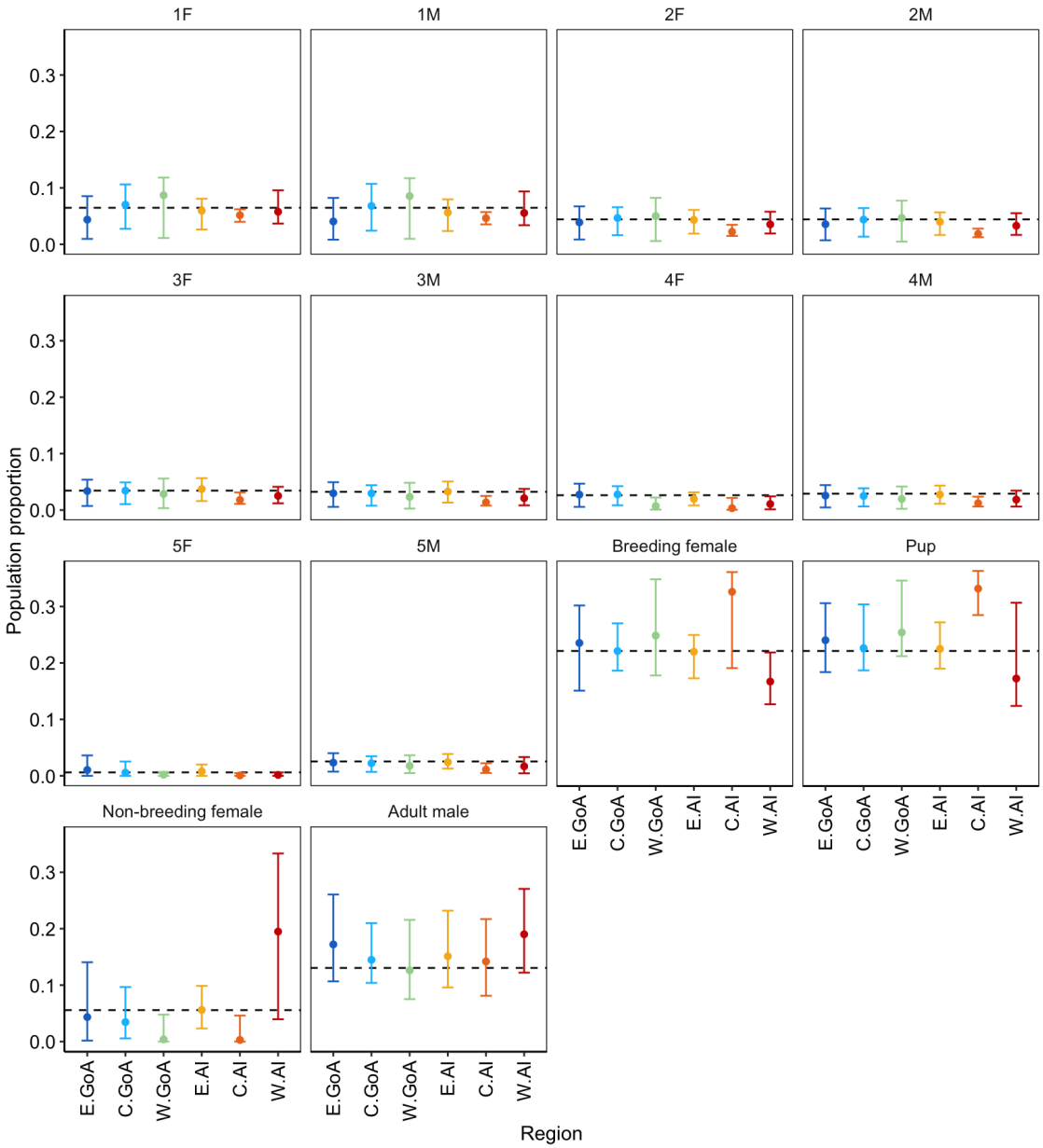

Figure B2: Posterior mean and 95% credible intervals of population age structure in each of the six wDPS subregions compared with the proportion expected according to a stable age distribution assumption (black dashed line).

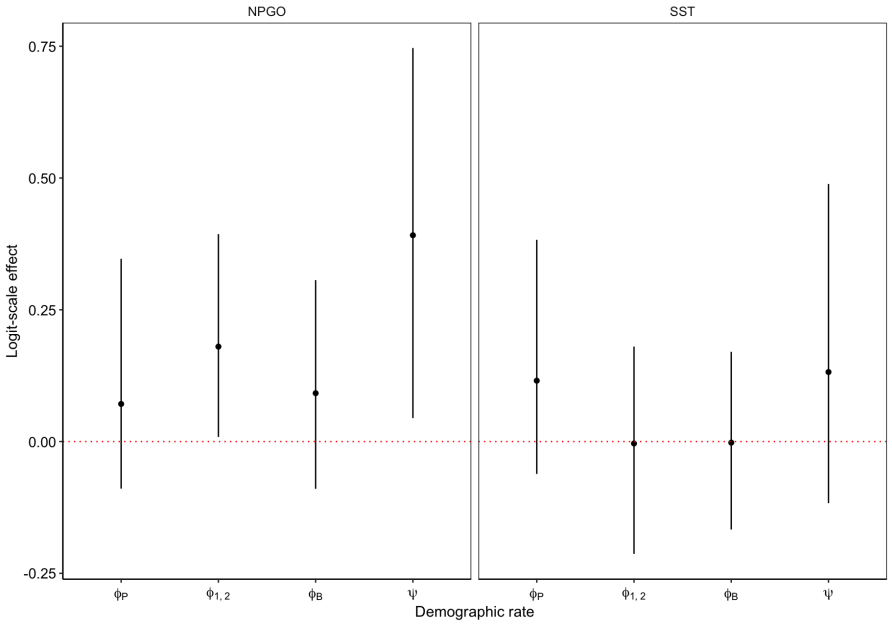

Figure B3: Mean and 95% credible intervals of logit-scale effects of environmental conditions on male and female pup and yearling survival, breeding female survival, and first-time and repeat pupping probabilities.

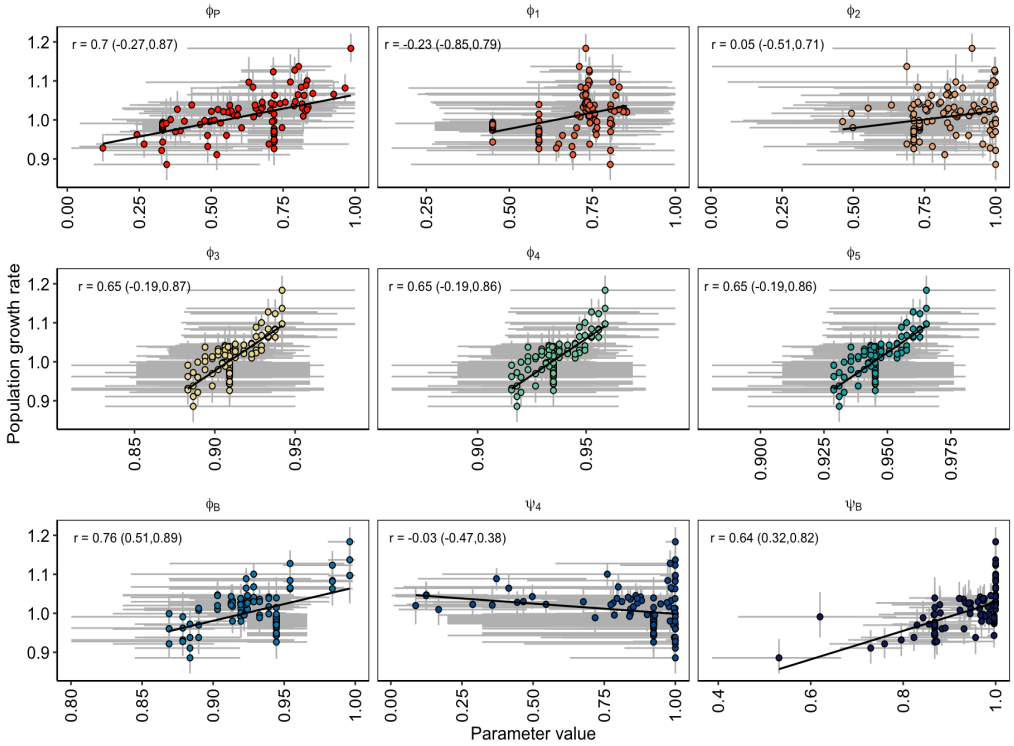

Figure B4: Posterior mean and 95% credible intervals for correlation coefficients between population growth rates and female time-varying demographic rates.

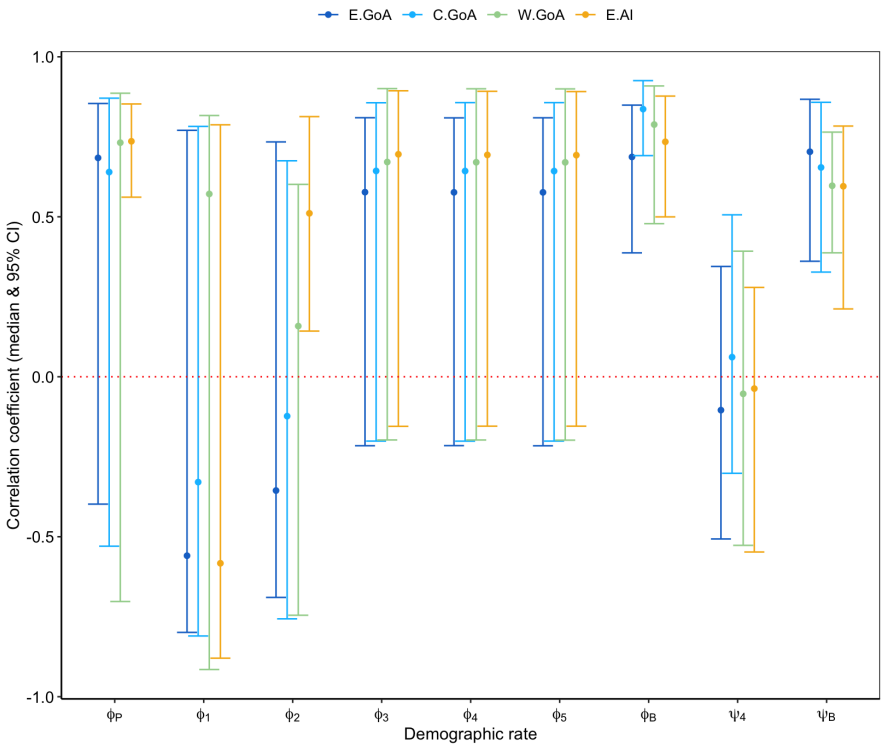

Figure B5: Posterior mean and 95% credible intervals for correlation coefficients between population growth rates and female time-varying demographic rates across the six wDPS subregions.

APPENDIX C

Sensitivity of demography, abundance, and viability to underlying assumptions of the aerial survey model in an IPM-based PVA for Cook Inlet belugas (Chapter 5)

Abundance estimated in this IPM is a product of the two subcomponent models: the mark-resight model that estimates demographic rates and the population size estimation model based on the aerial survey data. The aerial survey has to-date been conducted in a strategic manner rather than following a random or systematic track. This has led to previous assumptions that detection probability in this survey (represented here by the parameter p_{Ab_t}) is relatively high, but the proportion of the population that is missed on any given survey day remains highly uncertain. Differing assumptions underlying the aerial survey have also led to differing approaches of estimating abundance using the median daily survey counts versus the maximum daily survey count in a given year. As noted in the main text, to account for highly variable annual counts derived from the aerial survey data, population size is modeled as,

$$\widehat{N}_{\mu_t} \sim \mathrm{normal}(N_t, \widehat{\sigma}_t)$$

$$N_t \sim \mathrm{binomial}(N_{\mathrm{Tot}_t}, p_{\mathrm{Ab}_t})$$

$$p_{\mathrm{Ab}_t} \sim \mathrm{Beta}(\alpha, \beta)$$

where annual aerial survey population size estimates $\widehat{N}_{\mu_t}$ are modeled as arising from a normal distribution with mean equal to N_t (the population size in year *t* subject to detection in the aerial survey) and standard deviation $\widehat{\sigma}_t$. Both the annual estimates $\widehat{N}_{\mu_t}$ and their sampling standard deviations $\widehat{\sigma}_t$ were estimated by Boyd et al. (2019) and Shelden and Wade (2019). In turn, N_t is modeled as arising from a binomial distribution with index equal to the total abundance, N_{Tot_t},

from the IPM process model, and the probability equal to the aerial survey detection probability p_{Ab_t}.

We examined model results using both the "median" and "maximum" survey day data across four beta probability distribution rates that represented a range of uninformative to strongly informative priors to characterize uncertainty about the proportion of groups that are missed in the aerial survey. The flat, uninformative prior Beta(1,1) represents the most flexible option that allows the data to freely inform parameter estimation. The weakly informative prior of Beta(2,1) had most prior density between 0.8 and 0.9 with a broad tail that encompassed the space from 0 to 1.0. The moderately informative prior of Beta(10,3) also had the highest probability density around ~0.8 but a more truncated distribution tail that extends to ~0.4. The most informative prior, Beta(15,1), was estimated and used in previous studies (Boyd et al. 2019, Jacobson et al. 2020) and places a high prior density close to 1.0 with a relatively short tail that only extends to ~0.7.

The detection probability in the aerial survey subcomponent model provides information about how many individuals were not counted and therefore directly impacts the relative size of the abundance estimate: a lower estimated detection probability leads to a higher abundance estimate and vice versa. Therefore, when we relax the prior and allow for lower detection probabilities, we allow the potential for higher abundance estimates. In a traditional abundance estimation model, this sensitivity would only impact the relative scale of the abundance estimate. However, because the IPM framework facilitates all parameters being informed by both the mark-resight and aerial survey data sets, the demographic rates and abundance trends could also be affected depending on the relative contributions of each data set.

As expected, the annual detection probability estimates are sensitive to the choice of prior, where posterior means are higher with the strongly informative prior, but otherwise are similar across the other three approaches (Figure C1). As can be seen from the overlap of the prior and posterior distributions for detection probability, posterior means are higher and the distributions are tighter with the strongly informative prior. Posterior distributions are estimated fairly consistently and reliably under the flat and weakly informative priors (Figure C2), which guided our decision to allow the data to more freely inform estimation using the weakly informative prior Beta(2,1) while acknowledging that this approach may result in positively biased abundance estimates.

Demographic rate estimates were fairly robust to the choice of priors for the aerial survey detection probability, particularly adult survival (Figure C3). Where differences arose, they were slight and not systematically apparent, likely due to the strength of the mark-resight data informing the estimation of the demographic rate parameters. In contrast, the sensitivity of abundance estimates to the detection probability prior is evident, with abundance estimated using flat and weakly informative priors all being fairly similar, and notably higher than those estimated using the strongly informative prior (Figure C4). Population viability, growth rates, and extinction risk summary metrics varied across the choice of prior and survey day data, though much more notably for the latter (Figure C5, Figure C6, Figure C7).

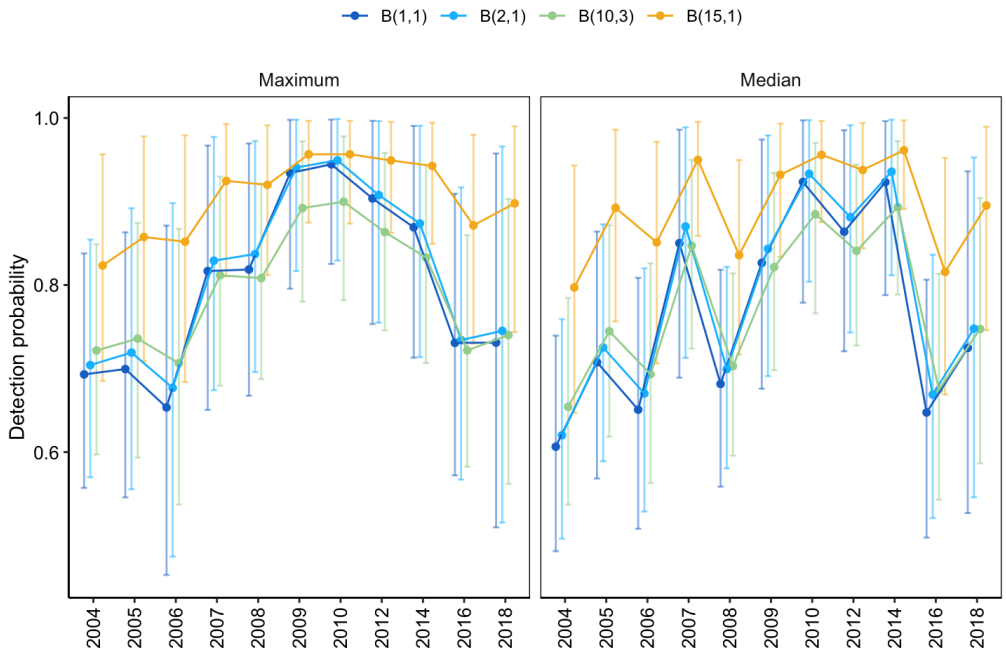

Figure C1: Posterior mean and 95% credible intervals for annual detection probabilities across priors for aerial survey detection probability using either maximum or median survey day counts.

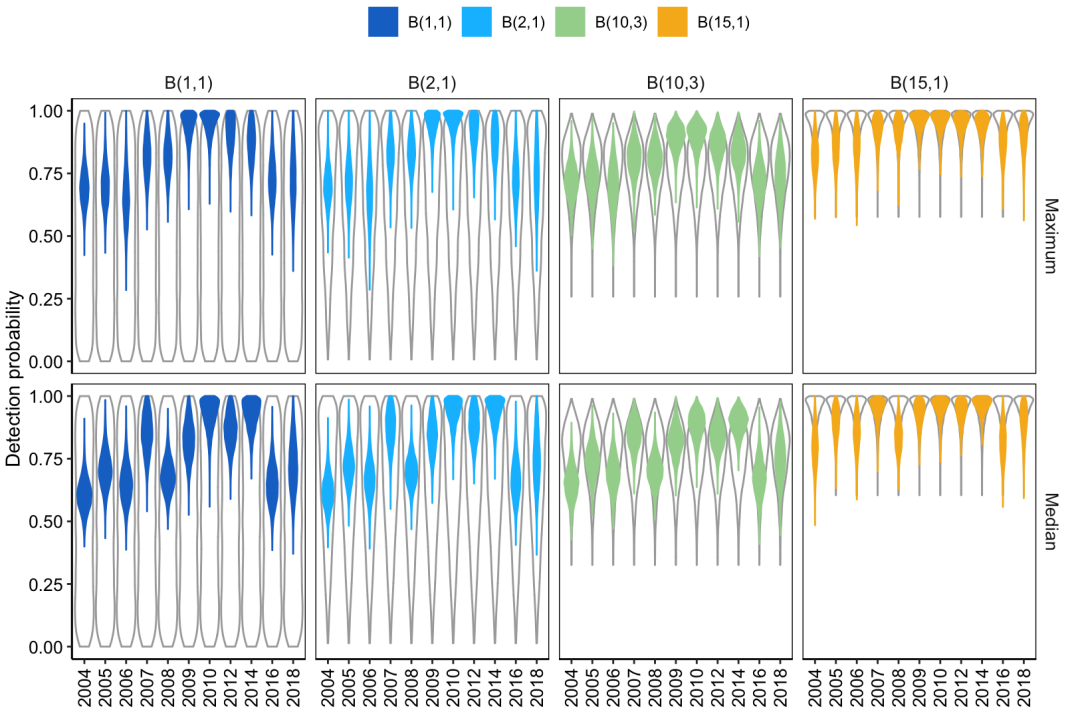

Figure C2: The overlap of prior (grey outline) and posterior (color fill) distributions across priors for aerial survey detection probability using either maximum or median survey day counts.

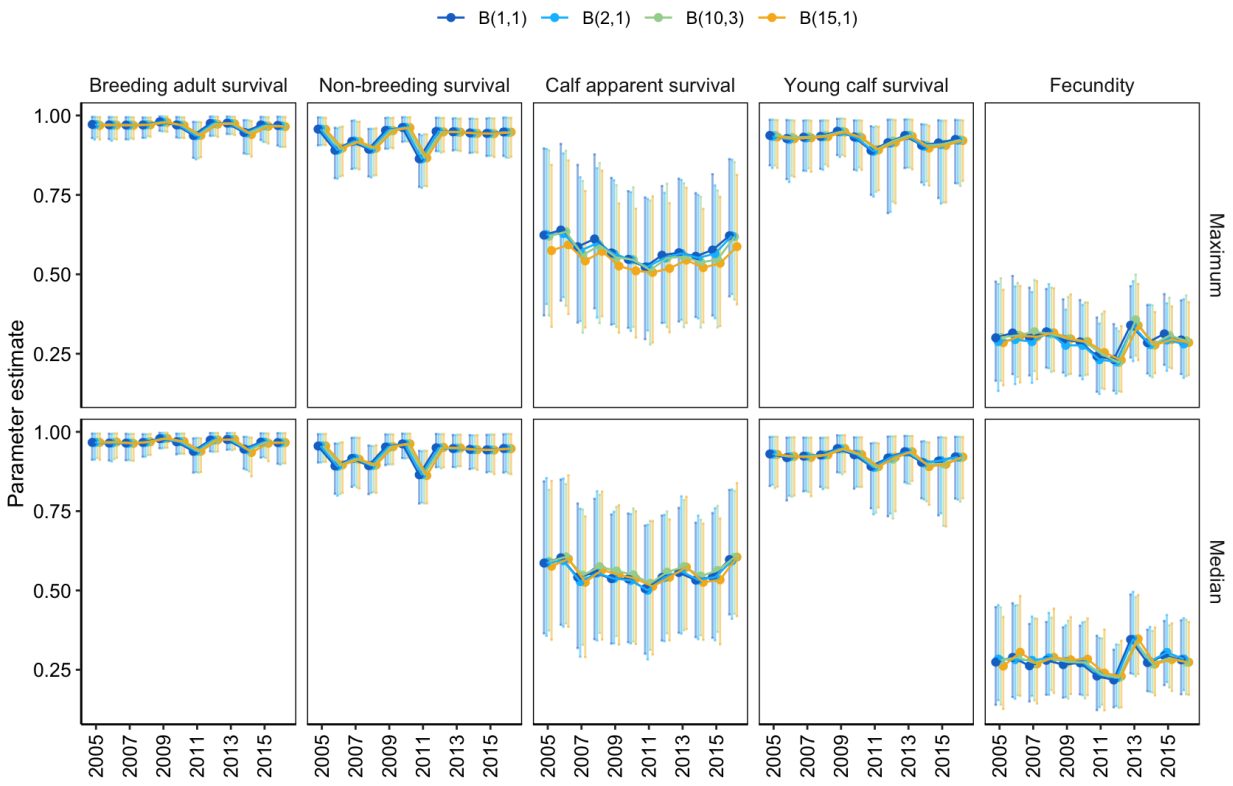

Figure C3: Posterior mean and 95% credible intervals for stage-based survival and fecundity estimated across priors for aerial survey detection probability using either maximum or median survey day counts.

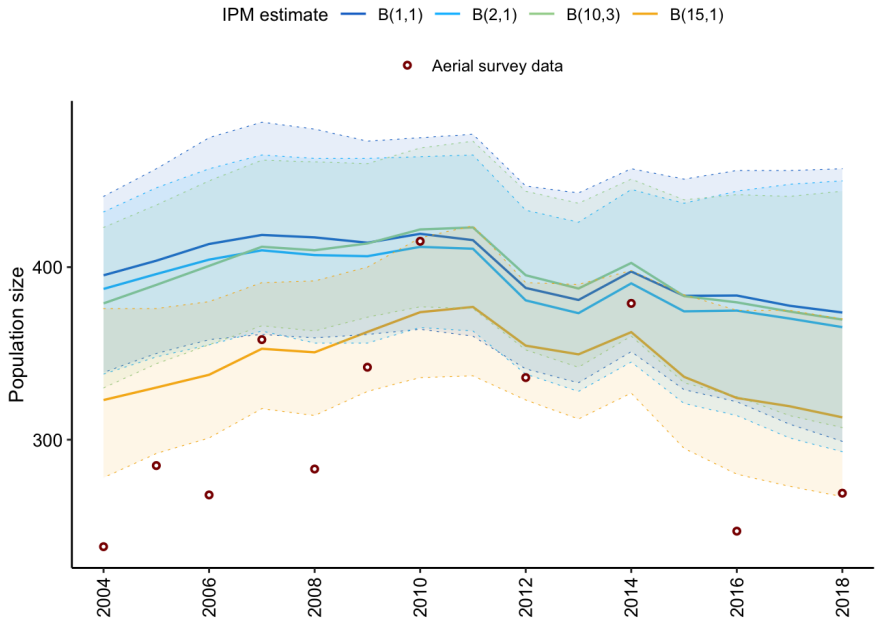

Figure C4: Abundance trend during the time period informed by data across priors for aerial survey detection probability estimated using the "median" survey day data.

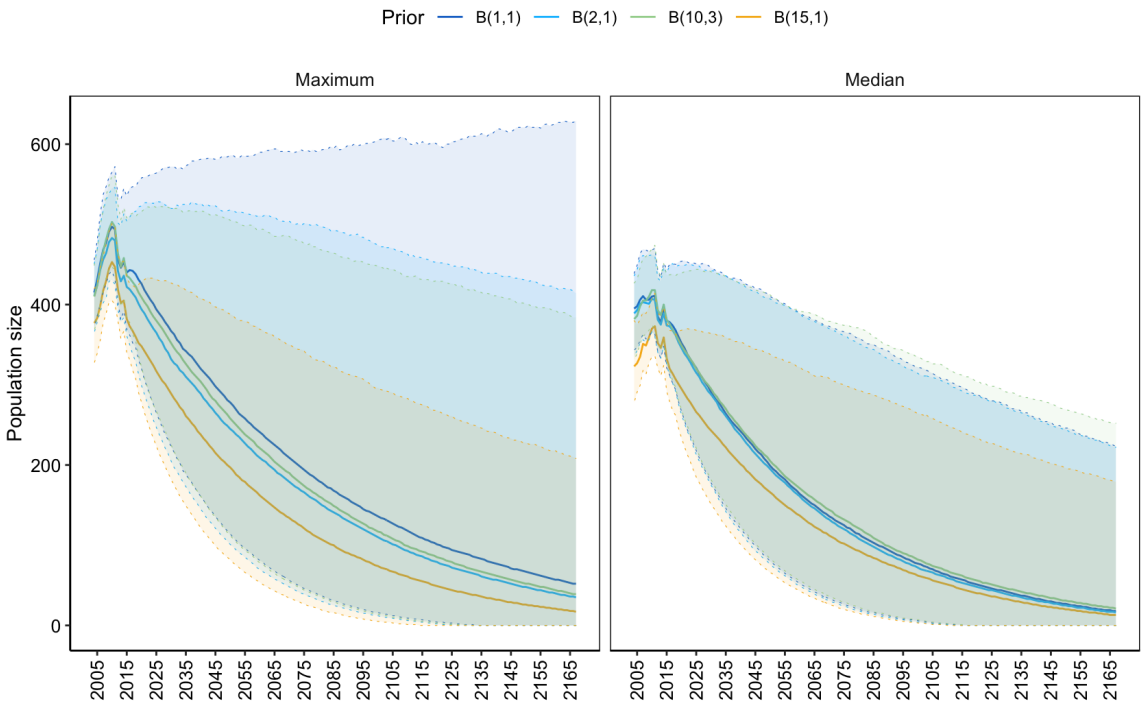

Figure C5: Posterior mean and 95% credible intervals for projected abundance trends across priors for aerial survey detection probability and median and maximum survey day data.

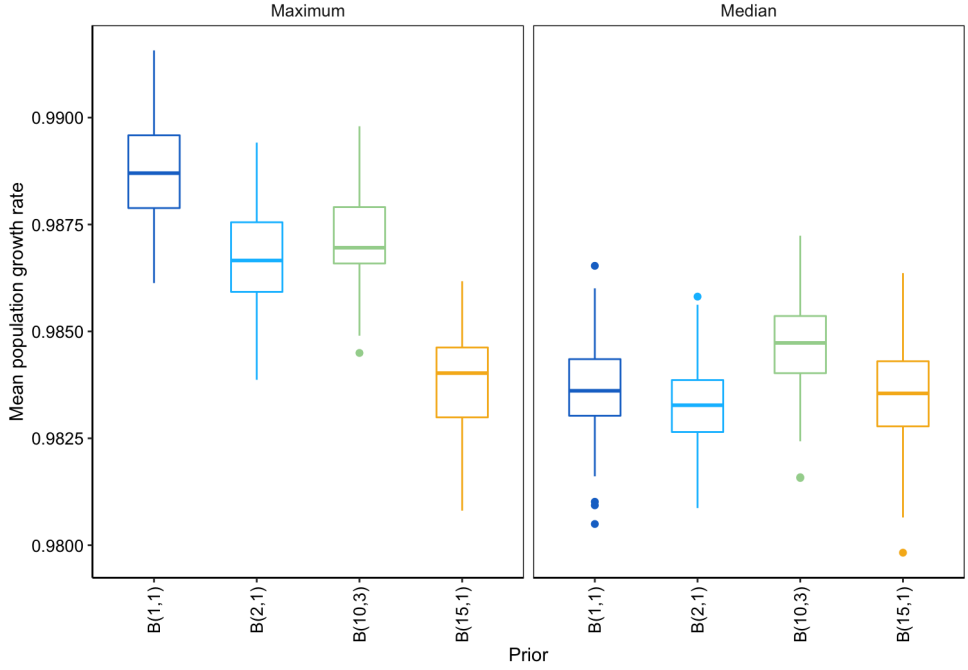

Figure C6: Posterior mean population growth rate across priors for aerial survey detection probability and median and maximum survey day data.

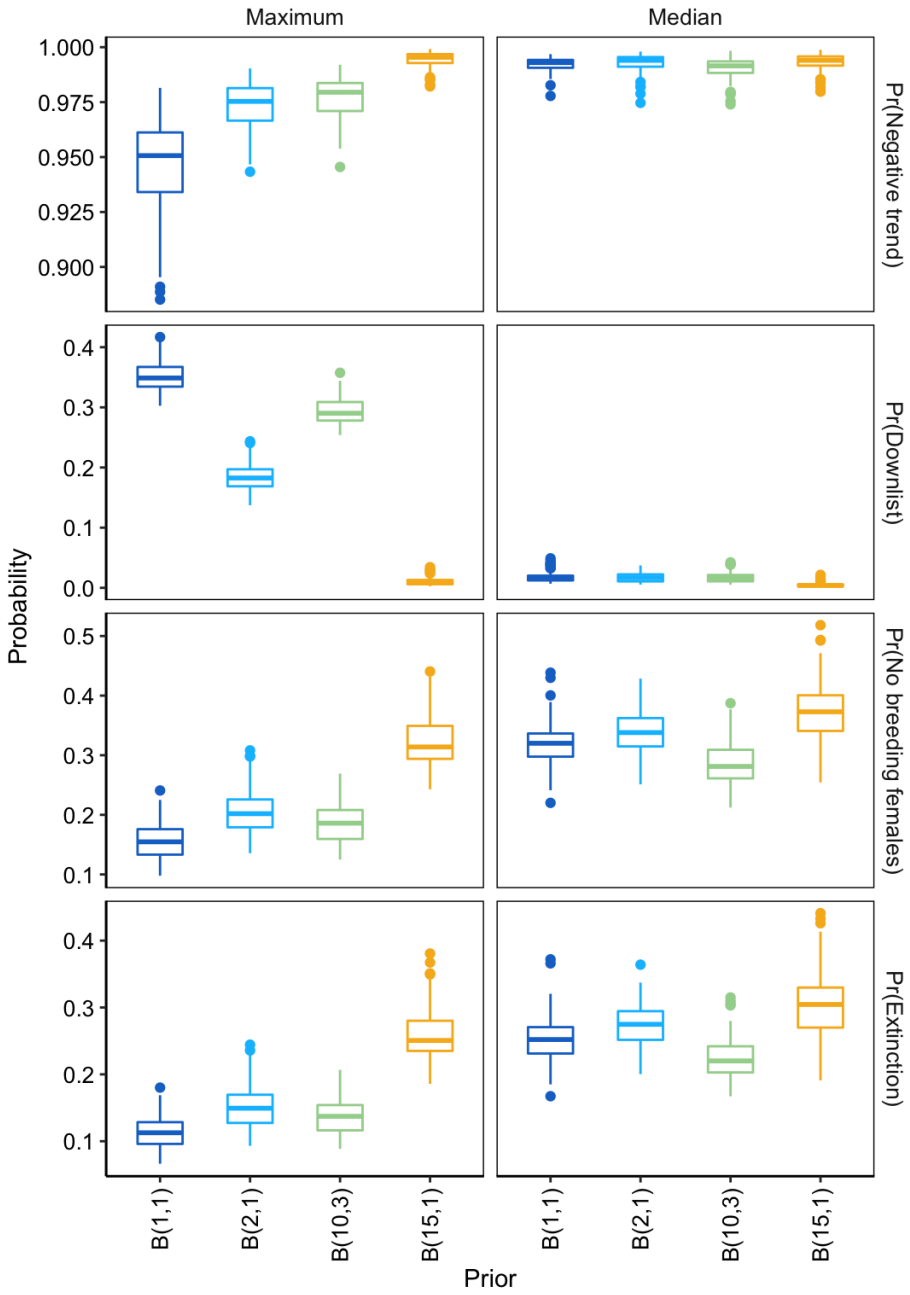

Figure C7: Posterior mean of population viability and extinction risk across priors for aerial survey detection probability and "median" and "maximum" survey day data.

APPENDIX D

Sensitivity of demography, abundance, and viability to age at first reproduction for Cook Inlet beluga whales (Chapter 5)

The integrated population model developed in this study combines parameters from the two subcomponent models (a multi-event model estimating vital rates using mark-resight data and a state-space model estimating annual population size using aerial survey data) using stochastic population growth equations to estimate population structure and total abundance. The population growth equations perpetuate the age structure that is established in the multi-event model, but as individual ages are unknown, we had to choose a minimum age at which females could enter the breeding population (i.e., age at first reproduction; AFR). Based on the best available information for the Cook Inlet and other beluga populations (Shelden et al. 2020, McGuire et al. 2020), we chose 10 years old as the AFR. However, there is some limited information that suggests AFR may be higher for Cook Inlet belugas, and we therefore examined the sensitivity of demographic rates, abundance estimates, and population viability across AFRs of 8, 10, 12, 14, and 16 years. The distinction mainly affects how many animals are eligible to become breeders, and therefore the reproductive rate. We assumed an older AFR might increase fecundity to compensate for fewer breeding females but likely would not have appreciable effects on projected population viability because while this age structure does create more subadult age classes, we apply the adult non-breeder survival rate to these age classes, which is lower than that of breeding adults but still relatively high.

As can be seen, demographic rates (Figure D1), detection probabilities (Figure D2), and abundance estimates (Figure D3) did not vary notably across the range of AFRs. We can, however, begin to see that population projections (Figure D4), growth rates (Figure D5), and

viability summary metrics (Figure D6) do vary slightly across AFRs, with higher extinction probabilities and lower downlisting probabilities when the AFR is set to 14 or 16 years of age.

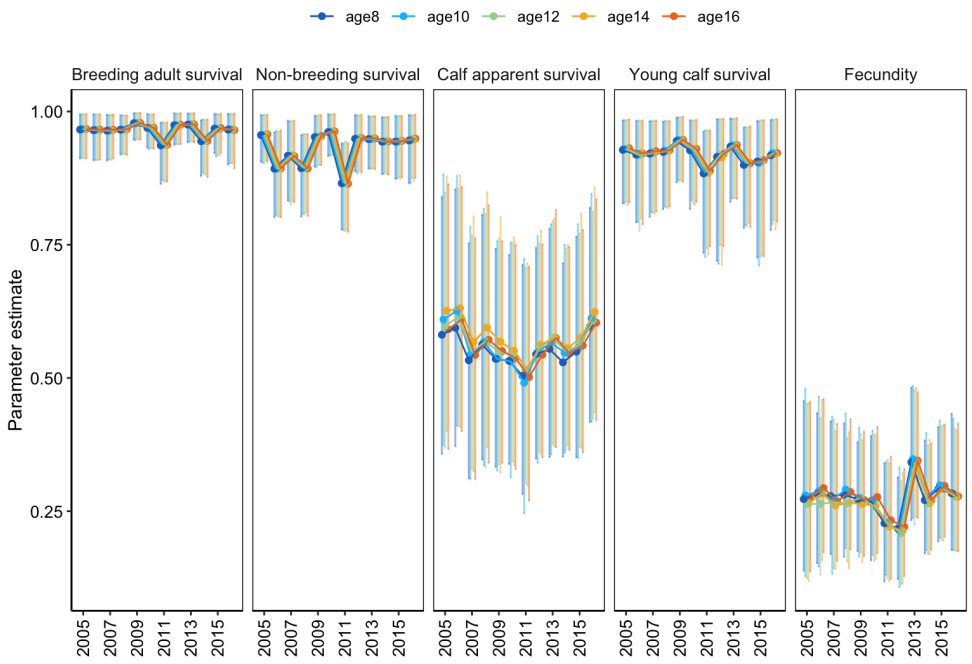

Figure D1: Posterior mean and 95% credible intervals for demographic rates across ages at first reproduction.

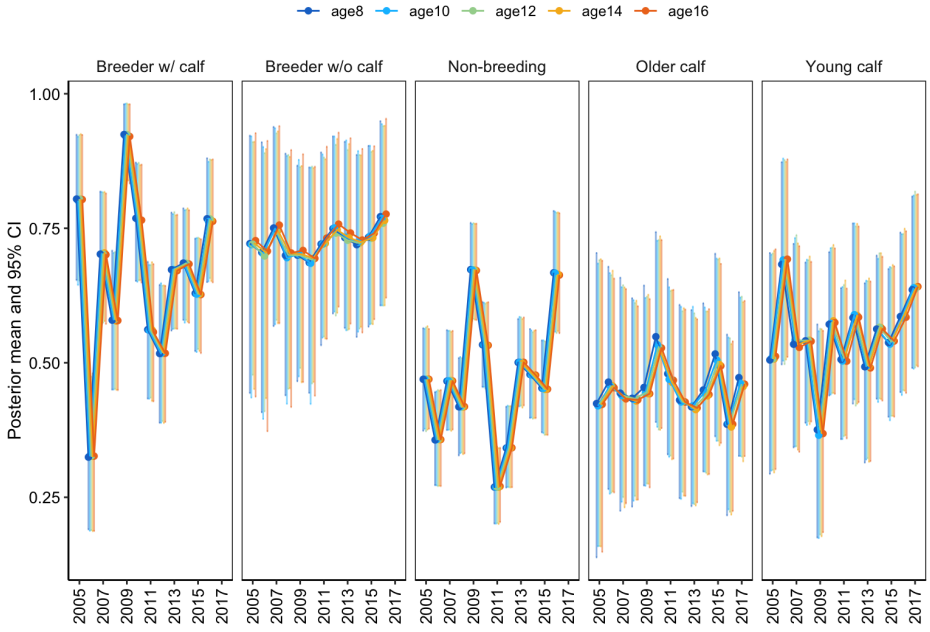

Figure D2: Posterior mean and 95% credible intervals for detection probabilities across ages at first reproduction.

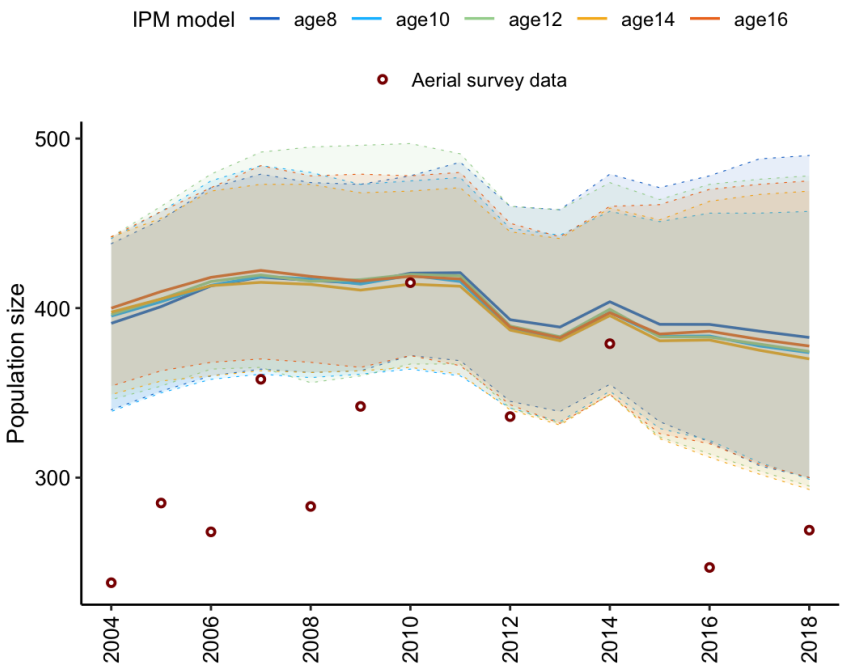

Figure D3: Posterior mean and 95% credible intervals for abundance estimates across ages at first reproduction.

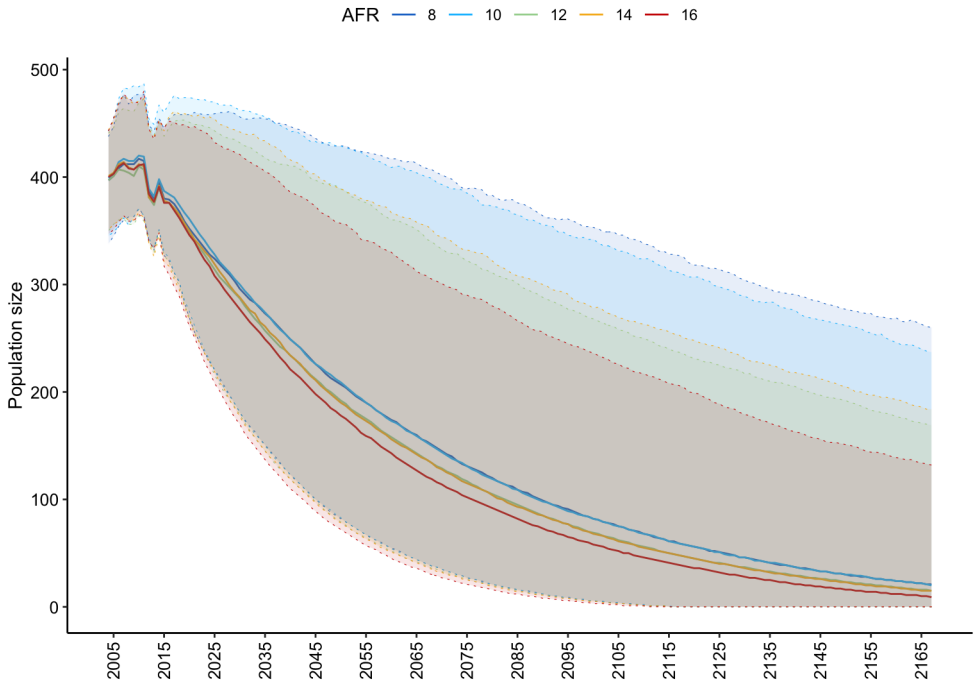

Figure D4: Posterior mean and 95% credible intervals for projected abundance estimates across ages at first reproduction.

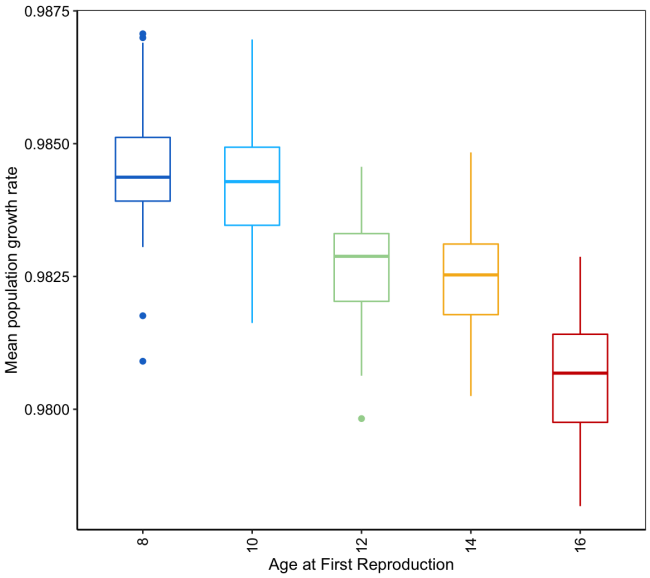

Figure D5: Posterior mean population growth rates over the 150-year projection period across ages at first reproduction.

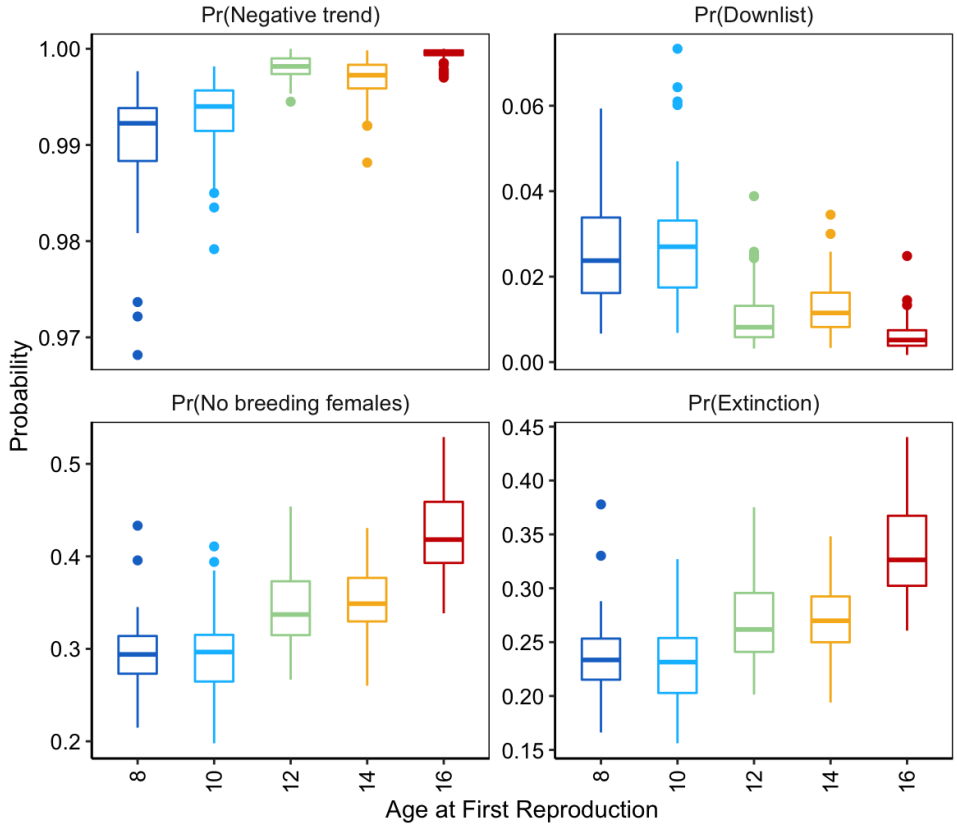

Figure D6: Posterior mean of population viability metrics, including the probability of a negative trend in abundance, of reaching the downlisting threshold (>520 individuals), of having no remaining female breeders, and of population extinction across a range of ages at first reproduction.

APPENDIX E

Defining a quasi-extinction threshold for Cook Inlet belugas (Chapter 5)

The Cook Inlet beluga whale Recovery Plan (NMFS 2016) describes the need to regularly reevaluate and update the population viability analysis (PVA) model framework underlying the estimation of extinction. Specifically, it is noted that quasi-extinction levels that account for small population effects should be addressed. Quasi-extinction risk (Ginzberg et al. 1982) has been defined as the point beyond which populations have little to no chance of recovering or when a population is "doomed" to extinction (Gerber and González-Suárez 2010) even if a handful of individuals remain. This highlights the perpetual challenges of consistently defining and estimating extinction risk thresholds for species across taxa in ways that are defensible and useful in the implementation of conservation actions. One of the reasons that developing consistent definitions for extinction risk and recovery criteria is that these metrics are highly context-specific. Extinction risk varies considerably depending on life history traits, historical and current population size, density dependence, geographic extent, sensitivity to environmental perturbations, and vulnerability to threats. We mention these broad issues not to embark on a recounting of the numerous approaches that have been debated and discussed in the literature (see Dulvy et al. 2004, Himes Boor 2014, Doak et al. 2015, Thompson et al. 2018), but to acknowledge that this is a complex issue and that established quasi-extinction thresholds are often inevitably subjective, as they require analysts and managers to (oftentimes arbitrarily) select an extinction risk time horizon (i.e., extinction at 100 years, 200 years, or 3 generations) and a level of risk tolerance (90% versus 95% probability of extinction) for that time horizon.

To examine population thresholds or quasi-extinction levels for Cook Inlet belugas, we used forward simulations to execute a grid search over a range of alternative quasi-extinction

population size thresholds n ranging from 20-300 individuals. This forward simulation was done 100 times for each MCMC sample i for a total of x = 600,000 total population projections. For each potential quasi-extinction population size threshold n, we performed the grid search over all x population trajectories where population size was n 50 years into the future and then stored the eventual probability of extinction at 250 years into the future. This longer 200-year time horizon (from t = 50-250; relative to that in the main text) was used to examine eventual extinction probabilities for larger population sizes.

This grid search approach resulted in a mean extinction probability for a given population size n that increases with decreasing population size threshold (Figure E1). Specifically, populations ranging from 30-35 individuals in 2068 (50 years into the projection) had a 95% probability of extinction ($\Pr(N_{\text{Tot}}<2)$) in 2268 (250 years into the projection). Similarly, populations ranging from 150-200 individuals had a 50% extinction probability and those ranging from 200-275 individuals had a 25% extinction probability (Figure E1). These results indicate that a population size ranging from 30-35 individuals could be considered a quasi-extinction threshold, or a level beyond which there is high certainty that the population will not recover. It should be noted, however, that these metrics are specific to the time horizon that was examined, and that larger population size thresholds (e.g., 150-200 individuals) may also have a high probability of extinction over longer time horizons (e.g., 300 years).

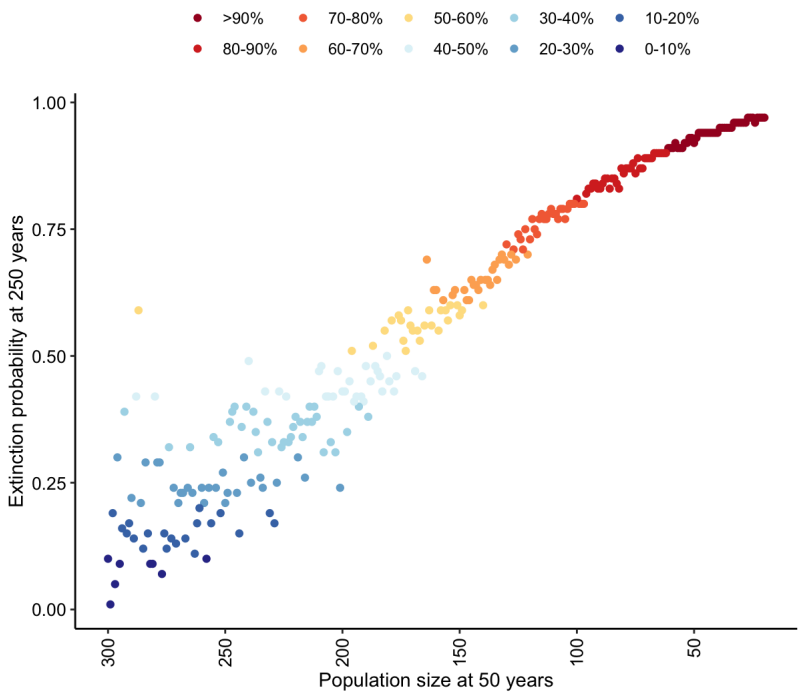

Figure E1. Results of a forward simulation grid search examining eventual extinction probabilities for population trajectories with a given population size at 50 years into the projection period.

References

Doak, D.F., Himes Boor, G.K., Bakker, V.J., Morris, W.F., Louthan, A., Morrison, S.A., Stanley, A., Crowder, L.B., 2015. Recommendations for Improving Recovery Criteria under the US Endangered Species Act. BioScience 65, 189–199. https://doi.org/10.1093/biosci/biu215

Himes Boor, G.K., 2014. A Framework for Developing Objective and Measurable Recovery Criteria for Threatened and Endangered Species. Conservation Biology 28, 33–43.

Dulvy, N.K., Ellis, J.R., Goodwin, N.B., Grant, A., Reynolds, J.D., Jennings, S., 2004. Methods of assessing extinction risk in marine fishes. Fish and Fisheries 5, 255–276. https://doi.org/10.1111/j.1467-2679.2004.00158.x

Gerber, L. & González-Suárez, M. 2010. Population Viability Analysis: Origins and Contributions. Nature Education Knowledge 3(10):15

Ginzburg, L.R., Slobodkin, L.B., Johnson, K., Bindman, A.G., 1982. Quasiextinction Probabilities as a Measure of Impact on Population Growth. Risk Analysis 2, 171–181. https://doi.org/10.1111/j.1539-6924.1982.tb01379.x

Thompson, G.G., Maguire, L.A., Regan, T.J., 2018. Evaluation of Two Approaches to Defining Extinction Risk under the U.S. Endangered Species Act. Risk Analysis 38, 1009–1035. https://doi.org/10.1111/risa.12927

APPENDIX F

Expanded covariate analysis for Cook Inlet belugas (Chapter 5)

One of the goals of this study was to examine the effects of environmental variability and anthropogenic stressors on the survival and reproduction of Cook Inlet beluga whales. However, this endeavor is complicated by numerous factors, including patchily available data on anthropogenic stressors that align with the spatio-temporal presence of whales, lack of specific evidence-based hypotheses about the impact of oceanographic conditions on vital rates, and strong correlations between environmental time series data on ocean conditions and prey availability. In the primary analysis described in the main text of the manuscript, we examined the effect of Gulf of Alaska sea surface temperature and a proxy for prey abundance that combined escapement data from multiple prey species over the summer months from several tributaries in Cook Inlet. However, we also conducted an expanded exploratory analysis that considered additional predictor variables with greater temporal specificity and present those findings here. As noted in the manuscript text, there are caveats and knowledge gaps pertaining to many of these covariate variables that we used as proxies for prey availability and anthropogenic stressors. Because many of these variables are strongly correlated, we fit the model using each as the sole covariate and examined whether there was an improvement in model fit compared to the model without covariates according to Watanabe-Akaike information criterion (WAIC; Watanabe 2010) values.

Data

In addition to yearly Gulf of Alaska sea surface temperature (SST) used as a predictor in the primary analysis, we fit models with additional local- and basin-scale indices of oceanographic variability. These included the Pacific Decadal Oscillation (PDO), North Pacific Gyre

Oscillation (NPGO), and upwelling. Localized summer (June-Oct) upwelling anomalies near Seward, AK (60°N, 149°W) were obtained from the NOAA Pacific Fisheries Environmental Laboratory. Summer sea surface temperatures (SST) in the Gulf of Alaska were obtained from a bounding box spanning approximately 54 to 60°N and -137 to -157°W using the NOAA GOES satellite data accessed from the ERDDAP server (Simons 2020). Basin-scale oceanographic covariates included the Pacific Decadal Oscillation (PDO; Zhang et al. 1997, Mantua et al. 1997) and the North Pacific Gyre Oscillation (NPGO; Di Lorenzo et al. 2008), both obtained at a monthly level from the NOAA National Center for Environmental Information (NOAA NCEI 2020) and NOAA Physical Science Laboratory (NOAA PSL 2020) and aggregated to seasonal values.

The Susitna River delta area contains many rivers with relatively large runs of multiple salmon species, and Cook Inlet beluga whales are known to forage in river mouths and along the delta during periods of the summer when salmon are entering these rivers (Castellote et al. 2021), but also in Turnagain Arm and, in late summer and early fall, in Knik Arm. Data are available for many of the largest salmon runs in upper Cook Inlet. Chinook, coho, pink, sockeye, and chum salmon escapement data from various tributaries and rivers in known beluga foraging áreas were obtained from the Alaska Department of Fish and Game. In addition to the combined-species metric of salmon abundance that was used in the primary analysis, we also fit models using each individual prey species (Chinook, coho, chum, pink, and sockeye salmon and eulachon) aggregated over the entire summer season and at a Monthly level where possible.

We also examined the effects of two proxies for forage fish availability: incidental catch of osmerids and eulachon in local commercial fisheries and the reproductive success of black-legged kittiwake and common murre on East Amatuli Island at the mouth of Cook Inlet (Kettle et

al. 2019). Data on hazardous waste spill volume was obtained from the Alaska Department of Environmental Conservation PPR Spills Database Search and used as a proxy for contaminants. Shipping traffic through the Port of Anchorate was compiled from the U.S. Department of Transportation's Repository and Open Science Access Portal and used as a proxy for underwater noise. Data were summed across all spills that occurred in the marine environment within Cook Inlet. Though developing a quantitative metric representing cumulative impacts on Cook Inlet belugas is challenging, we used the total human population size (based on the State of Alaska Department of Labor and Workforce Development) in Anchorage was used as an indirect proxy for cumulative impacts.

Covariate effects and WAIC values

In terms of the effects of local- and basin-scale oceanographic variability, the 95% credible intervals representing the effects of annual and season-specific predictors overlapped zero, indicating uncertainty about whether the direction of the effect was positive versus negative. However, there was weak evidence that adult survival was positively correlated with warmer spring and winter sea surface temperatures, stronger summer upwelling, and warm-phase PDO. Calf survival and fecundity were also positively correlated with warmer sea surface temperatures and stronger summer upwelling (Figure F1). Proxies for anthropogenic stressors were not notably correlated with vital rates. In terms of metrics of prey abundance and forage fish availability, Chinook salmon escapement was positively correlated with calf survival (in theory via lactation as calves do not consume adult salmon) and fecundity (Figure F2). The examination of these prey metrics at the monthly level revealed precisely when certain species may have a greater effect on demography. For example, Chinook abundance may have a positive effect on

calf survival in August while coho salmon may be more important in later summer and early fall (Figure F3).

Results indicated that model fit was improved with the addition of several of the covariates relative to when no covariates were included (Figure F4).

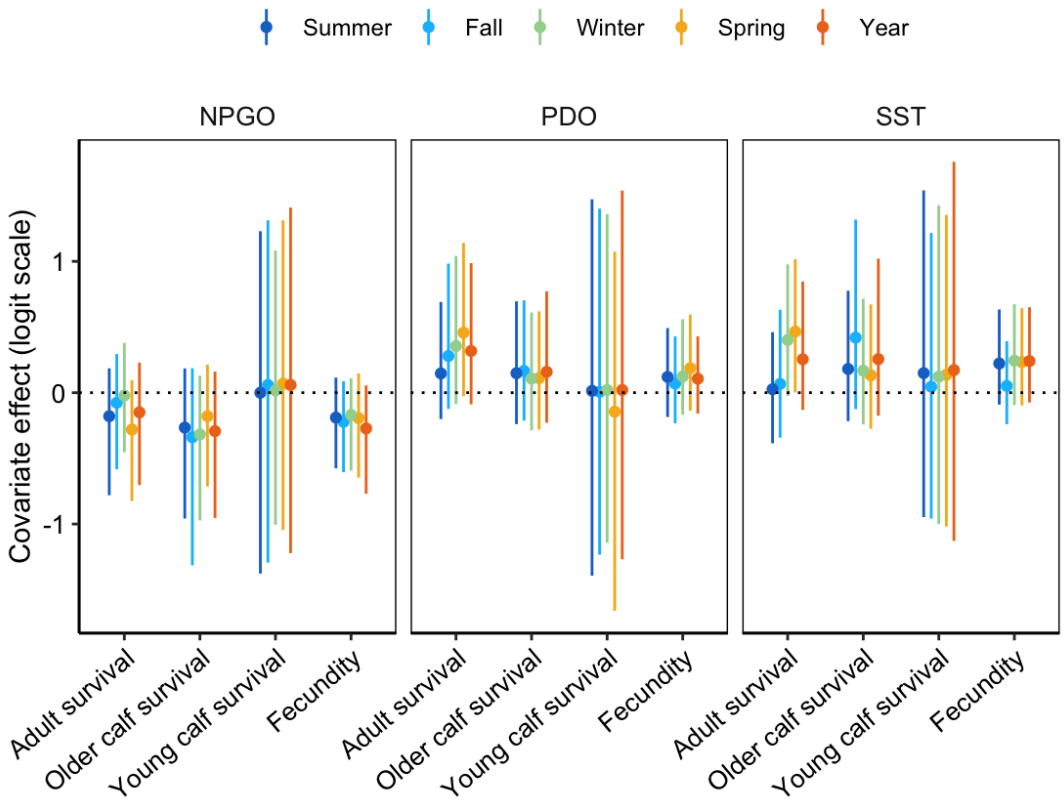

Figure F1: Mean and 95% CI of the logit-scale effects of seasonal and annual oceanographic covariate variables on beluga fecundity and adult, older calf, and young calf survival.

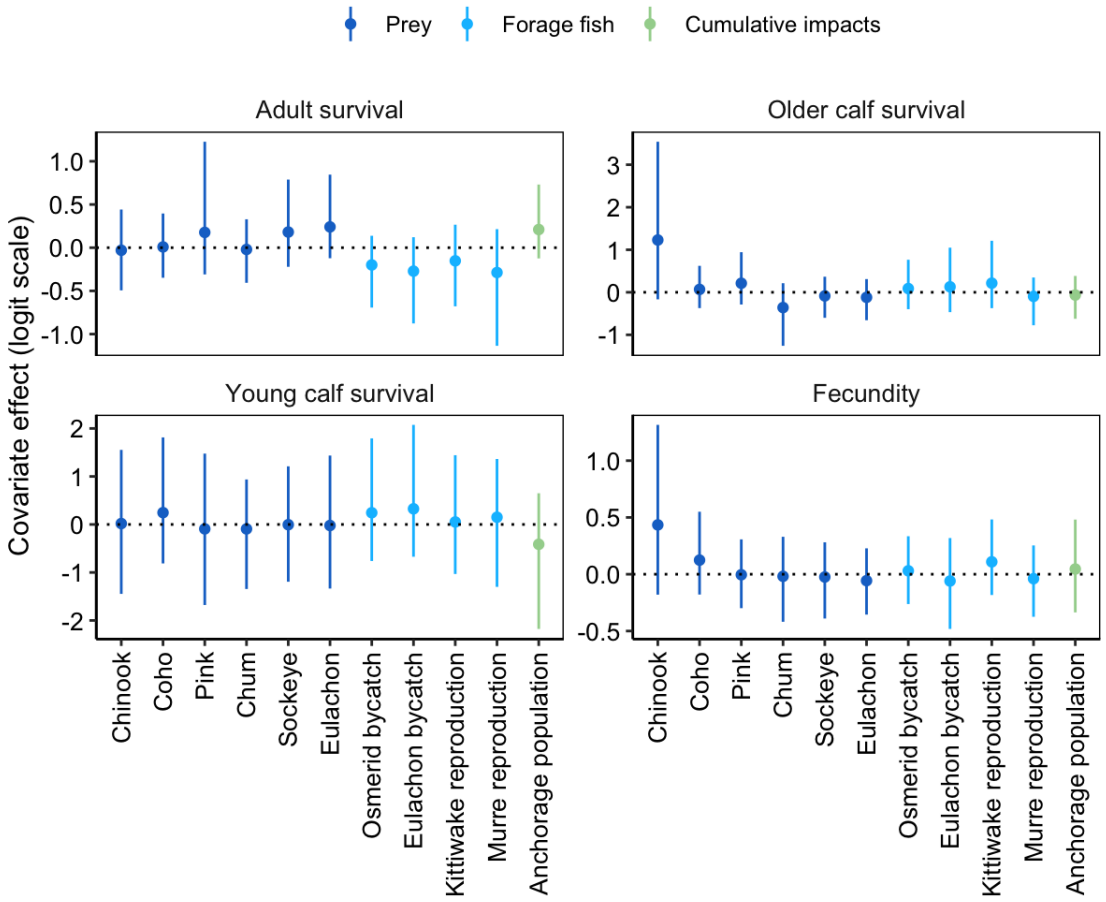

Figure F2: Mean and 95% CI of the logit-scale effects of annual covariate variables pertaining to proxies for prey availability, forage fish abundance, cumulative impacts, noise, and contaminants on beluga fecundity and adult, older calf, and young calf survival.

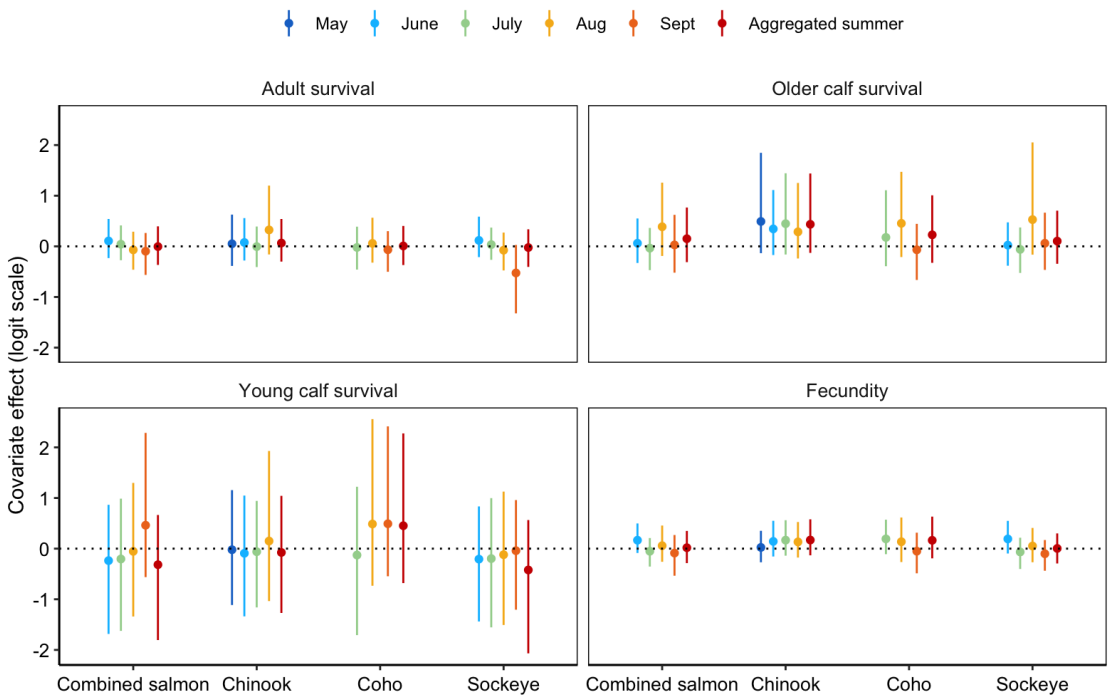

Figure F3: Mean and 95% CI of the logit-scale effects of seasonal prey-related covariate variables on beluga fecundity and adult, older calf, and young calf survival.

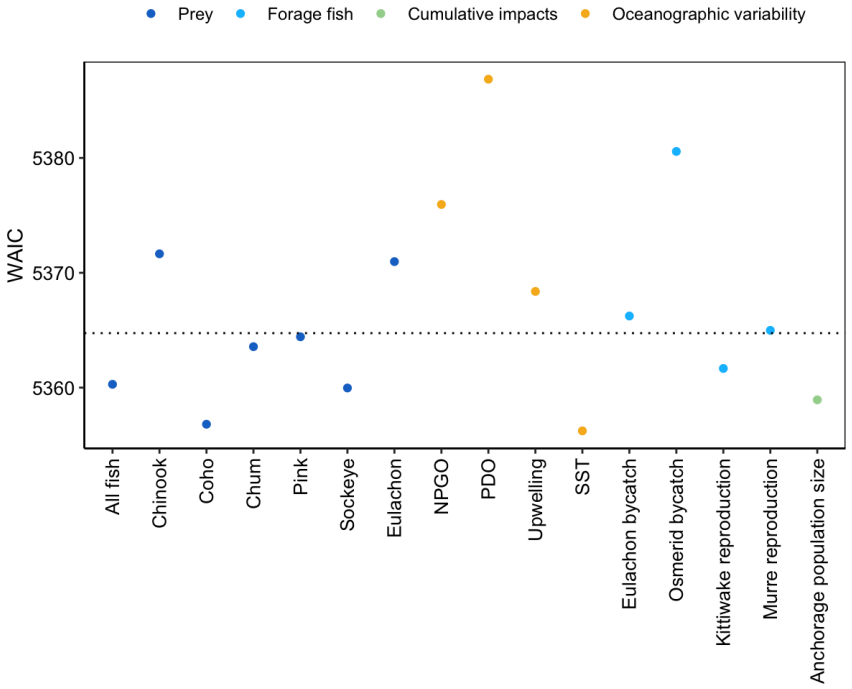

Figure F4: WAIC values for models where each annual covariate for stressor categories was used alone (colored dots) compared to when no covariates were included (interannual random effects only; dotted black line).

APPENDIX G

Detailed observation process model results for the multi-event subcomponent model in the IPM-based PVA for Cook Inlet belugas (Chapter 5)

Accounting for uncertainty within both the state and ecological processes is fundamental to hierarchical state-space mark-resight models. The complex observation process within the multi-event mark-resight model included parameters that describe the probabilities of detecting individuals given their life history states and the probabilities of correctly assigning calf ages given their true ages.

The mean of the state-specific detection probability intercept was 0.47 (95% credible interval: 0.38-0.57) for non-breeders (p_N), 0.68 (0.56-0.79) for breeders with calves (p_{B_C}), and 0.73 (0.6-0.87) for breeders without calves (p_{B_N}) (Figure G1). Variability in adult detection over the study period was greatest for breeders with calves (ranging from 0.33 to 0.92) and non-breeders (ranging from 0.27 to 0.67). Mean detection probability for older calves (δ_C) was approximately 0.55 (0.46-0.65) and that of younger calves was (δ_Y) 0.44 (0.3-0.56).

Calf age assignment probabilities were estimated relatively precisely, as in Himes Boor et al. (*In revision*). The probability of assigning an age category (γ) was approximately 0.93 and the probability of assigning calf age with perfect certainty (α) for younger and older calves was 0.5 and 0.05, respectively. The probability of assigning an uncertain age that matched the true age (ω) for younger and older calves was 0.97 and 0.6, respectively, and the probability of assigning an uncertain age different than the true age by one year (κ) for younger and older calves was 0.98 and 0.58, respectively.

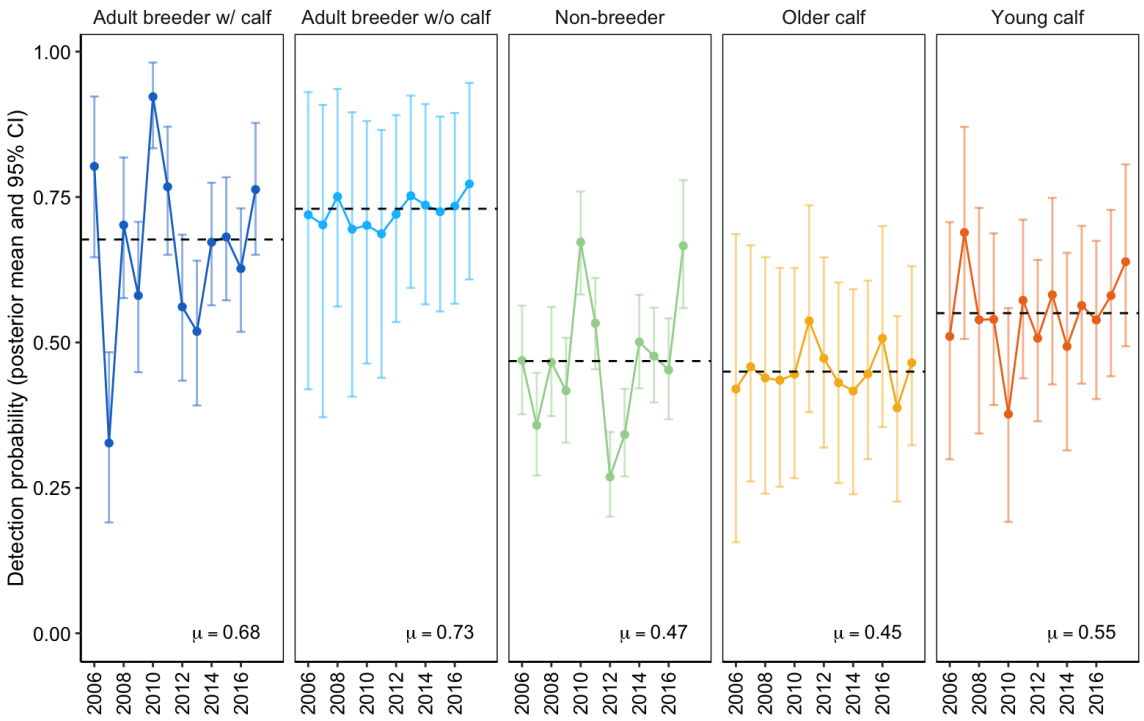

Figure G1: Posterior mean and 95% credible intervals for time-varying stage-specific adult and calf detection over the study period with median of mean rates represented by the dashed line.